Understanding the Anti-inflammatory Effect of C-peptide in Kidney

Thesis submitted for the degree of

Doctor of Philosophy

at the University of Leicester

by

Abdullah S. H. Alruwaili

Department of Infection, Immunity and Inflammation

College of Life Sciences

School of Medicine

University of Leicester

2019

Abstract

Patients with diabetes are at high risk of developing long-term complications, including diabetic kidney disease. Recent data suggest that type 1 diabetes might be a dual hormone deficiency disease in which secretion of insulin and C-peptide is insufficient. Insulin supplementation is provided as part of treatment regimes, however, C-peptide depletion remains untreated. In this study, the potential beneficial effect of C-peptide replacement on renal cell signalling and biochemical markers of inflammation was investigated. Using cultured human renal cells (HEK-293A and TERT/1), incubation with 0.3 to 10nM C-peptide resulted in stimulatory effects on the key intracellular signalling pathway to MAP kinase (ERK1/2).

This effect was further investigated in presence of 2.5mM inorganic phosphate (Pi), a plasma Pi concentration that occurs in in rodents but not in healthy humans. Both Pi and C-peptide activated ERK1/2 in TERT/1 cells, and a positive interaction (synergism) was found between the effects of Pi and C-peptide. This response to Pi occurred without detectable change in the intracellular Pi concentration and was mimicked by non-metabolisable Pi analogues orthovanadate, phosphite and hypophosphite, consistent with a recent report of sensing of extracellular Pi by SLC20 transporter proteins (PiT1 and PiT2) in the plasma membrane which then signal to ERK1/2. C-peptide (at a physiologically relevant concentration of 3nM) also decreased mRNA expression of Pi transporters PiT2 and XPR1 and the activity of total Na^+-linked Pi influx by 30% in TERT/1 cells, suggesting that C-peptide may contribute to regulation of renal Pi transport.

The proposed renoprotective effect of C-peptide was investigated *in vivo.* Streptozotocin-induced diabetes in rats resulted in upregulation of transforming growth factor-β and Type IV collagen. Administration of C-peptide prevented diabetes-induced overexpression of TGF-β and Col-IV mRNA, and TGF-β protein in kidney tissue. C-peptide administration also resulted in down-regulation of inflammatory marker proteins; monocyte chemo-attractant protein-1, inter-cellular adhesion molecule-1, vascular cell adhesion molecule-1, vascular endothelial growth factor-A, RANTES, tumour necrosis factor-α and interleukin-1β. Despite the older views that portrayed C-peptide as an inert molecule with no bioactivity, the data presented in this study, add to growing evidence supporting an

active role for C-peptide in the diabetic milieu, and suggest that (at least *in vitro*) the response to C-peptide may be enhanced at the elevated extracellular Pi concentration.

Acknowledgements

I would like to express my sincere gratitude and appreciation to my supervisor **Prof Nigel Brunskill**: thank you for giving me encouragement, guidance and constant support throughout my PhD journey. I also owe a great debt of gratitude to my supervisor **Dr Alan Bevington**, without whom I would not have come this far. Alan and Nigel, it has been a great pleasure and honour to be mentored by you.

I would also like to thank my PRP members, **Prof Jonathan Barratt** and **Dr Emma Watson** for their insightful feedback and constructive criticism.

Special thanks are due to **Mr Jeremy Brown** for his constant support during my PhD. I would also like to thank **Dr Nima Abbasian** and **Dr Ravinder Chana** for assistance with the mycoplasma screening testing of TERT/1 and HEK-293A cells. Very special thanks are due to **Dr Gary Willars** and **Dr Ali Janabi** for providing me, as a kind gift, with GPR146-EGFP plasmid and restriction enzymes used in chapter 3. My profound thanks also to **Miss Justina Kailey**, BSc project student, for her contribution in performing experiment (under my supervision) and producing data presented in figures 4.1, 4.2, 4.3, and 4.4 in chapter 4. My sincere gratitude to MSc student **Miss Yiqing Zeng** for performing (under my supervision) and producing data presented in figures 4.6 to 4.11 in chapter 4. I would like to thank Dr David Wimbury for his guidance in using Magnetic Luminex cytokine assays and Dr Karen Molyneux for providing unlimited access to the MAGPIX® Luminex reader.

It is a pleasure to acknowledge my sincere thanks to people in the renal lab, Safia Balbas, Violeta Diez Beltran, Ziyad Aldosari, Douglas Gould, Tom O'Sullivan, Patricia Higgins, Katherine Robinson, and Soteris Xenophontos, for their help and support, and for helping to create a positive and healthy environment inside the lab. I also would like to thank Dr Mohammed Imam for helping me tidying up my thesis.

My gratitude to the **Ministry of Education and Northern Border University (NBU)** for sponsoring and financially supporting me throughout my PhD study. Thanks to all the people I have met in the Medical Science Building at the University of Leicester for their kindness and support.

My final and most sincere thanks go to my parents, wife, and family for their unceasing help and for emotional support. Nevertheless, I cannot forget my lovely children, **Raghad**, **Lara**, **Reem**, and **Mohammed** for making everything worthwhile.

Statement of Originality

All of the work described in this thesis is my own work performed during my period of registration for the degree of Doctor of Philosophy in this university, with the exception of assistance and samples that were provided by others as follows:

Studies in this thesis on rat kidney and plasma were performed on samples from a study on the streptozotocin (STZ) model of type I diabetes in rats (see Chapter 1 & 5) which had previously been performed by Prof Nigel Brunskill and Mr Jeremy Brown (Department of Infection, Immunity & Inflammation, University of Leicester). All of the animal experiments were performed in the Preclinical Research Facility (PRF) at the University of Leicester under a project licence from the UK Home Office held by Prof Nigel Brunskill. This includes samples used to produce data presented in Chapter 5, and data presented in Appendix 5.

Table of Contents

Abstract.....I

Acknowledgements..... II

Statement of Originality.....IV

Table of Contents..... V

List of Figures.....XII

List of Tables XV

List of Abbreviations XVI

1 Chapter 1 Introduction 19

1.1 Biosynthesis of Insulin 19

1.1.1 Pancreatic islet structure and function 19

1.1.2 Islet Anatomy..... 19

1.1.3 Function of β-cells 19

1.1.4 Insulin and C-peptide exocytosis 19

1.2 Insulin action 20

1.3 Diabetes mellitus 20

1.3.1 Classification of DM..... 21

1.3.2 Type 1 diabetes (T1DM)..... 23

1.3.3 Type 2 diabetes (T2DM)..... 24

1.3.4 Gestational diabetes 25

1.4 Diabetic complications..... 27

1.4.1 Acute complications 27

1.4.2 Chronic complications 27

1.5 Anatomy of the kidney 31
1.5.1 Structure and function of the kidney 31
1.5.2 Nephrons 33
1.5.3 The vascular endothelium 33
1.6 Proinsulin C-peptide 34
1.6.1 Background and History 34
1.6.2 C-peptide and insulin biosynthesis and secretion 35
1.6.3 C-peptide structure 37
1.7 Intracellular signalling by C-peptide 38
1.7.1 Effect on MAPK ERK1/2 38
1.7.2 Effect on Na^+, K^+-ATPase 39
1.7.3 Effect on intracellular calcium (Ca^{2+}) 40
1.7.4 Effect on PI3K 40
1.7.5 Effect on eNOS 41
1.8 Anti-inflammatory effects of C-peptide 41
1.9 C-peptide receptor 42
1.9.1 C-peptide cell membrane interactions 42
1.10 G protein-coupled receptors (GPCR) 43
1.10.1 GPCR classification 44
1.10.2 The activation of heterotrimeric G proteins 44
1.10.3 GPCR signalling to ERK1/2 45
1.10.4 GPR146 47
1.11 C-peptide and diabetic kidney disease 49
1.11.1 Short-term effects in diabetic nephropathy 50
1.11.2 Effects on long-term glomerular and tubulo-interstitial damage 50
1.11.3 Effects of C-peptide in clinical trials of diabetic nephropathy 51

1.11.4 Phosphate and limitations on C-peptide action in humans 53

1.12 Background physiology of inorganic phosphate (Pi) 54

1.12.1 Extracellular Pi as a signaling molecule 55

1.12.2 Using Pi analogues as probes for Pi sensing..... 55

Figure *1*.7 The structure of inorganic phosphate (Pi) in comparison with its structural analogues. 57

1.13 Experimental models 58

1.13.1 Choice of cell culture models 58

1.13.2 Experimental animal models of T1DM 58

1.14 Aims and hypothesis in this project..... 59

2 Chapter 2 Materials and Methods 61

2.1 Materials..... 61

2.2 Tissue Culture 61

2.2.1 Cell lines 61

2.2.2 Cell culture procedure..... 61

2.2.3 Retrieving frozen cells 62

2.2.4 Collagen coating plates for HEK293A cells..... 63

2.2.5 Cell treatments 63

2.3 Western blotting..... 65

2.3.1 Cell stimulation and sample preparation 65

2.3.2 Sodium dodecyl sulphate polyacrylamide gel electrophoresis (SDS-PAGE).....65

2.3.3 Immunoblotting 65

2.3.4 Data Analysis and Band Quantification..... 66

2.4 Bio-Rad detergent-compatible (DC) protein assay 67

2.5 Lowry protein assay 67

2.6 Selective Pi assay 68

2.7 Pi transport studies using radiolabeled Pi [^{33}Pi] 68

2.8 Bacterial transformation 69

2.9 Plasmid purification 69

2.10 Restriction enzyme digestion to verify the integrity of GPR146-EGFP plasmid…… 70

2.11 TERT/1 transfection using TransFex reagent 71

2.12 HEK293A transfection (transient transfection) with calcium phosphate 72

2.13 HEK293A transfection using jetPRIME 73

2.14 RNA Extraction and RT-Q-PCR 73

2.15 Reverse transcription (RT) reaction (cDNA synthesis) 74

2.16 Quantitative real time-polymerase chain reaction (qPCR) 75

2.16.1 qPCR using Power SYBER®Green PCR Master Mix 75

2.16.2 qPCR using Taqman Master mix 76

2.17 Preparation of Samples for Luminex Assay 78

2.17.1 Preparation of Kidney Samples 78

2.17.2 Preparation of Plasma Samples 78

2.18 Magnetic Luminex cytokine assay 78

2.19 ELISA 79

2.20 Diabetic rat study 79

2.20.1 Induction of DM and animal groups 80

2.21 Statistical analysis 81

3 Chapter 3 Confirming C-peptide responsiveness in cultured human renal tubular epithelial cells 82

3.1 Introduction 82

3.2 Results 85

3.2.1 C-peptide-mediated activation of ERK1/2 in TERT/1 cells 85

3.2.2 C-peptide-mediated ERK1/2 activation in human embryonic kidney cells (HEK293A) 87

3.2.3 Time course of the effect of human C-peptide on ERK activation in TERT/1 and HEK 293A cells 89

3.2.4 Expression of GPR146 a candidate receptor for C-peptide 92

3.2.5 Attempted over-expression of EGFP-tagged GPR146 in TERT/1 and HEK293A cells 96

3.2.6 Verification of GPR146-EGFP plasmid integrity 96

3.2.7 Attempted transient expression of EGFP-tagged GPR146 or EGFP in TERT/1 and HEK293A cells 97

3.3 Discussion 98

3.3.1 C-peptide activates ERK1/2 in TERT/1 and HEK293A cells 98

3.3.2 Physiological significance of GPR146 101

3.3.3 Application of the work from this chapter. 101

4 Chapter 4 Interaction between C-peptide and inorganic phosphate (Pi) in TERT/1 cells… 102

4.1 Introduction 102

4.2 Results 103

4.2.1 Effect of C-peptide and inorganic phosphate (Pi) on ERK1/2 phosphorylation in TERT/1 and HEK293A cells 103

4.2.2 Using Pi analogues as probes for Pi sensing 106

4.2.3 The effect of extracellular vanadate (Vi) as a Pi analogue with C-peptide on ERK1/2 phosphorylation 106

4.2.4 Effects of other Pi analogues phosphite and hypophosphite on the activation of ERK1/2 108

4.2.5 A model to explain interaction between C-peptide and Pi 110

4.2.6 The effect of Pi and C-peptide on the cell layer Pi concentration in TERT/1 cells and HEK293A cells. 111

4.2.7 The effect of a 90 min extracellular Pi load on the cell layer Pi concentration with or without 3nM C-peptide in HEK293A and TERT/1 cells 112

4.2.8 The effect of Pi and of Na^+-deprivation on cell layer Pi in TERT/1 cells and HEK293A cells. 113

4.2.9 The effect of extracellular Pi load with or without Na^+ on ^{33}Pi transport in TERT/1 cells 115

4.2.10 The effect of 90 min incubations with C-peptide on ^{33}Pi transport into TERT/1 cells 117

4.2.11 The effect of C-peptide on mRNA expression of Pi transporters in TERT/1 cells……. 119

4.3 Discussion 122

4.3.1 Pi is unlikely to be acting through phosphoprotein phosphatases 122

4.3.2 The mechanism of Pi signaling to ERK1/2 123

4.3.3 C-peptide effects on Pi transporter activity 123

4.3.4 C-peptide effects on Pi transporter expression 124

5 Chapter 5 C-peptide and disease progression markers in a rat model of Type I diabetes 126

5.1 Introduction 126

5.1.1 Diabetic nephropathy and inflammation..... 126

5.1.2 Chemo-attractants and immune cell recruitment and adhesion 128

5.1.3 Proinflammatory cytokines 129

5.1.4 TGF-β and renal fibrosis 129

5.1.5 Aims 131

5.2 Results 132

5.2.1 Effect of C-peptide treatment on protein content of MCP-1 and RANTES in diabetic rat kidney and plasma 132

5.2.2 Effect of C-peptide treatment on protein content of ICAM-1, VCAM-1, and VEGF-A in diabetic rat kidney and plasma 134

5.2.3 Effect of C-peptide treatment on proinflammatory cytokines in diabetic rat kidney and plasma 138

5.2.4 Effect of C-peptide treatment on renal fibrosis 140

5.3 Discussion 143

5.3.1 Effect of C-peptide treatment on chemokines and adhesion molecules……..……143

5.3.2 Effect of C-peptide treatment on proinflammatory cytokines during diabetes. 146

5.3.3 Effect of C-peptide treatment on renal fibrosis 147

5.3.4 Limitations in this study 148

6 Chapter 6 General discussion 150

6.1 Overview 150

6.2 C-peptide and TERT/1 cells 151

6.3 GPR146 and C-peptide 152

6.4 ERK1/2 signalling and Pi 152

6.5 The effects of C-peptide on inflammatory and fibrotic cytokines *in vivo* 153

6.6 Future research in this field 154

6.6.1 Biological significance of C-peptide effects on adhesion molecules in plasma *in vivo* 154

6.6.2 Links between Pi and the anti-inflammatory and anti-fibrotic effects of C-peptide *in vivo* 155

6.7 Conclusion 155

6.8 Limitations in this project 155

Appendix 157

Appendix 1: Reducing Lysis buffer 157

Appendix 2: Sample Buffer 157

Appendix 3: Resolving and Stacking Gel for Western Blot (×1 gel) 158

Appendix 4: Buffers..... 158

Appendix 5: Characteristics of the animals used in the diabetic rat study 159

Bibliography 162

List of Figures

Figure 1.1 The genetic and environmental factors involved in autoimmune response and beta-cell destruction…….24

Figure 1.2 Schematic showing the inner structure of the kidney..... 32

Figure 1.3 Gross structure of the glomerulus and the proximal tubule. 33

Figure 1.4 Enzymatic processing and secretion of insulin and C-peptide..... 36

Figure 1.5 Extracellular signal-regulated kinase 1/2 (ERK1/2) mitogen-activated protein (MAP) kinase cascade. 47

Figure 1.6 Amino acid sequence of human GPR146..... 49

Figure 1.7 The structure of inorganic phosphate (Pi) in comparison with its structural analogues. 57

Figure 2.1 Phase contrast images of human renal cell lines used in this project..... 62

Figure 2.2 Restriction map of the GPR146-EGFP plasmid..... 71

Figure 3.1 Concentration-dependence of stimulation of ERK1/2 phosphorylation by peptide in TERT/1 cells. 86

Figure 3.2 Concentration-dependent stimulation of ERK1/2 phosphorylation by C-peptide in HEK293A cells. 88

Figure 3.3 Time course effect of C-peptide treatment on ERK1/2 activation in TERT/1 cells. 90

Figure 3.4 Time course effect of C-peptide treatment on ERK1/2 activation in HEK293A cells. 91

Figure 3.5 The effect of 3nM human C-peptide on GPR-146 mRNA in cultured TERT/1 cells. 93

Figure 3.6 The effect of 3nM human C-peptide on GPR-146 mRNA in cultured HEK293A cells. 94

Figure 3.7 Gene expression of GPR146 following treatment with physiological concentrations of C-peptide, in STZ diabetic rat kidney 95

Figure 3.8 BioRadCchemi-doc image of fragments following restriction enzyme digest to confirm the GPR146-EGFP plasmid integrity. 96

Figure 3.9 Fluorescent cell imaging of HEK293A cells after attempted transient expression of either GPR146-EGFP or EGFP empty vector after 24 and 48h. 97

Figure 3.10 Fluorescent cell imaging of TERT/1 cells with transient expression of either GPR146-EGFP or EGFP at 24h. 98

Figure 4.1 The effect of 90 min of pre-incubation with 1mM and 2.5 mM Pi followed by a 5 minute incubation with C-peptide on ERK1/2 activation in TERT/1 cells**.** 104

Figure 4.2 The effect of 90 min of pre-incubation with 1mM and 2.5 mM Pi followed by a 5 minute incubation with C-peptide on ERK1/2 activation in HEK293A cells. 105

Figure 4.3 Effect of 90 min of pre-incubation with 100uM vanadate followed by a 5 minute incubation with C-peptide on ERK1/2 activation in TERT/1 cells. 107

Figure 4.4 Effect of 90 min incubation with either 1.5mM Phi or 1.5mM HPhi in presence of 1mM Pi on the activation of ERK1/2 in TERT/1 cells. 109

Figure 4.5 Schematic diagram of the hypothesis to explain the stimulatory effect of Pi and C-peptide together on ERK phosphorylation in TERT/1 cells. 111

Figure 4.6 The effect of 90 min incubation with a 1 mM and 2.5 mM concentration of extracellular Pi on the cell layer Pi concentration with or without 3nM C-peptide in the MEM incubation medium 112

Figure 4.7 The effect of 90 min incubation with a 1 mM and 2.5 mM concentration of extracellular Pi on the cell layer Pi concentration after replacing sodium ions (Na^+) with choline ions in MEM incubation medium 114

Figure 4.8 The effect on ^{33}Pi transport of incubating TERT/1 cells with an extracellular Pi load for 90 min in HBS medium with 1mM or 2.5mM Pi with or without Na^+. 116

Figure 4.9 The effect of pre-incubation with C-peptide for 90 min in DMEM on ^{33}Pi transport into TERT/1 cells..... 118

Figure 4.10 The gene expression of Pi transporters SLC20A1, SLC20A2 and XPR1 in TERT/1 cells. 120

Figure 4.11 The gene expression Pi transporter SLC20A1, SLC20A2 and XPR1 in TERT/1 cells. 121

Figure 5.1 Effect of C-peptide treatment on MCP-1 protein content in diabetic rat plasma quantified by luminex technique..... 133

Figure 5.2 Effect of C-peptide treatment on RANTES protein content in diabetic rat kidney (a) and plasma (b) quantified by luminex technique. 134

Figure 5.3 Effect of C-peptide treatment on ICAM-1 protein content in diabetic rat kidney (a) and plasma (b) quantified by luminex technique. 135

Figure 5.4 Effect of C-peptide treatment on VCAM-1 protein content in diabetic rat kidney (a) and plasma (b) quantified by luminex technique. 136

Figure 5.5 Effect of C-peptide treatment on VEGF-A protein content in diabetic rat kidney quantified by luminex technique..... 137

Figure 5.6 Effect of C-peptide treatment on TNF-α protein content in diabetic rat kidney (a) and plasma (b) quantified by luminex technique. 138

Figure 5.7 Effect of C-peptide treatment on IL-1β protein content in diabetic rat kidney (a) and plasma (b) quantified by luminex technique. 139

Figure 5.8 Effect of C-peptide treatment on IL-6 protein content in diabetic rat kidney quantified by luminex (a) and ELISA (b) assay. 139

Figure 5.9 Effect of C-peptide treatment on Col-IV gene expression in diabetic rat kidney quantified by RT-QPCR. 140

Figure 5.10 Effect of C-peptide treatment on TGF-β gene expression in diabetic rat kidney quantified by RT-QPCR. 141

Figure 5.11 Effect of C-peptide treatment on TGF-β protein content in diabetic rat kidney quantified by Luminex technique. 142

List of Tables

Table1.1 Aetiological classification of glycaemia disorders. 22

Table 2.1 Composition of HEPES-buffered saline (HBS) 64

Table 2.2 Details of antibodies used in this project 66

Table 2.3 Composition of digests that were used in GPR146-EGFP plasmid digestion.70

Table 2.4 Composition of mixtures for calcium phosphate transfection of HEK293A cells. 72

Table 2.5 Composition of reverse transcription master mix incubations. 75

Table 2.6 Primer sequences that were used for qPCR analysis of GPR146 expression. 76

Table 2.7 Details of Taqman gene expression assays that were used for qPCR analysis of the expression of genes encoding Pi transporters, GAPDH, GPR146 and fibrotic markers. 77

Table 5.1 Cytokines thought to play a role in inflammation, resolution, repair and fibrosis during diabetic nephropathy 127

List of Abbreviations

ADA	American Diabetes Association
AGEs	Advanced glycation end products
Akt	Protein kinase B, PKB
ATP	Adenosine tri-phosphate
[Ca2+]i	Intracellular calcium concentration
CKD	Chronic kidney disease
C-peptide	Connecting peptide
CTLA4	Cytotoxic T lymphocyte antigen-4 gene
CVD	Cardiovascular disease
DCCT	Diabetes Control and Complications Trial
DFBS	Dialysed foetal bovine serum
DKD	Diabetic kidney disease
DM	Diabetes mellitus
DMEM	Dulbecco's modified Eagle medium
ECM	Extracellular matrix
ECs	Endothelial cells
ERK1/2	Extracellular signal-regulated kinase 1/2
eNos	Endothelial nitric oxide synthase
ESRD	End-stage renal disease
EVs	Extracellular vesicles
FBS	Foetal bovine serum
FCM	Flow cytometry
GAPDH	Glyceraldehyde 3-phosphate dehydrogenase
GDM	Gestational diabetes
GFR	Glomerular filtration rate
GPCR	G-protein-coupled receptor
HbA1C	Glycated haemoglobin
HBSS	Hanks' balanced salt solution

HEK-293A	Human embryonic kidney cells
HLA	Human leucocyte antigen complex
ICAM-1	Intercellular adhesion molecule 1
IFIH1	Interferon-induced helicase C domain-containing protein1
IL	Interleukin
IL2RA	Interleukin 2 Receptor Subunit Alpha
iNOS	Inducible nitric oxide synthase
INS	Insulin gene
IR	Insulin receptor
LPS	Lipopolysaccharide
MAPK	Mitogen-activated protein kinases
MCP-1	Monocyte chemotactic protein-1
MEM	Minimum essential medium
MPs	Microparticles
NF-κB	Nuclear factor kappa light chain enhancer of activated B cells
NO	Nitric oxide
OK	Opossum kidney
PARP	Poly-ADP-ribose polymerase
PCA	Perchloric acid
Pi	Inorganic phosphate
PI3Ks	Phosphatidylinositol 3-kinases
PKC	Protein kinase C
PLC	Phospholipase C
PS	Penicillin-streptomycin
PTCs	Proximal tubular cells
PTPase	Protein tyrosine phosphatase
PTPN2	protein tyrosine phosphatase, non-receptor type 2 gene
PTPN22	protein tyrosine phosphatase, non-receptor type 22 gene

PTX	Pertussis toxin
RAGE	Receptor for advanced glycation end-products
RANTES	Regulated on activation, normal T cell expressed and secreted
RAS	Renin-angiotensin system
Rho	Ras-homologous
RTECs	Renal tubular epithelial cells
ROS	Reactive oxygen species
S.C.	Subcutaneously
SDS	Sodium dodecyl sulphate
SEM	Standard error of the mean
siRNA	Small interfering ribonucleic acid
STZ	Streptozotocin
T1DM	Type 1 diabetes
T2DM	Type 2 diabetes
TE	Trypsin-EDTA
TFE	Trifluoroethanol
TGF-β	Transforming growth factor-β
TNF-α	Tumour necrosis factor alpha
VCAM-1	Vascular cell adhesion molecule 1
VEGF	Vascular endothelial growth factor
Vi	(Ortho)vanadate

1 Chapter 1 Introduction

1.1 Biosynthesis of Insulin

1.1.1 Pancreatic islet structure and function

1.1.2 Islet Anatomy

In the human pancreas, islets of Langerhans form 1-2% of the mass of the tissue. They were discovered in 1869 by Paul Langerhans. They include a number of types of endocrine cells including α-cells that are responsible for producing glucagon, δ-cells which produce somatostatin, pancreatic polypeptide expressing cells, and β-cells that are responsible for synthesis and secretion of insulin and C-peptide (Kulkarni, 2004). The islets usually have an oval shape and they receive a rich blood supply (around 15% of the total pancreatic blood supply). Islets are supplied by autonomic nerve fibres both parasympathetic and sympathetic, and sensory nerves with terminals containing the classical neurotransmitters acetylcholine and noradrenaline, and a variety of biologically active neuropeptides such as pituitary adenlyate cyclase activating polypeptide, galanin and gastrin releasing peptide (Ahren, 2000).

1.1.3 Function of β-cells

To maintain plasma glucose, the main function of β-cells is to produce and secrete a sufficient amount of insulin (See Section 1.6.2). Insulin and C-peptide are stored together in the secretory granules of β-cells and released in equimolar amounts during exocytosis (Hutton, 1994). The major components of insulin storage granule are insulin and C peptide, along with zinc, calcium, adenine nucleotides, biogenic amines and some enzymes such as proinsulin converting enzymes, acid phosphatase and protein kinases (Howell, 1984; Mostafa, 2012). Insulin and C-peptide are released from storage granules by exocytosis, a process during which the storage granule membrane fuses with the plasma membrane leading to the release of the contents of the storage granule into the interstitial space (Easom, 2000; Mostafa 2012).

1.1.4 Insulin and C-peptide exocytosis

Elevation of blood glucose promotes the signalling cascade of insulin release in β-cells. When glucose is transported into β-cells through the insulin-independent plasma membrane-localized glucose transporter, GLUT2, glucose-6-phosphate is generated by the phosphorylation of glucose by glucokinase. Glucose-6-phosphate is then metabolised

via the Embden-Meyerhof glycolytic pathway (Lenzen, 2014) and mitochondrial oxidative phosphorylation which then lead to an increase in the intracellular levels of ATP. ATP-sensitive potassium channels are then closed by the elevated levels of intracellular ATP, causing a depolarization of the plasma membrane which promotes calcium ion (Ca^{2+}) influx via voltage-dependent calcium channels leading to increase in intracellular Ca^{2+} concentration $[Ca^{2+}]_i$. High levels of $[Ca^{2+}]_i$ promote SNARE protein complex formation to facilitate insulin exocytosis (Jewell *et al.* 2010, Rorsman and Renström 2003).

1.2 Insulin action

Insulin mainly targets liver, muscles (especially skeletal muscle), and adipose tissue. In the liver, insulin decreases gluconeogenesis and glycogenolysis thus decreasing the production and release of glucose. Insulin promotes the clearance of triglyceride-rich lipoproteins from plasma by upregulating lipase in adipose tissue. High levels of insulin in plasma promote the cellular uptake of glucose and its conversion to triglyceride and/or glycogen in adipose tissue and skeletal muscle respectively (Ruan and Lodish 2003). Insulin also plays an important role in the synthesis and storage of carbohydrates, lipids and proteins, maintaining energy homeostasis, and inhibiting the degradation carbohydrates, lipids and proteins (Saltiel and Kahn, 2001).

The action of insulin is initiated by its binding to its receptor. Insulin binds to the α-subunits of the receptor leading to autophosphorylation of the β subunits (which have tyrosine kinase enzyme activity) and subsequently phosphorylation of tyrosine residues on a number of other protein substrates including insulin receptor substrate 1 and 2 (IRS1 and IRS2) (De Meyts, 2016).

The phosphorylation of the IRS activates a signal transduction cascade leading to the activation of the PI3K/PKB pathway and the Ras-MAPK pathway which are responsible for most of the metabolic actions of insulin, and control of cell growth and differentiation (Saltiel and Kahn, 2001, Taniguchi *et al*. 2006).

1.3 Diabetes mellitus

Diabetes mellitus (DM) is a group of diseases with various causes; the main feature is the inability to manage blood glucose levels over a long duration. There is disturbance of the

metabolism of proteins, fat and carbohydrates, as a result of defects in insulin secretion and/or insulin action (WHO Consultation, 1999). Diabetes mellitus is a serious public health issue, and according to recent estimates, although 4.7 % of adults over 18 years of age had diabetes in 1980, this has risen to 8.5 % in 2014. Roughly 422 million adults around the world suffered from diabetes in 2014, a number which is anticipated to more than double in the coming 20 years (WHO Global report on diabetes, 2016). Focusing on the UK, the number of people affected by diabetes in 2016 was found to have increased by 65 % over the previous 10 years, reaching more than 4 million (Diabetes UK, 2016). Due to the long-term complications, diabetes is one of the top ten causes of mortality globally. It caused the deaths of approximately 4.2 million people worldwide in 2017 (International Diabetes Federation, 2017). Diabetes results in a decrease in quality of life as well as life expectancy, and is a huge financial burden on health care services. In 2017, more than 10% of funds dedicated to health globally were used on diabetes (International Diabetes Federation, 2017).

1.3.1 Classification of DM

Previously, DM was categorized according to the pharmacological treatment (insulin-dependent and non-insulin dependent). This classification has been subject to change as the aetiology of DM varies widely. Based on the aetiology of the disease, new classification criteria were applied to classify the disease (Gavin *et al.*, 1997). Today, the most widely used classification has divided the disease into two categories: type 1 DM (T1DM) and type 2 DM (T2DM): there are also gestational DM (GDM) and other specific types of DM (Table 1.1).

Types	Description
Type 1	β cell destruction, usually leading to absolute insulin deficiency. Autoimmune or idiopathic.
Type 2	Ranging from predominantly insulin resistance with relative insulin deficiency to a predominantly secretory defect with or without insulin resistance.
Gestational diabetes	Carbohydrate intolerance resulting in hyperglycaemia of variable severity with onset or first recognition during pregnancy.
Other specific types	• Monogenic diabetes - Monogenic defects of β-cell function - Monogenic defects in insulin action • Diseases of the exocrine pancreas -Various conditions that affect the pancreas can result in hyperglycaemia (trauma, tumor, inflammation, etc.) • Endocrine disorders -Occurs in diseases with excess secretion of hormones that are insulin antagonists • Infection-related diabetes -Some viruses have been associated with direct β-cell destruction • Uncommon specific forms of immune-mediated diabetes • Other genetic syndromes sometimes associated with diabetes - Many genetic disorders and chromosomal abnormalities increase the risk of diabetes

Table1.1 Aetiological classification of glycaemia disorders.
Adapted from WHO Consultation, 2019.

1.3.2 Type 1 diabetes (T1DM)

Approximately 10% of cases of diabetes can be attributed to T1DM; despite the fact that it can develop at any point, this type is generally diagnosed during childhood and teenage years (Leslie, 2010). The majority of type 1 cases, namely 70 - 90 %, are autoimmune-mediated. On the other hand, the cause of the remaining 10 - 30% is unknown (idiopathic) (Eisenbarth, 2007). The development of autoimmune-mediated T1DM is determined by abnormal immune activity which results in the destruction of functional β cells. This then leads to the emergence of inflammatory responses to the pancreatic β cells. Among others, CD4+ T-cells, CD8+ T-cells, CD68+ macrophages and dendritic cells (DCs) are associated with the pathogenesis of T1DM (Morran *et al.*, 2008; Zerif *et al.*, 2017).

In genetically susceptible diabetics, these immunological abnormalities lead to the production of antibodies which generally target β cell antigens, insulin, glutamic acid decarboxylase and the protein tyrosine phosphatase IA2 (among others). It has been suggested that these autoantibodies can make an appearance some time before the clinical manifestation of T1DM (Steck *et al.*, 2016). One of the most significant factors which influences the development of T1DM is genetic predisposition. So far, over 50 DNA loci have been linked with T1DM, with the HLA class II genes having the strongest link (accounting for 40 – 50% of genetic predisposition) (Noble & Erlich, 2012). These DNA regions can lead (via a mechanism that remains unknown) to the autoimmune destruction of pancreatic β cells. Moreover, environmental factors also have a part with regards to the development of T1DM such as drugs, pollutants, food, stress, infections, and gut microbiota (Wang *et al.*, 2017). Most of these prompt the immune system to respond to novel antigens, and these factors either directly or indirectly induce epigenetic alterations (Javierre *et al.*, 2011). DNA methylation, histone modifications and miRNA regulation, as well as other kinds of epigenetic modifications, may cause alterations in gene expression, which in turn can result in the development of an autoimmune disease via a range of mechanisms (Figure 1.1) (Wang *et al.*, 2017).

Seeing as T1DM is generally linked to absolute insulin deficiency, its management consists of regular administration of insulin to fulfil the body's needs. Insulin with different duration of actions can be accessed, so as to provide the basal control (Chaudhury *et al.*, 2017). While there are many ways to deliver insulin, others are still being developed (Atkinson *et al.*, 2014). There are also complementary options to insulin therapy that can assist with controlling T1DM. For instance, the amylin analogue

pramlintide is an oral hypoglycaemic medication which has been approved by the Food and Drug Administration (FDA). Pramlintide decreases glucagon secretion from pancreatic α cells, in turn lowering the rate of gastric emptying and promoting satiety: this leads to a decreased need for higher insulin doses (Chaudhury *et al.*, 2017). Despite this, even when receiving insulin replacement therapy, T1DM patients can suffer many complications (see **Section 1.4**).

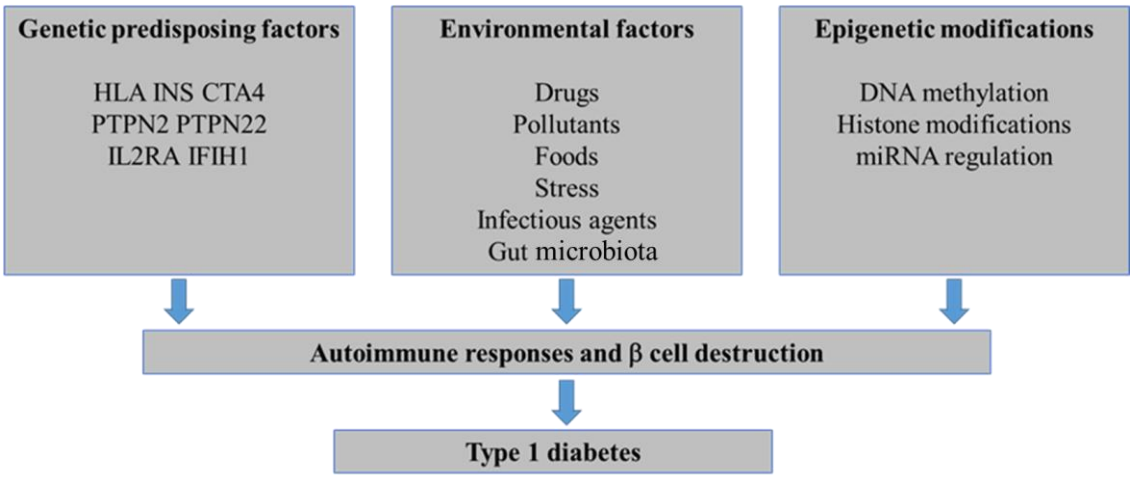

Figure 1.1 The genetic and environmental factors involved in autoimmune response and beta-cell destruction.
Taken from (Wang *et al.*, 2017).

1.3.3 Type 2 diabetes (T2DM)

In contrast to type 1, the development of type 2 diabetes is mainly caused by insulin resistance. This resistance is the result of deficient responses of insulin-dependent cells (mainly myocytes and adipocytes) to normal insulin levels (Unger & Parkin, 2010). This resistance leads the pancreatic β cells to hypersecrete insulin to sustain normal levels of blood glucose. On the other hand, β cell compensation in patients dealing with T2DM is linked to an eventual decline in their ability to secrete insulin (β cell failure) (Leahy, 2005). This points to the fact that the clinical manifestation of T2DM occurs in individuals with insulin resistance after the occurrence of β cell dysfunction (Prentki & Nolan, 2006; Campbell, 2009).

Roughly 60 – 90% of T2DM patients are obese (Muoio & Newgard, 2008), as determined by their body mass index (BMI). The BMI can be defined by the measurement of body weight and height (kg/m^2). It gives an indication of body fat levels and helps to identify an individual's risk of developing certain diseases (Eknoyan & Quetelet, 2008). WHO

states that a BMI of 25 to 30 is classed as overweight, while a number higher than 30 is obese. One of the main causes of insulin resistance is obesity or weight gain, which raises the risk of developing T2DM by over 90-fold (Anderson *et al.*, 2003). Obesity impedes insulin-mediated signalling cascades in both adipose tissue and liver through the upregulation of endoplasmic reticulum (ER) stress over a long period of time (Ozcan *et al.*, 2004). By the year 2030, approximately 366 million individuals worldwide will develop T2DM, given the escalating obesity rates (Wild *et al.*, 2004). Having said that, not all subjects diagnosed with T2DM suffer from obesity. Moreover, 40 potential susceptibility DNA loci predisposing to T2DM have been discovered, and more probably remain to be discovered (McCarthy, 2010).

When starting the management of T2DM, non-pharmacological treatment (lifestyle change) is first used, such as adjustments to diet, exercise and weight loss. These usually not only lead to improved health but also raise insulin sensitivity (Umpierre *et al.*, 2011; Tuso, 2014). With regards to pharmacological treatment for T2DM, glucose-lowering agents and insulin therapy can be used. Hypoglycaemic drugs target one or more pathways, leading to increased insulin secretion, insulin sensitivity, and the enhancement of the incretin system. Incretins are a group of metabolic hormones that are released after a meal to stimulate a decrease in blood glucose levels and augment the secretion of insulin by a blood glucose-dependent mechanism. This can occur via activation of the glucagon like peptide-1 (GLP-1) receptor, inhibition of GLP-1 degradation or interference with carbohydrate absorption (Chaudhury *et al.*, 2017). The preferred option concerning oral hypoglycaemic drugs is usually metformin to manage T2DM, unless the patient suffers from a condition which is incompatible with the drug, such as renal failure (Chatterjee *et al.*, 2017). Often, however, even the use of dual hypoglycaemic agents is not enough to keep levels of blood glucose under control, and patients may have to turn to insulin therapy (Swinnen *et al.*, 2009; Meneghini, 2009). As with T1DM patients, those with T2DM are at a risk of developing similar acute and chronic complications (Luzi *et al.*, 2007).

1.3.4 Gestational diabetes

Gestational diabetes (GDM) is a condition in which blood glucose levels are high during pregnancy. GDM affects approximately 14% of pregnancies worldwide. Women with GDM are at risk of developing pre-eclampsia, depression, and the need for a Caesarean section. Infants of mothers with poorly treated and/or untreated GDM are at risk of having

low blood sugar after birth, jaundice, stillbirth, and ultimately being overweight and developing T2DM. The majority (80%) of GDM cases include β-cell dysfunction as a result of increased insulin resistance (Buchanan & Xiang, 2005). It is believed that the dysfunction of β-cells in GDM is because of increased insulin production due to high energy consumption and insulin resistance (Pendergrass *et al*, 1995).

The classical factors that are involved in developing GDM include; overweight/obesity, excessive gestational weight gain, genetic polymorphisms, advanced maternal age, intrauterine environment (low or high birthweight), family and personal history of GDM, and other diseases of insulin resistance, such as polycystic ovarian syndrome (PCOS). Each one of these risk factors has been shown to be involved in the reduction of insulin sensitivity and/or impairment of β-cell function either directly or indirectly (Plows *et al*, 2018).

During pregnancy, the placenta produces a variety of hormones including estrogen, cortisol, and human placental lactogen in order to provide adequate nutrients and water for the fetus. These hormones can have contra-insulin effects (blocking effect on insulin). As the placenta grows, the production of these hormones increases. During normal pregnancy, the pancreas is able to produce a sufficient amount of insulin to overcome the diabetogenic effects of these hormones, but when the production of insulin is insufficient to overcome the effect of the placental hormones, gestational diabetes can lead to a number of pathophysiological changes. The pathophysiology of GDM includes distinct features such as peripheral maternal insulin resistance, inflammation, and placental and endothelial dysfunction. Insulin sensitivity declines during pregnancy leading to increase in the levels of glucose and fatty acids in order to provide extra energy to meet the needs of the fetus (Binder *et al.* 2015, Law & Zhang, 2017). Moderate inflammation is indicated during pregnancy in association with insulin resistance and GDM (Kirwan *et al.* 2002, Wolf *et al.* 2004). In early pregnancy, the secretion of pro-inflammatory cytokines has been shown to increase followed by increased insulin resistance in the third trimester, suggesting the involvement of pro-inflammatory cytokines such as TNF-α and IL-6 in the onset of insulin resistance during pregnancy (Abell *et al.* 2015). Glucose transporter 1 and 3 (GLUT-1 and GLUT-3) are both localised in the placenta. While GLUT-1 is localised in the synctiotrophoblast and involved in the uptake of glucose from the maternal circulation, GLUT-3 is localised in the endothelial cells of the placenta and is involved in the glucose transfer to the fetus (Illsley, 2000). GDM is associated with

altered placental glucose metabolism (Osmond *et al.* 2001, Jansson *et al.* 2006) and altered amino acid transport (Jansson *et al.* 2002) and lipid (Segura *et al.* 2017) concentrations. This leads to increase of the expression of GLUT-1 in trophoblasts, thus increasing glucose uptake (Gaither *et al.* 1999). The expression of GLUT-3 was also shown to increase in the placenta during GDM (Dekker Nitert *et al.* 2014), thus leading to increased glucose transmission to the fetus, hence contributing to fetal overgrowth (Nguyen-Ngo *et al.* 2019).

1.4 Diabetic complications

1.4.1 Acute complications

The inability to control blood glucose levels both over a short and long period of time means that T1DM and T2DM patients can face many complications, which in turn greatly increase their morbidity and mortality rates. Diabetic ketoacidosis (DKA), hyperglycaemic hyperosmolar state (HHS) and hypoglycaemia (as a result of inappropriate diabetic medication) are acute diabetic complications which occur often with T1DM and T2DM sufferers and are life-threatening. DKA and HHS are similar in the sense that they are both associated with severe hyperglycaemia and insulinopaenia: the level of dehydration and metabolic acidosis is the only clinical difference between them (Umpierrez & Korytkowski, 2016). Although DKA mortality occurs in less than 1% of all USA diabetics (adults and children), HHS mortality is 10-fold higher (Kitabchi *et al.*, 2009). These short-term complications can be fatal and necessitate immediate attention. However, once a treatment of intravenous fluids and insulin has been given, they are fully relieved.

1.4.2 Chronic complications

1.4.2.1 Macrovascular complications

Complications associated with suffering from diabetes over a long period of time can emerge after years or possibly decades of having the disease, and impact both the macrovasculature and microvasculature. The main macrovascular complications are cardiovascular diseases (CVD) such as atherosclerosis, myocardial infarction and strokes, as well as myocardial damage and coronary artery disease, which lead to diabetic cardiomyopathy associated with diastolic dysfunction (Forbes & Cooper, 2013). More than 50% of deaths of diabetes sufferers are caused by CVD (Laing *et al.*, 2003; Haffner *et al.*, 1998).

1.4.2.2 Microvascular complications

On the other hand, it is suggested that the development of nephropathy, neuropathy and retinopathy, the most common disastrous consequences of diabetes, are to a certain extent promoted by the *micro*vascular changes, despite the fact that the exact aetiology of these complications possibly involves multiple factors.

1.4.2.2.1 Diabetic nephropathy

Diabetic nephropathy (DN) is one of the serious complications of DM and it has been recognised as the leading cause of end-stage renal disease (ESRD), and cardiovascular morbidity and mortality worldwide (Gilbertson *et al.*, 2005). Data obtained from NHANES (Third National Health and Nutrition Examination Survey) demonstrates that approximately 35 % of diabetic patients in the United States develop DN, this occurs about 10-20 years after onset of diabetes (de Boer *et al.*, 2011). This complication is characterised by a range of changes occurring in the kidney that can be structural and functional, where the glomerular basement membrane becomes thicker and the mesangial matrix expands. This leads to a decline in the glomerular filtration rate (GFR) and microalbuminuria, which generally leads to proteinuria (Fioretto *et al.*, 2014).

The development of DN can be split into five separate stages, its progression being complicated by the fact that there are many different types of cells present in the kidney, as well as by the renal system's numerous physiological roles (Forbes & Cooper, 2013). Moreover, an individual with diabetes can develop DN despite their blood glucose levels being under control (Diabetes Control and Complications Trial Research Group, 1993). As blood glucose control alone cannot prevent DN, it can be said that other predisposing factors possibly contribute to its development. A noticeable feature of DN is an inappropriately activated renin-angiotensin system (RAS) (Huang *et al.*, 2001; Rudberg *et al.*, 2000), which leads to increased glomerular capillary pressure and hyperfiltration. In addition, impairment of renal endothelial nitric oxide synthase (eNOS) exacerbates the impact of RAS dysfunction on the renal vessels. eNOS has a potentially crucial role in the pathogenesis of DN, given that the production of glomerular and vascular nitric oxide (NO) decreases in DN (Takahashi & Harris, 2014).

Due to high cellular glucose availability and insulin-independent glucose uptake, glucose enters several pathways, such as the polyol pathway (Brownlee, 2001). These metabolic

changes have damaging effects, including the formation of advanced glycation end products, increased reactive oxygen species (ROS) and activation of protein kinase C (PKC) (Craven *et al.*, 1990; Sheetz & King, 2002; Forbes *et al.*, 2003; Wendt *et al.*, 2003). In addition, they are also associated with higher levels of pro-inflammatory cytokines, chemokines and adhesion molecules (see Chapter 5 of this thesis), along with dysregulation of transcription factors and collagen accumulation (fibrosis) in the kidneys (Wada & Makino, 2012; Reidy *et al.*, 2014).

1.4.2.2.2 Diabetic peripheral neuropathy

Diabetic peripheral neuropathy (PDN) is also a damaging microvascular complication of diabetes. Changed nerve function is common with long-term diabetes. Moreover, diabetic neuropathy contributes notably to cardiovascular disease, erectile dysfunction and diminished wound healing. This syndrome involves the peripheral nervous system's autonomic and somatic parts (Forbes & Cooper, 2013). PDN's exact aetiology is not fully known, however, it is a progressive syndrome which has been linked with vascular abnormalities such as endothelial hyperplasia, a thicker capillary basement membrane and endoneurial ischaemia (Forbes & Cooper, 2013). In serious cases, the nerve fibres are extensively damaged, resulting in the patient showing reduced sensation or altered sensation (such as increased sensitivity to pain or touch). Moreover, injuries, infections and ulceration can occur following the loss of sensation (Fowler, 2008). This can then mean that the affected area needs to be amputated, and this complication can also directly lead to death. Furthermore, 40 – 50 % of diabetics with PDN experience pain, thereby significantly decreasing quality of life (Obrosova, 2009). Orthostatic hypotension, gastroparesis and erectile dysfunction, among other issues, can also be caused by damaged autonomic nerves (Forbes & Cooper, 2013).

Research conducted with experimental animals indicated that early changes of diabetic neuropathy involve elevated polyol pathway activity, impaired Na^+, K^+-ATPase and reduced NOS activity (Sima, 2003; Sima & Sugimoto, 1999). This can result in the build-up of intra-axonal sodium and decreased endoneurial blood flow. This suggests that, at this stage of diabetic neuropathy, the structural changes which lead to altered functions and early changes could be biochemical and reversible (Li & Sima, 2004).

1.4.2.2.3 Diabetic retinopathy

Diabetic retinopathy usually develops in individuals suffering from diabetes after around 20 years, with various degrees of lesions in the retina. This is the leading cause of blindness in diabetics under 65 (Tarr *et al.*, 2013). Retinopathy can be categorized into nonproliferative and proliferative. The early nonproliferative stages involve the impairment of retinal blood vessel integrity, followed by altered vascular permeability as a result of thicker membrane basement and intramural pericyte death (Frank, 2004). On the other hand, many diabetics do not suffer from visual impairment during these stages. Diabetic retinopathy can advance towards a proliferative stage, which involves the degeneration of capillaries found in the retina as a consequence of ischaemia, in turn causing compensatory angiogenesis. Visual impairment can be caused by neovascularisation (the formation of new blood vessels) and macula oedema, as a result of fluid retention within the retina (Frank, 2004). It is thought that the development of diabetic retinopathy is due to multiple factors.

Many of these factors have also been suggested to play a part in DN, including sorbitol accumulation (polyol pathway activation), protein glycation, inappropriate PKC activity, RAS dysfunction, inflammation, oxidative stress and growth factors, most notably, vascular endothelial growth factor (Tarr *et al.*, 2013). Invasive treatments are available to reduce vision loss, such as laser photocoagulation, triamcinolone injections and more recently, vascular endothelial growth factor antagonists. Recently, the U.S. FDA approved EYLEA (aflibercept) to treat diabetic retinopathy.

In addition to retinopathy, a number of other complications have been shown to be associated with diabetes including glaucoma. Glaucoma is a neurodegenerative disorder of the optic nerve in which retinal ganglion cell (RGC) death leads to characteristic patterns of visual field loss. The most common type of glaucoma is open-angle glaucoma (in which the drainage angle for fluid within the eye remains open) and it is mainly caused by elevated intraocular pressure leading to a mechanical stress (Types of Glaucoma, 2020). Mechanical stress caused by elevated intraocular pressure is thought to take place at the lamina cribrosa (in contact with the optic nerve fibers). The optic nerve fibers form the axons of the RGCs. Mechanical stress caused by elevated intraocular pressure leads to thinning of the lamina, causing disrupted axonal transport. As a result, the RGCs undergo apoptosis along with loss of neuroretinal rim tissue of the optic disc and corresponding enlargement of the optic cup (Quigley *et al*, 1981; Song *et al*, 2016).

1.4.2.2.4 Other complications

Other complications are also linked with diabetes, such as depression (Nouwen *et al.*, 2011), dementia (Cukierman *et al.*, 2005) and impaired sexual function (Adeniyi *et al.*, 2010; Thorve *et al.*, 2011). In comparison with the general population, those suffering from diabetes have a lower life expectancy and decreased quality of life. Even when taking into account the efforts made to control blood glucose levels (with insulin), long-term complications related to diabetes cannot be fully prevented, though they can be delayed (Madsbad, 1983; Ceriello, 2005). Secondary complications as a result of diabetes affect tissues which are classically insulin independent. This indicates that it is not the lack of insulin as such, and may only partly be the presence of intracellular glucose availability in those tissues. There are alternative treatments which are still being developed to prevent secondary complications which do not necessitate blood glucose control, including proinsulin connecting peptide (C-peptide) (Section 1.4).

1.5 Anatomy of the kidney

1.5.1 Structure and function of the kidney

As the main complication of T1DM considered in this thesis is DN, it is important to consider how this relates to the structure and function of the kidney. The mammalian kidney has a number of important biological functions, mainly to filter blood and produce urine. The structure of the kidney relates closely to the function. The macroscopic structure of the kidney is composed of: the **renal capsule** forming the outside; and within the capsule two major divisions of the tissue, the outside layer which is called the **cortex** and the inside layer which is called the **medulla**. There are also the **renal pyramids** that are surrounded by the cortex. These pyramids are separated from one another by the **renal columns** that carry blood vessels to the cortex. Through the renal pyramids, the urine is carried in small tubules called **collecting ducts**. These collecting ducts run through the renal pyramids and through the **renal papilla** which is where the renal pyramids meet with the **minor calyx** which passes urine to the **major calyx**. The major calyx passes urine to the **renal pelvis** from which the urine passes to the **ureter** and then to the bladder. The blood supply to the kidney is carried through the **renal artery,** and the **renal vein** takes blood from the kidney. The renal artery, the renal vein, and the ureter enter the kidney in an area called the **hilum** which is surrounded by perinephric fat (Moinuddin & Dhanda, 2015; Fine, 1995) (Figure 1.2).

The kidneys play a big part in the removal of body wastes such as urea, ammonium, and creatinine (by excretion in the urine) and re-absorption of water, inorganic phosphate (Pi) and glucose, along with many other nutrients and metabolites. However, they are also essential for the regulation of body homeostasis, biosynthesis, catabolism, and blood pressure (Lote, 2001; Hladky & Rink, 1986). In fact, one of their main physiological functions is to maintain homeostasis of the blood plasma and electrolytes, especially sodium and potassium (Edmund Lamb, 2011), as well as synthesis of the enzyme renin, which maintains blood pressure at an appropriate level. They also synthesize important hormones such as **erythropoietin** (EPO), which stimulates bone marrow to produce red blood cells (RBC), and **calcitriol**, which is associated with calcium absorption by the gastrointestinal tract (GIT). Moreover, another major physiological function of the kidneys is the metabolism of **insulin** (both degradation and reabsorption) (Feehally *et al*., 2008; Edmund Lamb, 2011).

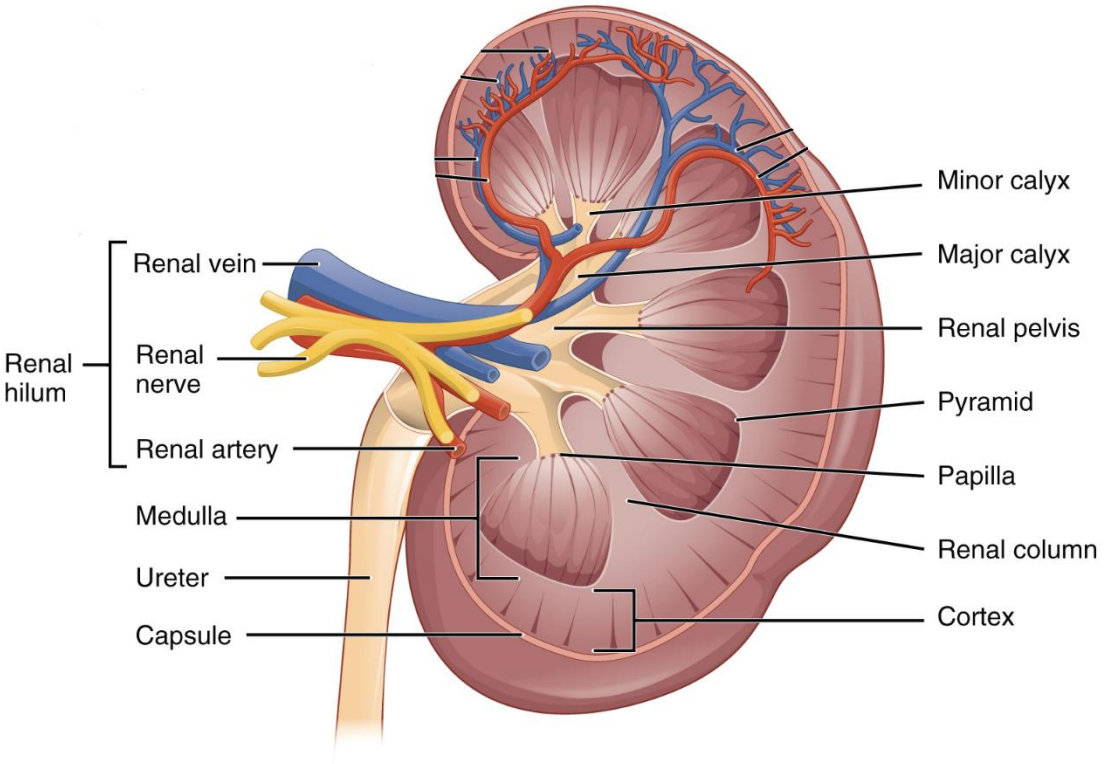

Figure 1.2 Schematic showing the inner structure of the kidney.
Picture taken from Biga et al., 2019.

1.5.2 Nephrons

The nephrons are the functional units of the kidney; occurring both within the cortex of the kidney and within the medulla. The parts in the cortex are the glomerulus, the proximal tubule, and the distal tubule, whereas the loop of Henle descends into the medulla and then back into the cortex. There are two major types of nephrons; cortical nephrons and juxtamedullary nephrons. The glomerulus is the part of the nephron in which the blood is filtered. The glomerulus is surrounded by Bowman's capsule. The blood enters the glomerulus through the afferent arteriole and exits from the efferent arteriole after being filtered by the capillaries inside the glomerulus and then the filtrate flows out through the capillary walls into the lumen of the proximal tubule (Chmielewski, 2003; Moinuddin & Dhanda, 2015) (Figure 1.3).

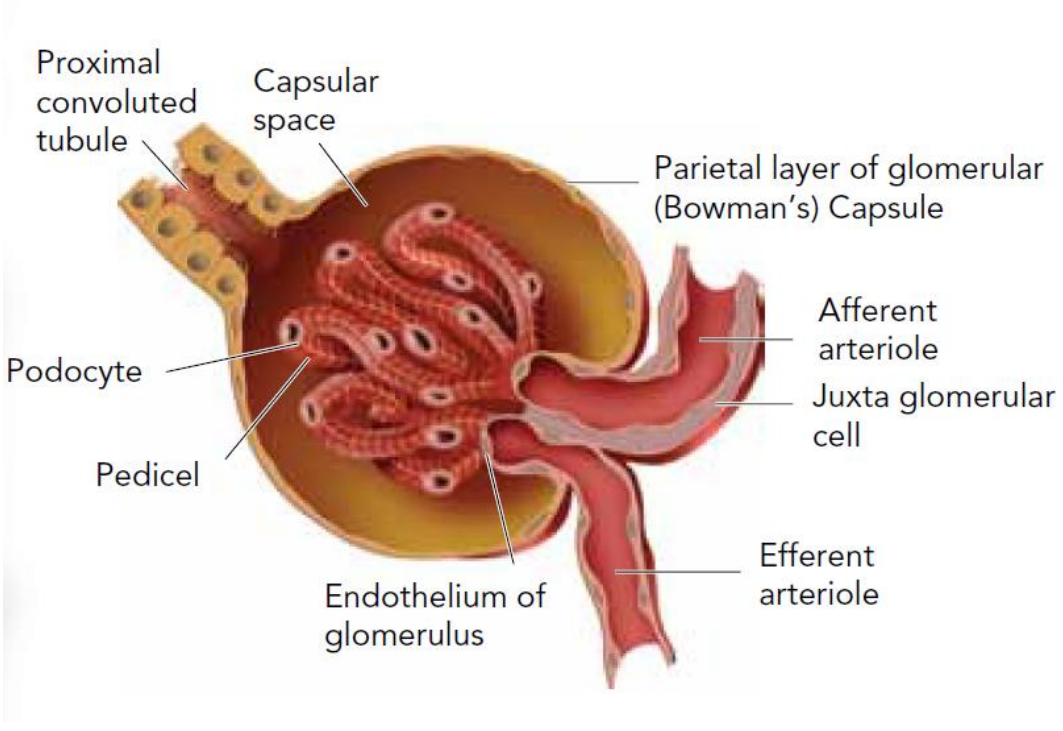

Figure 1.3 Gross structure of the glomerulus and the proximal tubule.
Taken from Serhan *et al.*, 2010.

1.5.3 The vascular endothelium

As many of the complications of T1DM are vascular and involve endothelial dysfunction, it is also important to consider the structure and function of the blood vessels, with a particular focus on the vascular endothelium. In the human body, the vascular system comprises of blood vessels which supply tissue with oxygen and nutrients and remove

metabolic waste through the blood circulation (Pugsley & Tabrizchi, 2000). These vessels are: arteries, capillaries, and veins. The vessels are made of three layers; **tunica intima** (a thin layer of endothelial cells (ECs), **tunica media** (the middle layer of the blood vessel consisting of vascular smooth muscle), and **tunica adventitia** (the external layer of the blood vessel consisting of connective tissue) (Tortora & Bryan, 2014). The cellular lining of the blood vessel is called the endothelium and it performs crucial secretory, metabolic and immune activities (Verma & Anderson, 2002). The layer of ECs has a significant role in both the normal physiology and in the pathophysiology of the vasculature, as they are located in an important position between the blood and the underlying tissue. ECs have been reported to conduct essential functions (Pearson, 2000), including modulation of inflammation, immune responses and coagulation processes. They participate in the homeostasis of the vasculature by synthesis and secretion of numerous classes of biological mediators notably vasodilators, antiproliferative and proproliferative factors, antithrombotic and prothrombotic agents, inflammatory markers, permeability factors, and angiogenesis factors (Verma & Anderson, 2002). To satisfy the specific physiological requirements of different tissues, ECs possess some structural heterogeneity. For example, the blood brain barrier is maintained by continuous endothelium, whereas the kidney glomerulus is lined by fenestrated endothelium (Cines *et al.*, 1998). ECs in different tissues are also different in other aspects such as: response to stimuli, release of mediators, and antigen presentation (Pries & Kuebler, 2006). They also exhibit diversity in phenotype according to the surrounding microenvironment. For example, when grown on lung derived extracellular matrix, aortic ECs express the lung adhesion molecule Lu-ECAM-1, whereas the same cells develop fenestrae when grown on kidney derived extracellular matrix (Cines *et al.*, 1998).

1.6 Proinsulin C-peptide

1.6.1 Background and History

Those suffering from DM are very likely to develop long-term complications, including DKD and CVD. Prior research has demonstrated that vascular complications due to diabetes cannot be fully prevented by strict glycaemic control (Section 1.4.2.2.4). Findings from said research indicate that, other than insulin deficiency, there are other factors which contribute to disease development. One possible factor is proinsulin C-peptide.

The pancreatic ß-cells are where insulin is synthesised from its precursor, proinsulin. Thereafter, proinsulin is cleaved into insulin and its connecting peptide (C-peptide). The stimulation of ß-cells by secretagogues such as D-glucose causes the release of C-peptide in conjunction with insulin. In patients with T1DM, defective or destroyed pancreatic ß-cells release a small amount, if any, of insulin and C-peptide. Although insulin is part of the treatment administered to all T1DM and some T2DM patients, C-peptide levels in patients with T1DM, and in the later stages of T2DM, are deficient (Bell & Ovalle, 2006; Wahren, J. *et al.*, 2016a).

1.6.2 C-peptide and insulin biosynthesis and secretion

In the human body, the protein preproinsulin is the precursor of insulin and C-peptide. It consists of 110 amino acids, including residues for the A- and B-chains of insulin, C-peptide and the signal peptide. The signal peptide is cleaved enzymatically in the endoplasmic reticulum (ER) of pancreatic β cells (Figure 1.4) by a signal peptidase, leaving proinsulin. The oxidation of cysteine moieties of insulin results in the formation of two inter-chain disulfide bonds between the A- and B-chain as well as one intra-chain disulfide bond within the A-chain. After this, proinsulin is translocated to the Golgi apparatus and packaged in the secretory vesicles (granules) of the pancreatic β cells. In the secretory vesicles, proinsulin is enzymatically cleaved by two very specific serine endoproteases, prohormone convertase 1/3 (PC1/3) and 2 (PC2) at site R32/E33 and at site R65/G66 respectively, leading to distinct C-peptide and insulin polypeptides (Muller & Lindberg, 1999; Zhou *et al.*, 1999). C-peptide and the B-chain of insulin are processed by another highly specific enzyme, carboxypeptidase E (CPE) (Fricker *et al.*, 1986), in order to cleave terminal basic amino acid residues, which results in mature C-peptide and insulin (Figure 1.4).

C-peptide is eventually released along with insulin in equal concentrations into the blood stream as a result of increased blood D-glucose levels. Increased extracellular glucose concentrations lead to elevated cytoplasmic glucose levels in β cells via entry through glucose transporter 2 (GLUT 2). This in turn leads to increased ATP level, causing the closure of ATP-sensitive potassium channels. The consequent occurrence of membrane depolarization and the opening of voltage-sensitive calcium channels translates into an increase in intracellular Ca^{2+} levels (Ashcroft & Rorsman, 1989), and the fusion of secretory vesicles to the plasma membrane occurs, releasing their contents by exocytosis.

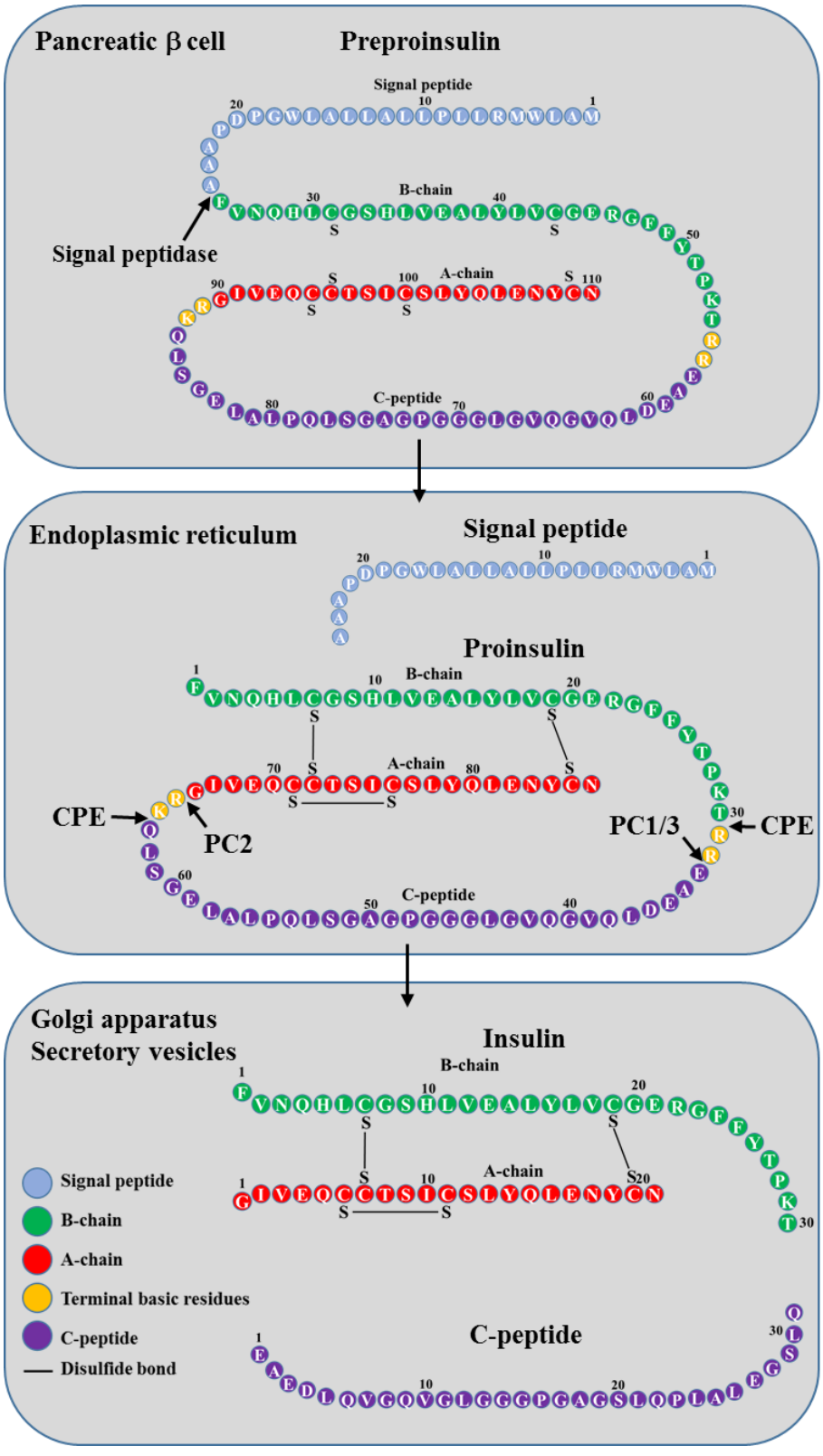

Figure 1.4 Enzymatic processing and secretion of insulin and C-peptide.
Taken from Janabi, 2017. Proinsulin is post-translationally cleaved by endopeptidase type I and II, and carboxypeptidase E, which liberates equimolar concentrations of insulin and C-peptide into the circulation (Hills and Brunskill 2009). For further details and abbreviations see text.

1.6.3 C-peptide structure

Although C-peptide is composed of only 30 – 35 residues, its amino acid sequence can greatly vary among species. In humans, this highly acidic peptide has five acidic amino acid residues, whilst it can have up to seven in other species (Wahren *et al.*, 2004). Apart from only a few species with a single basic residue, C-peptide generally does not have aromatic and basic amino acids. On the other hand, insulin chains' amino acid sequences show less variability than those of C-peptide. In certain species, rats and mice for instance, there are two distinct isoforms for C-peptide. However, 8 residues in the amino acid sequence of human C-peptide are relatively conserved among species, notably glutamic acid (E) residues at positions 1, 3, 11 and 27; glutamine (Q) residues at positions 6 and 31, and leucine (L) residues at positions 12 and 26 (Wahren *et al.*, 2004; Wahren *et al.*, 2000). The C-peptide structure's partial conservation indicates that the acidic residues (E in particular) are of importance to biological activity such as membrane interactions. In fact, the residue E27 is thought to be of particular importance with regards to C-peptide-membrane interactions (Pramanik *et al.*, 2001). Moreover, proinsulin's E59 residue is well-conserved, and its removal results in proinsulin aggregation as opposed to the usual generation of disulphide bonds and subsequent C-peptide cleavage (Chen *et al.*, 2002; Wang *et al.*, 2012).

It was previously thought that C-peptide does not have a stable secondary structure, whether in its free or insulin-attached form under physiological conditions (Weiss *et al.*, 1990). Nevertheless, findings from equilibrium denaturation studies indicate that the C-peptide structure is not a random coil; instead, its structure is ordered both when alone or within proinsulin (Brems *et al.*, 1990). The enzymatic activity of protein tyrosine phosphatase 1B (PTP-1B) is increased by the N-terminal pentapeptide (EAEDL) (Jägerbrink *et al.*, 2009). In contrast, the mid-portion of C-peptide (13 – 25), which is rich in glycine (G, 5 residues), lacks the characteristics of stable secondary structure and shows the least conservation with regards to both length and sequence across species (Henriksson *et al.*, 2005). It is thought that the middle section of the C-peptide is needed to facilitate the correct folding of proinsulin, meaning that the sequence itself does not necessitate conservation as much as length and relative flexibility of the region. Some studies have shown that the C-terminal pentapeptide (comprising residues 27 - 31 in many species) brings about a lot of the same effects as full-length C-peptide does (Rigler *et al.*, 1999; Pramanik *et al.*, 2001; Jägerbrink *et al.*, 2009; Landreh *et al.*, 2014a).

Although C-peptide's structural variability among species is sizeable, it is not exceptional in comparison with other bioactive peptides, and does not exclude hormone-like action and specific binding of C-peptide to cell membranes (Rigler *et al.*, 1999). Additionally, the extent of co-evolution (intramolecular coevolution and correlated residue substitutions) is higher between C-peptide, insulin and the insulin receptor (IR) than either proinsulin or preproinsulin, indicating that the amino acid contribution to protein structure and therefore C-peptide function is quite well conserved (Wang *et al.*, 2012).

1.7 Intracellular signalling by C-peptide

There is increasing evidence that C-peptide is a bioactive mediator (Brunskill, 2017). C-peptide works by stimulating a range of signalling pathways in different cell types. Outlined below are the intracellular pathways which are activated by C-peptide.

1.7.1 Effect on MAPK ERK1/2

ERK1/2 is an important subfamily of mitogen-activated protein kinases (MAPK) which regulates numerous cellular processes (cell growth and differentiation, for instance) by phosphorylating specific target protein substrates' serines and threonines. At physiological concentrations, C-peptide activates ERK1/2 phosphorylation in a concentration-dependent manner in the Swiss 3T3 fibroblast cell line (Kitamura *et al.*, 2001). This was decreased after pre-treatment with the G-protein inhibitor pertussis toxin (PTX) or a MAPK inhibitor. Additionally, C-peptide activates ERK1/2 in capillary ECs of mouse lungs (Kitamura *et al.*, 2002). C-peptide also induces ERK1/2 phosphorylation in rat aortic ECs, leading to a higher level of eNOS protein expression (Kitamura *et al.*, 2003). Other research demonstrated that C-peptide improved the healing of wounds in mice with diabetes and promoted human umbilical vein endothelial cells (HUVEC) migration via ERK1/2-mediated action (Lim *et al.*, 2015). In opossum proximal tubular epithelial cells (PTECs), C-peptide strongly stimulates ERK1/2 in a way that is concentration-dependent (Al-Rasheed *et al.*, 2004). Of note, PKC-dependent translocation of the small GTPase, Ras gene homolog family member A (RhoA) to the cell membrane has been implicated in the activation of one or several downstream components of the MAPK system (Wahren & Larsson, 2015).

1.7.2 Effect on Na^+, K^+-ATPase

The Na^+, K^+ pump is an electrogenic transmembrane ATPase. It is localized in the plasma membrane of the cells. For every ATP molecule consumed, Na^+ , K^+ ATPase delivers $2K^+$ into the cell in exchange for transport of 3 Na^+ out of the cell (Pivovarov *et al*, 2019). This process is important to maintain osmotic equilibrium and membrane potential in cells. It is also crucial in regulation of cell volume and cell signal transduction (Pivovarov *et al*, 2019) along with its important role in other physiological processes including active transport of solutes in the nephrons, neuronal action potential, and motility of sperms (Clausen *et al*, 2017). Abnormal expression levels or activity of the Na^+, K^+ pump are found in a number of disorders including; cardiac disease, Alzheimer's disease, chronic kidney disease, diabetes, hypertension, and in various tumors such as breast, cancer, melanoma, and bladder cancer (Khajah *et al*, 2018). Defective Na^+, K^+-ATPase activity is a common problem seen in tissues damaged by DM, and is associated with the pathogenesis of diabetic vascular complications. For example, when the tissues of rats with diabetes were investigated, altered Na^+, K^+-ATPase function was noted. Moreover, human studies conducted by Val *et al*. (2004) have shown that in RBCs of individuals suffering from diabetes, the activity of the Na^+, K^+-ATPase pump is decreased. A major reason for this is the activation of Na^+, K^+-ATPase by insulin (Sweeney & Klip, 1998). However, prior research has also indicated favourable effects for C-peptide replacement on Na^+, K^+-ATPase function. For instance, in individuals with T1DM, a significant increase in Na^+, K^+-ATPase activity of RBCs was seen after a short-term C-peptide infusion, and the magnitude of Na^+, K^+-ATPase activation significantly correlated with plasma C-peptide levels (Forst *et al.*, 2009). Moreover, *in vitro* incubation of diabetic RBCs with 6 nmol/L C-peptide was able to bring Na^+, K^+-ATPase function back to normal (Djemli-Shipkolye *et al.*, 2000).

It has also been noticed that the Na^+, K^+-ATPase pump in the renal and nervous systems of individuals suffering from T1DM is dysfunctional. Through *in vivo* and *in vitro* experiments, it has been demonstrated that reduced Na^+, K^+-ATPase in hyperglycaemic conditions can be regulated by C-peptide treatment. This has been shown with diabetic animals, where C-peptide successfully re-established Na^+, K^+-ATPase activity in renal tubule segments in a dose-dependent manner (Ohtomo *et al.*, 1996). This effect was terminated by PTX pre-treatment and linked with an increase in intracellular Ca^{2+} concentration ($[Ca^{2+}]i$). Moreover, Na^+, K^+-ATPase protein expression was elevated when PTECs were treated with 1nmol/L C-peptide when high glucose and normal glucose

concentrations were present (Galuska *et al.*, 2011). It is also known that the activation of PKC and ERK1/2 mediates this effect (Galuska et al., 2011). Furthermore, levels of neural Na^+, K^+-ATPase activity were normalised in diabetic rats after C-peptide administration (Ekberg *et al.*, 2007).

1.7.3 Effect on intracellular calcium (Ca^{2+})

Several studies have established that [Ca^{2+}] plays a part in C-peptide intracellular signalling. In rat, opossum and human PTECs, physiological amounts of C-peptide resulted in a sudden and sustained increase in [Ca^{2+}]i (Ohtomo *et al.*, 1996; Shafqat *et al.*, 2002; Al-Rasheed, *et al.*, 2004). However, pre-treating cells with PTX stopped this effect, suggesting that there is a dependency on a PTX sensitive G-protein-coupled receptor (Ohtomo *et al.*, 1996).

It is suggested that the rise in [Ca^{2+}]i levels which occurs after C-peptide stimulation is due to calcium influx across the cell membrane as opposed to a release from the intracellular stores. The addition of EDTA to the culture medium to bind extracellular calcium impaired C-peptide's effect on NO release from ECs (Wallerath *et al.*, 2003). Inhibiting components in the intracellular signalling pathway of calcium demonstrated that C-peptide's effect on renal Na^+, K^+-ATPase activity is impaired (Ohtomo *et al.*, 1996). Overall, there exists a good amount of evidence indicating that modulation of $[Ca^{2+}]_i$ is an important aspect with regards to transducing signals generated by C-peptide.

1.7.4 Effect on PI3K

The phosphatidylinositol 3-kinases (PI3Ks) are members of a distinct and conserved family of intracellular lipid kinases that phosphorylate the 3′-hydroxyl group of phosphatidylinositol and phosphoinositides. Activation of these kinases triggers a host of intracellular signalling pathways which are responsible for functions such as cell metabolism, survival and polarity, and vesicle trafficking (Engelman *et al.*, 2006). PI3K signalling pathways can be stimulated in a range of cell types with the application of C-peptide. Examples of said cells are: L6 myoblasts (Grunberger *et al.*, 2001), opossum kidney cells (Al-Rasheed *et al.*, 2004), SHSY5Y neuroblastoma cells (Li, Zhen-guo *et al.*, 2003), swiss 3T3 fibroblasts (Kitamura *et al.*, 2001), and CD4+ T-cells (Walcher *et al.*, 2006). The activation of PI3K via C-peptide is associated with certain physiological functions such as enhanced T-cell migration (Walcher *et al*., 2006), increased neuronal growth (Li *et al*., 2003), increased glycogen synthesis in skeletal muscle (Grunberger *et*

al., 2001), and increased renal tubular cell proliferation and renal PPAR-ϒ activity (Al-Rasheed *et al.*, 2004).

1.7.5 Effect on eNOS

The endothelial nitric oxide (NO) system mediates, at least in part, C-peptide's vascular effects. As has been demonstrated in several reports, C-peptide treatment enhances NO release from ECs. In accordance with this, NO liberation from bovine aortic ECs was increased in a concentration- and time-dependent manner by human C-peptide, which also led to elevation in $[Ca^{2+}]i$. However, blockade of NOS activity in these cells terminated C-peptide action (Wallerath *et al.*, 2003). Nevertheless, C-peptide did not seem to have an effect on eNOS expression or phosphorylation in the study previously mentioned. In contrast, Giebink *et al*., (2013) did not report any NO release or Ca^{2+} influx in bovine pulmonary artery ECs when administering treatment with up to 100nM human C-peptide. It should be noted, however, that almost double the control levels of NO production were reported when C-peptide-stimulated RBCs were perfused under the cultured ECs within a microfluidic device. RBC-derived ATP was put forward as an alternative indirect mechanism for NO liberation. Whereas ATP stimulates NO release from ECs by acting on its purinergic receptors (Burnstock, 2014), C-peptide stimulates NO release from HUVECs in absence of RBCs in other studies (Lim *et al.*, 2015; Bhatt *et al.*, 2013). Moreover, a study conducted by Kitamura *et al*. (2003) demonstrated that rat aortic ECs treated with human C-peptide had increased mRNA and protein levels of eNOS via ERK-dependent up-regulation of eNOS gene transcription.

1.8 Anti-inflammatory effects of C-peptide

The fact that C-peptide has anti-inflammatory effects on a range of tissues in response to multiple stimuli has been demonstrated in experimental studies on animals. For example, with non-diabetic kidney injury, C-peptide decreases the abundance of inflammatory cells in renal tissue (Chima *et al.*, 2011). Additionally, C-peptide protects the heart against damage related to ischaemia-reperfusion (Young *et al.*, 2000). C-peptide can lessen the inflammatory response caused by haemorrhagic shock in lung tissue and plasma (Chima *et al.*, 2011). As well as this, C-peptide also protects lung tissue in the event of lipopolysaccharide (LPS)-induced endotoxic shock (Vish *et al.*, 2007). Furthermore, in rat mesentery exposed to thrombin, human C-peptide lessens the vascular inflammatory response. It was also noticed that after C-peptide administration, P-selectin and ICAM-1

surface expression were inhibited on the mesenteric venules, and this effect was linked with elevated eNOS mRNA levels (Scalia *et al.*, 2000). In diabetic rats, it was found that C-peptide downregulates the inflammatory status in brain tissue (Sima *et al.*, 2009). C-peptide reduces the inflammatory response which occurs following exposure to high glucose in vascular cells. For example, C-peptide has anti-inflammatory effects on human aortic ECs which have been damaged by high glucose (Luppi *et al*, 2008). The expression of VCAM-1, and IL-8 and MCP-1 secretion, was reduced when co-treatment with C-peptide was introduced in human aortic ECs (Luppi *et al.*, 2008). Furthermore, C-peptide represses NF-κB, the pro-inflammatory nuclear transcription factor, in human SMCs exposed to a hyperglycaemic environment (Cifarelli *et al.*, 2008). Such anti-inflammatory effects of C-peptide in a rat model of T1DM are explored further in Chapter 5 of this thesis.

1.9 C-peptide receptor

1.9.1 C-peptide cell membrane interactions

Although the C-peptide is able to activate multiple signaling pathways in different tissues, the mechanism behind the C-peptide binding/interaction with the cell membrane is not well understood. A number of studies have been carried out in an attempt to identify a receptor for C-peptide. Flatt *et al.* (1986) were the first to explore this by using a radio-ligand binding technique (^{125}I-C-peptide) which showed that C-peptide binds specifically and in a displaceable manner to the cell membrane of cultured pancreatic adenoma ß-cells. A direct, non-chiral interaction of C-peptide with cell membranes has also been suggested, this interaction would depend on a specific sequence of amino acids, however, this is not likely, given the hydrophilic nature of the C-peptide molecule (Landreh *et al.*, 2014b).

Later, fluorescence correlation spectroscopy demonstrated stereospecific binding of rhodamine-labelled human C-peptide or (Rh-C-peptide) to the surface of various human cell types, such as renal tubular cells, dermal fibroblasts and ECs of saphenous vein. In these experiments, the displacement of fluorescent-labelled C-peptide occurred following administration of unlabelled full-length C-peptide, or the addition of its C-terminal pentapeptide segment. Scrambled C-peptide, insulin, IGF-I and IGF-II did not have the ability to displace labelled C-peptide from cell membranes, pointing to the specificity of the C-peptide interaction. Moreover, pre-incubating the cells with PTX greatly hindered

this binding (Rigler *et al.*, 1999), suggesting that the C-peptide receptor may be a Gαi-linked G-protein-coupled receptor (GPCR) or at least a Gαi/o-coupled receptor. According to many researchers, C-peptide binding and some downstream intracellular signalling are sensitive to PTX (Al-Rasheed, 2006; Maezawa *et al.*, 2006).

It has also been found that C-peptide is internalised across the plasma membrane. In aortic ECs and umbilical artery SMCs, internalization of AlexaFluor-labelled C-peptide results in initial localisation to early endosomes before termination at the lysosomes (Cifarelli *et al.*, 2011). Via the use of confocal microscopy and Rh-C-peptide, internalization and localisation of C-peptide to the cytoplasm and to the nucleoli of Swiss 3T3 fibroblasts and human embryonic kidney cells (HEK-293) were noted (Lindahl *et al.*, 2007). These studies' results indicate that C-peptide modulates gene transcription and triggers ribosomal RNA expression. This points to the importance of the C-peptide in terms of regulating cellular activities like cell growth and survival.

In a more recent study, a possible C-peptide receptor or a partner for the C-peptide receptor complex was uncovered by Yosten *et al*. (2013) by using deductive ligand-receptor matching. The orphan GPCR, GPR146, was found to mediate cFos mRNA expression elicited by 1 nmol/L C-peptide in HEK-293 cells, human gastric tumour cells (KATOIII) and human erythroleukemia cells (TF-1) cells. Co-localization of C-peptide and GPR146 on the plasma membrane was noted, whilst C-peptide stimulation mediated GPR146 internalisation, which agrees with general GPCR behaviour upon ligand binding (Brunskill, 2017). Moreover, according to this study, siRNA-mediated knockdown of GPR146 blocked *cFos* transcription induced by C-peptide in KATOIII cells, although this was not the case when other orphan GPCRs were tested. However, the role of GPR146 in C-peptide mediated ERK1/2 signalling has since then not been confirmed (Janabi, 2017).

1.10 G protein-coupled receptors (GPCR)

G protein-coupled receptors (GPCRs), also known as seven-transmembrane domain receptors (7TM) are the largest family of plasma membrane receptors. They are composed of seven membrane-spanning domains or transmembrane α helices connected by three extracellular loops (ECLs) and three intracellular loops (ICLs) with an extracellular N-terminus and an intracellular C-terminus. GPCRs are found only in eukaryotes, including yeast and animals. GPCR ligands include hormones, light-sensitive compounds, ions,

neurotransmitters, odours, pheromones and sensory stimuli. They involve a variety of cellular functions including metabolism, morphology, secretion, and motility (Stevens *et al*., 2013). GPCRs are activated by external stimuli leading to conformational changes in the receptor causing activation of G proteins.

1.10.1 GPCR classification

GPCRs are divided into six classes (A-F) based on their amino acid sequences and functional similarities (Hu *et al*., 2017). Class A, which is also known as the "rhodopsin-like family" is the largest group of GPCRs. This class accounts for around 80% of GPCRs and include hormone, neurotransmitter, and light receptors. It is formed of seven transmembrane helices and an eighth helix and a palmitoylated cysteine at the C terminus (Heilker *et al*., 2009; Millar *et al*., 2010). Class B, also known as the "secretin receptor family", is characterized by its relatively long N-terminal domain (120 residues stabilized by disulfide bonds) along with seven transmembrane helices. This class contains around 70 receptors including receptors for calcitonin, parathyroid hormone, vasoactive intestinal peptide, corticotropin-releasing factor and many members from the glucagon hormone family (including glucagon, GLP-1 and secretin) (Kristiansen, 2004). Class C, the glutamate family, is characterized by its large N-terminal domain, which is a ligand binding site, with around 600 residues along with seven transmembrane helices. It includes receptors like GABA receptors, calcium-sensing receptors, the metabotropic glutamate receptor family, and taste receptors (Brauner-Osborne *et al*., 2007). There are also classes D, E, and F. Class D includes fungal mating pheromone receptors. Class E includes cAMP receptors. Class F includes frizzled/taste receptors (Hu *et al*., 2017).

An alternative classification system, called "GRAFS" has identified GPCRs based on the phylogenetic tree of approximately 800 human GPCR sequences into five main families; Glutamate (G), Rhodopsin (R), Adhesion (A), Frizzled/Taste2 (F), and Secretin (S) (Fredriksson *et al*., 2003).

1.10.2 The activation of heterotrimeric G proteins

During the rest (inactive) state GPCRs are bound to a heterotrimeric G protein complex. Heterotrimeric G proteins contain three subunits α, β and γ. The α subunit (Gα) is bound to guanosine diphosphate GDP (during the inactive state) or guanosine triphosphate GTP (during the active state) which act as a switch for the activation of G-protein. β and γ subunits are associated together forming a βγ complex (Gβγ). The activated GPCR acts

as a guanine nucleotide exchange factor (GEFs). Activation of GPCRs by agonist binding results in conformational change of the receptor leading to exchange of GTP in place of GDP in the Gα sub-unit which triggers the dissociation of Gα-GTP from the Gβγ complex and from the receptor. The resultant Gα-GTP and Gβγ complex can then interact with various intracellular proteins to carry out further signalling cascades. This includes interaction with enzymes and ion channels and leads to a number of cellular functions (Hanlon and Andrew, 2015). Gα proteins are GTPases which catalyze the hydrolysis of GTP to GDP (Sowa *et al*., 2000; Magalhaes *et al*., 2012). Such activity allows Gα-GDP to rebind with the Gβγ complex to regenerate the inactive form of the G protein heterotrimer that is ready to initiate another signalling transduction cycle.

There are four main subclasses of Ga proteins: each can activate a specific type of signalling cascade. Gα(s), Gα(i), and Gα(o) all regulate the activity of adenylate cyclase. The Gα(s) subclass stimulates the activity of adenylate cyclase, while (the second subclass) Gα(i) and Gα(o) inhibit it. The third subclass is Gα(q/11) which stimulates phospholipase C (PLC) which cleaves phosphatidylinositol 4, 5-bisphosphate (PIP2) into inositol 1, 4, 5 trisphosphate (IP3) and diacylglycerol (DAG) that stimulates PKC isoforms. The fourth subclass is Gα(12/13) which stimulates the activity of Rho (Hanlon and Andrew, 2015).

1.10.3 GPCR signalling to ERK1/2

Extracellular signal-regulated kinases are common intracellular molecules that are involved in a number of cellular functions including mainly proliferation, differentiation, survival, apoptosis and stress. The ERK pathway can be activated by different stimuli including cytokines, growth factors, virus infection, and ligands for heterotrimeric G protein-coupled receptors. ERK activation is mainly initiated at the level of membrane receptors such as receptor GPCRs and receptor tyrosine kinases (RTKs). These receptors transmit signals to adaptor proteins (e.g. GRB2) and exchange factors such as SOS which then lead to activation of Ras by binding to GTP. The GTP-bound Ras then sends a signal to Rafs (Raf-1, A-Raf, and B-Raf). The activated Raf then activates mitogen-activated protein kinase kinase (MEK1 and MEK2). The activated MEK1/2 then activate ERK1/2 (Wortzel & Seger, 2011). There are several substrates that can be activated by ERK1/2 including ribosomal S6 kinase which, upon activation, can lead to the activation of several transcription factors such as CREB and c-Fos. ERK1/2 can also translocate into the nucleus and activate transcription factors including ternary complex factor (TCF) which

is a transcription factor that regulates immediate early gene (IEG) expression (Zhang & Liu, 2002). Although ERK1/2 are considered to have the same function and to be regulated in a similar manner, they actually can have cell-specific differences. Depending on the stimuli and specific signalling cascade, ERK1/2 can regulate different cellular functions such as cell proliferation, differentiation, survival and death (Wortzel & Seger, 2011). Dysfunction of ERK1/2 signaling has been shown to be associated with many human diseases, including hearing loss, cancer, asthma, stroke and Alzheimer's disease (Birkner, *et al*, 2017).

GPCRs can activate ERK1/2 by different G protein subclasses and transduce the signal by different pathways. The four classes of G protein (Gs, Gi, Gq and G12) can all regulate ERK1/2 (Goldsmith and Dhanasekaran, 2007). ERK1/2 is activated by the "Ras-Raf-MEK-ERK pathway", a pathway wherein Ras activates c-Raf, followed by mitogen-activated protein kinase kinase (MEK). The Gαi mediated activation of ERK1/2 is PTX sensitive (Pace *et al*., 1995; Mochizuki *et al*., 1999). PTX alters the function of G protein by catalysing the ADP-ribosylation of the cysteine residue on the C terminus of Gαi. This results in preventing the G protein from interacting with GPCRs. It also keeps the Gαi locked in the GDP-bound form (inactive), thus interrupting downstream signals (Burns, 1988).

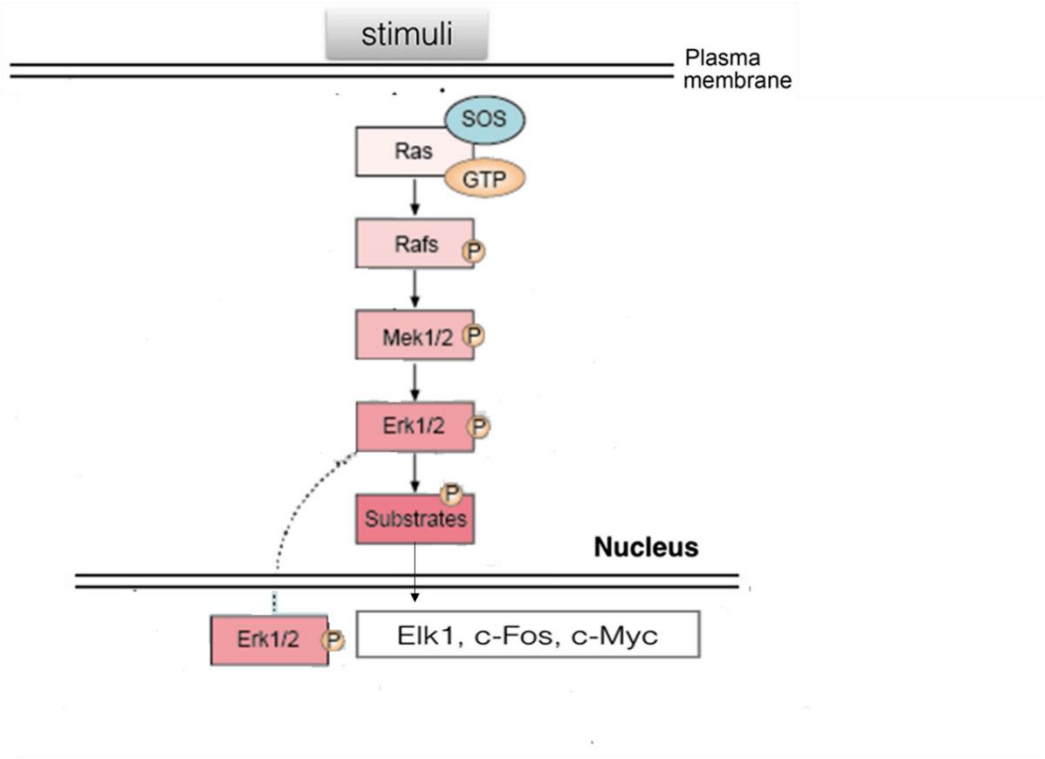

Figure 1.5 *Extracellular signal-regulated kinase 1/2 (ERK1/2) mitogen-activated protein (MAP) kinase cascade, adapted from ERK Signaling Pathway - Creative Diagnostics, 2021.*

The ERK1/2 MAP kinase, which occurs in the cytoplasm and can be translated into the nucleus, catalyzes the phosphorylation of a number of cytosolic proteins and nuclear transcription factors. A comprehensive list of ERK1/2 substrates has been reviewed elsewhere (Yang, et al, 2019).

1.10.4 GPR146

In terms of structure, GPR146 is related to GPCR Family A (rhodopsin) receptors. Given that its ligand has not yet been identified, it is classed as an orphan receptor. Human GPR146 is otherwise known as PGR8, given that it was first identified as a partial sequence of 150 amino acids in the nr (non-redundant) database (Gloriam *et al.*, 2005). Human GPR146 is a 333-amino acid polypeptide with a chromosomal location of 7p22.3 and encoded by a single exon gene (Gloriam *et al.*, 2005). GPR146 orthologs have been found in animals including mice, rats and monkeys. There is 74 % homology between the human sequence of GPR146 and rodent orthologs (Gloriam *et al.*, 2005).

The hidden Markov models (HMMs) structural prediction software of pfam in conjuction with 7TM prediction analysis were used in order to carry out an analysis of GPR146 amino acid sequence. Results demonstrated that GPR146 belongs to Family A GPCR.

This receptor does however have a fairly low amino acid identity with other GPCRs (Kelley *et al.*, 2015). Nevertheless, the fact that it is part of Family A GPCRs is clear, given that it has motif sequences which are known to be diagnostic for this family. This includes D/ERY in transmembrane helix 3 (TM3) and NPxxY at the end of TM7 represented by DHY (at the boundary of TM 3 and the second intracellular loop, as shown in Figure 1.6, yellow colour) and TPLLY (at the boundary of TM 7 and the C-terminus as show in Figure 1.6, green colour) (Gloriam *et al.*, 2005). Although these motifs are important in terms of functions and receptor stability, they are not present in the other families of GPCR such as B and C. These motifs are highly conserved in the rhodopsin family. However, numerous variations can be found in one or more substituted amino acids in this family. Similarly, these motif variants can also be present in some amine receptors, the purine receptors and melatonin receptors.

Gloraim *et al*. 2005 conducted a phylogenetic analysis which showed that GPR146 is closely related to the γ group of the rhodopsin family. BLAST searches for nine orphan GPCRs, including GPR146, revealed that chemokine receptors CMKLR2 and CXCR2 had the biggest degree of similarity to GPR146. The presence of serine- and tyrosine-linked potential phosphorylation sites (shown in red in Figure 1.6) and asparagine (N)-linked glycosylation sites (shown in purple colour in Figure 1.6) was also detected.

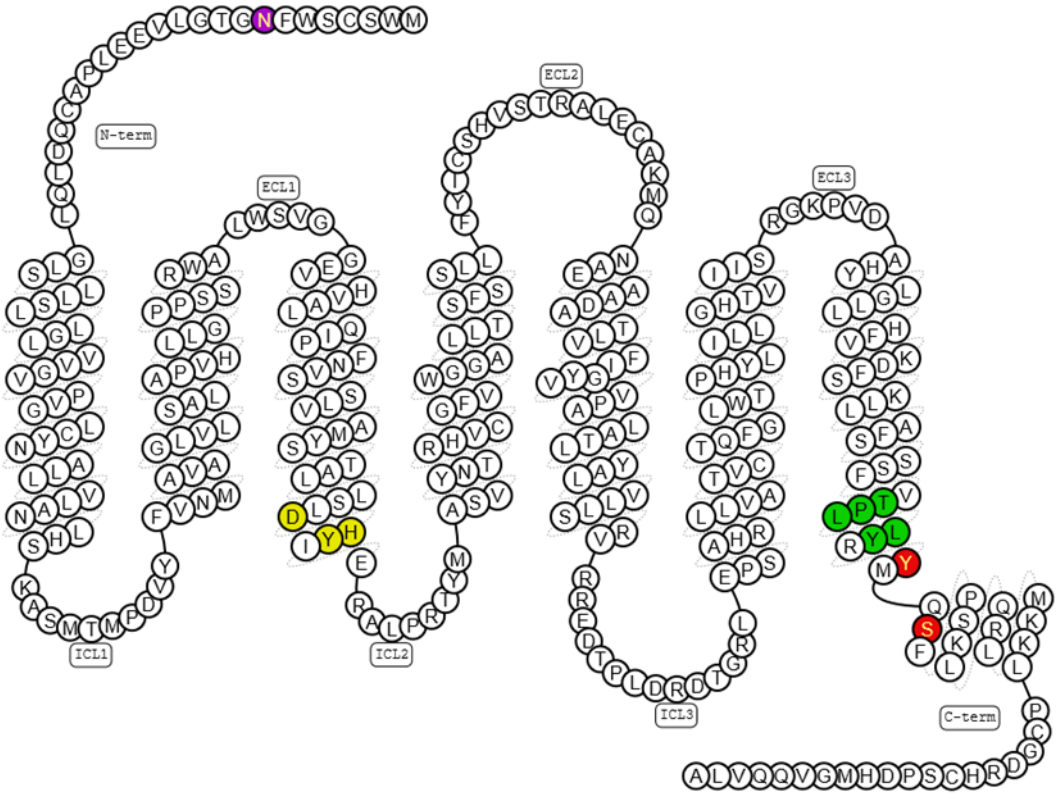

Figure 1.6 Amino acid sequence of human GPR146.
It shows seven transmembrane helices together with an extracellular C-terminus and intracellular N-terminus. Taken from the GPCR database http://gpcrdb.org/protein/.

1.11 C-peptide and diabetic kidney disease

When C-peptide was first discovered by Steiner *et al*. (1967), it was thought to be an inert by-product of insulin metabolism. At the start of the 1990s, however, the idea that C-peptide might actually be a biologically active molecule was investigated. A sizeable improvement in nerve conduction, peripheral circulation and kidney function was seen when T1DM patients were administered with physiological concentrations of C-peptide (Wahren, 2017). This then led to exploring the therapeutic possibilities of this peptide. Over the last 20 years, more evidence has been gathered which points to its beneficial effects, consistent with the molecular studies which have recorded activation of multiple signalling pathways in various tissues by C-peptide (Section 1.6 and (Hills, Brunskill 2009)). It is now seen as an active biomolecule which could be a useful tool in the fight against the development of renal and vascular (as well as other) complications in those suffering from diabetes.

1.11.1 Short-term effects in diabetic nephropathy

In order to determine whether C-peptide plays a role in protecting the kidneys, various experiments and clinical trials have been conducted. A study conducted in 1998 investigated the role of C-peptide on renal function in STZ-induced diabetic rats (see Section 1.10.2). When a human C-peptide infusion was continuously administered to the STZ-induced diabetic rats for 60 minutes, glomerular hyperfiltration and proteinuria decreased. Additionally, there was an improvement in the renal function reserve. A negative control (scrambled) C-peptide resulted in no significant difference (Sjöquist *et al.*, 1998). Similar findings have also been published, with research indicating that C-peptide is able to improve glomerular hyperfiltration to a similar extent as captopril, which is an angiotensin converting enzyme (ACE) inhibitor drug. The impact of C-peptide on blood flow was, however, lower than that of captopril. When both C-peptide and captopril were used in conjunction, no additive effects were found (Samnegård *et al.*, 2004).

1.11.2 Effects on long-term glomerular and tubulo-interstitial damage

Investigations into the effects of C-peptide administered over a long time period on the morphology and function of the kidneys has also been researched. This is important because the severity of long-term damage to the glomeruli, resulting in tubulo-interstitial damage in the rest of the kidney (in human chronic kidney disease (CKD) including DN) has been found to correlate tightly with the rate of decline of renal function assessed as the glomerular filtration rate (GFR) (Hodgkins & Schnaper, 2012). Over a two-week period, when C-peptide was intravenously infused into STZ-induced diabetic rats at physiological concentrations, glomerular hypertrophy, albuminuria and glomerular hyperfiltration were all inhibited. Alongside this, the existing renal function in the diabetic rats was maintained and a partial alleviation in the glomerular volume expansion arising from the diabetes was observed. The glomerular volume of the rats that received treatment increased by up to 23% when compared to the study controls; whereas a higher glomerular volume increase of 63% was observed in the untreated rats (Samnegård *et al.*, 2001; Huang *et al.*, 2002).

Furthermore, in STZ-induced diabetic rats, a dose-dependent decrease in the glomerular hyperfiltration rate by 40 % and a 50 % decrease in the amount of urinary albumin excreted was observed when C-peptide was administered. C-peptide had no impact on control rats (Huang *et al.*, 2002). A few years after this publication, C-peptide's benefits

with regards to improving renal function were further outlined. When STZ-induced diabetic rats were treated with C-peptide for a duration of 4 weeks, mesangial matrix expansion and glomerular hypertrophy were prevented (Samnegård *et al.*, 2005a). The impact of treating STZ-induced diabetic rats for 7 days with C-peptide on renal function was similar to the aforementioned studies. This 7-day treatment led to a decrease in microalbuminuria and reduction in the glomerular expression of type IV collagen, and the pro-fibrotic cytokine transforming growth factor-β (TGF-β) (Maezawa *et al.*, 2006b).

Studies have also performed both microperfusion and microdissection in mice and rats which were induced to be diabetic. It was found that the afferent glomerular arterioles were constricted and efferent glomerular arterioles dilated, due to the administration of C-peptide. This may provide an insight as to how C-peptides can work to reduce glomerular hyperfiltration (Nordquist *et al.*, 2008; Nordquist *et al.*, 2009). Furthermore, it has been shown that the loss of sodium from urine was lower in STZ-induced diabetic rats, which were treated with C-peptide for 4 weeks, in comparison to control rats that were not treated with C-peptide. Additionally, the C-peptide treated rats were found to have other improvements in their renal function (Rebsomen *et al.*, 2006).

A limitation on these longer-term studies in T1DM models however was that they only lasted for a few weeks, whereas very prolonged T1DM may be required in order to observe significant tubulo-interstitial damage in rats and possible effects of C-peptide on this. For this reason the effects of C-peptide administration in a 29 week rat T1DM model were investigated in the experiments described in Chapter 5 of this thesis.

1.11.3 Effects of C-peptide in clinical trials of diabetic nephropathy

Clinical trials involving patients suffering with T1DM have been conducted to elucidate how effective C-peptide is in terms of renoprotective properties. These trials assessed the effect of long- and short-term effects of administering C-peptide, along with the administration of C-peptide alone or in conjunction with insulin. C-peptide was administered to young T1DM individuals and its immediate effect was investigated by testing subjects one hour after delivery (Johansson *et al.*, 1992). There was found to be a 7 % decrease in the glomerular (hyper)-filtration rate and a 2% decrease in the renal filtration fraction from 19% to 17%. A slight increase in renal blood flow was also reported, showing the improvements in renal function. Furthermore, this research group investigated the effects of C-peptide over a longer time period (2 to 4 weeks) in T1DM

individuals presenting with hyperfiltration and microalbuminuria. Individuals who were treated with C-peptide alone had a reduction of 6 % in GFR after 2 and 4 weeks, along with a 40 % decrease in albuminuria after week 2, and a 55 % decrease in albuminuria after the fourth week. When individuals received a treatment of insulin alone, no improvements were found (Johansson *et al.*, 1993). A later study found that T1DM individuals who received an administration of both C-peptide and insulin had decreased microalbuminuria after a three-month duration (Johansson *et al.*, 2000)

The aforementioned studies correlate with findings from other research, where the diabetic renal lesions of T1DM patients who were subject to pancreas transplants were reversed (Fioretto *et al.*, 1998). Moreover, kidney and islet transplants in T1MD patients were found to have a better renal prognosis when compared to patients undergoing kidney transplants alone (Fiorina *et al.*, 2003).

Successful transplants of islets in T1DM and kidney graft patients have been linked with an improvement in microalbuminuria, restoration of Na^+, K^+-ATPase pump activity, reduction in natriuresis and better kidney graft survival rates. Therefore, it has been assumed that the beneficial effects of islet transplant are due to the fact that endogenous secretion of C-peptide as well as insulin is restored, along with the restoration of glyco-metabolic control. A retrospective study looked at 2,000 patients suffering from T2DM who were followed up after 14 years; they were found to have increased C-peptide levels in the blood, along with decreased microvascular complications. Therefore, the conclusion can be made that C-peptide therapy may also have a renoprotective role in T2DM (Bo *et al.*, 2012) although excessive levels of C-peptide that occur in some T2DM patients have been reported to be harmful owing to their pro-inflammatory effect (Vasic & Walcher, 2012). C-peptide was found to exhibit a proinflammatory effect by depositing in the intima of the vessel wall in the thoracic aorta of 21 subjects. In these subjects 77% showed infiltration of monocytes/macrophages and 57% infiltration of CD4+ lymphocytes (Marx *et al*, 2004). The effects of C-peptide on cell proliferation have been further investigated. It was found that proliferation of human and rat vascular smooth muscle cells was increased *in vitro* by high levels (10 nmol/L) of C-peptide in a concentration dependent manner (Walcher *et al*, 2006). High levels of C-peptide were also demonstrated to have an indirect proinflammatory effects in kidneys. High levels of C-peptide (10 nmol/L) were found to induce proliferation of kidney human mesangial cells in a concentration-dependent manner (Vasic & Walcher, 2012).

The manner in which C-peptide benefits and protects renal function and structural abnormalities in diabetic patients is not fully understood, though there are a few possible explanations. Firstly, it can be hypothesised that eNOS stimulation in renal capillaries may regulate intraglomerular blood pressure, thus reducing hyperfiltration and diminishing microalbuminuria (Kitamura *et al.*, 2003). A second hypothesis into the beneficial effects of C-peptide administration is the increase in Na^+, K^+-ATPase activity in glomeruli and tubular cells (Ohtomo *et al.*, 1996; Tsimaratos *et al.*, 2003). Finally, it can also be hypothesised that mitogen-activated protein kinase (MAPK) pathways and genes corresponding to the nuclear factor–κB (NF-κB) activated by C-peptide, may induce growth and tubular cell survival (Al-Rasheed *et al.*, 2004; Al-Rasheed, 2006).

1.11.4 Phosphate and limitations on C-peptide action in humans

The clinical trials outlined above provide encouraging evidence that C-peptide may have beneficial effects at least in the short-term in preventing complications of T1DM. However, even though experimental C-peptide therapy applied to rat models of diabetic neuropathy apparently led to functional improvement (Sima *et al.*, 2001); a more recent clinical trial in T1DM patients did not show any significant improvement in diabetic neuropathy (Wahren *et al.*, 2016). This implies a difference in the effectiveness of C-peptide between species. A possible explanation for a difference in potency of C-peptide between rats and humans is that there is a significant difference in the plasma concentration of inorganic phosphate (Pi) between these two species. In mammals the plasma Pi concentration correlates inversely with body mass, with the plasma Pi being relatively higher in smaller animals such as rats and mice (Sestoft, 1979). The plasma Pi concentration is about 1mM in healthy humans, but in rats it is commonly about 2 to 2.5mM (Haut *et al.*, 1980). Some intracellular signalling pathways which are known to be dependent on protein phosphorylation in mammalian cells have been shown to be disturbed if the extracellular Pi concentration is elevated from 1 to 2.5mM (Abbasian *et al.*, 2015). Such disturbance can include enhanced phosphorylation of ERK1/2 (Cargnello & Roux, 2011) which (as discussed above) are key mediators of C-peptide action.

As Pi may amplify some protein phosphorylation signals in mammalian cells by inhibiting phosphoprotein phosphatases (Abbasian *et al.*, 2015) it is possible that Pi can also amplify certain functional effects of hormones which signal through protein phosphorylation. There is some evidence that this might be true for insulin signalling

(Nowicki *et al.*, 1996; Lu *et al.*, 2001) and in principle this might also be true for C-peptide signalling to ERK1/2 phosphorylation. As both C-peptide and Pi can signal through ERK, this might mean that in rats the higher plasma Pi concentration might amplify the signal from C-peptide to P-ERK, giving effects that are stronger than those observed with the lower plasma Pi concentration that is found in humans.

1.12 Background physiology of inorganic phosphate (Pi)

Phosphorous is a key mineral in living organisms. It is the second most abundant mineral in humans. Phosphate metabolites such as ATP, DNA, phospholipids and phosphoproteins are present within the human body, and play an essential role in cellular metabolism and structure. In the case of mammals, inorganic phosphorus is present as free phosphate ions, as either HPO_4^{2-} or $H_2PO_4^-$ (Werner *et al.*, 1998; Phillips *et al.*, 2009; Bansal, 1990). In solution, free phosphates are referred to as inorganic phosphate (Pi).

The homeostatic control of Pi is performed via the transport of Pi through the kidney's proximal tubular epithelial cells (PTECs). Transportation of Pi through the PTECs' brush border membranes from glomerular ultrafiltrate is reliant on Na^+-dependent transporters i.e. this transportation is dependent on sodium being present in the extracellular fluid. The Na^+-dependent transporters are either from the SLC20 gene family (SLC20A1 or PiT1; and SLC20A2 or PiT2) or SLC34 gene family (SLC34A1 or NaPi-IIa; and SLC34A3 or NaPI-IIc) (Forster *et al.*, 2006). In contrast the movement of Pi between the basolateral side of the epithelial cells and the cytosol of these cells is mediated by the Na^+-*in*dependent transporters of the SLC53 gene family (SLC53A1 or XPR1) (Ansermet *et al.*, 2017).

Less than 1% of the total phosphorous present in the human body is in the plasma. Despite the percentage of plasma Pi being relatively low, it is essential for cellular processes as this pool of Pi is in equilibrium with the Pi present in the extracellular fluid and also influences the Pi concentration inside cells. The aforementioned transporters present in the PTECs control and regulate the amount of Pi present in plasma. Any excess Pi from dietary consumption is normally removed by the kidneys and excreted in urine. Individuals who suffer from kidney failure, such as CKD patients (including those with advanced DN), therefore fail to excrete excess Pi from their diet, and have higher levels of Pi present in their plasma (Abbasian *et al.*, 2015).

Cellular signaling pathways are influenced by Pi ions, as they can act as signaling molecules (Michigami, 2013). Therefore, an increased amount of plasma Pi can result in enhanced entry of Pi into cells and lead to the disruption of signaling pathways. For example in vascular endothelial cells such disruption can cause the release of pro-coagulant endothelial microparticles, which can subsequently increase the risk of cardiovascular related mortality in CKD patients (Abbasian *et al.*, 2015).

1.12.1 Extracellular Pi as a signaling molecule

Pi has a key role in regulating the metabolism of intracellular energy as well as cell signalling. (Bevington *et al.*, 1992; Buzalaf *et al.*, 1998; Szajerka & Kwiatkowska, 1984; Zhang & VanEtten, 1991). Such signals require the presence of Pi sensors to detect extracellular Pi concentration. It has been suggested (Bevington *et al.*, 1992) that Pi directly modulates the activity of some **enzymes** and **signalling proteins**. These Pi responsive enzymes possess important biological activities including, anaerobic glycolysis, modulation of oxygen transport, ion transport, phospho-protein turnover, muscle contraction, gluconeogenesis, and mitochondrial, glycogen, glutamine, purine nucleotide, and nucleic acid metabolism (Bevington *et al.*, 1992). Of particular importance is the fact that Pi has been shown to exhibit inhibitory effects on protein-tyrosine phosphatases and serine/threonine phosphatases (Adam *et al.*, 2004; Rath *et al.*, 1995; Buzalaf *et al.*, 1998; Zhang & VanEtten, 1991). It has also been shown that Pi can inhibit the activity of phosphoprotein phosphatases (PPP) I and II (Khandelwal & Kamani, 1980).

In addition to such intracellular effects of Pi, a recent study has suggested that Pi does not have to be transported into the cell to induce its effect. In their study Bon *et al*, have shown that Pi can signal to ERK1/2 in murine preosteoblastic MC3T3-E1 cells through heterodimerization of the high-affinity sodium-dependent Pi transporters PiT1/Slc20a1 and PiT2/Slc20a2 (Bon *et al.*, 2018). Extracellular Pi is thought to bind to this heterodimer and signal to ERK1/2 independent of Pi transport into the cell.

1.12.2 Using Pi analogues as probes for Pi sensing

Pi analogues; vanadate (Vi) (also known as orthovanadate), phosphite (Phi) and hypophosphite (HPhi) (Figure *1.7*) are structurally and chemically similar to Pi. They also possess stability within the cell i.e. they cannot be metabolized. However, they are able to mimic the action of Pi in terms of binding to proteins. For example vanadate is

commonly used as a protein tyrosine phosphatase (PTP) inhibitor. Hence, it was previously used to mimic the action of insulin by promoting insulin-dependent tyrosine phosphorylation events (Lu *et al.*, 2001). Vanadate does not become metabolized within the cell, yet it can bind to regulatory sites on enzymes such as protein tyrosine phosphatases (PTP1B) (Huyer *et al.*, 1997). Although the effect of phosphite and hypophosphite in mammalian cells is not well understood, phosphite has been shown to mimic the effect of Pi in plants (Varadarajan *et al.*, 2002).

There is a possibility that Pi induces its biological effects on cells (and possible modulatory effects on C-peptide action) either because it becomes metabolized and converted into organic phosphates, or because it binds non-covalently to regulatory proteins. In the experiments described in Chapter 4 of this thesis, non-metabolisable Pi analogies (Figure 1.6) were used to distinguish these two possibilities.

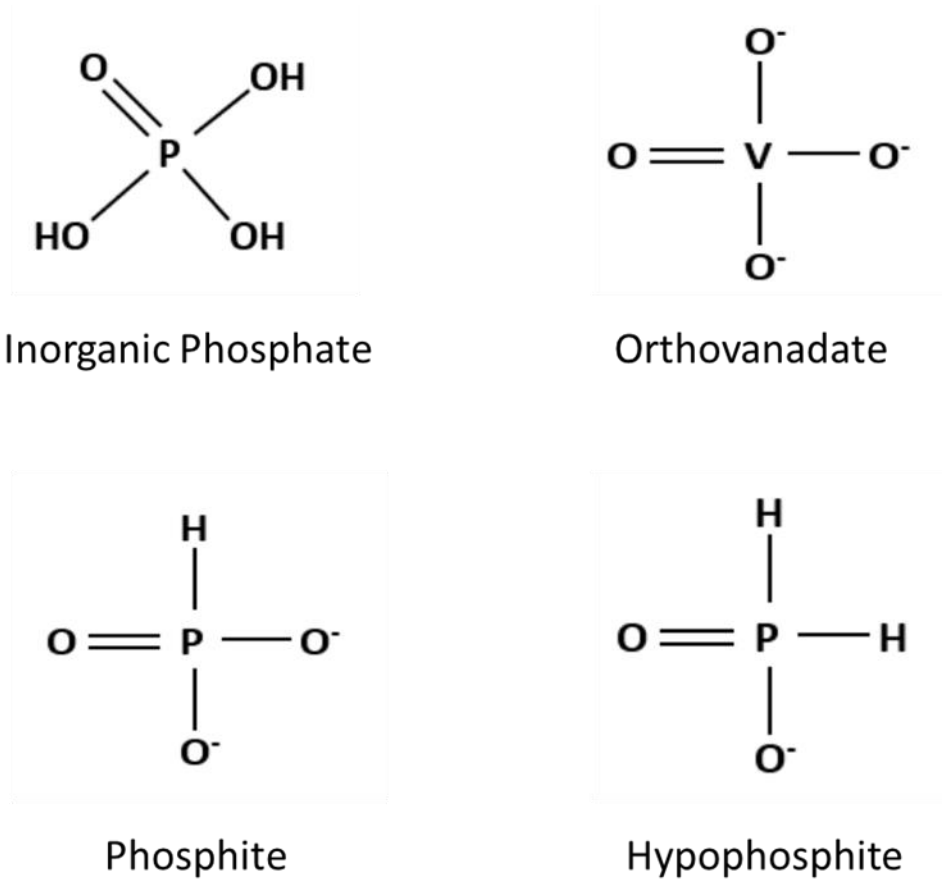

Figure *1.*7 The structure of inorganic phosphate (Pi) in comparison with its structural analogues.

1.13 Experimental models

As the main focus of this thesis is the potential role of C-peptide in DN (especially inflammatory tubulo-interstitial disease) and its possible modulation by Pi, models were required to study mechanisms relevant to DN and C-peptide action both *in vitro* and *in vivo*.

1.13.1 Choice of cell culture models

Two renal cell lines were utilized to carry out experimentation outlined in this project: TERT/1 (Crean *et al.*, 2015) and HEK293A (Simmons, 1990; Thermo-Fisher 2016). RPTEC/ TERT/1 cells have been shown to maintain morphological and functional characteristics like dome formation, sodium dependent phosphate uptake and sustaining genomic stability for up to 90 passages. These cells are a useful system for cell biology, drug screening, toxicology, and tissue engineering (Crean *et al.*, 2015). HEK293A cells are a sub-clone of HEK293 and have a flat morphology and better adherence to culture vessels than is the case for the parent HEK293 cell line. They grow rapidly and are easily transfected but show few of the differentiated characteristics of human proximal tubular epithelial cells.

1.13.2 Experimental animal models of T1DM

There is a variety of animal models for performing diabetic studies and each model is meant to represent certain aspects of the disease. Depending on the purpose of the research, whether it is pathogenesis of DM or testing a new therapeutic method, the choice of the model varies. To study the auto-immune aspect of T1DM, models of spontaneous or transgenic DM are commonly used (King & Bowe, 2016). For therapeutic methods studies, however, diabetogenic agents that destroy β-cells by non-immunological mechanisms (such as streptozotocin (STZ) and alloxan), are used to induce DM (King & Bowe, 2016). Both agents enter β-cells via glucose transporter-2 (GLUT-2) (Islam & Wilson, 2012; Lenzen, 2008). Alloxan promotes cell death as a result of ROS generation. However, alloxan has low efficacy compared to STZ: it also causes direct adverse effects on the liver and kidney (Islam & Wilson, 2012). STZ is commonly considered as the agent of choice for the DM induction in animals due its ability to produce stable long-term hyperglycaemia (Lenzen, 2008). A single injection of STZ is enough to produce irreversible damage to cellular DNA by alkylation. STZ selectively destroys β-cells as a

result of their high expression of GLUT-2 (Lenzen, 2008) and this model was used in the long-term rat study that is described in Chapter 5 of this thesis.

1.14 Aims and hypothesis in this project

The overall aim of the experimental work described in this thesis was to investigate the regulation of the anti-inflammatory effects of C-peptide in kidney by testing two related hypotheses:

1) That an elevated extracellular Pi concentration enhances the effectiveness of C-peptide in signalling to ERK1/2 in proximal tubular epithelial cells *in vitro.*
2) That in the relatively hyperphosphataemic environment of a rat, using a prolonged (29 week) STZ model of T1DM, C-peptide administration suppresses complications of T1DM, demonstrated by suppression of markers of inflammation and fibrosis in kidney tissue and in plasma.

The specific experimental objectives were as follows:

In Chapter 3

1) To determine by immunoblotting for the phospho-activated form of ERK1/2 whether this could be used as a convenient read-out of intracellular response to C-peptide in HEK-293A and hTERT cells
2) To investigate whether these cell lines could be used to assess the possible role of GPR146 in C-peptide signalling (a) by investigating the effect of C-peptide on GPR146 expression, and (b) by attempting to over-express GPR146 by transfection of these cells with a plasmid incorporating human GPR146 cDNA.

In Chapter 4

To investigate the effect of an extracellular Pi load on the phosphorylation of ERK1/2 and whether it enhances the ERK1/2 response to C-peptide in TERT/1 and HEK293A cells.

In Chapter 5

1) To confirm in a prolonged (29 week) rat STZ model of T1D the inflammatory and fibrotic effects of DM that have been reported previously (Section 1.7), and

2) To investigate the effect of prolonged C-peptide treatment on the following parameters in the diabetic animals:

- Chemo-attractants and immune cell recruitment and adhesion
- Inflammatory cytokines
- TGF-β and renal fibrosis

Overall:

To test the hypothesis that C-peptide is a beneficial anti-inflammatory and anti-fibrotic therapy potentially of value in suppressing diabetic nephropathy.

2 Chapter 2 Materials and Methods

2.1 Materials

Plastic sterile consumables for tissue culture were purchased as follows; 25 cm^2 and 75 cm^2 flasks and 22 mm diameter 12-well plates were purchased from Corning Costar, Petri dishes and 35 mm diameter 6-wells were purchased from Thermo Scientific. All the reagents and chemicals used, including the molecular grade reagents, were purchased form Sigma-Aldrich, unless otherwise stated. Growth media and supplements for tissue culture were from Gibco™ Life Technologies (Paisley, UK).

2.2 Tissue Culture

2.2.1 Cell lines

Immortalized human proximal tubular epithelial cell line (RPTEC, TERT/1) (Figure 2.1 A) (LGC ref. ATCC® ACS-4007™) was obtained from LGC Promochem – ATCC, UK). The human embryonic kidney cell line (HEK293A) (Figure 2.1 B) (LGC ref. ATCC® CRL-1573™) was a kind gift from Dr Terry Herbert (Department of Cell Physiology and Pharmacology, University of Leicester, UK).

2.2.2 Cell culture procedure

Both cell lines were cultured between passages 3 and 20 to minimize morphological and phenotypic variations that might result from prolonged serial -passaging.

TERT/1 cells were grown in a serum-free defined medium comprising DMEM / Nutrient Mixture Ham's F-12 (D6421, Gibco™) supplemented with 5pM tri-iodo-L-thyronine (Sigma-Aldrich® 6397), 10ngml^{-1} recombinant human EGF (E9614, Sigma-Aldrich®), 3.5 µg ml^{-1} ascorbic acid (A4403, Sigma-Aldrich®), 5µg ml^{-1} human transferrin (T2036, Sigma-Aldrich®), 5µg ml^{-1} insulin (I6634, Sigma-Aldrich®), 25ng ml^{-1} prostaglandin E1 (P8908, Sigma-Aldrich®), 25ng ml^{-1} hydrocortisone (HD135, Sigma-Aldrich®), 8.65 ng ml^{-1} sodium selenite (S5261, Sigma-Aldrich®), 1.2g L^{-1} sodium bicarbonate ($NaHCO_3$) (S8761, Sigma-Aldrich®), 0.1ng ml^{-1} G418 (ant-gn-5, Invitrogen™), penicillin (10,000 units per ml) + streptomycin (10 mg ml^{-1}) (15140-122, Gibco®), and 2mM L-glutamine (25030-024, Gibco®).

HEK293A cells were grown in a DMEM medium with high glucose (Sigma D6429) supplemented with 100 U / ml penicillin G, 100 µg/ml streptomycin and 10 % v/v heat inactivated foetal bovine serum (FBS).

For propagation and maintenance of stock, both cell lines were plated at a density of 10 x 10^4 cells per 9cm Petri dish, and were passaged when 70-80% confluent. For experiments, they were plated at density of 25 x 10^4 cells / 3.5 cm 6-well in 2ml of growth medium.

Both cell lines were grown in a culture incubator at 37°C with humidified air, 5% CO_2. For passaging, the growth medium (GM) was aspirated and each vessel was rinsed with 5ml of (1x) Hank's balanced salt solution (HBSS, Life Technologies-1754651) and then incubated with 2ml of (1x) trypsin-EDTA (T/E) (Invitrogen 25300) for 5 min at 37°C in the culture incubator to detach the cells from the plastic vessel. The cells were then re-suspended in 10 ml of the GM and centrifuged at 500g for 5 minutes. After centrifugation, the supernatant was discarded, the cell pellet was re-suspended in another 10 ml of GM, and the suspension counted using a haemocytometer and plated at the cell densities described above.

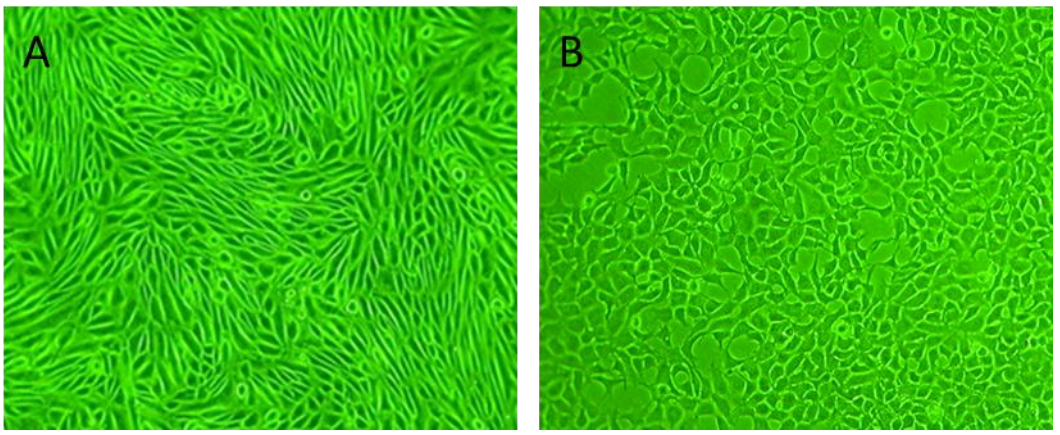

Figure 2.1 Phase contrast images of human renal cell lines used in this project.
(A) TERT/1 cells and (B) HEK293A cells after 3 days in culture in their respective growth media. (x200 magnification)

2.2.3 Retrieving frozen cells

A cryotube containing 1 ml of frozen cell suspension was taken out from liquid nitrogen and incubated at room temperature for 5 minutes to allow the liquid nitrogen to evaporate.

The cell suspension was then rapidly dipped in a 37^0C water bath, transferred to a 30ml universal tube containing 10 ml of GM, which had been pre-warmed in a humidified 37ºC incubator under 5% CO_2, and spun down on a centrifuge at 200g for 5 min. The supernatant was then aspirated and the re-suspended cells were transferred to a 9cm diameter Petri (for HEK293A cells) or T75 flask (for TERT/1 cells) containing pre-warmed complete GM.

2.2.4 Collagen coating plates for HEK293A cells

To enhance HEK293A attachment to plastic plates, collagen coated plates were used for all HEK293A cells experiments. Bovine (calf skin) collagen, type I (1mg/ml or 0.1% w/v stock in 0.1M acetic acid) (Sigma C8919) was used to coat the 6-well plates. The collagen stock solution was diluted in sterile 0.1 M acetic acid to 50µg/ml before use and applied at a concentration of 5µg/cm^2. The culture plates were left in the culture hood with the lid off overnight to dry out the collagen solution. The following morning, they were rinsed thrice with 0.40 ml HBSS per 2.2 cm well to remove any residual acetic acid, then the plates were securely sealed and kept at 4°C.

2.2.5 Cell treatments

Minimum essential medium (MEM) (21090, Life Technologies) supplemented with 2 mM L-glutamine, penicillin (100 IU / ml) and streptomycin (100 µg / ml) was used in all experimental incubations. An additional 4.6ml of 7.5% w/v $NaHCO_3$ per 500ml of culture medium was added in all experiments to bring the pH of the media to 7.4. TERT/1 and HEK293A were grown to 80% confluence in 6-well plates, and then the desired experimentally modifed MEM was added to the cultures after discarding the previous medium. (Further specific details of cell treatments are explained in the figure legends of Chapters 3, 4 and 5 below). To achieve quiescence of the cells and to remove endogenous C-peptide from serum in the GM, experiments were preceded by overnight serum-free MEM incubation.

Synthetic human C-peptide (ref CCP1163, Cohesion, Generon) dissolved in sterile 0.9% w/v NaCl was used to stimulate TERT/1 and HEK293A cells. In studies that involved high inorganic phosphate (Pi) treatment, the Pi stock solution was prepared by using $NaH_2PO_4.2H_2O$ (ref 71505, Sigma). The stock solution was added to MEM in sufficient amount to raise the Pi concentration of the medium from 1mM Pi (the original Pi concentration in MEM) to 2.5mM, to mimic conditions described (Abbasian *et al*., 2015).

For experiments investigating the effect of Na^+ deprivation, the control medium was HEPES-buffered saline (HBS) pH 7.4 made as shown in Table 2.1 and the Na^+ deprivation medium was HBS in which the NaCl was replaced by equimolar choline chloride. Pi was added to the medium in the form of NaH_2PO_4 (or KH_2PO_4 for Na^+ deprivation experiments). Plates were then incubated at 37ºC for 90 minutes. At the end of the 90 min incubation, the cell monolayer was rinsed with ice-cold 0.9% w/v NaCl, and 150µl of 0.3 M perchloric acid (PCA) was then added to each well. The cell monolayer was scraped in the acid with a rubber policeman and transferred to a 1.5ml microcentrifuge tube on ice. The tubes were then left on ice for 30 min to allow protein to precipitate followed by microcentrifugation at 3000rpm with a 7cm radius rotor for 10min 4^0C. The supernatant was then transferred to fresh tubes and 2µl of Universal pH indicator (Acros Organics 422435000) was added to each 100µl of supernatant. The resulting red PCA extract was then neutralized by titrating with a volume of 4.3M KOH / 0.6M imidazole sufficient to turn the universal indicator yellow-green (i.e. ~ pH 7). The neutralised perchlorate extract was then stored at -80^0C.

At the end of other experimental incubations, test media were removed and cell monolayers were either lysed for Western blotting (Section 2.3) or scraped with perchloric acid (PCA) for protein determination with the Lowry protein assay (Section 2.5).

Component	**Formula Weight**	**Weight (g)**	**Concentration (mM) when made up to 1L**
NaCl	58.44	8.1816	140
HEPES Acid	238.3	4.7660	20
$MgSO_4.7H_2O$	246.5	0.6163	2.5
KCl	74.55	0.3728	5.0
$CaCl_2.2H_2O$	147.02	0.1470	1.0
Phenol Red	----------	0.010g	10mg/L

Table** 2.1 **Composition of HEPES-buffered saline (HBS)

2.3 Western blotting

2.3.1 Cell stimulation and sample preparation

After incubation with experimental test media (Section 2.2.5) for the required time, the culture plates were immediately put on ice and then the test medium was removed. The monolayer was then washed once with HBSS (1ml) and scraped in 110µl of pre-chilled Lysis buffer (Appendix 1). Each lysate was then transferred to a pre-chilled 1.5ml micro centrifuge tube and centrifuged on a refrigerated micro centrifuge at 13,000rpm for 10 minutes at 4°C to remove insoluble debris. In order to determine the sufficient amount of cell lysate required to load 20µg of protein, a Bio-Rad DC protein assay was performed (Section 2.4). The required amount of cell lysate was then mixed with an equal amount of SDS-reducing sample buffer (Appendix 2) and heated on a heating block (Grant QBT2) at 100°C for 5 minutes.

2.3.2 Sodium dodecyl sulphate polyacrylamide gel electrophoresis (SDS-PAGE)

To separate the proteins in cell lysates (Section 2.2.5) gel electrophoresis was performed. Laemmli resolving gels of 10% acrylamide were prepared and cast in-between glass plates (Mini-PROTEAN®, Bio-Rad Laboratories, Hemel Hempstead, UK) then covered with isopropanol to obtain a uniform gel edge. The resolving gel was then left for 30 min to set and the isopropanol was washed out with water. The stacking gel (10 %) (Appendix 3) was then prepared and poured over the resoling gel followed by a well-forming comb. The gels were then placed in an electrophoresis tank containing running buffer (Appendix 4). Samples (Section 2.3.1) were loaded into the sample wells; except the first well which was loaded with molecular weight standards (Full-Range Rainbow MW Markers 10 - 250 kDa, Fisher Ref 11580684). The electrophoresis was run on a Bio-Rad Mini-Protean® system using a POWER PAC 300 (Bio-Rad, Hemel Hempestead, UK) at a voltage of 200V until the bromophenol blue dye front reached the end of the resolving gel.

2.3.3 Immunoblotting

After protein separation by SDS-PAGE, a wet transfer was performed onto a 0.45 µm nitrocellulose membrane (Fisher Ref 10773485) by using cool (4°C) transfer buffer (Appendix 4) at 100volts for one hour with continuous stirring. An ice block was used to keep the transfer cool. Membranes were then washed with 10 ml of x1 Tris-buffered saline with 0.5% Tween 20 (TTBS) three times for 5 minutes each time, and blocked with 5% w/v milk powder in x1 TTBS for one hour with continuous rocking to minimize

nonspecific binding; followed by three washes with 10 ml of x1 TTBS for 5 min. At the end of the third time of washing, the membranes were incubated overnight at 4°C on a rocker with the primary antibodies (Table 2.2). After incubation with the primary antibody, membranes were washed for three further washes with x1 TTBS, then secondary antibodies were applied and incubated for one hour at room temperature to detect the primary antibody. The membranes were then washed with 10 ml of x1 TTBS three more times, 10 minutes each. ECL reagent (Thermo Scientific-34080) was then applied for chemiluminescence generation. The fluorescence was detected on ChemiDoc™ Touch Imaging System. To confirm the size of the proteins of interest, bands were compared with molecular the weight standards ladder.

Primary antibody	***Dilution with 1xTTBS***	***Secondary antibody***	***Supplier and ref number of primary antibodies***
a) Antibodies used for functional assays			
Phospho – P44/42 ERK1/2 (Thr202/Tyr 204)	1:1000	1: 1000 Goat anti-rabbit (Dako, refP0448)- Affinity purified antibody	Cell Signalling, Ref # 91015
b) Antibodies used for loading controls			
P42MAP Kinase (ERK2) antibody	1:1000 1:2000	1:2000 Goat anti Rabbit (Dako P0448)- affinity purified antibody	Cell Signalling, Ref # 91085
β actin	1:10000	1:2000 Rabbit anti mouse (Dako-P0260)	Sigma (Clone AC-40), ref A4700

Table 2.2 Details of antibodies used in this project

2.3.4 Data Analysis and Band Quantification

Digital images of the membrane were taken on ChemiDoc™ Touch Imaging System and quantified by using Image Lab TM software. Densitometry data are presented as the ratio of

the intensity for the protein of interest/housekeeping protein, expressed as a % of the corresponding ratio under control conditions.

2.4 Bio-Rad detergent-compatible (DC) protein assay

To measure the protein content of cell lysate for Western blotting, a Bio-Rad detergent-compatible (DC) protein assay kit (Bio-Rad 500-0113) was used. 5µl of cell lysate or standards (0-2000 µg/ml BSA in 1% IGEPAL detergent) was added to 96 well plates in triplicate and 25 µl of kit Reagent A (an alkaline copper tartrate solution), then supplementary reagent S was added in 1:50 volume ratio to reagent A, followed by 200µl of Reagent B a diluted Folin-like reagent, and incubated for 15 min at room temperature. The absorbance after that was read at 750nm.

2.5 Lowry protein assay

At the end of cell stimulation with test media, cells were washed thrice with ice cold 0.9% w/v NaCl and scraped in 150 µl of 0.3M PCA, then centrifuged at 3000 g at 4°C for 10 minutes in a microcentrifuge to sediment the precipitated protein content. Cell monolayers precipitated in PCA were then dissolved in 200 µl of 0.5M NaOH followed by heating to 70°C for 30 minutes in a water bath. The Folin method of Lowry *et al* (1951) was performed to determine the protein content of the cell monolayer. The NaOH digest was further diluted with 0.5M NaOH then standards were prepared form BSA at final concentrations of 0, 50, 100, 150, 200, 300, 400, 500, and 600 µg/ml. To prepare reagent C, Lowry reagents A and B were mixed at 50:1 volume ratio then 50 µl of the NaOH digest and standards were loaded into 3ml tubes and mixed with 600 µl of reagent C and vortexed thoroughly, and incubated for 10 minutes. Then Folin-Ciocalteu reagent (FCR) (Sigma F-9252) was freshly diluted 1 in 4 with water and added to each tube, vortexed and incubated for a further 30 minutes at room temperature. 300 µl of the final mixture was transferred into a 96-well plate and absorbance was read at 600nm using a microplate reader (Labtech LT-4500).

2.6 Selective Pi assay

To avoid interference from organic phosphate compounds in cell extracts such as ATP, inorganic phosphate (Pi) was assayed by converting Pi into phosphomolybdate which was then rapidly separated from organic phosphates by solvent extraction. Neutralized PCA cell extracts (Section 2.2.5) were rapidly centrifuged by pulsing on a microcentrifuge to sediment precipitated potassium perchlorate. Then 145µl of the clear yellow-green supernatant (or Pi standards prepared from NaH_2PO_4 at final concentrations of 0, 0.01, 0.02, 0.03, 0.04, 0.05mM) were loaded into fresh 1.5ml tubes on ice. Then 655µl of ultra-pure water and 200µl of acidified ammonium molybdate were mixed with 200µl of a 4:1 vol/vol mixture of isobutanol/petroleum ether (IBPE) (made by mixing 400ml of 2-methylpropan-1-ol (isobutanol, BDH 10062 AnalaR) and 100ml of petroleum spirit (petroleum ether) (b.p. 80-100 degrees C, BDH 10180 AnalaR). The resulting mixture was vigorously vortexed for 30 seconds then the aqueous and organic solvent phases were separated by pulsing on a microcentrifuge. A 100µl aliquot of the phosphomolybdate extract from the pink organic (IBPE) top phase was transferred to a fresh microcentrifuge tube, followed by 150µl of ethanol and 10µl of a freshly prepared solution of 4% w/v $SnCl_2$ in 1.65M HCl. A 200ul aliquot of the resulting blue solution was then transferred to a 96 well plate and absorbance was read at 750nm.

2.7 Pi transport studies using radiolabeled Pi [^{33}Pi]

After incubation of cells in experimental medium as shown in Section 2.2.5, the test medium on each culture well was removed and replaced with 250µl of fresh HBS with or without Na^+ (Table 2.1), supplemented with 0.1mM Pi in the form of KH_2PO_4. A 20µl aliquot of radioactive ^{33}Pi (ARC (UK) Ltd, 0.5µCi per well) was then added followed by rapid mixing by swirling and incubated for exactly 5 min at room temperature. At the end of the incubation the plates were immediately placed on ice and the medium was aspirated. Each well was then washed thrice with 0.9% w/v NaCl to remove remaining extracellular ^{33}Pi. The cell monolayer was then harvested by scraping in 200µl of 0.05 mM NaOH and transferred to a 1.5ml microcentrifuge tube followed by 30 min incubation at 70^0C in a water bath to digest the cells. 120ul of this digest was added to 4ml of Ecoscint A scintillant and counted using an LKB Wallac 1219 liquid scintillation counter.

2.8 Bacterial transformation

Shot® TOP10 Chemically Competent *E. coli* (C4040-Invitrogen) were thawed on ice and 2µl of stock GPR146-EGFP plasmid (GPR146 cDNA inserted into pDXA vector; kindly provided by Dr Gary Willars, Department of Molecular & Cell Biology, University of Leicester) was added to the cells in a 0.5 ml thin-walled tube and incubated on ice for 20 min. This was then was exposed to heat shock by putting the tube in a water bath at 42°C for 1.5 min, and returned to ice for another 2 min. Lennox Broth (LB) (300µl) medium was added to the tube and incubated at 37°C for 1 h and then split onto two 10 cm microbiology grade Petri dishes containing 25ml of LB agar with 50 µg/ml antibiotic (kanamycin). The plates were incubated in an incubator at 37°C overnight. Next day, a single bacterial colony was selected and transferred into a 30 ml tube containing 5 ml LB broth (with 50 µg/ml kanamycin) and then incubated for ~ 8 h at 37°C in a shaking incubator (230 rpm). Then 400 µl of the culture was added to 200 ml LB medium (with 50 µg/ml kanamycin) in a1L flask and incubated in a shaking incubator overnight at 37°C.

2.9 Plasmid purification

At the end of the overnight incubation, plasmid purification was performed using a GeneJETTM Plasmid Maxiprep Kit (K0491, Life Technologies) according to the manufacturer's instructions. Briefly, the bacterial cells were centrifuged at 5000 x g at 4ºC for 10 min then the supernatant was removed and the pelleted bacteria were resuspended in 6 ml of Resuspension Solution from the kit followed by thorough vortexing. The resuspended bacterial cells were then lysed by adding 6 ml of Lysis Solution and incubated at room temperature for 3 min. The lysate was then neutralized by adding the Neutralizing Solution and mixed by inverting the tube 8 times. The Endotoxin-binding Reagent was then added to the tube followed by gentle but thorough mixing by inverting the tube and incubated at room temperature for 5 min. The tube was then centrifuged at 5000 x g for 40 min after adding 6ml of 96% ethanol to the mixture. The supernatant was transferred to a fresh 50ml tube followed by adding 6ml of 96% ethanol with immediate mixing. A 20 ml aliquot of the sample was then transferred to the separation column from the kit and centrifuged for 3 min at 2000xg. The flow-through was discarded followed by adding 8 ml of Wash Solution I, and centrifuged for 2 min at 3000 x g. The flow-through was discarded, and the column washing step was repeated twice with Wash Solution II. The column was transferred to a fresh 50 ml collection tube.

A 1 ml aliquot of Elution Buffer was then added to the centre of the purification column membrane, incubated for 2 min at room temperature and centrifuged for 5 min at 3,000 × g to elute plasmid DNA. The purified plasmid DNA was quantified by using a Thermo Scientific NANO DROP 1000 Spectrophotometer and was stored at -20°C.

2.10 Restriction enzyme digestion to verify the integrity of GPR146-EGFP plasmid

Three reactions using restriction enzymes (Janabi, 2017) and a control incubation without restriction enzyme were set up as shown in Table 2.3 confirm the integrity of the GPR146-EGFP plasmid (Figure 2.2). The components were mixed gently then incubated at 37ºC for at least 1 hour. Aliquots of 20µl from these mixes and 5ul of a DNA ladder were loaded into a 1 % agarose gel. The gel electrophoresis was performed at 150V for 60 min using a POWER PAC 300 (Bio-Rad, Hemel Hempstead, UK) and a picture of the resultant gel was obtained using a ChemiDoc™ Touch Imaging System.

Name of digest	H_2O	Plasmid DNA	BSA 10X	Buffer3 10X	Buffer2	*BamH I*	*Not I*	*Hind III*	DNA loading buffer
GFP	14	5	2	2	0	0.5	0.5	0	3
GPR146	14	5	2	0	2	0.5	0	0.5	3
GPR146-GFP	14	5	2	0	2	0	0.5	0.5	3
Intact construct	17	5	2	0	0	0	0	0	3

Table 2.3 Composition of digests that were used in GPR146-EGFP plasmid digestion. *(with all volumes shown in µl)*

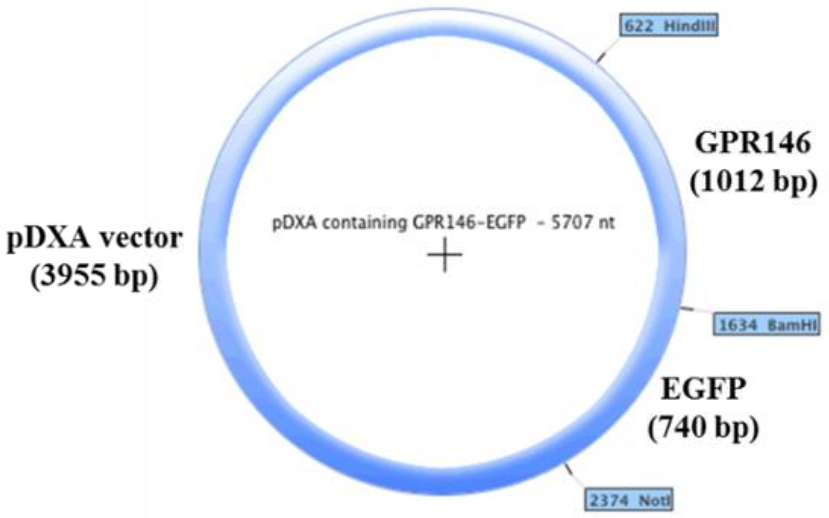

Figure 2.2 Restriction map of the GPR146-EGFP plasmid.
Copied from *(Janabi, 2017)****.***

2.11 TERT/1 transfection using TransFex reagent

TransfeX™ Reagent (a specialised transfection reagent recommended by ATCC for transfection of TERT/1 cells) was used to conduct the transfection experiments on TERT/1 cells according to the manufacturer's instructions. Briefly, cells were plated at the manufacturer's recommended density in growth medium and incubated at 37°C with 5% CO_2. On the day of transfection, the old growth medium was replaced with fresh medium. Then the transfection complex was prepared as follow; pre-warmed Tranfex Reagent, plasmid DNA, and Opti-MEM (Gibco / Life Technologies) were mixed, followed by gentle vortexing. (A range of volumes of Transfex Reagent, plasmid DNA and Opti-MEM was tested in an attempt to optimise the transfection). The Opti-MEM / plasmid DNA mixture was loaded into a sterile microcentrifuge tube and mixed thoroughly followed by adding Transfex reagent to the mixture without allowing the reagent to come in contact with the plastic sides of the tube. Concentrations were scaled to meet the required ratio that was recommended by the manufacturer. The whole mixture was then mixed thoroughly and incubated at room temperature for 15 min. The mixture was then added drop-wise to the cell monolayer to different areas of the well followed by gentle rocking of the plate to distribute the transfection mixture evenly. The cells were then incubated for up to 72 hours with replacement of the growth medium every 24 hours post transfection.

2.12 HEK293A transfection (transient transfection) with calcium phosphate

Calcium phosphate transfection of HEK293A cells was performed using a ProFection® Mammalian Transfection System (Promega UK ref. E1200) according to the manufacturer's instructions. Briefly, cells were plated at 25 x 10^4 cells / well in collagen coated 35mm 6-well plates in 2ml of growth medium (Section 2.2.2). GPR146-EGFP plasmid or GFP-empty vector (2µg of plasmid DNA) were mixed with $CaCl_2$ and nuclease-free water to give a total volume of 120 µl in a 1.5ml tube as shown in Table ***2.4***. The plasmid mixture was then mixed with an equal volume of 2X HBS buffer (a HEPES-buffered saline containing the phosphate that is required for the precipitation) in a fresh tube dropwise to ensure thorough mixing. The resulting mixture was then added in a dropwise manner to each well followed by gentle but thorough rocking back and forth to ensure even distribution of the transfection mixture over the cell monolayer. The plate was then incubated at 37°C for 24 hours. The medium containing the transfection mix was then replaced with 2 ml of fresh medium followed by a further 24 hour incubation. Cell imaging was then performed by using a BIO-RAD ZOE™ Fluorescent Cell Imager (Ref 1450031) to screen the cultures for EGFP expression.

	GFP-empty vector (µl) per well		GPR146-eGFP (µl) per well	
	Tube 1 (µl)	**Tube 2 2x HBS (µl)**	**Tube 1 (µl)**	**Tube 2 2x HBS (µl)**
Plasmid	**0.4**	**120**	**0.6**	**120**
$CaCl_2$	**15**		**15**	
Nuclease-free water	**104.6**		**104.4**	

Table 2.4 Composition of mixtures for calcium phosphate transfection of HEK293A cells.

2.13 HEK293A transfection using jetPRIME

HEK293A cells were plated at a density of 25 x 10^4 cells / well in collagen coated 35mm 6-well plates in 2ml of growth medium (Section 2.2.2), then the cells were exposed to transient transfection using jetPRIME® DNA transfection reagent from Polyplus (USA) according to the manufacturer's instructions. In brief, when the cells were around 80% confluent, 2μg of the plasmid was mixed with 200μl of jetPRIME buffer followed by vortexing. Then, the jetPRIME transfection reagent was added to the diluted DNA in a ratio of l2μl of jetPRIME per μg of DNA followed by 10 seconds of vortexing and pulse centrifugation on a microcentrifuge to pool the mixture at the bottom of the tube. The mixture was then left for 10 minutes at room temperature, and 200μl was then added to the cell monolayer dropwise followed by rocking the plate back and forth to ensure distribution of the transfection mixture over the cell monolayer. The plate was then incubated for 4 hours in the culture incubator. The medium containing transfection agent was then replaced with fresh growth medium. The plate was incubated for up to 72 hours with checking every 24 hours for to screen for EGFP expression using fluorescence microscopy (BIO-RAD ZOE™ Fluorescent Cell Imager Ref 1450031).

2.14 RNA Extraction and RT-Q-PCR

RNA was extracted from rat kidney tissue (Section 2.20) by homogenising using a Fast Prep 24, 5G bead tissue homogenizer (MP Biomedicals) with TRIzol reagent (Gibco / Life Technologies Ref 15596). Approximately 2mg of rat kidney tissue was homogenised in 1.5 ml of TRIzol and incubated at room temperature for 15 minutes. For cultured cells which had been incubated with experimental medium as described in Section 2.2.5, Trizol reagent (Invitrogen,) was added (600 μl / 35mm culture well) and left to stand at room temperature for 10 minutes to allow the cells to rupture and release RNA.

The crude RNA extract in Trizol was then transferred to RNAase-free 2ml screw-cap plastic tubes. Chloroform (200 μl of molecular biology grade reagent per ml of Trizol extract) was added to the tubes and vortexed for 15 seconds then left to stand at room temperature for 2-3 minutes, then centrifuged on a pre-chilled Sarsted Biofuge microcentrfuge at 13000 rpm for 15 minutes. The upper (i.e. aqueous) phase was taken and transferred to fresh autoclaved tubes. Isopropyl alcohol (500 μl per 1ml of original Trizol extract) was added. The sample was left to stand for 10 minutes to allow

precipitation of RNA and again vortexed vigorously. The tube was then microcentrifuged at 10,000 rpm for 10 minutes. After centrifugation, a faint RNA pellet could be seen at the bottom of the tube. Then the isopropyl alcohol was carefully removed from the tube and the pellet was washed in 1ml of pre-chilled (-20^{0}C) 75% ethanol (RNAase free). The tubes were vortexed and microcentrifuged (10,000 rpm for 5 minutes at 4°C), the ethanol was removed and the tube left to stand upside down to air dry. Finally, 20µl of diethylpyrocarbonate (DEPC)-treated water was added to the pellet and incubated at 65°C for 10 minutes to dissolve the RNA.

The concentration of RNA per µl was determined on a Nano Drop Spectrophometer, at 260nm in duplicate. The RNA was stored at -80°C.

2.15 Reverse transcription (RT) reaction (cDNA synthesis)

To synthesise cDNA from the RNA extracted in Section 2.14, an AMV Reverse Transcription System (Promega A3500) was used, following the manufacturer's instructions. The RNA samples above were diluted with DEPC water to achieve 1µg in a 2µl aliquot in thin walled PCR tubes (Abgene 0.5ml Thermo-Tube, Ref Ab-0350). The RT master mix (18µl per RNA sample) was prepared as shown in Table 2.5 in a thin walled PCR tube with 2µl of RNA sample to achieve a concentration of 1µg of total RNA per reaction, then the tubes were placed on a PCR thermal cycler (Techne Genius, TC-3000X) and subjected to heating as follows:

- 42°C for 1 h for cDNA synthesis
- 99°C for 5 min for enzyme inactivation.
- 4°C for at least 5 min for cooling

At the end, the samples were stored at -20°C.

Reagent	Volume for 1 reaction (µl)
$MgCl_2$ (25mM)	4
Reverse Transcriptase 10X Buffer	2
dNTP Mixture, 10mM	2
Recombinant RNasin ribonuclease inhibitor	0.5
AMV reverse Transcriptase (15U/µl)	0.75
Oligo$(dT)_{15}$ Primer	1
DEPC water	7.75
Total volume for reaction	**18**

Table 2.5 Composition of reverse transcription master mix incubations.

2.16 Quantitative real time-polymerase chain reaction (qPCR)

2.16.1 qPCR using Power SYBER®Green PCR Master Mix

The qPCR reaction was performed by adding cDNA (1µl) to Power SYBER®Green PCR Master Mix (12.5µl) (Applied Biosystems; Cat No. 4367659) mixed with nuclease-free water (10.5µl) followed by adding 0.5µl forward primer and 0.5µl of reverse primer (Table 2.6). Samples were then mixed by gentle pipetting. Negative control samples were also prepared by adding 1µl of DEPC water in place of the cDNA to the mixture above. The relative gene expression level was normalized to housekeeping gene (GAPDH), and the relative gene expression was calculated as fold change in relation to the control condition in the experiment (control cultures without C-peptide) using the $2^{-\Delta\Delta C_T}$ method. qPCR efficiency was measured by running the qPCR at a range of template cDNA concentrations and plotting a standard curve. The primer efficiency was calculated from the slope of the curve using the equation (10^(-1/slope)*100).

2.16.2 qPCR using Taqman Master mix

The qPCR reaction was performed by adding 1µl of the cDNA prepared in Section 2.15 to 3.5µl of nuclease-free water, 5µl of Taqman Master mix (Fisher ref. 10525395) and 0.5µl of the required Taqman Gene expression assay primers (Thermo Fisher ref. 4331182) (Table 2.7). Negative control samples were prepared by using 1µl of DEPC water instead of the cDNA in the mixture above. The above mixtures were loaded into 96-well PCR plates, and the plates were covered with self-adhesive sealing sheets to minimize evaporation. To perform real-time PCR, An Applied Biosystems 7500 Fast Real-Time PCR System (Applied Biosystems, Life Technologies) was used. The relative gene expression level was normalized to housekeeping gene (GAPDH), and the relative gene expression was calculated as fold change in relation to the control condition in the experiment (control cultures without C-peptide) using the $2^{-\Delta\Delta C_T}$ method.

Gene	Forward Sequence	Reverse Sequence	PCR Efficiency (%)	NCBI reference
Hu GPR146	ACTTTGTCAACATGGCAGTGGCAG	TGGACACATGGCTGCAGATGTAGA	96.25	NM_001303474.2
GAPDH	CATGTAGTTGAGGTCAAGGA	CGAGCCACATCGCTCAG	97.36%	NM_001289746.1

Table 2.6 Primer sequences that were used for qPCR analysis of GPR146 expression

Primer	Reference number
Human SLC20A1	Hs00965587_m1
Human SLC20A2	Hs00198840_m1
Human XPR1	Hs00173707_m1
Human SLC34A1	Hs01092910_m1
Human SLC34A3	Hs02341453_g1
Human GAPDH	Hs02758991_g1
Rat GPR146	1756385_250µl
Rat TGF-β1	0057210_250µl
Rat Col6a4	01445285_250µl

Table 2.7 Details of Taqman gene expression assays that were used for qPCR analysis of the expression of genes encoding Pi transporters, GAPDH, GPR146 and fibrotic markers. Choice of the primers based on previous research in the lab

(Abbasian *et al.*, 2015).

2.17 Preparation of Samples for Luminex Assay

2.17.1 Preparation of Kidney Samples

Approximately 2mg of rat kidney tissue was homogenised using a Fast Prep 24, 5G bead tissue homogenizer (MP Biomedicals) in 300µl of cell lysis buffer (RIPA buffer 89900, ThermoFisher). Samples were then incubated on ice for 30 min. At the end of the 30 min incubation, the samples were microcentrifuged at 13,000 rpm for 15 minutes at 4°C. The resulting supernatant was then stored at -80°C.

2.17.2 Preparation of Plasma Samples

Samples were collected in EDTA tubes. Samples were then centrifuged at 1200 x g for 10 min within 30 min of collection. They were then immediately aliquoted and stored at -80ºC.

2.18 Magnetic Luminex cytokine assay

To quantify concentrations of cytokines in diabetic rat kidney tissue (Section 2.17) and plasma, a Rat Premixed Luminex assay kit (ProcartaPlex Immunoassays PPX-02-MXGZFN4, PPX08-MXDJXYD, EPX01A-30249-901 ThermoFisher) was used, according to the manufacturer's instructions. The Luminex technology allows detection and quantification of multiple biomarkers in a mixed solution via antibody capture of the molecule of interest using binding to fluorescent dye microspheres. In this project, 10 biomarkers were selected that could in principle be involved in inflammation during diabetes mellitus or in the progression of tubulo-interstitial disease in the kidney. These biomarkers were; TGF-beta-1, sVCAM, sICAM, bNGF, IL-1beta, IL-6, MCP-1, RANTES, TNF-alpha, and VEGF-A. Total protein concentration was determined for the kidney tissue lysates by DC protein assay (Section 2.4), and all samples were diluted in cell lysis (RIPA) buffer to a final concentration of 500 µg/ml (Hulse 2010). Magnetic beads were vortexed for 30 seconds followed by adding 50 µl of the beads to each well of a 96-well plate (supplied in the kit). Samples (or standards for the proteins of interest) were added in 25 µl aliquots to each dedicated well containing 25 µl of 1X Universal Assay Buffer (supplied in the kit). This was followed by a 2h incubation on a microplate shaker at 800 rpm at room temperature, then the plates were washed with wash buffer followed by isolation of the beads with their bound proteins using a Luminex magnetic separator. The detection antibody (biotin-labelled secondary antibody) was then added to

each well and incubated for 1h at room temperature. Then the plates were washed as above to remove the excess antibody followed by incubation with 50µl streptavidin-phycoerythrin (PE) substrate for 30 min at room temperature, followed by a final wash. Beads were then resuspended in 120 µl of the reading buffer (supplied in the kit) followed by a 5 min incubation at room temperature. Data were then acquired immediately on a MAGPIX® Luminex reader.

2.19 ELISA

To supplement the Luminex assay of the IL-6 concentration in diabetic rat kidney (Sections 2.17 and 2.18), an ELISA kit (R&D, ref. R6000B) was used following the manufacturer's instruction. Briefly the assay was performed as follows. Standards were prepared at 8 different concentrations from 0 to 4000 pg/ml. Standards, samples and a recombinant IL-6 positive control were loaded into a 96-well plate (supplied with the kit) precoated with capture antibody, followed by 2 h incubation at room temperature. At the end of the 2 h incubation, the plate was washed 5 times using ELISA washing buffer. A 100µl aliquot of an HRP conjugated anti-rat IL6 antibody was added to each well followed by 2 h incubation at room temperature. The plate was then washed 5 further times using ELISA washing buffer followed by adding 100µl of Substrate Solution to each well and then incubating for 30 minutes at room temperature in the dark. Data were acquired using a 96 well microplate reader (Varioskan Flash, ThermoFisher) at 450 nm.

2.20 Diabetic rat study

Studies in this thesis on rat kidney and plasma were performed on samples from a study on the STZ model of T1DM in rats (see Chapter 1) which had previously been performed by Prof Nigel Brunskill and Mr Jeremy Brown (Department of Infection, Immunity & Inflammation, University of Leicester). All of the animal experiments were performed in the Preclinical Research Facility (PRF) at the University of Leicester under a project licence (reference PPL 40/3539) from the UK Home Office held by Prof Nigel Brunskill (under the Animals (Scientific Procedures) Act 1986 and in accordance to Animal Research: Reporting of In Vivo Experiments (ARRIVE) regulations). Key characteristics of the animals used in this study are presented in Appendix 5.

2.20.1 Induction of DM and animal groups

A single intravenous dose of 65mg / kg body weight of STZ solution prepared in citrate buffer was given to male Wister rats (280-300g) after overnight fasting, to induce DM. Two days after STZ injection, the development of the disease model was confirmed by measurement of blood glucose. Only rats with blood glucose level greater than 14 mM were included in this study. Standard rat chow diet and water *ad libitum* was provided to rats throughout the study. Animals were randomly assigned into five experimental groups (each of 8 animals) as follows: diabetic group (STZ), C-peptide treated group (STZ+C-pep), angiotensin converting enzyme (ACE) inhibitor group (STZ+ACEI), C-peptide and ACE inhibitor treated group (STZ+ACEI + C-pep), and healthy control group (2 rats that matched the age and sex of the diabetic animals but did not receive STZ treatment). (As both ACEI groups were not relevant to the aims of this thesis, these animals were excluded from the analysis described here). The C-peptide treated group were injected with subcutaneous 0.5mg/kg synthetic long-acting pegylated C-peptide (Polypeptide Laboratories, San Diego, USA) twice a week throughout the study. The vehicle of C-peptide (0.9% w/v NaCl) was injected into all non-C-peptide treated groups. All diabetic (STZ) rats were provided with subcutaneous long acting insulin (3 units of Hypurin Bovine (Protamine Zinc) insulin) at sufficient intervals to maintain blood glucose concentration between 25-33mM and to avoid severe weight loss. During the study, blood glucose, plasma C-peptide, and body weight were monitored periodically.

Streptozotocin (STZ) administration to render the rats diabetic at the start of the study

STZ stock solution was made up aseptically fresh each day at a concentration of 50mg/ml in 20mM citrate buffer pH 4.5. Sufficient STZ stock was injected intravenously into each rat to achieve a dose of 65mg/Kg body weight. For a 250g rat this required 325µl of the STZ stock. Volume to be administered =

Dose to be administered (mg/kg) X weight of rat (g) /Weight of STZ (mg).

C-peptide administration to *TREATED* STZ diabetic rats throughout the study

Pegylated Rat C-Peptide stock solution was made up aseptically at a concentration of 1.0 mg/ml (0.31mmol/L) in 0.9% w/v NaCl, 5mM HEPES pH 7.4. C-peptide stock was injected into each rat sub-cutaneously twice per week to achieve a dose of 0.5mg/Kg body weight. For a 250g rat this required 125µl of the C-peptide stock.

Vehicle administration to *CONTROL* STZ diabetic rats throughout the study

Control STZ diabetic rats which did not receive C-peptide received the same volume of C-peptide vehicle (i.e. sterile 0.9% w/v NaCl, 5mM HEPES pH 7.4) twice per week instead.

Respite insulin administration to *ALL* STZ diabetic rats throughout the study

Hypurin ® bovine (protamine Zinc) insulin (100 IU/ml stock) was administered subcutaneously twice a week to all of the STZ rats to allow the animals to maintain their body weights while allowing blood glucose concentration to remain in the range (~25 - 33mM). A dose of 2 IU (20µl of stock) was administered on each occasion.

2.21 Statistical analysis

Data were analysed with GraphPad Prism 7.0 and are shown as the mean ± SEM. In experiments which involved multiple comparisons, repeated measures one-way analysis of variance (ANOVA) was performed and followed with *post hoc* testing with Tukey's multiple comparisons test. Experiments involving two experimental variables (e.g. C-peptide and Pi in Chapter 4) were analysed by 2-way ANOVA followed by Dunnett's multiple comparisons test. $P<0.05$ was considered statistically significant.

3 Chapter 3 Confirming C-peptide responsiveness in cultured human renal tubular epithelial cells

3.1 Introduction

As noted in Chapter 1, in the past two decades C-peptide has been recognized as a biologically active molecule, and a number of studies (Wahren & Larsson, 2015; Hills, & Brunskill, 2009; Yosten *et al.*, 2014a) have reviewed its intracellular signalling, largely from studies on cultured cell lines. C-peptide has also been reported to exert beneficial effects on diabetic complications *in vivo*, including retinopathy, neuropathy, impaired wound healing, and nephropathy (Hills *et al.*, 2010). *In vitro*, it has also been shown to regulate the activation of MAPK, Na^+/K^+ ATPase regulation and expression, and activation of NO production (Wahren *et al.*, 2012). C-peptide is also reported to inhibit ROS production and inhibit inflammation (Bhatt *et al.*, 2013b). It also may be involved in controlling D-glucose uptake (Johansson *et al.*, 1992). All of these beneficial findings were found to be abolished by pre-treatment of cells with PTX, and accompanied by the binding of C-peptide to cell membranes shown by Rigler and colleagues (1999). These findings suggest that there is a direct interaction between C-peptide and a specific GPCR at the C-terminal pentapeptide region of C-peptide at physiological concentrations (Hills & Brunskill, 2009).

Efforts have been made to identify this receptor or receptors. The initial evidence that C-peptide interacts with a cell membrane receptor(s) (obtained in (Rigler *et al.*, 1999; Flatt *et al.*, 1986); was followed by further studies (Al-Rasheed, 2006; Lindahl *et al.*, 2007) in which C-peptide membrane-binding was detected in HEK 293 cells, Swiss 3T3 fibroblasts, kidney tubule cells and endothelial cells. This receptor, clearly is not the insulin receptor as the binding of C-peptide to cell membranes was not displaced by insulin, IGF-I or IGF-II (Yosten *et al.*, 2014b). As the pathway through which C-peptide signals is likely to be through a GPCR and is PTX sensitive (as reported in T-cells (Walcher *et al.*, 2004), renal proximal tubular cells (Shafqat *et al.*, 2002; Al-Rasheed *et al.*, 2004a; Al-Rasheed *et al.*, 2004; Zhong *et al.*, 2005; Al-Rasheed *et al.*, 2006), macrophages (Marx *et al.*, 2004), fibroblasts (Kitamura *et al.*, 2001; Lindahl *et al.*, 2007), and podocytes (Maezawa *et al.*, 2006)), it was hypothesized that the C-peptide receptor

was an orphan GPCR (Yosten *et al.*, 2014). To identify this C-peptide receptor, Yosten *et al* used a strategy developed in their laboratory, called the "Deductive Ligand Receptor Matching Strategy". Three cell lines, that were known to respond to C-peptide (Rigler *et al.*, 1999; Yosten *et al.*, 2012), were screened for the expression of a series of orphan GPCRs (Yosten *et al.*, 2012). These cell lines were HEK293, TF-1, and KATOIII. These authors evaluated the sequence homology, the function and the known distribution of 24 orphan receptors by using a bioinformatics database in order to narrow down the receptor candidates to test experimentally. Then, they followed an elimination strategy in which they used siRNA to knock down single receptors in KATOIII cells and test the response to C-peptide. Their study showed that the knock-down of only one of these orphan receptors (GPR146) blocked the intracellular signalling effects of C-peptide to *cFOS* in KATOIII cells. They also observed a co-localization between GPR146 and C-peptide at very low levels by using confocal microscopy (Yosten *et al*., 2013).

C-peptide has been reported to activate the three major mitogen-activated protein kinases (MAPKs): ERK, p38, and JNK. However, only ERK has been shown to be consistently activated by C-peptide (Nordquist *et al.*, 2008). C-peptide stimulates ERK1/2 activation in a number of cells including proximal tubular cells. C-peptide was first seen to activate ERK1/2 in (Grunberger *et al.*, 2001; Kitamura *et al.*, 2001). Kitamura and colleagues reported that C-peptide activates ERK1/2 in Swiss 3T3 within 10 minutes of stimulation. They also reported that this activation was entirely abolished by PTX indicating that G-protein Gαi isinvolved in the C-peptide-modulated ERK1/2 activation. Grunberger and colleagues in 2001 reported a similar effect in rat L6 myoblasts.

As the main clinical interest in this thesis is to investigate C-peptide effects that may be of therapeutic value in treating progressive tubulo-interstitial damage in diabetic nephropathy (Chapter 1), it is desirable to study cultured human proximal tubular epithelial cells (HPTC). In primary cultures of HPTC, it was shown that stimulation with 0.1 to 10 nM C-peptide for 5 minutes activated ERK1/2 in a concentration dependent manner (Al-Rasheed *et al.*, 2004). However an important limiting factor in the further characterisation of such effects is the availability of healthy human kidney tissue from which to culture primary HPTCs. For this reason the initial experimental aim in this project was to investigate whether the established human proximal tubular epithelial cell line TERT/1 could be used as an acceptable substitute for primary cultures of HPTCs in studies of C-peptide. The TERT/1 cell line is an immortalized line that has been reported

to show a close resemblance in its physiology to human proximal tubular epithelial cells *in vivo*, including expression of HPTC-specific marker proteins (Wieser *et al.*, 2008). In contrast the human embryonic kidney cell line HEK293A fails to show such highly differentiated characteristics but is easier to culture and transfect than TERT/1 cells and was therefore included in this chapter as a comparison cell line.

The specific experimental aims in this chapter were as follows:

1) To determine whether immunoblotting for the phospho-activated form of ERK1/2 could be used as a convenient read-out of intracellular response to C-peptide in HEK-293A and TERT/1 cells.
2) To investigate whether these cell lines could be used to assess the possible role of GPR146 in C-peptide signalling (a) by investigating the effect of C-peptide on GPR146 expression, and (b) by attempting to over-express GPR146 by transfection of these cells with a plasmid incorporating human GPR146 cDNA.

3.2 Results

3.2.1 C-peptide-mediated activation of ERK1/2 in TERT/1 cells

To determine whether TERT cells are responsive to C-peptide, using phospho-ERK1/2 as a known and consistent readout for intracellular response to C-peptide, TERT/1 cells were exposed to serum starvation overnight (to avoid any interaction with serum C-peptide and other growth factors, prior to exposure to different doses of C-peptide namely (0.01, 0.03, 0.1, 0.3, 1, 3, 10 nM C-peptide, and 10% DFBS as a positive control) (Figure 3.1). The same volume of C-peptide vehicle was used for the treatment of control (0) cells. The expression of phospho-ERK1/2 protein was then determined by Western blotting.

Stimulation of TERT/1 cells with C-peptide for 5 minutes increased phosphorylation of ERK1/2 (Thr202/Tyr204) significantly in comparison to control cells, with an apparent maximal increase at 0.3, 3 and 10 nM C-peptide (Figure 3.1).

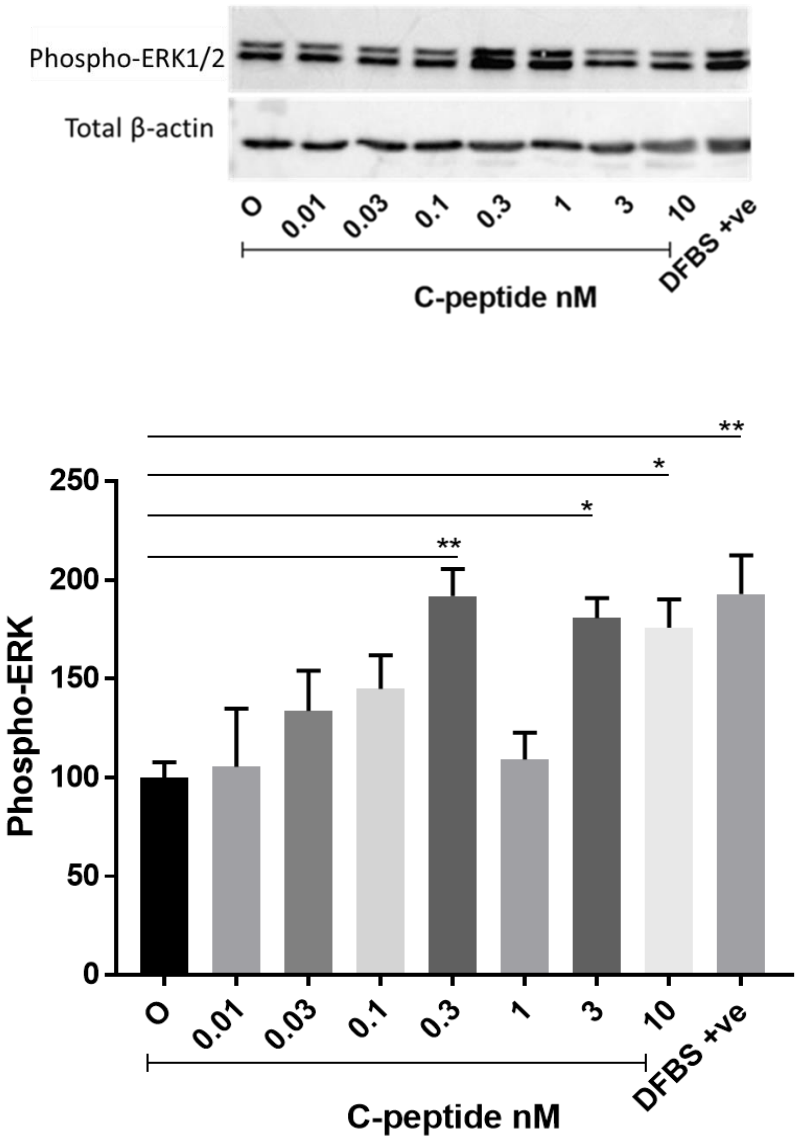

Figure 3.1 Concentration-dependence of stimulation of ERK1/2 phosphorylation by peptide in TERT/1 cells.

*After overnight serum-starvation, cells were treated with the indicated concentrations of C-peptide for 5 min. Phospho-ERK1/2 (Thr202/Tyr204) and total β-actin as a loading control were detected by immunoblotting. The presented densitometry values are mean ± SEM of 3 independent experiments. Both bands of phospho-ERK1/2 were pooled and values expressed as the ratio relative to β-actin using Image J software. (One-way ANOVA and post hoc testing showed a significant stimulatory effect of C-peptide relative to the unstimulated control, 0 is considered 100% (*P<0.05; **P<0.01)*

3.2.2 C-peptide-mediated ERK1/2 activation in human embryonic kidney cells (HEK293A)

Although C-peptide has previously been shown to have no effect on the activation of MAP kinase (ERK1/2) signalling in HEK293A cells (Janabi, 2017), in this study, stimulation of the HEK293A cell line, (which is a subclone of the parent HEK293 line which shows improved adherence on culture surfaces and consequently shows flatter morphology than the parent line) did show a response (Figure 3.2). HEK293A cells were exposed to serum starvation overnight (to avoid any interaction with serum C-peptide) prior to exposure to 0.01, 0.03, 0.1, 0.3, 1, 3, or 10 nM C-peptide or 10% DFBS (Figure 3.2). The same volume of C-peptide vehicle was used for the treatment of control (0) cells. The expression of phospho-ERK1/2 protein was then determined by Western blotting. Stimulation of HEK293A cells with C-peptide for 5 minutes increased phosphorylation of ERK1/2 (Thr202/Tyr204) significantly in comparison to control cells. The concentration-response curve demonstrated a more gradual increase of ERK1/2 phosphorylation than in TERT/1 cells, with the phospho-ERK1/2 response only reaching maximum in HEK293A cells at a concentration of ~ 0.3, 3 and 10 nM (Figure 3.2).

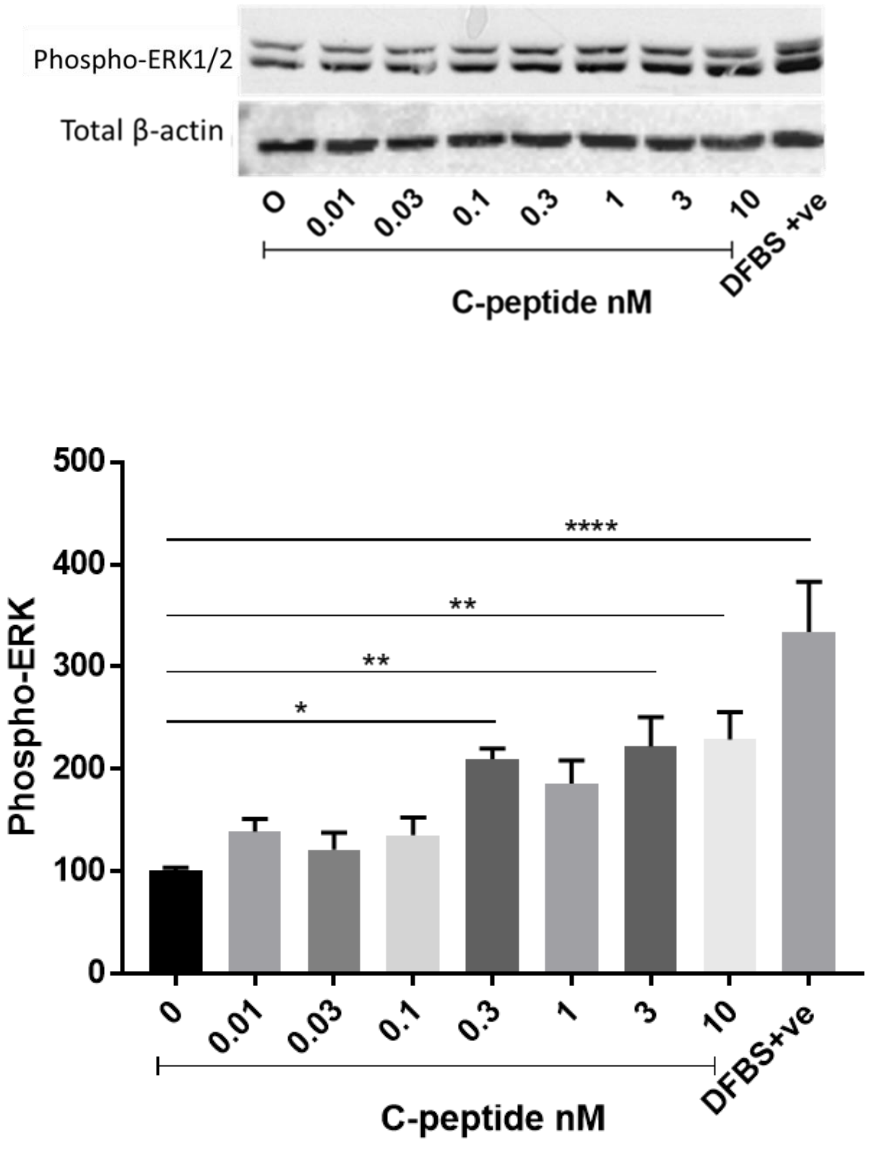

Figure 3.2 Concentration-dependent stimulation of ERK1/2 phosphorylation by C-peptide in HEK293A cells.

*After overnight serum-starvation, cells were treated with the indicated concentrations of C-peptide for 5 min. Phospho-ERK1/2 (Thr202/Tyr204) and total β-actin as a loading control were detected by immunoblotting. The presented densitometry values are mean ± SEM of 3 independent experiments. Both bands of phospho-ERK1/2 were pooled and values expressed as the ratio relative to β-actin using Image J software. (One-way ANOVA and post hoc testing showed a significant stimulatory effect of C-peptide relative to the unstimulated control, (0) is considered 100% (*P<0.05; **P<0.01; ****P<0.0001)*

3.2.3 Time course of the effect of human C-peptide on ERK activation in TERT/1 and HEK 293A cells

It has been previously reported that C-peptide stimulates the phosphorylation of ERK1/2 within 5 to 10 minutes in a number of cell types (Al-Rasheed, *et al.*, 2004; Kitamura *et al.*, 2001). This study aimed to determine whether a similar effect of C-peptide can be seen in TERT/1 and HEK293A cell. In these experiments, both TERT/1 and HEK293A cells were serum-starved overnight then treated with 3nM C-peptide for up to 60 min (Figure 3.3). A concentration of 3nM of C-peptide was chosen because this had previously been shown in Figure 3.1 and Figure 3.2) to induce a significant stimulation at 5 min. At each time point control cells were incubated with C-peptide vehicle for comparison. An early maximal stimulation of ERK1/2 phosphorylation after 5 minutes was observed in both TERT/1 (Figure 3.3) and in HEK293A (Figure 3.4) cell lines. Longer periods of stimulation did not affect pERK levels.

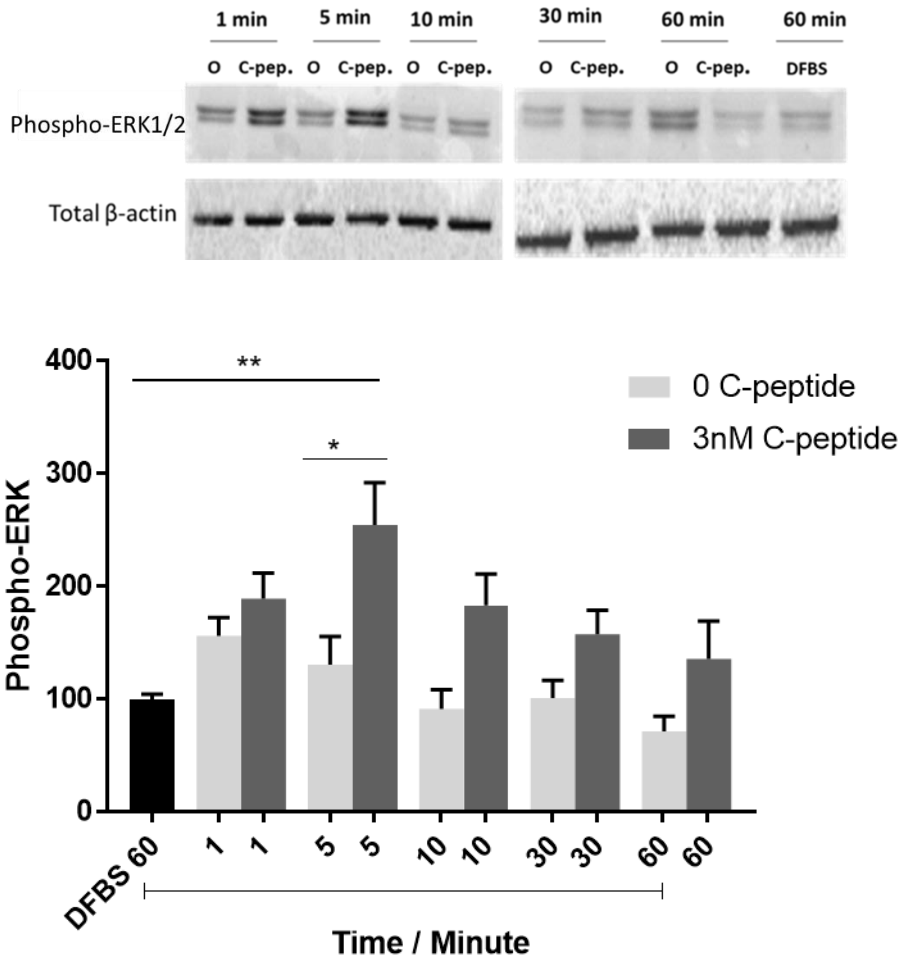

Figure 3.3 Time course effect of C-peptide treatment on ERK1/2 activation in TERT/1 cells.

*Expression of pERK1/2 in TERT/1 cell treated with 3nM C-peptide for up to 60 min following overnight serum starvation analysed by Western blotting. Control (0) cells were treated with C-peptide vehicle for the same duration and assigned as 100%. Densitometry analysis for ERK1/2 is presented as the relative ratio to β-actin. Data are expressed as fold change compared to the pERK1/2 band intensity in a lysate on each membrane derived from cultures stimulated for 60 min with DFBS. Densitometry was performed using Image J software. The presented values are mean ± SEM of 3 independent experiments. (one-way ANOVA showed significant effect of C-peptide (*P<0.05; **P<0.01).*

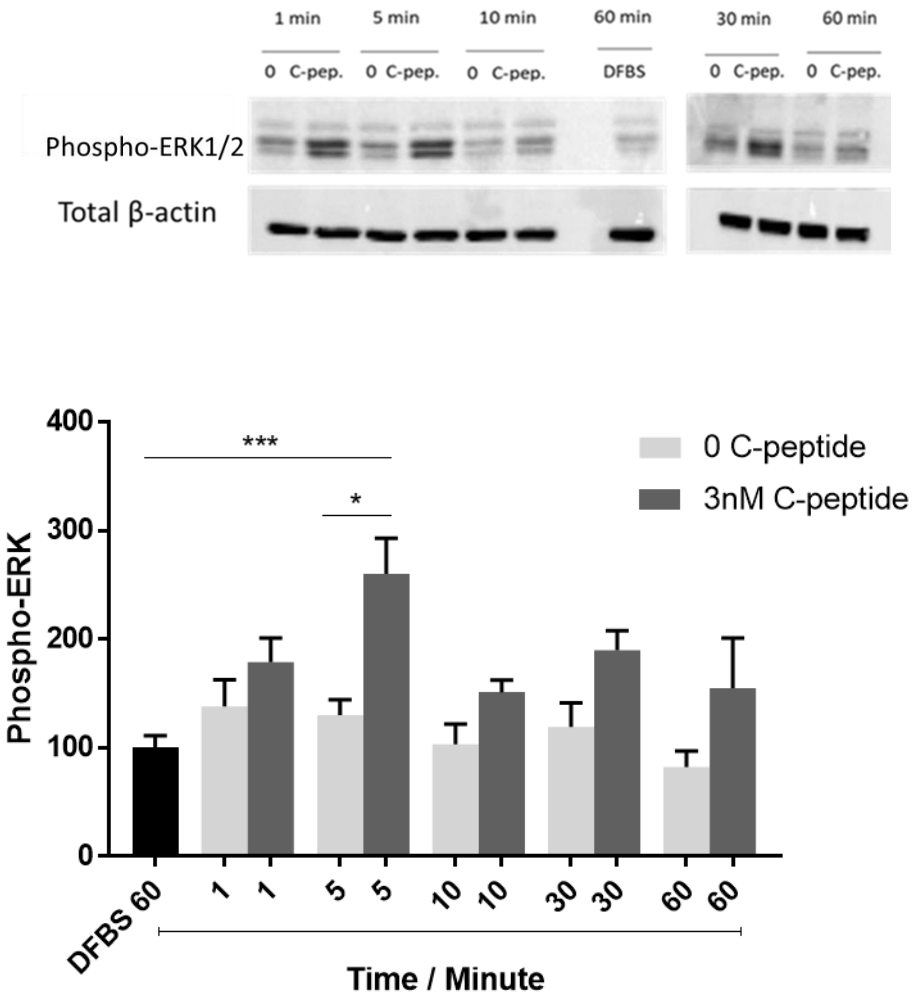

Figure 3.4 Time course effect of C-peptide treatment on ERK1/2 activation in HEK293A cells.

*Expression of pERK1/2 in HEK293A cell treated with 3nM C-peptide for up to 60 min following overnight serum starvation analysed by Western blotting. Control (0) cells were treated with C-peptide vehicle for the same duration and assigned as 100%. Densitometry analysis for ERK1/2 is presented as the relative ratio to β-actin. Data are expressed as fold change compared to the pERK1/2 band intensity in a lysate on each membrane derived from cultures stimulated for 60 min with DFBS. Densitometry was performed using Image J software. The presented values are mean ± SEM of 3 independent experiments. (one-way ANOVA showed significant effect of C-peptide (*P<0.05; ***P<0.001).*

3.2.4 Expression of GPR146 a candidate receptor for C-peptide

As GPR146 has been proposed as a possible receptor for C-peptide (Yosten *et al.*, 2013) and as TERT/1 and HEK293A cells seemed to respond to physiologically relevant concentrations of C-peptide, an attempt was made to detect GPR146 mRNA expression in these cells, by using RT-Q-PCR. Expression was readily detectable in both cell lines (Figures 3.5 and 3.6). As at least one GPCR (the luteinizing hormone receptor) has been reported to show down-regulation of its mRNA in response to ERK signalling triggered by the receptor's ligand (Menon *et al.*, 2011), experiments were performed in order to assess whether there was any effect of C-peptide on the expression of GPR-146 mRNA. Both TERT/1 and HEK293A cells were serum-starved overnight and treated with 3nM C-peptide for 2, 4, and 24h. (Figures 3.5 and 3.6). For comparison the effect of 10% DFBS was also tested. Cells treated with C-peptide showed no statistically significant change in the expression of GPR-146 mRNA in either cell line when compared to untreated control cells. In contrast, 10% DFBS (Figures 3.5 and 3.6) showed a statistically significant decrease in GPR-146 mRNA expression after 2h in both cell lines.

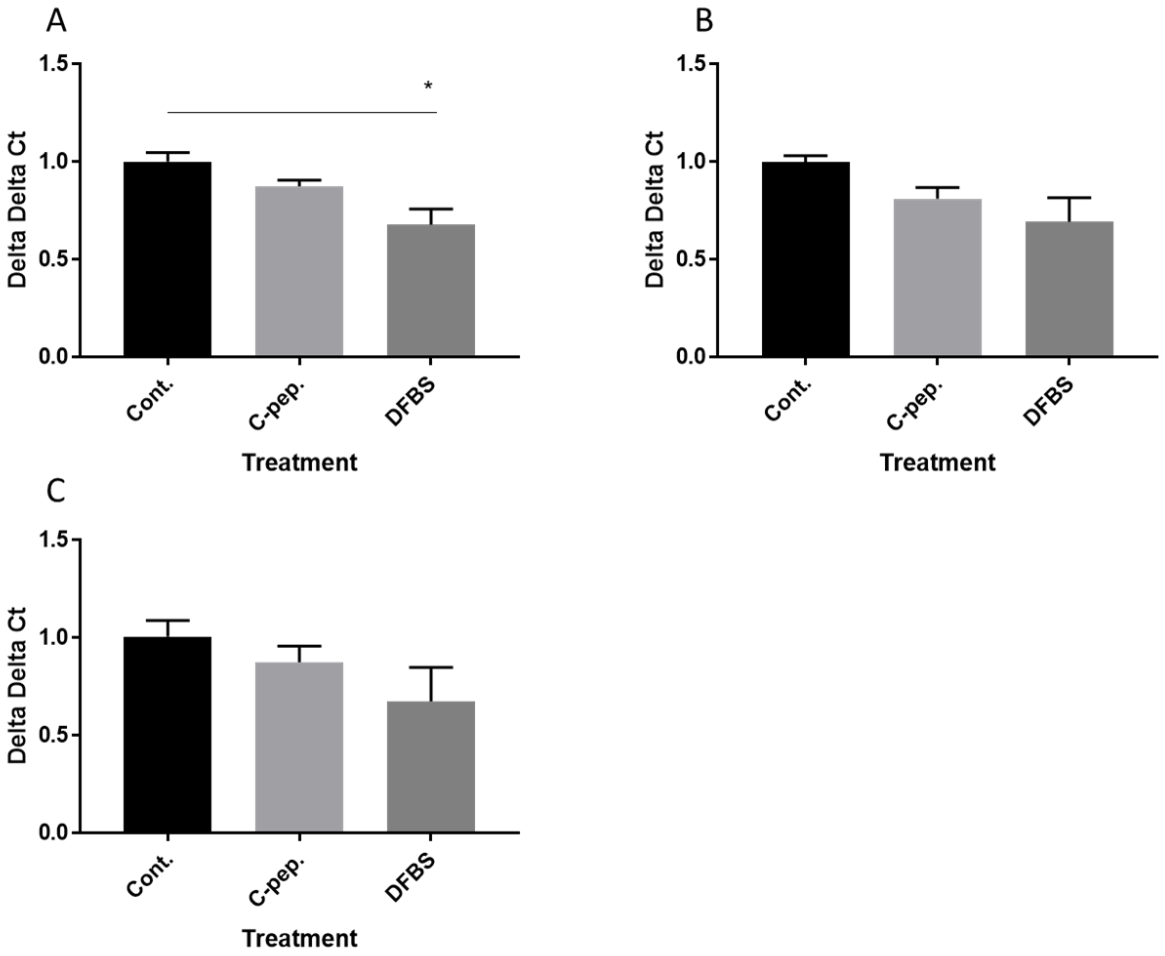

Figure 3.5 The effect of 3nM human C-peptide on GPR-146 mRNA in cultured TERT/1 cells.

*After overnight serum-starvation, cells were incubated for 2h (A), 4h (B) or 24h (C) hours in medium with 3 nM C-peptide or 10% DFBS. Relative GPR-146 mRNA expression was calculated using the delta delta CT value method, relative to GAPDH as a house-keeping control gene. Pooled data are shown from n=3 independent experiments. (One-way ANOVA and post hoc testing showed a significant down-regulation effect of DFBS relative to the unstimulated control after 2h stimulation, the control untreated cells considered as 1 (*P<0.05).*

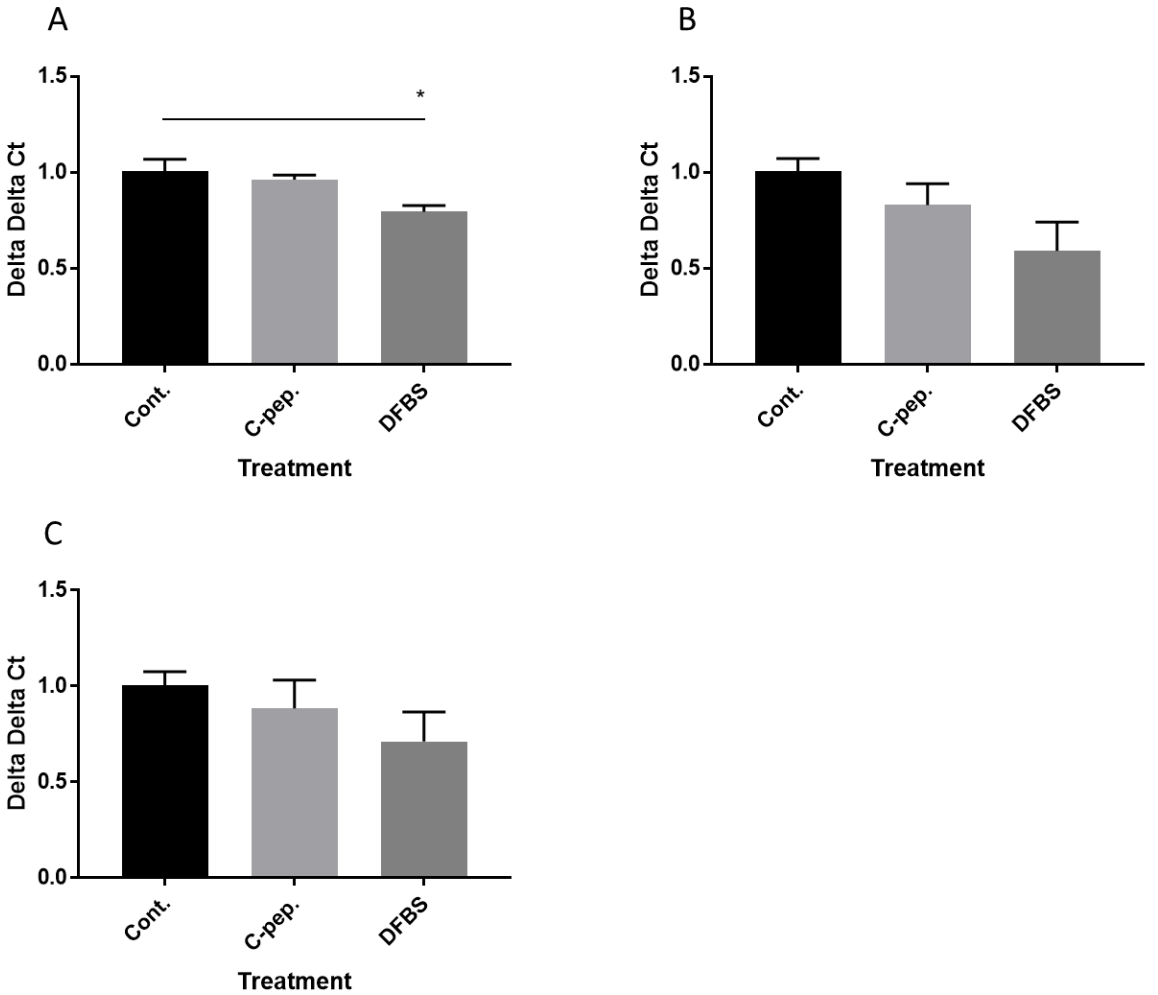

Figure 3.6 The effect of 3nM human C-peptide on GPR-146 mRNA in cultured HEK293A cells.

*After overnight serum-starvation, cells were incubated for 2h (A), 4h (B) or 24h (C) hours in medium with 3 nM C-peptide or 10% DFBS. Relative GPR-146 mRNA expression was calculated using the delta delta CT value method, relative to GAPDH as a house-keeping control gene. Pooled data are shown from n=3 independent experiments. (One-way ANOVA and post hoc testing showed a significant down-regulation effect of DFBS relative to the unstimulated control after 2h stimulation, the control untreated cells considered as 1 (*P<0.05).*

For comparison with these experiments in TERT/1 and HEK293A cells, the effect of C-peptide on GPR146 mRNA expression in rat kidney in a diabetic milieu was investigated in kidneys from the diabetic rats that are described in detail in Chapter 5. Again C-peptide administration exerted no detectable effect on GPR146 mRNA (Figure 3.7)

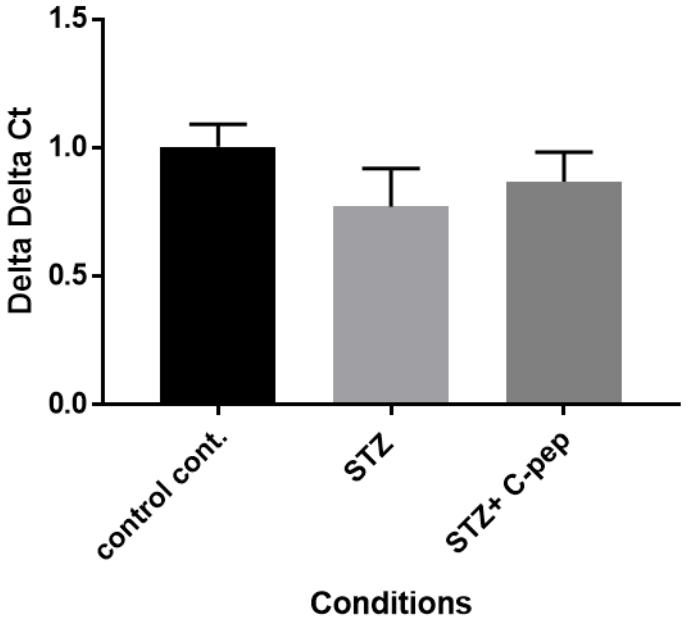

Figure 3.7 Gene expression of GPR146 following treatment with physiological concentrations of C-peptide, in STZ diabetic rat kidney
*(As described in Chapter 2 and Chapter 5)**.** For the C-peptide treatment group, diabetic rats were treated with long-acting C-peptide 0.5mg/kg subcutaneously twice weekly for 29 weeks. Results are expressed as mean ± SEM of 8 rats from the STZ group, 6 rats STZ+C-peptide groups and 2 rats from the healthy control group. GPR146 mRNA expression was calculated relative to the corresponding GAPDH signal for each sample and relative gene expression is presented as ($2^{-\Delta\Delta CT}$).*

3.2.5 Attempted over-expression of EGFP-tagged GPR146 in TERT/1 and HEK293A cells

To investigate whether there was any effect of GPR146 expression on C-peptide signalling, an attempt was made to over-express GPR146 in TERT/1 and HEK293A cells. Plasmid encoding EGFP tagged GPR-146 (as described in Chapter 2) was kindly provided by Dr Ali Janabi (Department of Cell Physiology and Pharmacology University of Leicester) (Janabi, 2017) and was used in attempted transfection experiments with the two cell lines, TERT/1 and HEK293A, that had been shown to respond to C-peptide.

3.2.6 Verification of GPR146-EGFP plasmid integrity

To confirm the identity and integrity of the GPR146-EGFP plasmid, digestion with restriction enzymes, *BamHI*, *HindIII* and *NotI* was performed as described in (Janabi, 2017). The expected restriction sites and fragment sizes derived from the digest are listed in Table 2.3 and were confirmed to be similar to those previously reported in (Janabi, 2017) using a 1% agarose gel to resolve the fragments (Figure 3.8). The plasmid digest DNA was separated successfully into three fragments at expected sizes; 1752 bp, 740 bp, and 1012 bp respectively. The undigested plasmid gave a band at ~ 5000 bp.

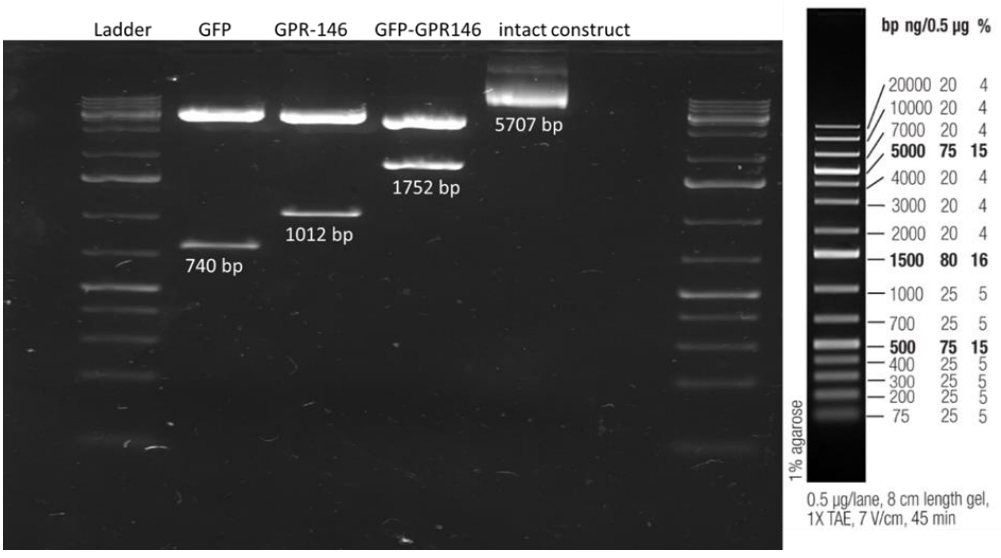

***Figure 3.8 BioRad*C*chemi-doc image of fragments following restriction enzyme digest to* confirm *the GPR146-EGFP plasmid integrity*.**
Lane 2 HindIII/notI/BamHI digest yielding GFP ; lane 3, HindIII/BAMHI digest yielding GPR146; lane 4, NOTI/HINDIII digest yielding GFP-GPR146; and lane 5 undigested GPR146-EGFP plasmid.

3.2.7 Attempted transient expression of EGFP-tagged GPR146 or EGFP in TERT/1 and HEK293A cells

The EGFP-tagged GPR146 (GPR146-EGFP) containing plasmid verified in **Section 3.26** was transfected into TERT/1 and HEK293A cells using jetPRIME and calcium phosphate transfection reagent for HEK293A cells; and Transfex reagent for TERT/1 cells as described in Chapter 2. After 24h and 48h of transfection, cells were stained with DAPI stain and assessed under fluorescent cell imaging. The images showed no significant expression of EGFP-GPR146 in either cell line (Figure 3.9 and Figure 3.10). However, there was a very small expression of the EGFP alone containing no GPR146 cDNA (empty vector) in HEK293A cells (Figure 3.9B and Figure 3.9D).

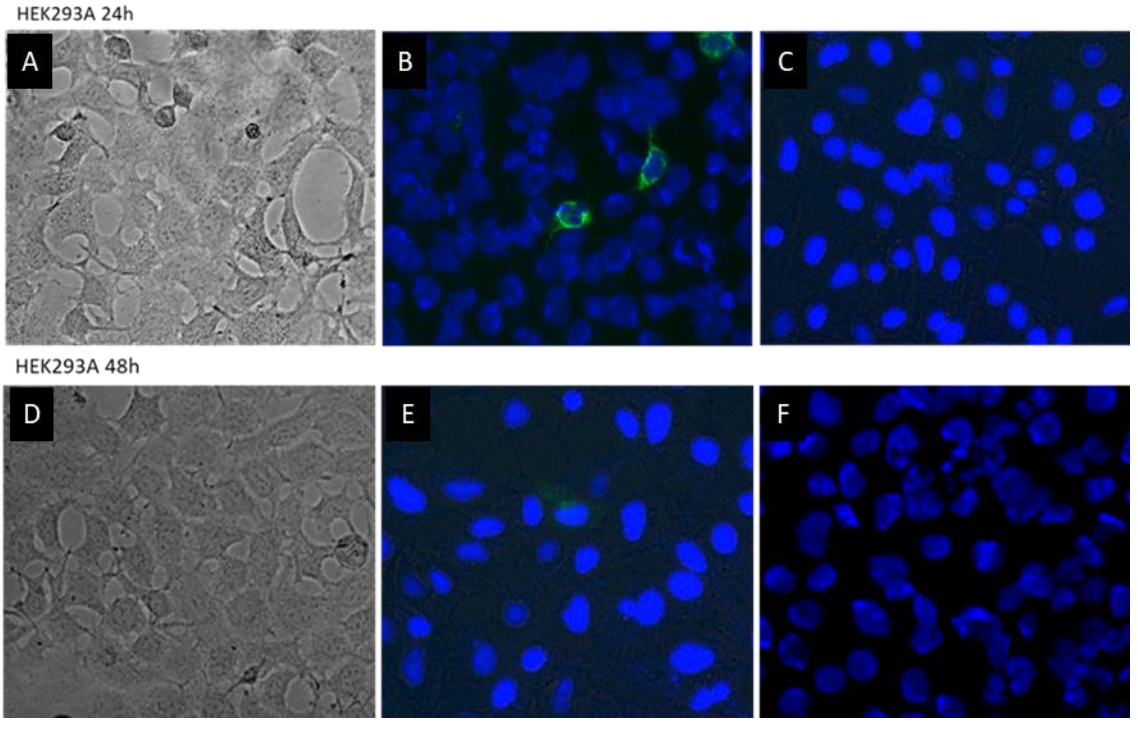

Figure 3.9 Fluorescent cell imaging of HEK293A cells after attempted transient expression of either GPR146-EGFP or EGFP empty vector after 24 and 48h.
HEK293A-GPR146-EGFP or HEK293A-EGFP were imaged by fluorescent cell imaging following addition of DAPI stain as described in Methods (Chapter 2). The images are represented either as a white light channel (A) and (D) for the non-transfected cells, or as merged image of blue, green and white light channel for the transfected cells. (B) empty vector 24 h, (E) empty vector 48h, (C) EGFP-GPR146 24h, and (F) EGFP-GPR146 48h. Fluorescent cell images are representative of 15 independent experiments.

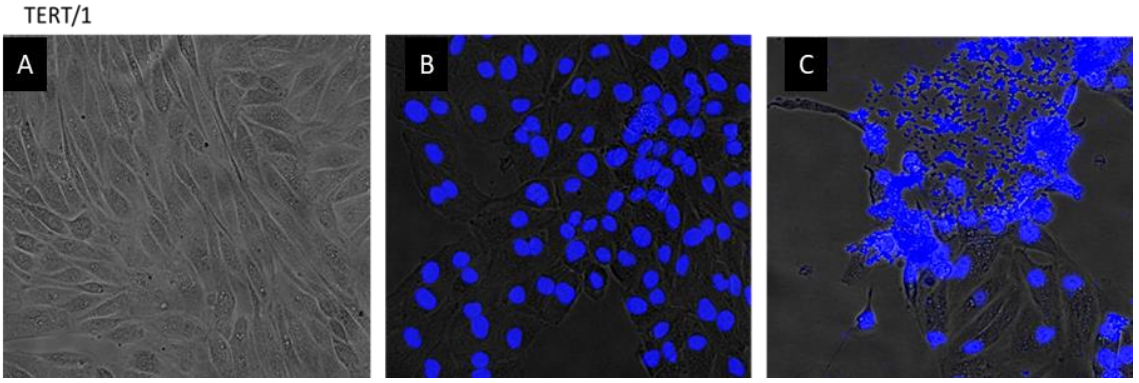

Figure 3.10 Fluorescent cell imaging of TERT/1 cells with transient expression of either GPR146-EGFP or EGFP at 24h.
TERT/1-GPR146-EGFP or TERT/1-EGFP were imaged by fluorescent cell imaging following addition of DAPI stain as described in Methods (Chapter 2). The images are represented either as a white light channel (A) for the non-transfected cells, or as merged image of blue, green and white light channel for the transfected cells. (B) empty vector 24 h, and (C) EGFP-GPR146 24h. Fluorescent cell images are representative of 15 independent experiments.

3.3 Discussion

3.3.1 C-peptide activates ERK1/2 in TERT/1 and HEK293A cells

Data in this chapter show a clear phospho-activation of MAPK ERK1/2 in response to physiological concentration of C-peptide in both TERT/1 and HEK293A cells. The ability of C-peptide to stimulate the phosphorylation of ERK1/2 has previously been reported in OK cells and Swiss 3T3 fibroblasts (Al-Rasheed *et al.*, 2004) (Henriksson *et al.*, 2005).The study of concentration-response effect of low concentrations of C-peptide (0.01 to 10 nM) on ERK1/2 in TERT/1 cell resulted in an approximately bell shaped curve, and similar effects were also shown in OK cells by (Al-Rasheed *et al.*, 2004). HEK293A cells are a sub-clone of the parent HEK293 line showing improved adherence and more flattened morphology (Thermo-fisher 2016) which might have an impact on the cell surface expression or function of the putative C-peptide receptor. Although it has been reported that HEK293A cells did not respond to C-peptide (Janabi, 2017), in this study HEK293A cells did show a response to low concentrations of C-peptide (0.01 to 10 nM). The reason for this difference is unknown. . This effect, however, is in a monophasic concentration-dependent manner, unlike the bell shaped curve shown in this chapter with TERT/1 cells, and previously with OK cells (Al-Rasheed *et al.*, 2004b). It is also unlike the sigmoidal shaped curve that was previously reported in human renal tubular cells (Zhong *et al.*, 2005) and capillary endothelial cells of mouse lung (Kitamura *et al.*, 2002).

The precise molecular basis behind this variation in the concentration response curve of C-peptide is not well understood. However, this may be due to the rapid elimination of the C-peptide receptor, or as a result of activation of multiple types of C-peptide receptors in these cells.

Exposing TERT/1 and HEK293A cells to 3nM human C-peptide showed a rapid (5 minutes) but transient activation of ERK1/2, such effects have also been demonstrated for C-peptide (0.1 to 3 nM) in OK Cells (Al-Rasheed *et al.* 2004) and rat myoblast L6 cells (Essid, 2016). The activity of ERK1/2 was seen to descend over longer exposure to C-peptide, suggesting either inactivation of the receptor of C-peptide or degradation of some aspect of the ERK1/2 signaling pathway over time. As this time course was obtained using a single dose of C-peptide (3nM), it would be of interest in future work to compare the time course observed with other doses, for example with 0.3nM which gave significant activation of ERK1/2 in Fig 3.1.

It has previously been established that the majority of C-peptide signalling is sensitive to PTX (Al-Rasheed *et al*., 2004). This suggests that the signalling of C-peptide is mediated by a $G\alpha_{i/o}$-coupled receptor.

It has previously been reported that C-peptide signalling is mediated by orphan GPCR (GPR146) (Yosten *et al.*, 2013). Taking *cFOS* expression as a known intracellular effect of C-peptide that could be used as a convenient read-out, the authors showed that C-peptide signalling to *cFOS* was blunted by knocking down GPR146. However, cFOS expression induced by foetal bovine serum (FBS) was also blocked by the knock-down of GPR146 (Yosten *et al.*, 2013). As there are likely to be many factors in serum (in addition to C-peptide) that can activate *cFOS*, this suggests that the silencing of GPR146 might be acting directly on *cFOS* signalling rather than acting exclusively on the C-peptide receptor. To test this alternative explanation, the authors showed that even though applying siRNA against GPR146 in KATOIII cells significantly decreased the expression of GPR146, these transfected KATOIII cells still showed a significant increase in the expression of *cFOS* after treatment with 30nM neuronostatin – a peptide that signals through a different GPCR (Yosten *et al.*, 2012). It therefore seems unlikely that GPR146 silencing acts by knocking out all *cFOS* signalling.

Further evidence that GPR146 may be a component of the C-peptide receptor has come from a more recent study using different methods i.e. targeting the GPR146 protein (Richards *et al*., 2014). The presence of the GPR146 protein has been reported in immunoblotting experiments with anti-GPR146 antibody in KATOIII cells, TF-1 cells and human erythrocytes. When human erythrocytes are exposed to a low oxygen concentration, ATP is released from the cells. A physiological C-peptide concentration blunted this effect. However, when the cells were pre-incubated with an antibody that recognises an extracellular epitope of GPR146, this effect of C-peptide was abolished, suggesting that the antibody blocks C-peptide binding to GPR146 and therefore acts as a neutralising antibody for the C-peptide receptor. However, the putative receptor is yet to be further investigated. In the present study, if GPR146 is the receptor of C-peptide, the mRNA expression of the receptor in the TERT/1 and HEK293A cells that were shown to be responsive to C-peptide and in diabetic rat kidney might have been expected show response to treatment with C-peptide (by analogy with the previously reported effect of luteinising hormone on its GPCR (Menon *et al.*, 2011). Stimulation of TERT/1 and HEK293A cells and prolonged stimulation of diabetic rat kidney *in vivo* with C-peptide, in this study, did not show any effect of C-peptide on the expression of the proposed receptor GPR146 (Figure 3.5 – Figure 3.7). However stimulation of these cells (TERT/1 and HEK293A) with 10% DFBS led to a decrease in GPR146 mRNA expression after 2 hr of exposure (see Section 3.3.2 below).

A further complication in research on the C-peptide receptor is that several studies have suggested that insulin and C-peptide signalling interact (Wahren *et al.*, 2012; Luppi, *et al.*, 2011) and some have reported that the insulin receptor interferes with $G\alpha_q$ coupled GPCR signalling. This is relevant because Wahren (2012) showed that C-peptide signalling is likely to be through G_{aq}. Yosten 2013 reported, after treatment with C-peptide, an infrequent co-localization between GPR146 (C-peptide receptor) and the insulin receptor was detected, suggesting that it might be necessary to stimulate with insulin along with C-peptide to observe the full interaction between GPR146 and insulin receptor. However, stimulation with both C-peptide and insulin did not cause internalisation of the receptor in either HEK293-GPR146-EGFP or HEK293A-GPR146-EGFP (Janabi, 2017).

In order to further examine the claim that GPR146 is C-peptide's receptor, a transient expression of EGFP-GPR146 was attempted in the two cell lines that had been shown to

respond to C-peptide (Figure 3.1 and Figure 3.2) (TERT/1 and HEK293A). In spite of repeated attempts, only very low transfection efficiency was observed. The reason for this is unknown, but some of the experiments with the GPR146-EGFP construct were accompanied by morphological changes suggesting declining cell viability.

3.3.2 Physiological significance of GPR146

Abundant evidence accumulated elsewhere (Janabi, 2017) suggests that GPR146 is unlikely to be a direct receptor for C-peptide. Furthermore, recent work has suggested that, at least in hepatocytes, the biological function of GPR146 is to signal through phospho ERK1/2 (P-ERK1/2) and through activation of hepatic sterol regulatory element binding protein 2 (SREBP2) to promote VLDL secretion and hence reduce the plasma concentration of cholesterol in mice, and possibly in humans. Also the knockout of GPR146 remarkably reduces plasma cholesterol levels in both wild-type and LDL receptor (LDLR)-deficient mice (Yu *et al.*, 2019). GPR146's natural ligand(s) is (are) still unknown but (like C-peptide) the natural ligand is thought to increase on feeding (Yu *et al.*, 2019) and might be a lipid ligand encountered in plasma, possibly consistent with the apparent down-regulation of GPR146 mRNA by serum that was observed in Fig 3.5 and Fig 3.6.

3.3.3 Application of the work from this chapter.

The clear detection of C-peptide signalling to P-ERK1/2 in the two renal cell lines that were studied in this chapter suggests that these cells may be suitable models in which to investigate further the factors (such as the inorganic phosphate concentration) that may control C-peptide sensitivity *in vitro*. Experiments of this type are the subject of the next chapter of this thesis.

4 Chapter 4 Interaction between C-peptide and inorganic phosphate (Pi) in TERT/1 cells

4.1 Introduction

Hyperphosphatemia is a common complication of CKD, especially end-stage CKD. The loss of kidney function leads to elevation in Pi levels in plasma causing hyperphosphatemia (Bevington *et al.*, 1990). It has been shown that changes in the extracellular Pi concentration may lead to alteration in the intracellular Pi concentration, for example in cultured vascular endothelial cells (Abbasian *et al.*, 2015). It has also been shown that Pi can act as a signalling molecule (Bon *et al.*, 2018; Michigami, 2013) which leads to direct alteration in the cellular physiology and gene expression in mammalian cells (Michigami, 2013; Camalier *et al.*, 2013). This direct alteration in intracellular signalling includes changes in protein phosphorylation, including increased phospho-activation of MAPK ERK1/2 in primary mouse calvaria-derived osteoblasts and osteoblasts (MC3T3-E1 cells).(Julien *et al.*, 2009).

Even though there is evidence that administration of C-peptide produced marked effects in improving the diabetic neuropathy observed in a rodent model of T1DM (Sima *et al.*, 2001), this improvement could not be seen in a more recent clinical trial in humans (Wahren *et al.*, 2016b). One key difference between humans and rodents is the plasma Pi concentration. The plasma Pi concentration in humans is approximately 1mM, while in rodents it is 2 to 2.5mM (Haut *et al.*, 1980; Cargnello & Roux, 2011). Abbasian *et al.*, 2015 showed that extracellular Pi concentration could modulate protein phosphorylation signaling pathways in mammalian cells. This includes the key regulatory protein kinase MAP ERK1/2 which has been shown to be phosphorylated in response to higher extracellular Pi concentration (Cargnello & Roux, 2011) possibly because of the ability of intracellular Pi to inhibit phosphoprotein phosphatases (Abbasian *et al.*, 2015) or because of direct sensing of extracellular Pi concentration by Pi transporters of the SLC20 gene family (Bon *et al.*, 2018). This suggests that extracellular Pi concentration might also play a role in altering the effects of hormones and other agonists that signal through protein phosphorylation events. As both C-peptide and Pi (Bon *et al.*, 2018) can signal through MAP ERK1/2, C-peptide may be such a hormone.

The initial aim of the study described in this chapter was therefore to investigate the effect of a Pi load on the phosphorylation of ERK1/2 and whether it enhances the ERK1/2 response to C-peptide in TERT/1 and HEK293A cells.

4.2 Results

4.2.1 Effect of C-peptide and inorganic phosphate (Pi) on ERK1/2 phosphorylation in TERT/1 and HEK293A cells

In these experiments, cells were pre-incubated for 90 min with medium containing 1mM or 2.5mM Pi, then treated with various concentrations of C-peptide (0.01, 0.03, 0.1, 0.3, 1, 3, and 10 nM) for 5min in the presence of 1mM or 2.5mM Pi. As observed previously in Chapter 3, in the presence of medium containing the normal Pi concentration of 1mM, C-peptide showed a dose-dependent stimulation of ERK1/2 phosphorylation, reaching a maximum at a dose of 0.3 nM, followed by a decline at 1 nM or above (Figure 4.1). In the absence of C-peptide, 2.5mM Pi alone also strongly stimulated ERK1/2 phosphorylation (Figure 4.1). However, the effects of C-peptide and of Pi were not simply additive and there might be an interaction between C-peptide and Pi load on the activation of ERK1/2. In the 2.5mM Pi medium, the stimulation of ERK1/2 phosphorylation by C-peptide seemed to give a biphasic response, achieving a maximal response with as little as 0.03 nM C-peptide and again at 1-3nM (Figure 4.1), the response here with as little as 0.03nM implied that Pi was increasing the sensitivity of the cells to C-peptide. This impression was confirmed by 2-way ANOVA which demonstrated independent statistically significant effects of C-peptide and of Pi, but also demonstrated a statistically significant interaction between C-peptide and Pi (summarised in the legend of Figure 4.1). Pi and C-peptide therefore seem to reinforce one another's effect, i.e. a Pi load may increase the sensitivity of C-peptide on activation of ERK1/2 in TERT/1 cells.

In contrast in HEK293A cells there was no significant effect of an extracellular Pi load on the ERK1/2 phosphorylation response. As in Chapter 3, in the presence of 1mM Pi, C-peptide gave a gradual monophasic increase in ERK1/2 phosphorylation, reaching a maximum with 10 nM C-peptide, the highest dose tested (Figure 4.2). Raising the Pi concentration in the medium to 2.5mM had no detectable effect of the basal ERK1/2 phosphorylation response, nor did 2-way ANOVA detect any significant interaction between the effects of C-peptide and Pi (summarised in the legend of Figure 4.2).

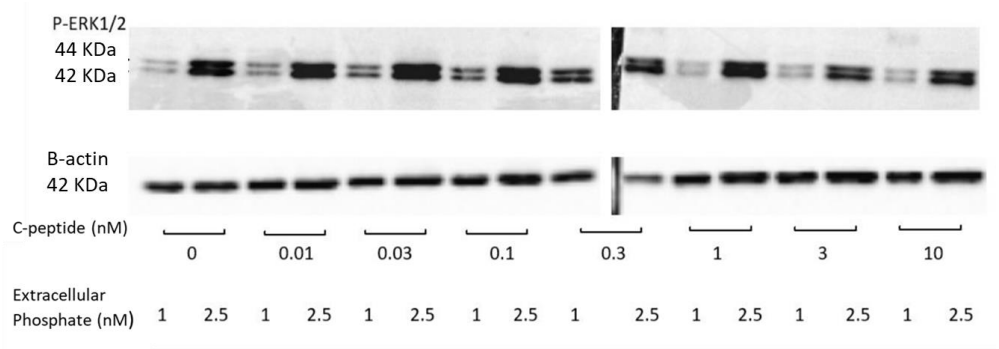

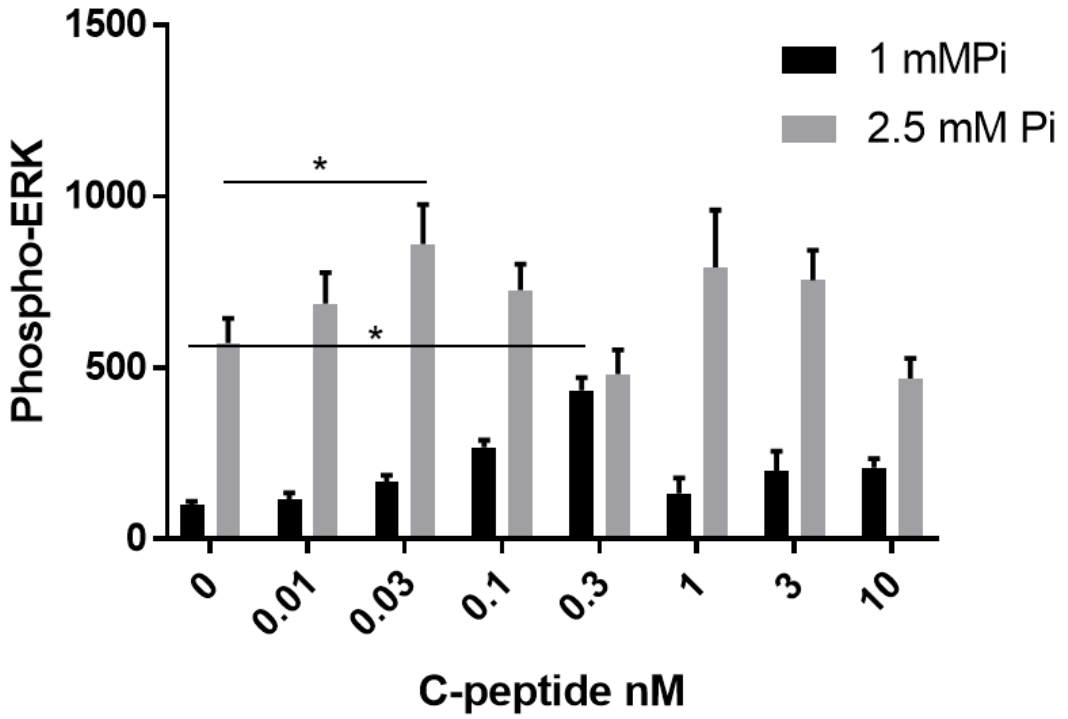

Figure 4.1 The effect of 90 min of pre-incubation with 1mM and 2.5 mM Pi followed by a 5 minute incubation with C-peptide on ERK1/2 activation in TERT/1 cells.

*TERT/1 cells were incubated with either 1 or 2.5 mM Pi in presence of a range of C-peptide concentrations (0.01, 0.03, 0.1, 0.3, 1, 3, and 10 nM). Densitometric analysis for ERK1/2 is presented as the ratio relative to β-actin. Data are expressed as control (0)-fold change (i.e. the ERK1/2 densitometry signal divided by the corresponding actin densitometry signal, expressed as a % of the value observed in control medium with 1mM Pi and no C-peptide). 2-way ANOVA showed a significant effect of Pi (P<0.0001); significant effects of C-peptide (*P<0.05); and significant interaction between Pi and C-peptide (P<0.001). The presented values are mean ± SEM, n = 4.*

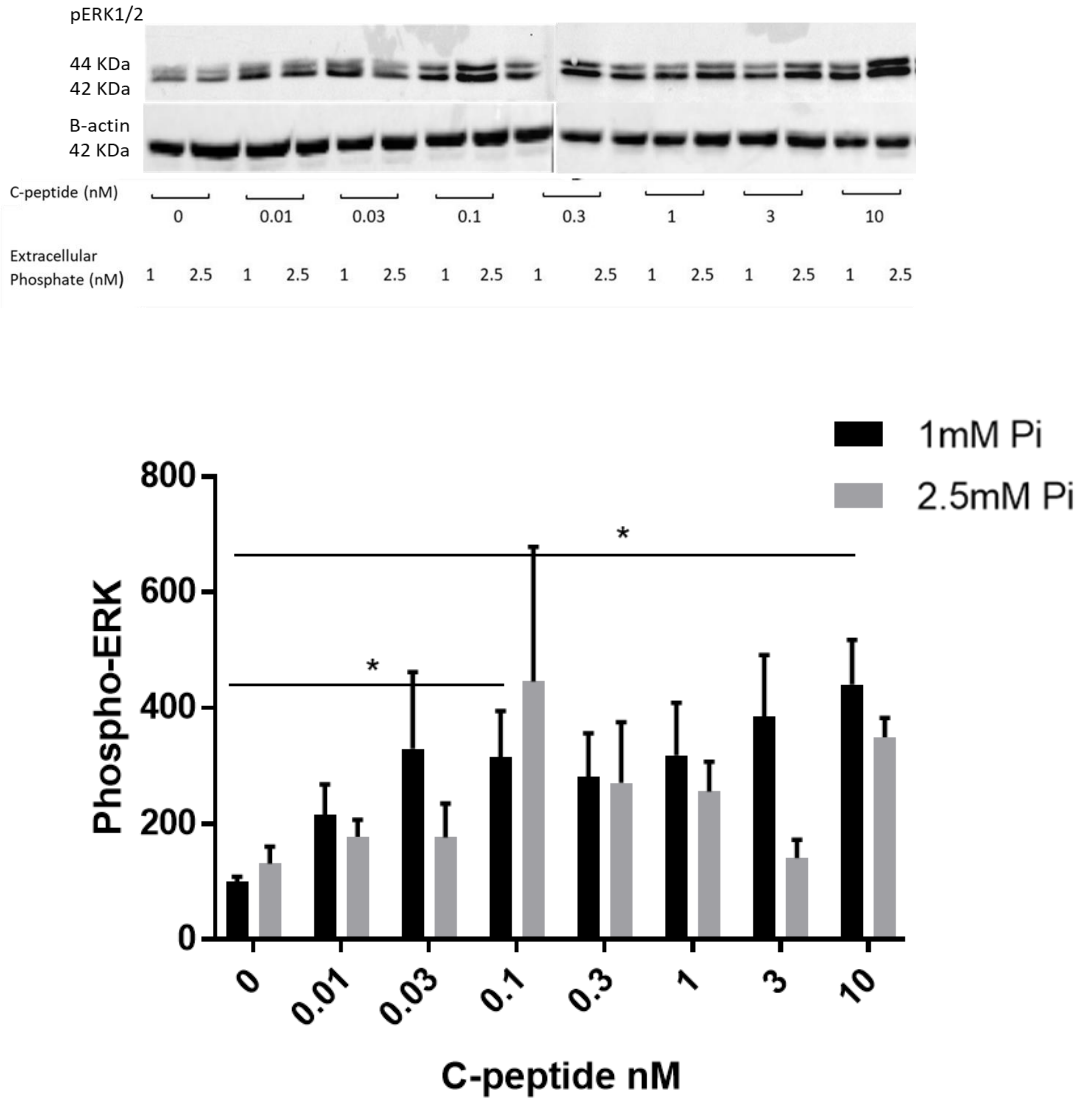

Figure 4.2 The effect of 90 min of pre-incubation with 1mM and 2.5 mM Pi followed by a 5 minute incubation with C-peptide on ERK1/2 activation in HEK293A cells.
*HEK293A cells were incubated with either 1 or 2.5 mM Pi in presence of a range of C-peptide concentrations (0.01, 0.03, 0.1, 0.3, 1, 3, and 10 nM). Densitometric analysis for ERK1/2 is presented as the relative ratio to B-actin. Data are expressed as control (0)-fold change as in Fig 4.1. 2-way ANOVA showed a significant effect of C-peptide (*P<0.05); but no significant effect of Pi (P= 0.1765); and no significant interaction between Pi and C-peptide (P= 0.6412). The presented values are mean ± SEM (n=3).*

4.2.2 Using Pi analogues as probes for Pi sensing

As was outlined in Chapter 1 (Section 1.6.3), structural analogues of Pi can be used to probe the biological effects of Pi on intact cells. As the analogues vanadate (Vi), phosphite (Phi) and hypophosphite (HPhi) are not regarded as metabolisable to organic phosphate analogues in mammalian cells, probably acting by non-covalent binding to target proteins such as phosphoprotein phosphatases or Pi transporters (Section 1.6.3), they can be used to test whether the effect of Pi in Section 4.2.1 requires incorporation of Pi into organic phosphates.

4.2.3 The effect of extracellular vanadate (Vi) as a Pi analogue with C-peptide on ERK1/2 phosphorylation

To investigate the effect of a vanadate load on the phosphorylation of ERK1/2 and whether it enhances the cell response to C-peptide in TERT/1 cells, cells were pre-incubated for 90 min with 100µM vanadate in a medium containing 1mM Pi then treated with various concentrations of C-peptide (0.01, 0.03, 0.1, 0.3, 1, 3, and 10 nM) for 5min in presence of 100µm vanadate. Like Pi, vanadate was found to exert a stimulatory effect on P-ERK1/2 suggesting that both Pi and its structural analogue vanadate might exert their effects on the TERT/1 cells via a similar mechanism. However, unlike Pi, vanadate and C-peptide did not significantly reinforce one another's effect on ERK1/2 phosphorylation (Figure 4.3). In this experiment C-peptide in the presence of 1mM Pi induced an apparent maximal stimulation of ERK phosphorylation at a dose of 0.3nM as in Fig 4.1, but in Fig 4.3 this fell short of statistical significance.

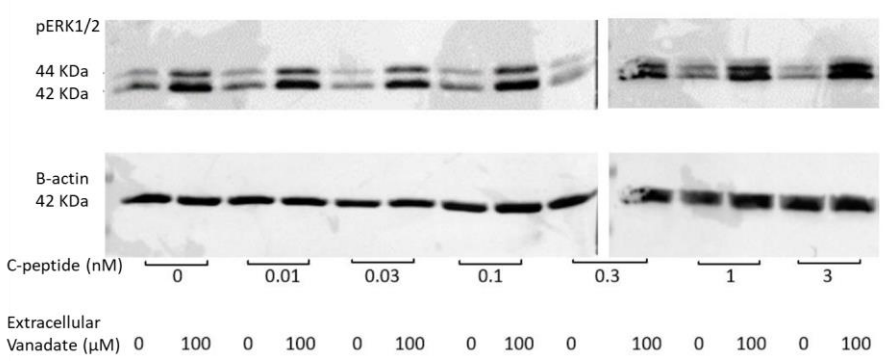

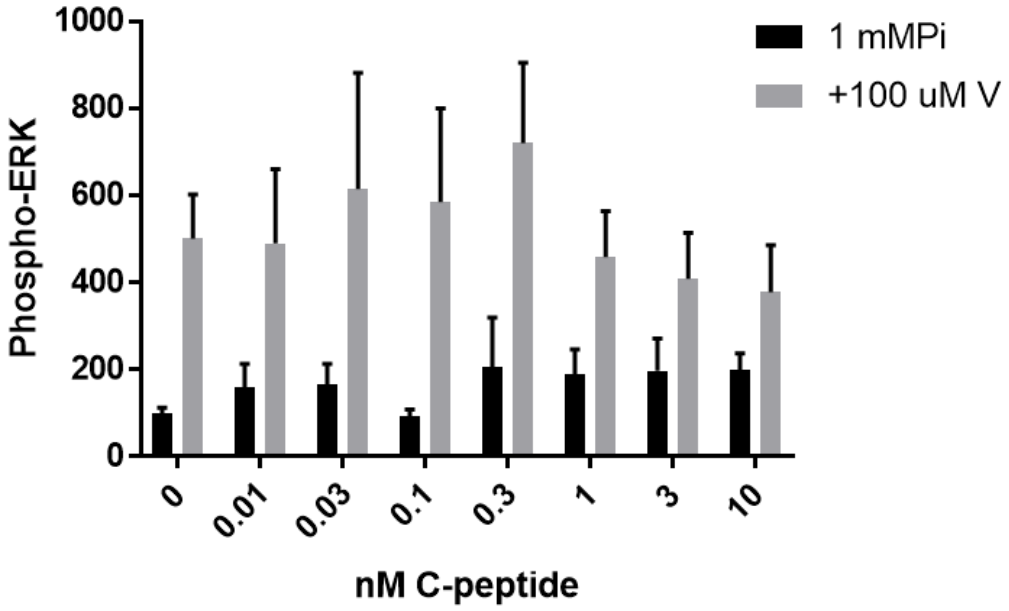

Figure 4.3 Effect of 90 min of pre-incubation with 100uM vanadate followed by a 5 minute incubation with C-peptide on ERK1/2 activation in TERT/1 cells.

TERT/1 cells were incubated with either 1mM Pi or 1mM Pi + 100μM vanadate in presence of a range of C-peptide concentrations (0.01, 0.03, 0.1, 0.3, 1, 3, and 10 nM). 2-way ANOVA showed a statistically significant effect of vanadate (P<0.05) but no significant effect of C-peptide on the response of ERK1/2, nor any interaction between C-peptide and vanadate. Densitometric analysis for ERK1/2 is presented as the ratio relative to β-actin. Data are expressed as fold change relative to the control (no C-peptide with 1mM Pi). The presented values are mean ± SEM (n=3).

4.2.4 Effects of other Pi analogues phosphite and hypophosphite on the activation of ERK1/2

To investigate the effect of other Pi analogues on the activation of ERK1/2 in TERT/1 cells, the cells were incubated with basal medium containing 1mM Pi supplemented with either an extra 1.5mM Pi, or 1.5mM Phi, or 1.5mM HPhi for 90 minutes. As shown in Fig 4.4, these Pi analogues stimulated the activation of ERK1/2 in TERT/1 cells compared with the control value obtained with 1mM Pi alone. Vanadate was used as a positive control as it had been shown previously (Figure 4.4) to have a statistically significant effect on the activation of ERK1/2. Both Phi and HPhi were shown to have statistically significant effects in increasing the phosphorylation of ERK1/2.

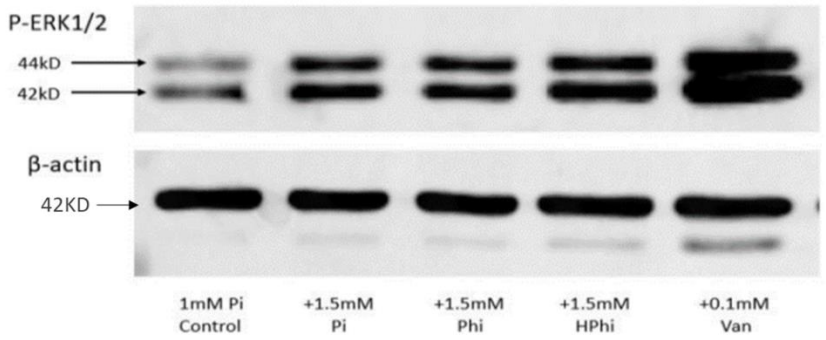

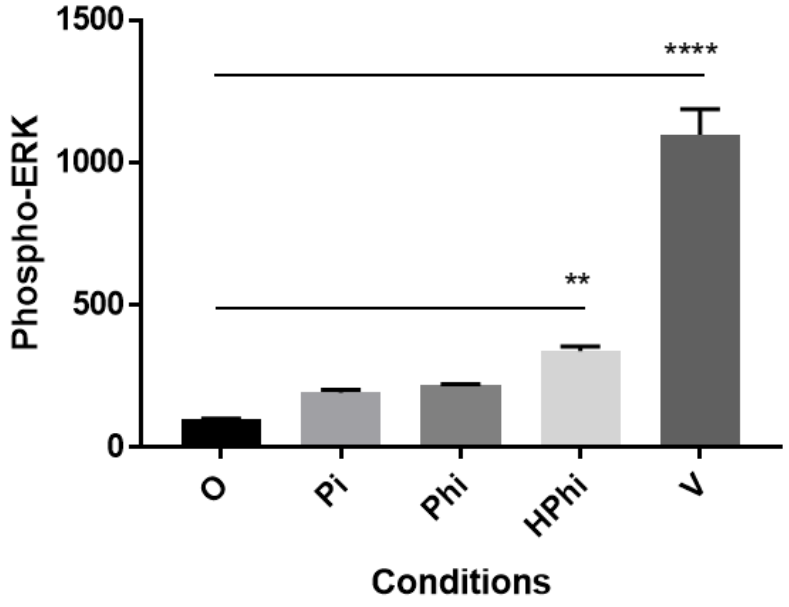

Figure 4.4 Effect of 90 min incubation with either 1.5mM Phi or 1.5mM HPhi in presence of 1mM Pi on the activation of ERK1/2 in TERT/1 cells.
*TERT/1 cells were incubated for 90 minutes with either 1.5mM additional Pi, 1.5mM Phi, or 1.5mM HPhi, comparing with control medium "O" which contained a basal concentration of 1mM Pi. 100μM vanadate was used as a positive control. Densitometric analysis for ERK1/2 is presented as the relative ratio to β-actin. Data are expressed as fold change relative to the control (0). One way ANOVA showed a significant effect of Phi (**P<0.01) and HPhi (****P<0.0001). The presented values are mean ± SEM (n=3).*

4.2.5 A model to explain interaction between C-peptide and Pi

Two possible mechanisms have been published in the literature which suggest how extracellular Pi signals to ERK1/2;

Mechanism 1: involves heterodimerization of the plasma membrane Pi transporter proteins PiT1 and PiT2, which can directly sense the extracellular Pi. The downstream signalling from this heterodimer then leads to the activation of ERK1/2. This may be a direct signal from the heterodimer rather than from the uptake of Pi through the PiT1 and PiT2 transporters (Bon *et al.*, 2018).

Mechanism 2: involves the uptake of extracellular Pi leading to a rise in the intracellular Pi concentration which then inhibits phosphoprotein phosphatases (Dick *et al.*, 2011). This then leads to phosphoprotein accumulation, including phospho-activated ERK1/2 (Abbasian *et al.*, 2015).

The aim of the experiments described in the remainder of this chapter is to investigate **Mechanism 2** by testing the following hypothesis which is outlined in the schematic diagram in Figure 4.5;

a) The stimulatory effect of Pi and C-peptide together on ERK phosphorylation in TERT/1 arises due to Pi uptake via Na^+-dependent active Pi transporters of the SLC20 and SLC34 gene families which increase the intracellular Pi concentration which then inhibits phosphotyrosine protein phosphatase(s) inside the cell thus increasing ERK phosphorylation.
b) The reinforcing effect of Pi on C-peptide signalling to ERK in TERT/1 cells that was seen in Fig 4.1 is due to up-regulation of Na^+-dependent Pi transporters by C-peptide, thus further increasing the intracellular Pi concentration.

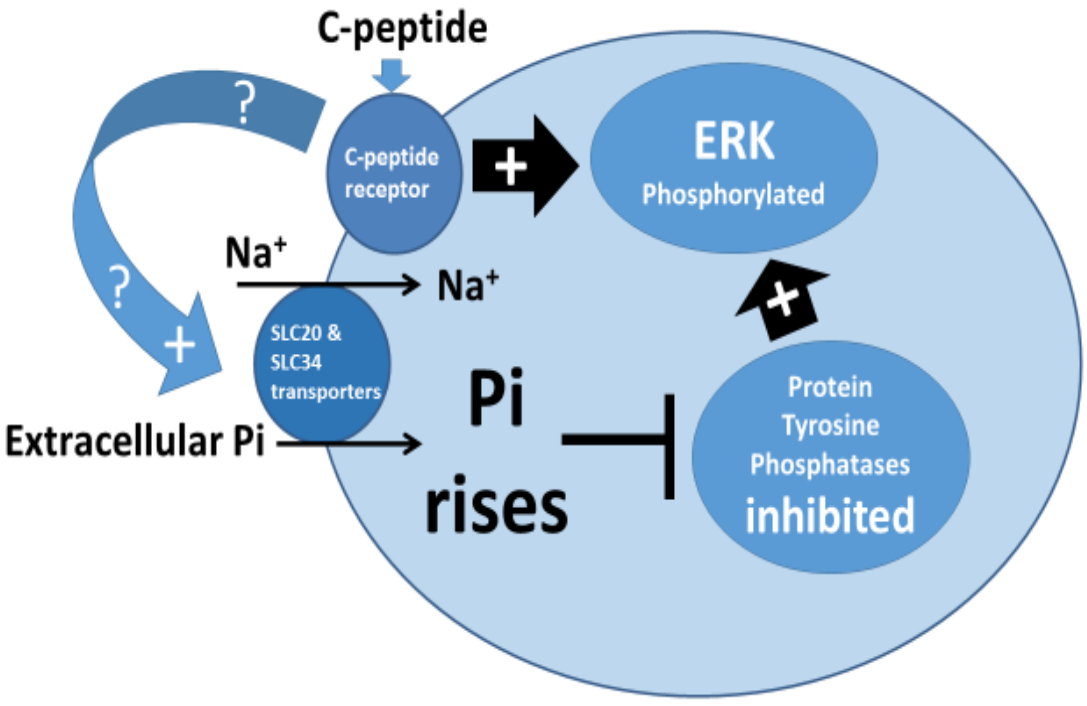

Figure 4.5 Schematic diagram of the hypothesis to explain the stimulatory effect of Pi and C-peptide together on ERK phosphorylation in TERT/1 cells.

4.2.6 The effect of Pi and C-peptide on the cell layer Pi concentration in TERT/1 cells and HEK293A cells.

It was shown above (Figure 4.1) that higher extracellular Pi concentration (2.5mM) induced a rapid increase in the phosphorylation of ERK1/2 both in presence and in absence of C-peptide in TERT/1 cells. Data in Figure 4.1 suggest that C-peptide and higher extracellular Pi may interact in signalling to ERK1/2 in TERT/1 cells. As discussed above (Section 4.2.5 and Figure 4.5), Pi might signal to ERK1/2 indirectly by entering the cell and raising the cellular Pi concentration leading to inhibition of phosphoprotein phosphatases. The first experimental aim was therefore to measure Pi in the cells to determine whether an extracellular Pi load could raise the concentration and whether this concentration was further increased by C-peptide.

4.2.7 The effect of a 90 min extracellular Pi load on the cell layer Pi concentration with or without 3nM C-peptide in HEK293A and TERT/1 cells

When HEK293A and TERT/1 cells were incubated with extracellular Pi at a concentration of 1mM or 2.5mM for 90 min with and without 3nM C-peptide, in both cell types, incubation with the higher extracellular Pi concentration for 90 min failed to increase the intracellular Pi, and no further increase was seen in presence of 3nM C-peptide (Figure 4.6).

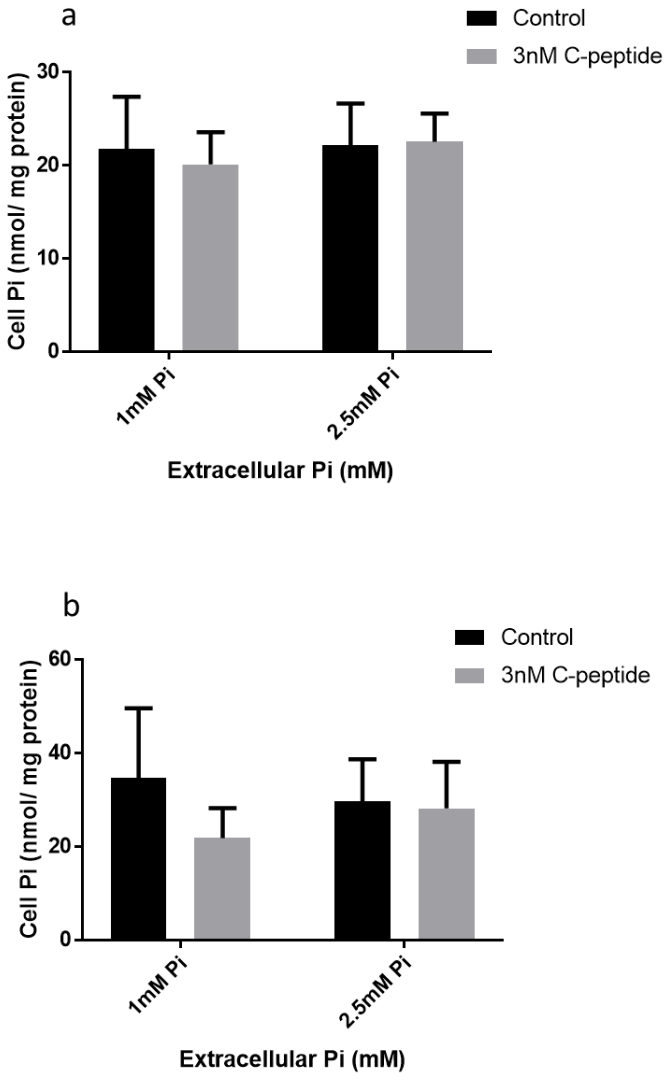

Figure 4.6 The effect of 90 min incubation with a 1 mM and 2.5 mM concentration of extracellular Pi on the cell layer Pi concentration with or without 3nM C-peptide in the MEM incubation medium

(a) in HEK293A cells and (b) in TERT/1 cells. The presented values are mean ± SEM (n=4).

4.2.8 The effect of Pi and of Na^+-deprivation on cell layer Pi in TERT/1 cells and HEK293A cells.

As the selective Pi assay above did not show a detectable effect of the higher extracellular Pi on the cellular Pi, it was therefore necessary to confirm that the assay is detecting intracellular Pi rather than for example extracellular Pi trapped in the cell layer. A possible way to confirm this is by measuring the intracellular Pi after depletion of sodium ions (Na^+) from the medium. As discussed in Chapter 1, in the brush border membrane, the reabsorption of Pi into tubular epithelial cells is carried out through Na^+-dependent transporters of the SLC20 and SLC34 gene families (Forster *et al.*, 2006).

HEK293A and TERT/1 cells were therefore incubated again with extracellular Pi concentrations of 1mM or 2.5mM for 90 min as in Figure 4.6 but sodium ions (Na^+) were removed from the medium in some of the cultures (replaced with choline ions), which should inhibit active Na^+-linked Pi transporters, thus lowering the intracellular Pi concentration. Although, a slight downward trend may have occurred in TERT/1 cells after Na^+ depletion (Figure 4.7), the effect was not statistically significant, whereas a statistically significant decrease in cellular Pi was observed in HEK293A cells ($P < 0.05$) (Figure 4.7) confirming the ability of this assay method to detect changes in intracellular Pi.

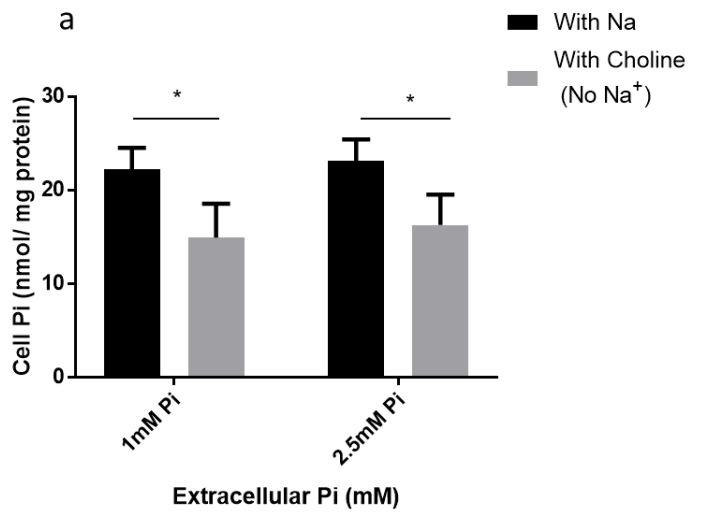

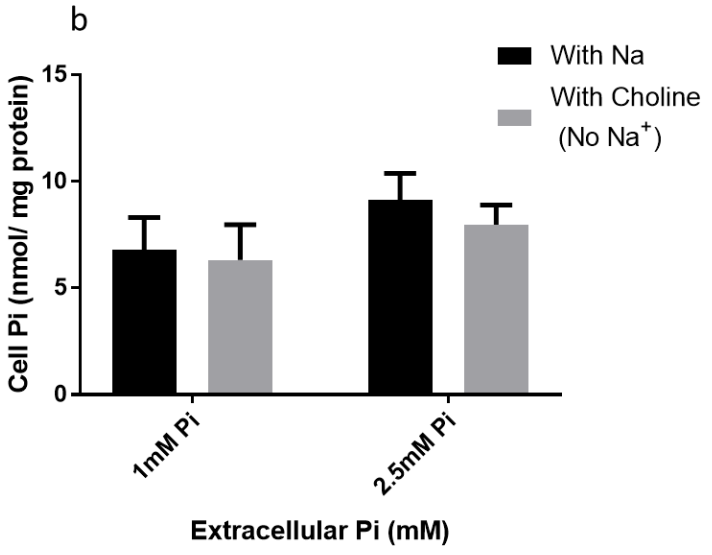

Figure 4.7 The effect of 90 min incubation with a 1 mM and 2.5 mM concentration of extracellular Pi on the cell layer Pi concentration after replacing sodium ions (Na^+) with choline ions in MEM incubation medium

*(a) in HEK293A cells (*P < 0.05) and (b) in TERT/1 cells. The presented values are mean ± SEM (n=4).*

4.2.9 The effect of extracellular Pi load with or without Na^+ on ^{33}Pi transport in TERT/1 cells

As the selective Pi assay and the depletion of sodium ions (Na^+) from the medium above did not show a detectable effect of the higher extracellular Pi on the cellular Pi in TERT/1 cells, it was therefore necessary to further confirm that the assay is detecting intracellular Pi rather than for example extracellular Pi trapped in the cell layer or mitochondrial Pi. Another possible way to confirm this is by measuring the activity of Na^+-dependent Pi transporters in TERT/1 cells which can be assayed directly by measuring transfer of radioactive^{33}Pi (per mg of cell protein) from the extracellular medium into the cells by using a liquid scintillation counter. Such a radioactive ^{33}Pi transport assay was used to investigate further whether Na^+-dependent Pi transporters are expressed in TERT/1 cells (see Section 1.9). At the end of 90 min of incubation with Pi, the uptake of ^{33}Pi into TERT/1 cells was measured in a 5 min incubation in HBS medium containing 0.1mM Pi with or without sodium (Na^+) as shown in Figure 4.8. As expected the depletion of Na^+ significantly decreased ($P<0.01$) ^{33}Pi transported into TERT/1 cells. However, pre-incubation for 90 min with 2.5mM Pi (without Na^+ depletion) had no effect on the Pi transport, indicating that a high (2.5 mM) Pi load does not down-regulate the Na^+-dependent -transporters in TERT/1 cells (this is in contrast to the effect of extracellular Pi previously reported in the LLC-PK1 porcine renal tubular cell line (Caverzasio *et al.*, 1985)).

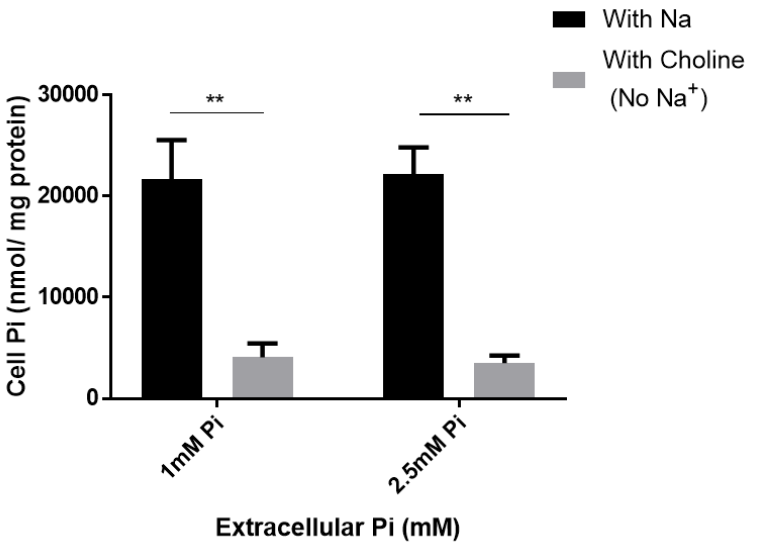

Figure 4.8 The effect on ^{33}Pi transport of incubating TERT/1 cells with an extracellular Pi load for 90 min in HBS medium with 1mM or 2.5mM Pi with or without Na^+.
*After 90 minutes, uptake of ^{33}Pi into the cells was measured in a 5 min incubation in HBS medium with 0.1mM Pi with or without sodium (Na^+). (*P < 0.01). The presented values are mean ± SEM (n=3).*

4.2.10 The effect of 90 min incubations with C-peptide on ^{33}Pi transport into TERT/1 cells

To test the possibility that synergism might have occurred between Pi and C-peptide in signaling to ERK1/2 in TERT/1 cells was because of activation of the Na^+-dependent Pi transporters (Hypothesis Figure 4.5) by C-peptide, the activity of ^{33}Pi transport in TERT/1 cells was measured after stimulation with C-peptide. TERT/1 cells were incubated with extracellular Pi concentration 1mM and 2.5mM for 90 min in the presence of different concentrations of C-peptide (0.01, 0.03, 0.1, 0.3, 1, 3, and 10nM). After 90 minutes, uptake of ^{33}Pi into the cells was measured in a 5 min incubation in HBS medium with 0.1mM Pi with or without sodium (Na^+) (Figure 4.9). The incubations without Na^+ were performed to confirm that uptake of ^{33}Pi was arising mainly from transport through Na^+-dependent transporters as outlined in Section 1.9. The highest concentrations of C-peptide tested (3 or 10 nM) were shown to cause a significant decrease in the Na^+-dependent Pi transport by about 30% in medium containing 2.5mM Pi (Figure 4.9b).

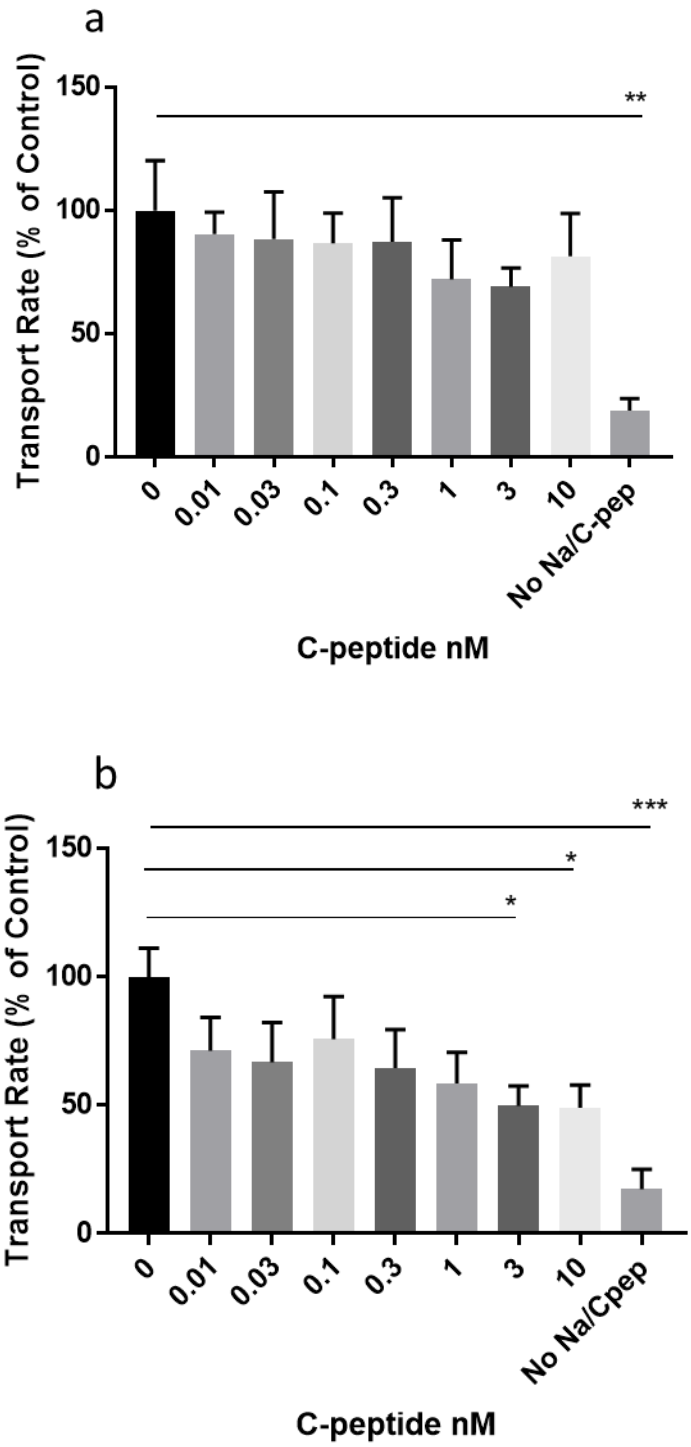

Figure 4.9 The effect of pre-incubation with C-peptide for 90 min in DMEM on ^{33}Pi transport into TERT/1 cells.

*After 90 minutes, uptake of ^{33}Pi into the cells was measured in a 5 min incubation in HBS medium with 0.1mM Pi with or without sodium (Na^+). The presented values are mean ± SEM (n=4). *P< 0.05; **P<0.01; ***P<0.001. (a) Pre-incubation with 1mM Pi in the medium. (b) Pre-incubation with 2.5mM Pi in the medium.*

4.2.11 The effect of C-peptide on mRNA expression of Pi transporters in TERT/1 cells

To identify the Na^+-dependent or Na^+-independent Pi transporters that are expressed in TERT/1 cells and which may be involved in the effect shown in Fig 4.9, RT-Q-PCR Taqman gene expression assays were performed to study the expression of several candidate genes: PiT1 (SLC20A1), PiT2 (SLC20A2), NaPi-IIa (SLC34A1), NaPi-IIc (SLC34A3) and XPR1 (SLC53A1). Briefly, these genes were selected in this study because they are expressed in renal tubular epithelium: NaPi-IIa and NaPi-IIc are responsible for Pi reabsorption in kidney across the brush border (Forster *et al.*, 2006), XPR1 is responsible for the basolateral transport of Pi (Ansermet *et al.*, 2017), and PiT1 and PiT2 are reported to signal directly to ERK1/2 by forming a heterodimer acting as a Pi sensor in the plasma membrane (Bon *et al.*, 2018) (although this heterodimer signaling has not so far been reported in renal tubular epithelial cells)..

The effect of C-peptide on the gene expression was studied at two different time points. To study the expression of these genes in response to short C-peptide stimulation as in Figure 4.1, 5 minute stimulations with C-peptide were performed. In addition, prolonged physiological stimulation of renal tubule is reported to alter Pi transporter gene expression (Jacquillet & Unwin, 2019). Therefore to assess such effects (which might be relevant to the decline in the Pi transporter activity in Figure 4.9), a prolonged stimulation (24h) of TERT/1 cells with different concentrations of C-peptide was performed in presence of 1mM or 2.5mM Pi.

Even though rapid (~ 10 min) effects on mRNA stability sometimes occur (Ross, 1995) and may affect NaPi-IIa mRNA (Jacquillet & Unwin, 2019), 5 min stimulations with C-peptide had no detectable effect of the gene expression of PiT1 (SLC20A1), PiT2 (SLC20A2), and XPR1 (SLC53A1) (Figure 4.10). In contrast, 3nM C-peptide, in 24h stimulations, showed a significant down-regulatory effect (about 30 – 50%) on gene expression of PiT2 and XPR-1 in presence of 1mM Pi (Figure 4.11). In presence of 2.5mM Pi, some down-regulation in the gene expression of PiT2 and XPR-1 may also have occurred but this did not reach statistical significance (Figure 4.11). The gene expression of NaPi-IIa (SLC34A1) and NaPi-IIc (SLC34A3) in TERT/1 cells was undetectable in some cultures and very low in others and has not therefore been presented here.

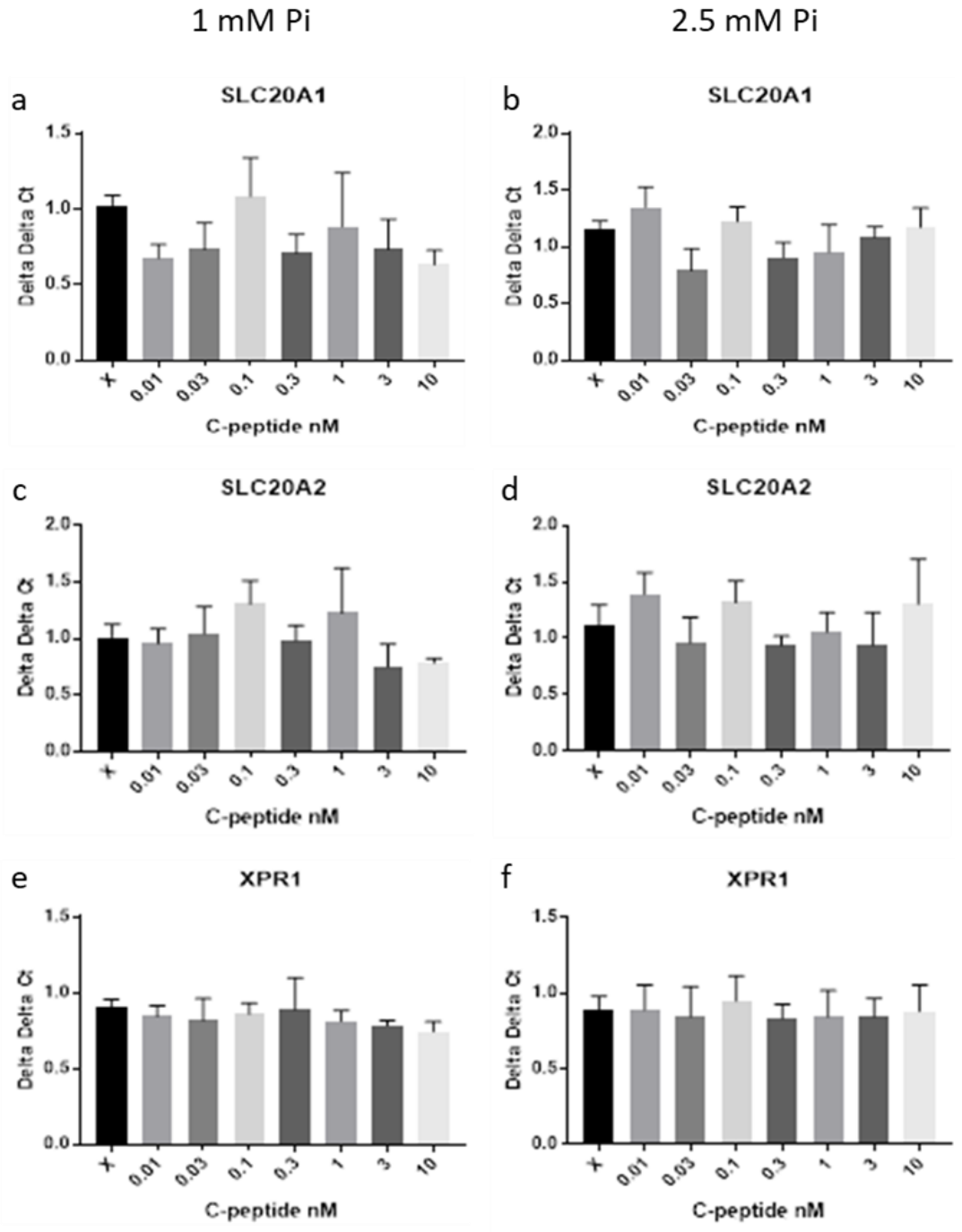

Figure 4.10 The gene expression of Pi transporters SLC20A1, SLC20A2 and XPR1 in TERT/1 cells.

5 min incubations with different concentrations of C-peptide were performed followed by Taqman RT-qPCR assays. (a) PiT1 (SLC20A1) in 1mM Pi medium, (b) PiT1 (SLC20A1) in 2.5mM Pi medium, (c) PiT2 (SLC20A2) in 1mM Pi medium, (d) PiT2 (SLC20A2) in 2.5mM Pi medium, (e) XPR1 (SLC53A1) in 1mM Pi medium and (f) XPR1 (SLC53A1) in 2.5mM Pi medium. Relative mRNA expression of each transporter was calculated using the delta delta CT value method, relative to GAPDH as a house-keeping control gene. Pooled data are shown from n=3 independent experiments. (One-way ANOVA and post hoc testing showed no significant effect of C-peptide relative to the unstimulated control after 5 min stimulation.

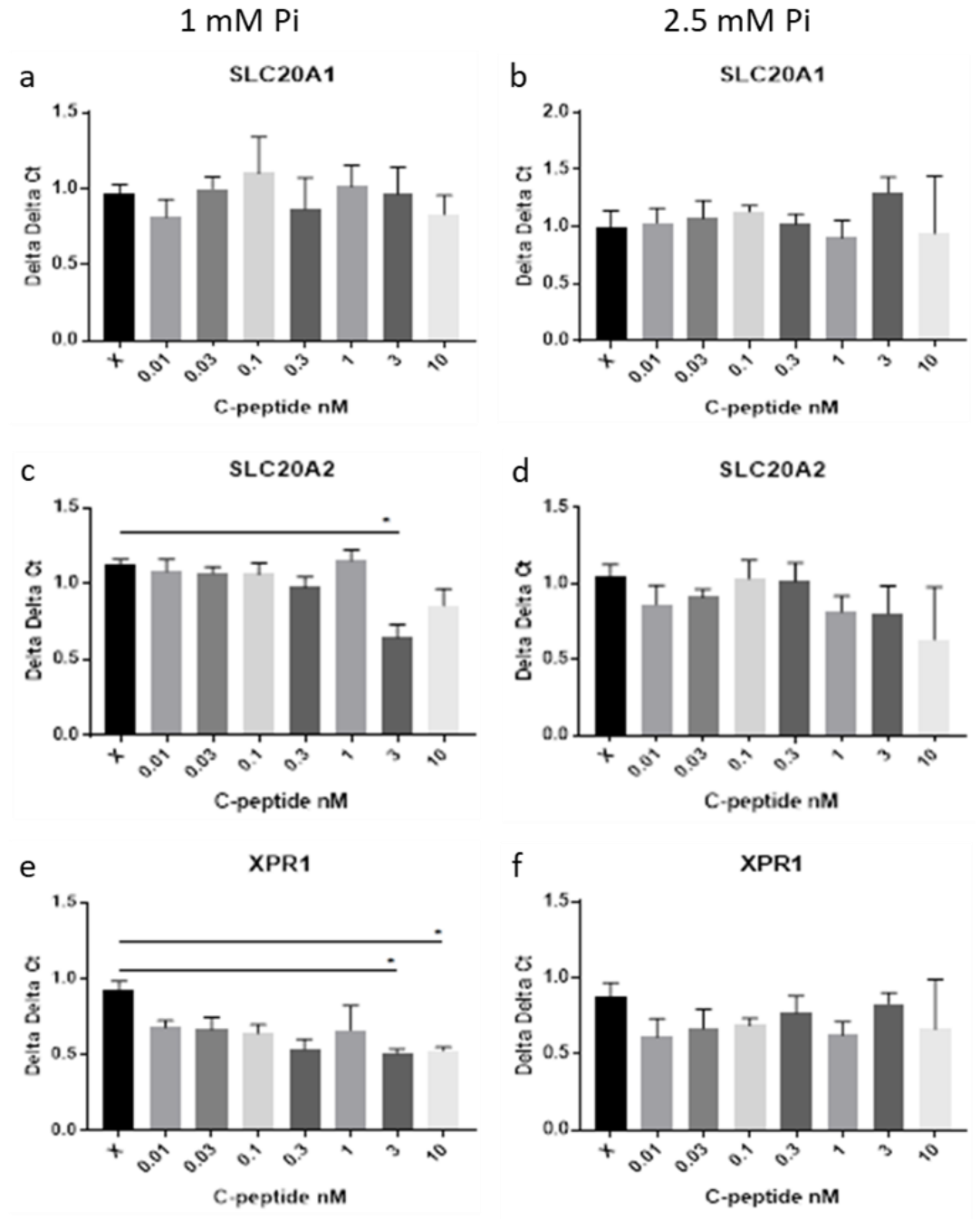

Figure 4.11 The gene expression Pi transporter SLC20A1, SLC20A2 and XPR1 in TERT/1 cells.

*24h incubations with different concentrations of C-peptide were performed followed by Taqman RT-qPCR assays. (a) PiT1 (SLC20A1) in 1mM Pi medium, (b) PiT1 (SLC20A1) in 2.5mM Pi medium, (c) PiT2 (SLC20A2) in 1mM Pi medium, (d) PiT2 (SLC20A2) in 2.5mM Pi medium, (e) XPR1 (SLC53A1) in 1mM Pi medium and (f) XPR1 (SLC53A1) in 2.5mM Pi medium. Relative mRNA expression of each transporter was calculated using the delta delta CT value method, relative to GAPDH as a house-keeping control gene. Pooled data are shown from n=3 independent experiments. (One-way ANOVA and post hoc testing showed a significant down-regulation effect of 3nM C-peptide (c), 3 and 10 nM of C-peptide (e) relative to the unstimulated control after 24h stimulation (*P<0.05).*

4.3 Discussion

Data in this chapter demonstrate a clear activation of a key intracellular signalling element (ERK1/2) mediated by C-peptide at physiological concentrations in TERT/1 cells, an observation that is consistent with the earlier experiments in Chapter 3. This activation was found to be enhanced by higher extracellular Pi concentration (2.5mM), a concentration that occurs in TID patients with CKD and in rodents. Pi has been reported to play a key role in mediating cell signalling and this role might be through a rise in intracellular Pi concentration inhibiting phosphotyrosine protein phosphatases (PTPases) and phosphoserine/threonine protein phosphatases (PSPases) as proposed in Mechanism 2 above (Section 4.2.5).

4.3.1 Pi is unlikely to be acting through phosphoprotein phosphatases

From the experiments presented in this chapter however, it seems unlikely that Mechanism 2 is correct. In both renal epithelial cell lines that were studied here HEK293A and TERT/1, C-peptide and higher extracellular Pi failed to increase the cell monolayer Pi concentration. It has been shown that, in renal tubular epithelium *in vivo*, Pi is transported into cells via Na^+-dependent transporters of the SLC20 and SLC34 gene families (Forster *et al.*, 2006). Therefore, Na^+ depletion was a possible way to test the validity of the method that was used here to measure the intracellular Pi concentration. In HEK293A cells this did result in detectable depletion of cell layer Pi, confirming the ability of the assay to detect changes in cell layer Pi. However, in TERT/1 cells, the depletion of Na^+ did not show a statistically significant effect in decreasing the intracellular Pi, possibly because in these more highly differentiated renal tubular epithelial cells, much of the cell layer Pi is in mitochondria rather than the cytosol, and therefore not directly influenced by the plasma membrane Pi transporters. It was also noted that the Pi concentration detected in the cell monolayer (Fig 4.6b and Fig 4.7b) showed wide variation between replicate experiments. In principle calcium phosphate precipitation into the cell monolayer from the culture medium could contribute to this, a possibility that could be investigated in future experiments by measuring deposition of $^{45}Ca^{2+}$.

This means that the mechanism by which Pi enhances the effect of C-peptide on ERK1/2 is still unknown, but it apparently does not involve altering the intracellular Pi concentration. It therefore seems that Mechanism 2 in Section 4.2.5 (involving a rise in

intracellular Pi concentration resulting in inhibition of intracellular phosphoprotein phosphatases) is unlikely to be correct. This is also consistent with the observation that Pi analogues Phi and HPhi which (unlike Vi) are not thought to be phosphoprotein phosphatase inhibitors, successfully mimic the effect of Pi on ERK phosphorylation (Figure 4.5). In future work it would also be of interest to determine their effect on ERK phosphorylation in the presence of C-peptide. It has also recently been shown in this laboratory that the potent broad-spectrum phosphotyrosine phosphatase inhibitor methyl 3,4-dephostatin (which might be expected to act in a similar way to Vi) failed to increase ERK1/2 phosphorylation in TERT/1 cells (Zeng 2019). A possible explanation is that, in intact cells, inhibiting phosphotyrosine phosphatases does not lead directly to an increase in the phosphorylation of tyrosine residue 204 on p42 ERK2/MAP kinase which is detected by the phospho-specific antibody used in this study (Table 2.2). Instead, the main effect of phosphotyrosine phosphatase inhibition in intact cells has been reported to be inhibition of *Ras*, a stimulatory protein which lies upstream of ERK, thus tending to inhibit rather than activate ERK phosphorylation (Dube *et al.*, 2004).

4.3.2 The mechanism of Pi signaling to ERK1/2

In view of the above, it therefore seems more likely that the other mechanism through which Pi was proposed to signal to ERK1/2 applies in TERT/1 cells (Bon *et al.*, 2018) (i.e. **Mechanism 1** in Section 4.2.5), in which sensing of extracellular Pi (and possibly also Vi, Phi and HPhi) occurs by SLC20 transporter proteins (PiT1 and PiT2 in the plasma membrane) forming a heterodimer which seems to be acting like a receptor for extracellular Pi, allowing the extracellular Pi to bind then signal to ERK1/2 without the need to transport Pi into the cell. The data in this chapter are consistent with the Bon *et al* 2018 heterodimer Pi sensor mechanism, as both PiT1 and PiT2 mRNA were shown to be expressed together in TERT/1 cells (Fig 4.10 and 4.11), although it was not proved that these mRNAs are translated, nor was it shown that the resulting proteins dimerise.

4.3.3 C-peptide effects on Pi transporter activity

The other part of the hypothesis that was proposed in this chapter (Section 4.2.5) was that C-peptide up-regulates Na^+-dependent Pi transporter activity, thus further increasing the intracellular Pi concentration when the extracellular Pi concentration is elevated. It is well established that in diabetic milieu, Na^+-K^+-ATPase is impaired and this impairment enhances the progression of some diabetic complications (Gerbi *et al.*, 1997). Erythrocyte membrane Na^+-K^+-ATPase activity was shown to be lower than normal in diabetic

patients (Dufayet *et al.*, 1998). C-peptide has been shown to activate Na^+-K^+-ATPase through the ERK1/2 signaling pathway in human primary tubular cells (Zhong *et al.*, 2004), and has also been shown to increase the activity of Na^+-K^+-ATPase when injected in TIDM patients (Forst *et al.*, 2000). Na^+-K^+-ATPase maintains the electrochemical gradient of Na^+ across the plasma membrane which is used to drive transport of Pi into cells through Na^+-dependent Pi transporters. It would therefore be reasonable to expect C-peptide to activate Na^+-dependent Pi transport (Section 4.2.5).

However, data presented in Fig 4.9 did not support this hypothesis: - on the contrary, within 90 min 3 nM and 10 nM C-peptide decreased the Na^+-dependent ^{33}Pi transporter activity, in spite of the probable increase in Na^+-K^+-ATPase activity that accompanied this. However, this effect on ^{33}Pi transporter activity only reached statistical significance in the presence of the higher extracellular Pi concentration (2.5mM), possibly because this elevated Pi concentration partly inhibits Na^+-K^+-ATPase as has been shown elsewhere (Huang, W. H. & Askari, 1984).

4.3.4 C-peptide effects on Pi transporter expression

Three gene families (SLC17 family), (SLC34 family), and (SLC20 family) have been shown to perform sodium-phosphate co-transporter activity in mammalian cells (see Chapter 1). In this study, the decrease of Pi transport in response to C-peptide (Figure 4.9) was further investigated by reverse-transcription polymerase chain reaction (RT-PCR). C-peptide was shown to down-regulate the level of mRNA expression of SLC20A2 and SLC53A1 Pi transporters (Figure 4.11) at a concentration of about 3nM (i.e. consistent with the C-peptide concentration that seemed to decrease transporter activity in Figure 4.9). This apparent down-regulation does not explain the apparent synergism between the effects of C-peptide and Pi loading on ERK1/2 signaling that was observed in Fig 4.1, but the possible physiological significance of inhibition of renal Pi transporters by C-peptide is discussed further in Chapter 6.

4.3.5 Conclusion

The data presented in this chapter are consistent with the idea that Pi may interact with C-peptide signalling in its action on cells, which may provide a partial explanation of why C-peptide effects *in vivo* are sometimes more clearly observed in rodents (with 2.5mM plasma Pi) than in humans with 1mM Pi. The idea that C-peptide may exert further potent physiological effects (on inflammatory and disease progression markers) in the relatively hyperphosphataemic environment of a T1DM rat model is tested further in the next chapter.

5 Chapter 5 C-peptide and disease progression markers in a rat model of Type I diabetes

5.1 Introduction

5.1.1 Diabetic nephropathy and inflammation

Traditionally, diabetic nephropathy was not regarded as an inflammatory disease. However, more recent studies have shown that inflammatory processes are vital to the progression of the disease (Lim & Tesch, 2012). There is increasing awareness about cytokines that are involved in the pathogenesis of diabetic nephropathy. Some of the main cytokines that are involved in the promotion and the progression of diabetic nephropathy are summarized in Table 5.1 and are the subject of the work described in this chapter. In addition to the chemokines and cytokines that directly promote inflammation, a key cytokine in the accompanying processes of resolution of inflammation and tissue repair is TGF-β (Serhan *et al.*, 2010b), and there is abundant evidence that if the accompanying TGF-β response becomes excessive, this leads to tubulo-interstitial fibrosis and progression of diabetic nephropathy (see Section 5.1.4 below).

These cytokines (Table 5.1) arise not only from immune cells infiltrating the kidney, but also from renal cell populations, especially tubular epithelial cells (TECs) (see Section 5.1.4.1).

If inflammation is an important process in the development of diabetic nephropathy in T1DM, in principle the absence of C-peptide in T1DM may contribute to this inflammation, and administering C-peptide therapy might suppress the inflammation. There is considerable evidence that C-peptide therapy is anti-inflammatory in T1DM (Haidet *et al.*, 2009; Bhatt *et al.*, 2014; Wahren *et al.*, 2012), although paradoxically the high circulating concentration of C-peptide that occurs in T2DM may be pro-inflammatory (Vasic & Walcher, 2012).

cytokine	function
MCP-1	Chemoattractant which promotes macrophage recruitment into diabetic kidneys
RANTES	Chemoattractant which promotes recruitment of T cells, monocytes, and macrophages
ICAM-1	Adhesion molecule facilitating leukocyte-endothelial adhesion and infiltration into diabetic kidneys
VCAM-1	Adhesion molecule facilitating leukocyte-endothelial adhesion and infiltration into diabetic kidneys
TNF-α	Promotes production of reactive oxygen species, induces cell injury, and increases endothelial permeability
VEGF-a	Chemoattractant which promotes macrophage recruitment into diabetic kidneys
IL-1	Stimulates expression of cell adhesion molecules and profibrotic growth factors and increases endothelial permeability
IL-6	Promotes mesangial cell proliferation, glomerular hypertrophy, fibronectin production and endothelial permeability
TGF-β	A pleiotropic cytokine, promotes resolution of inflammation, and tissue repair by enhancing the synthesis and cross-linking of extracellular matrix and suppressing its degradation. It displays proinflammatory properties by being a potent chemoattractant for neutrophils and promoting inflammation.

Table 5.1 Cytokines thought to play a role in inflammation, resolution, repair and fibrosis during diabetic nephropathy

(Serhan et al., 2010)

5.1.2 Chemo-attractants and immune cell recruitment and adhesion

Chemokines are a family of small cytokines that have a significant role in the chemoattraction and recruitment of inflammatory cells. The hemodynamic and the metabolic effects of diabetes upregulate a number of inflammatory chemokines, mainly MCP-1 (monocyte chemotactic protein-1) and RANTES (regulated on activation, normal T cell expressed and secreted). These chemokines participate in the pathogenesis of DN (Ruster & Wolf, 2008).

Levels of MCP-1 have been shown to be high in patients who developed DKD in both urine and kidney biopsies, as well as facilitating the macrophage infiltration in the tubulointerstitium (Perez-Morales *et al.*, 2019). In cultured human mesangial cells, the expression of MCP-1 correlates with levels of glucose due to the activation of transcription factor NF-kappaB (Panee, 2012). RANTES is another chemokine that is upregulated in a similar way to MCP-1 and plays an important role in DN. RANTES is expressed in a number of renal cells and it is a chemoattractant for monocytes, macrophages, granulocytes and T cells (Lloyd *et al.*, 1997).

The predominantly endothelial adhesion molecules ICAM-1 and VCAM-1 also have a role in facilitating leukocyte-endothelial adhesion and infiltration into diabetic kidneys. Intercellular adhesion molecule 1 (ICAM) is involved in the attachment of leukocytes to endothelium. ICAM-1 has been reported to be induced by hyperglycaemia and it was also found to be highly expressed in T1DM models (Galkina & Ley, 2006b). The high expression of ICAM-1 has been reported to be involved in the progression of DN. High circulating levels of ICAM-1 were also reported to have a role on the induction of microalbuminuria alongside the soluble form of vascular cell adhesion molecule 1 (VCAM-1) (Chow *et al.*, 2005b; Okada *et al.*, 2003b) which is another adhesion molecule that is involved in the adhesion and recruitment of leukocytes. The expression of VCAM-1 was shown to be elevated in kidneys of diabetic patients and rodents during diabetes (Seron *et al.*, 1991; Ina *et al.*, 1999). In T1D diabetic patients, high circulating levels of VCAM-1 were also shown to be associated with albuminuria (Lim H. & Tesch, 2012).

Vascular endothelial growth factor (VEGF) is an important cytokine that has a key role in the pathogenesis of endothelial dysfunction during diabetes (Connolly *et al.*, 1989; Connolly *et al.*, 1989). It is also involved in the progression of diabetic nephropathy as its mRNA levels were found to elevate in response to high glucose in cultured rat mesangial cells. VEGF, in diabetic patients, was also found to correlate with proteinuria.

In early stages of DKD, VEGF was found to be upregulated mainly in glomerular epithelial cells, and found to be highly expressed in proximal tubule in advanced stages of the disease (Cha *et al.*, 2000).

5.1.3 Proinflammatory cytokines

TNF-α, in kidney, is produced by a number of cell types including renal tubular cells, mesangial cells, endothelial cells and podocytes (Jevnikar *et al.*, 1991; Lim & Tesch, 2012). TNF-α plays a crucial role in the pathogenesis of DN by promoting the production of reactive oxygen species, induction of apoptosis and necrosis, as well as increasing albumin permeability (Radeke *et al.*, 1990; McCarthy *et al.*, 1998). It is also involved in decreased glomerular filtration rate and recruiting leucocytes (Lim. & Tesch, 2012; Baud & Ardaillou, 1995). Interleukin-1β (IL-1β) expression was shown to be elevated in kidney of diabetic rats (Navarro *et al.*, 2006). IL-1β was shown to elevate the levels of ICAM-1 and VCAM-1 in rat mesangial cells (Lim & Tesch, 2012). It was also found along with interleukin 6 (IL-6) to be involved in the stimulation of fibroblast proliferation, TGF-*β* production, mesangial cell proliferation, and endothelial cell permeability (Pfeilschifter *et al.*, 1989; Vesey *et al.*, 2002; Ruef *et al.*, 1990). IL-6 was found to be high in T1DM patients and diabetic animals and it correlates with kidney hypertrophy and albuminuria (Aso *et al.*, 2004; Lim & Tesch, 2012).

5.1.4 TGF-β and renal fibrosis

5.1.4.1 Collagen type IV and diabetic nephropathy in cell culture and animal models

Tubulointerstitial fibrosis, which is characterized by increase of the extracellular matrix components and increase of the basement membrane component collagen type IV, is a major complication of diabetic nephropathy (Zeisberg & Kalluri, 2004). Tubulointerstitial fibrosis is one important contributor to diabetic nephropathy, as it correlates to the severity of the damage in renal function (Zeisberg & Kalluri, 2004; Ziyadeh 1996). One of the main characteristics of tubulointerstitial fibrosis is accumulation of extracellular matrix components. The tubulointerstitium is composed of interstitial fibroblasts and predominantly tubular epithelial cells (TECs) (Harris, 2001). The TECs during tubulointerstitial fibrosis produce fibrotic growth factors, pro-inflammatory cytokines and chemokines (Harris, 2001). They also enhance the accumulation of ECM components in kidney (Harris, 2001). The fibroblasts mainly

produce the ECM.They are low in number in normal interstitium however they increase in number and change in function and morphology in the case of renal fibrosis. This is thought to be a major contributor to ECM accumulation during renal fibrosis (Strutz *et al.*, 2000; Jinde *et al.*, 2001; Iwano *et al.*, 2002).

In normal kidney, TECs produce collagen type IV (Col-IV) and fibroblasts produce collagen types I and III (Razzaque *et al.*, 1995; Han *et al.*, 1999; Lam *et al.*, 2003). In case of renal fibrosis, the ECM components are increased and Col-IV is expressed not only in the glomerular basement membrane but also in the interstitium (Eddy *et al.*, 1995; Vleming *et al.*, 1995). It has been found that TGF-β is a crucial mediator in this fibrosis process (Blobe *et al.*, 2000) as the increase of TGF-β during kidney injury promotes the expression of the ECM components including Col-IV (Blobe *et al.*, 2000; Sharma & Ziyadeh, 1995). Treatment of STZ induced diabetic mice with anti TGF-β antibody blunted the gene expression of ECM components as well as attenuating renal hypertrophy (Sharma & Ziyadeh, 1995). It was shown that Col-IV was predominantly secreted by renal proximal tubular epithelial cells as well as cultured renal fibroblasts and mesangial cells, and diabetic rat kidneys in response to stimulation with TGF-β and/or high glucose. (Lam *et al.*, 2004; Li *et al.*, 2018)

TGF-β has been a major subject in studies investigating causes of the progression of diabetic nephropathy (Ziyadeh 1998; Reeves & Andreoli, 2000). TGF-β stimulates the formation of various components of the extracellular matrix including collagen type I and IV, as well as inhibiting proteases and activating protease inhibitors which decrease the matrix degradation (Sharma & Ziyadeh, 1997; Sharma & Ziyadeh, 1995; Heino *et al.*, 1989).

5.1.4.2 TGF-β and diabetic nephropathy in cell culture

In cell culture studies, high glucose has been found to provoke proximal tubular and mesangial cell hypertrophy (Wakisaka *et al.*, 1994; Ziyadeh *et al.*, 1994). In cultured proximal tubular, mesangial, glomerular endothelial, podocyte, and interstitial fibroblasts cells, it has been found that high glucose activates the production of extracellular matrix molecules (Miller *et al.*, 2014). High glucose upregulates the activity of TGF-β in most types of kidney cells (Loeffler & Wolf, 2013; Ziyadeh *et al.*, 1994). Blocking the TGF-β receptors by using neutralizing antibody (neutralizes TGF-β1, and TGF-β2 receptors) has

blunted high glucose induced matrix over-expression which indicates that TGF-β is positively involved in hyperglycaemic renal fibrosis (Ziyadeh *et al.*, 1994).

5.1.4.3 TGF-β and diabetic nephropathy in animal models

A considerable body of evidence in animal models suggests that TGF-β is a major factor targeting diabetic nephropathy (Hill *et al.*, 2000; Braga Gomes *et al.*, 2014). It has been shown, in diabetic rats and mice, that the levels of TGF-β I mRNA and protein were increased in the tubular and glomerular compartments (Miller *et al.*, 2014; Nakamura *et al.*, 1993). It has been found, in animal interventional studies, that high levels of renal TGF-β activity are responsible for the development of diabetic nephropathy. Antagonism with neutralising antibodies of all TGF-β isoforms was shown to prevent glomerular hypertrophy (Sharma *et al.*, 1996).

5.1.5 Aims

To test the hypothesis that C-peptide is a beneficial anti-inflammatory and anti-fibrotic therapy of value in suppressing diabetic nephropathy, the specific experimental aims of this chapter were therefore two-fold:

1) To confirm in a prolonged (29 week) rat STZ model of T1DM the inflammatory and fibrotic effects of DM that have been outlined above, and
2) To investigate the effect of prolonged C-peptide treatment on the following parameters in the diabetic animals:

- Chemo-attractants and immune cell recruitment and adhesion
- Proinflammatory cytokines
- TGF-β and renal fibrosis

5.2 Results

5.2.1 Effect of C-peptide treatment on protein content of MCP-1 and RANTES in diabetic rat kidney and plasma

To assess the effect of DM on the activation of MCP-1 and RANTES in plasma and kidney of STZ-diabetic rats, and whether C-peptide treatment could change this, kidney tissue and plasma from vehicle-treated healthy control (2 rats), STZ-diabetic (8 rats), and C-peptide treated STZ-diabetic rats (6 rats) were evaluated using the luminex technique. (Rats that did not receive C-peptide treatment were injected with the same volume of C-peptide vehicle (i.e. sterile 0.9% w/v NaCl, 5mM HEPES pH 7.4) twice per week, see Section 2.20.1) Data in Figure 5.1 show that induction of DM in rats resulted in a significant increase in protein content of MCP-1 in diabetic rat plasma, compared to healthy rats (Control). However, C-peptide treatment (STZ + C-pep) significantly downregulated MCP-1 protein in plasma. MCP-1 was not detectable in the rats' kidneys (data not shown).

Although, DM seemed to upregulate RANTES in kidney tissue, the effect was not statistically significant (Figure 5.2). C-peptide treatment, however, resulted in significant suppression of RANTES in kidney. In plasma, the effect of DM on RANTES was not significant compared to the control group (Control), neither was the effect of C-peptide treatment compared to the diabetic group. However the plasma data showed a trend that was similar to that in kidney (Figure 5.2b).

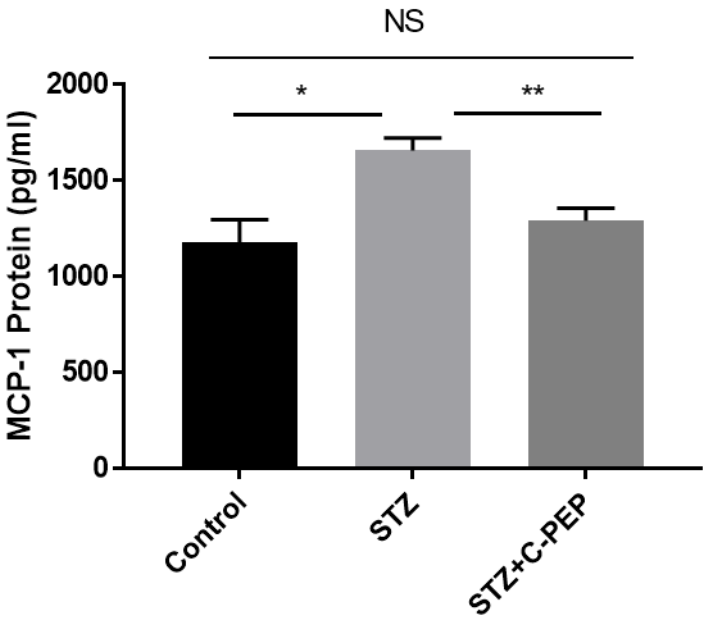

Figure 5.1 Effect of C-peptide treatment on MCP-1 protein content in diabetic rat plasma quantified by luminex technique.

*For the C-peptide treatment group, diabetic rats were treated with long-acting C-peptide 0.5mg/kg subcutaneously twice weekly for 29 weeks. Rats that did not receive C-peptide treatment were injected with the same volume of C-peptide vehicle twice per week. Results were expressed as mean ± SEM of 8 rats from the STZ group, 6 STZ+C-pep group rats, and 2 rats from the C-peptide vehicle treated healthy (control) group. * $P < 0.05$ compared to healthy control group and ** $P < 0.01$ compared to C-peptide treatment group.*

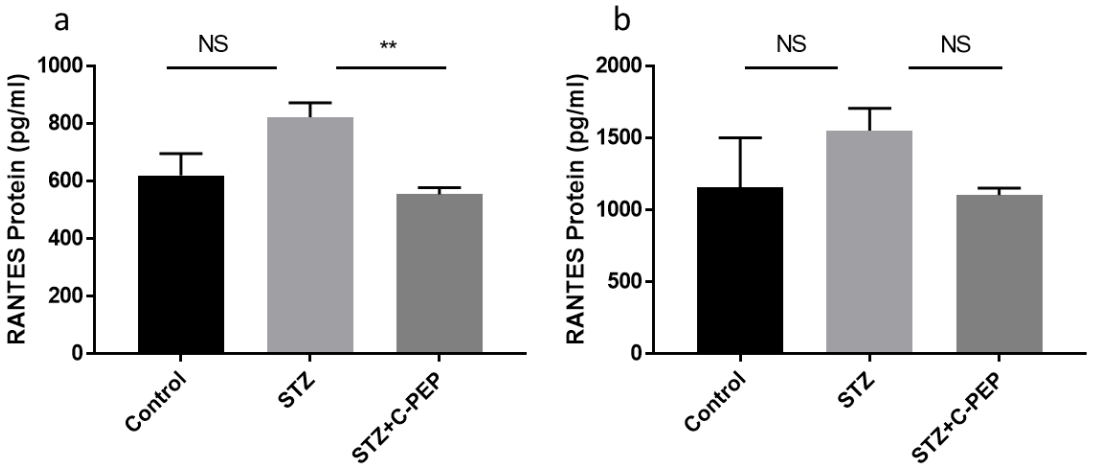

Figure 5.2 Effect of C-peptide treatment on RANTES protein content in diabetic rat kidney (a) and plasma (b) quantified by luminex technique.
*For the C-peptide treatment group, diabetic rats were treated with long-acting C-peptide 0.5mg/kg subcutaneously twice weekly for 29 weeks. Rats that did not receive C-peptide treatment were injected with the same volume of C-peptide vehicle twice per week. Results were expressed as mean ± SEM of 8 rats from the STZ group, 6 STZ+C-pep group rats, and 2 rats from the C-peptide vehicle treated healthy (control) group. NS no significant difference compared to healthy control group. ** P < 0.01 compared to C-peptide treatment group.*

5.2.2 Effect of C-peptide treatment on protein content of ICAM-1, VCAM-1, and VEGF-A in diabetic rat kidney and plasma

To assess the effect of DM on the activation of adhesion molecules (ICAM-1 and VCAM-1) in plasma and kidney of STZ rats and whether C-peptide treatment could change this, kidney tissue and plasma from vehicle-treated healthy control, STZ-diabetic, and C-peptide treated rats were evaluated by using the luminex technique. Data show that 29 weeks of DM in rats resulted in a significant increase in protein content of ICAM-1 in STZ rat kidney (Figure 5.3a) and plasma (Figure 5.3b) compared to healthy rats (Control). However, C-peptide treatment (STZ + C-pep) resulted in significant downregulation of ICAM-1 protein in kidney tissue, but not plasma. DM did not significantly induce VCAM-1 activation in kidney (Figure 5.4a). In plasma, however, the 29 weeks of DM significantly induced VCAM-1 activation (Figure 5.4b) and C-peptide treatment blunted this activation. Data in Figure 5.5 show that 29 weeks of DM in rats resulted in significant increase in protein content of VEGF-A in diabetic rat kidney, compared to healthy rats (Control). However, C-peptide treatment (STZ + C-pep) significantly suppressed this increase. VEGF-A was not detectable in plasma (data not shown).

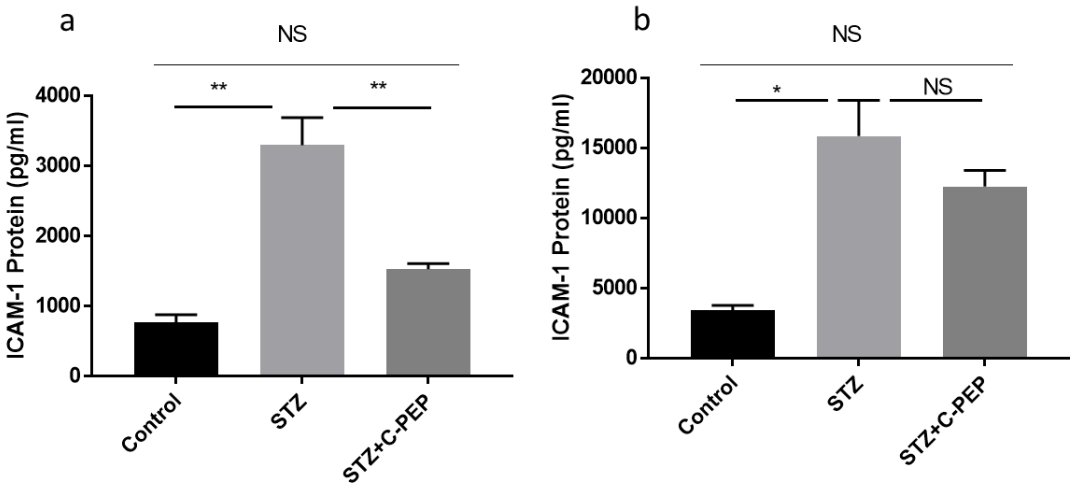

Figure 5.3 Effect of C-peptide treatment on ICAM-1 protein content in diabetic rat kidney (a) and plasma (b) quantified by luminex technique.

*For the C-peptide treatment group, diabetic rats were treated with long-acting C-peptide 0.5mg/kg subcutaneously twice weekly for 29 weeks. Rats that did not receive C-peptide treatment were injected with the same volume of C-peptide vehicle twice per week. Results were expressed as mean ± SEM of 8 rats from the STZ group, 6 STZ+C-pep group rats, and 2 rats from the C-peptide vehicle treated healthy (control) group. (a) ** $P < 0.01$ compared to healthy control group and compared to C-peptide treatment group. (b) * $P < 0.05$ compared to healthy control group, NS no significant difference compared to C-peptide treatment group.*

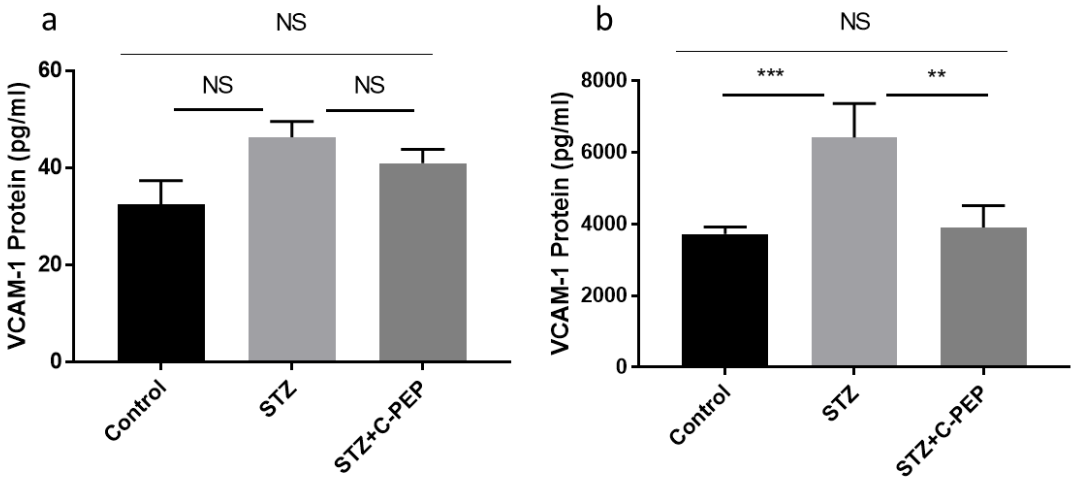

Figure 5.4 Effect of C-peptide treatment on VCAM-1 protein content in diabetic rat kidney (a) and plasma (b) quantified by luminex technique.

*For the C-peptide treatment group, diabetic rats were treated with long-acting C-peptide 0.5mg/kg subcutaneously twice weekly for 29 weeks. Rats that did not receive C-peptide treatment were injected with the same volume of C-peptide vehicle twice per week. Results were expressed as mean ± SEM of 8 rats from the STZ group, 6 STZ+C-pep group rats, and 2 rats from the C-peptide vehicle treated healthy (control) group. (a) NS no significant difference compared to healthy control group and compared to C-peptide treatment group. (b) *** P < 0.001 compared to healthy control group, ** P < 0.01 compared to C-peptide treatment group.*

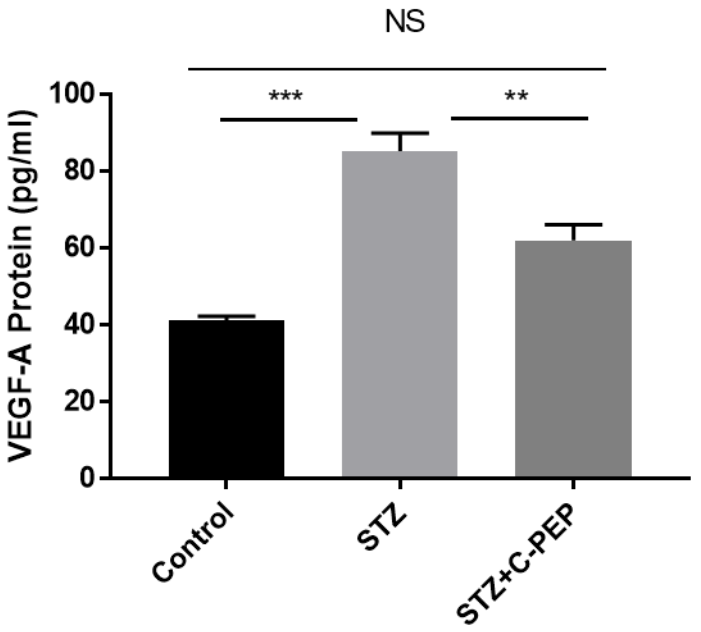

Figure 5.5 Effect of C-peptide treatment on VEGF-A protein content in diabetic rat kidney quantified by luminex technique.

*For the C-peptide treatment group, diabetic rats were treated with long-acting C-peptide 0.5mg/kg subcutaneously twice weekly for 29 weeks. Rats that did not receive C-peptide treatment were injected with the same volume of C-peptide vehicle twice per week. Results were expressed as mean ± SEM of 8 rats from the STZ group, 6 STZ+C-pep group rats, and 2 rats from the C-peptide vehicle treated healthy (control) group. *** P < 0.001 compared to healthy control group and ** P < 0.01 compared to C-peptide treatment group. NS no significant difference compared to healthy control group.*

5.2.3 Effect of C-peptide treatment on proinflammatory cytokines in diabetic rat kidney and plasma

To assess the effect of DM on the activation of proinflammatory cytokines (TNF-α, IL-1β, and IL-6) in plasma and kidney of STZ-diabetic rats and whether C-peptide treatment could change this, kidney tissue and plasma from vehicle-treated control, STZ-diabetic, and C-peptide treated STZ-diabetic rats were evaluated using luminex and ELISA (for IL-6 only). Data show that induction of DM significantly increased TNF-α and IL-1β in diabetic rat kidney (Figure 5.6a and Figure 5.7a), but not in plasma (Figure 5.6b and Figure 5.7b), compared to healthy rats (Control). C-peptide treatment resulted in significant downregulation of the levels of these cytokines in kidney tissue, however, there was no detectable effect in plasma.

In Figure 5.8, the luminex data did not show any effect of DM or C-peptide on the concentration of IL-6 in kidney tissue. This was unexpected in view of the earlier reports that IL-6 was found to be high in T1DM patients and diabetic animals (Aso *et al.*, 2004; Lim & Tesch, 2012). IL-6 was therefore also assayed by ELISA (Figure 5.8b) to confirm the luminex result. IL-6 was not detectable in plasma (data not shown).

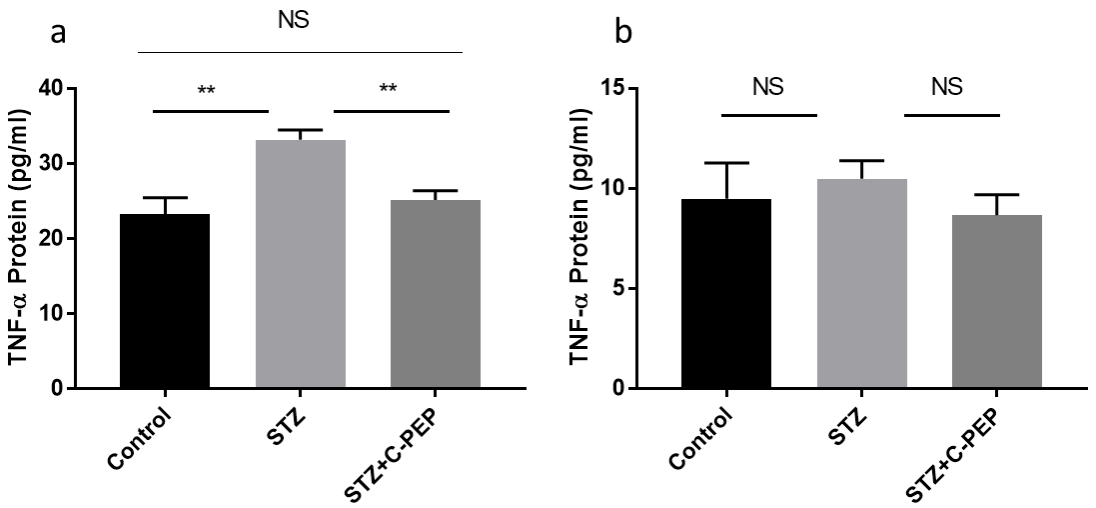

Figure 5.6 Effect of C-peptide treatment on TNF-α protein content in diabetic rat kidney (a) and plasma (b) quantified by luminex technique.
*For the C-peptide treatment group, diabetic rats were treated with long-acting C-peptide 0.5mg/kg subcutaneously twice weekly for 29 weeks. Rats that did not receive C-peptide treatment were injected with the same volume of C-peptide vehicle twice per week. Results were expressed as mean ± SEM of 8 rats from the STZ group, 6 STZ+C-pep group rats, and 2 rats from the healthy (control) group. (a) ** P < 0.01 compared to control group and to C-peptide treatment group. (b) NS no significant difference compared to healthy control group and compared to C-peptide treatment group.*

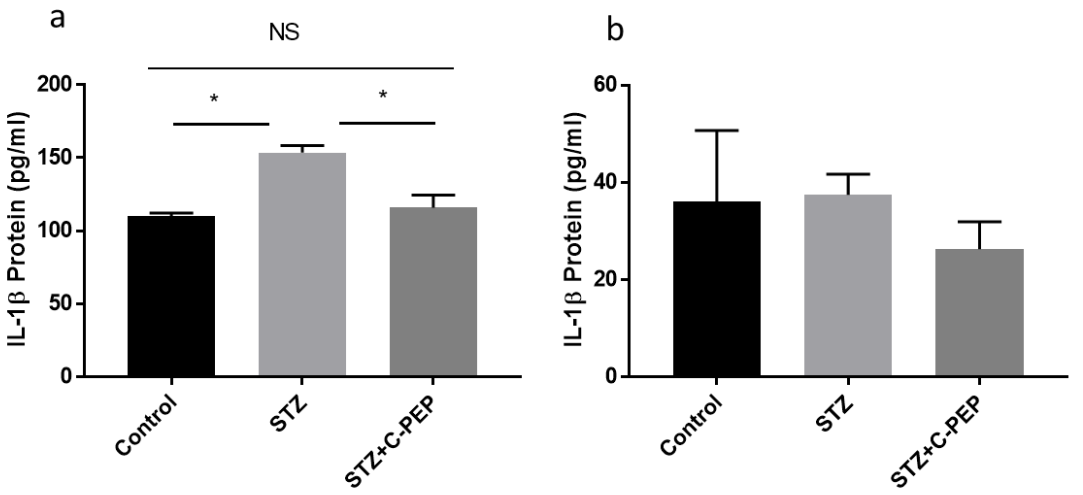

Figure 5.7 Effect of C-peptide treatment on IL-1β protein content in diabetic rat kidney (a) and plasma (b) quantified by luminex technique.

*For the C-peptide treatment group, diabetic rats were treated with long-acting C-peptide 0.5mg/kg subcutaneously twice weekly for 29 weeks. Rats that did not receive C-peptide treatment were injected with the same volume of C-peptide vehicle twice per week. Results were expressed as mean ± SEM of 8 rats from the STZ group, 6 STZ+C-pep group rats, and 2 rats from the healthy (control) group. (a) * P < 0.05 compared to healthy control group and to C-peptide treatment group. (b) NS no significant difference was detected.*

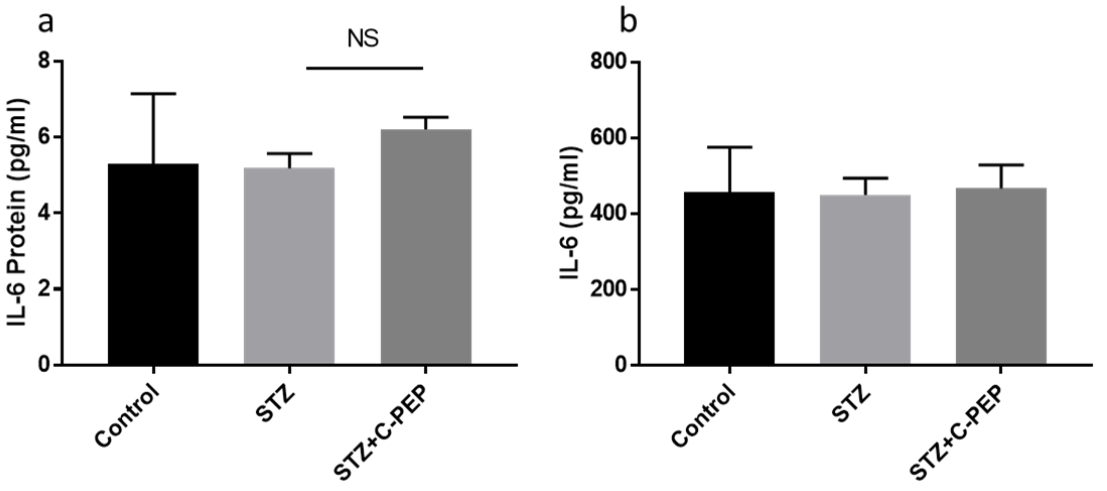

Figure 5.8 Effect of C-peptide treatment on IL-6 protein content in diabetic rat kidney quantified by luminex (a) and ELISA (b) assay.

For the C-peptide treatment group, diabetic rats were treated with long-acting C-peptide 0.5mg/kg subcutaneously twice weekly for 29 weeks. Rats that did not receive C-peptide treatment were injected with the same volume of C-peptide vehicle twice per week. Results were expressed as mean ± SEM of 8 rats from the STZ group, 6 STZ+C-pep group rats, and 2 rats from the healthy (control) group. No significant difference was detected.

5.2.4 Effect of C-peptide treatment on renal fibrosis

5.2.4.1 Effect of C-peptide treatment on the gene expression of collagen type IV in diabetic rat kidney

To assess the effect of DM on the gene expression of collagen type IV (Col-IV) in kidney of STZ-diabetic rats and whether C-peptide treatment could change this, kidney tissue from vehicle-treated control, STZ-diabetic, and C-peptide treated rats was evaluated by using RT-QPCR technique. Data in Figure 5.9 confirmed that 29 weeks of DM in rats significantly increased the gene expression of Col-IV in diabetic rat kidney compared to healthy rats (Control). Although C-peptide treatment (STZ + C-pep) resulted in apparent downregulation the gene expression of Col-IV compared to STZ group, this effect did not reach statistical significance. It was also noted that the effect of DM on the C-peptide treatment group (STZ+Cpep) was not significant compared to the healthy control group.

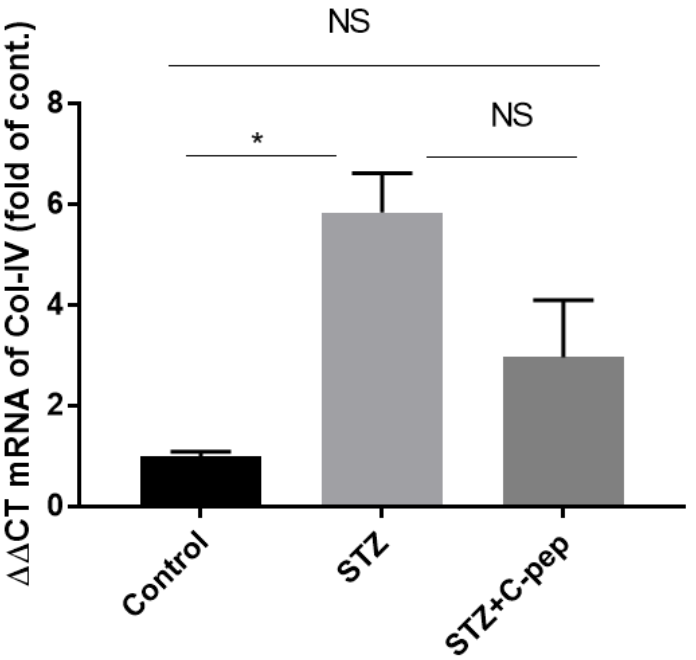

Figure 5.9 Effect of C-peptide treatment on Col-IV gene expression in diabetic rat kidney quantified by RT-QPCR.
*For the C-peptide treatment group, diabetic rats were treated with long-acting C-peptide 0.5mg/kg subcutaneously twice weekly for 29 weeks. Rats that did not receive C-peptide treatment were injected with the same volume of C-peptide vehicle twice per week. Relative Col-IV mRNA expression was calculated using the delta delta CT value method. Results were expressed as mean ± SEM of 8 rats from the STZ, 6 STZ+C-peptide group rats, and 2 rats from the Healthy control group. * P < 0.05 compared with healthy control group. NS no significant difference compared to C-peptide treatment group.*

5.2.4.2 Effect of C-peptide treatment on gene expression and protein content of TGF-β in diabetic rat kidney

To assess the effect of DM on the gene expression and the protein content of TGF-β in kidney of STZ-diabetic rats and whether C-peptide treatment could change this, kidney tissue from vehicle-treated control, STZ-diabetic, and C-peptide treated rats were evaluated by using RT-QPCR and Luminex technique. Data in Figure 5.10 and Figure 5.11 show that induction of DM in rats significantly increased both the gene expression and protein content of TGF-β in diabetic rat kidney compared to healthy rats (Control). However, C-peptide treatment (Diabetic + C-pep) resulted in a significant decrease in the gene expression and the protein content of TGF-β. Indeed in Fig 5.10 C-peptide almost reduced the TGF-β expression in the diabetic rats to the level observed in the non-diabetic control animals.

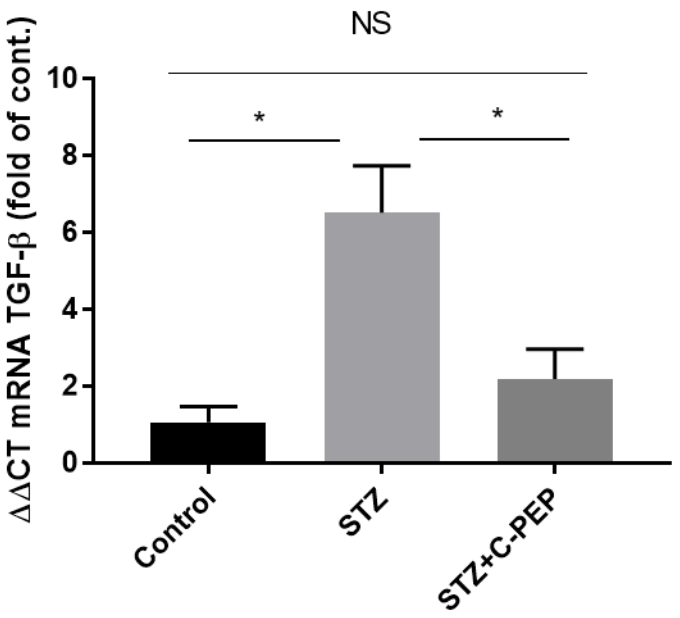

Figure 5.10 Effect of C-peptide treatment on TGF-β gene expression in diabetic rat kidney quantified by RT-QPCR.
*For the C-peptide treatment group, diabetic rats were treated with long-acting C-peptide 0.5mg/kg subcutaneously twice weekly for 29 weeks. Rats that did not receive C-peptide treatment were injected with the same volume of C-peptide vehicle twice per week. Relative TGF-β mRNA expression was calculated using the delta delta CT value method. Results were expressed as mean ± SEM of 8 rats from the STZ, 6 STZ+C-peptide group rats, and 2 rats from the control group. * P < 0.05 compared to Healthy control group and to C-peptide treatment group.*

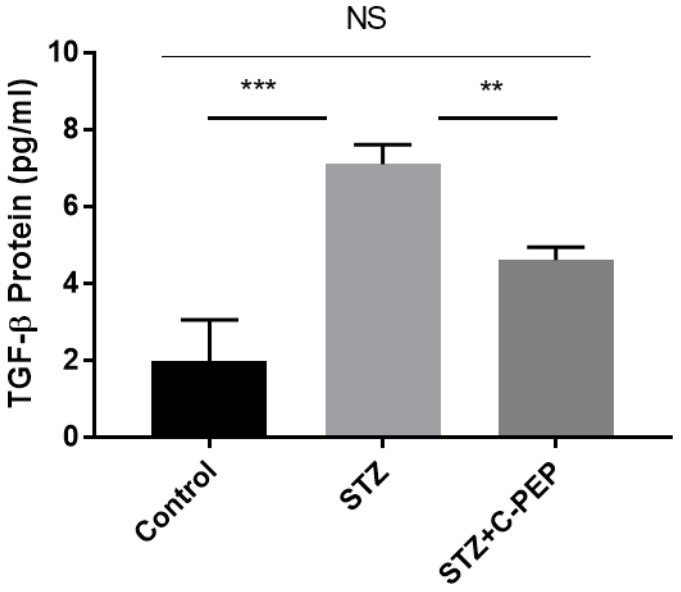

Figure 5.11 Effect of C-peptide treatment on TGF-β protein content in diabetic rat kidney quantified by Luminex technique.

*For the C-peptide treatment group, diabetic rats were treated with long-acting C-peptide 0.5mg/kg subcutaneously twice weekly for 29 weeks. Rats that did not receive C-peptide treatment were injected with the same volume of C-peptide vehicle twice per week. Results were expressed as mean ± SEM of 8 rats from the STZ, 6 rats from the STZ+C-peptide group rats, and 2 rats from the control group. . *** P < 0.001 compared to healthy control group and ** P < 0.01 compared to C-peptide treatment group.*

5.3 Discussion

5.3.1 Effect of C-peptide treatment on chemokines and adhesion molecules

A large body of evidence has shown that diabetic nephropathy is an inflammatory disease and it is characterized by infiltration of immune cells. The recruitment of these immune cells is facilitated by chemokines. MCP-1 is one of the main participant chemokines in the recruitment events in the diabetic milieu in kidney and circulation. MCP-1 has been reported to play a key role in recruiting monocytes and macrophages in diabetic patients and animals (Ruster & Wolf, 2008).

The expression of MCP-1 was also reported to be stimulated by high glucose in cultured human mesangial cells (Ueda *et al.*, 1997). Transcription factor NF-kappaB was shown to activate the transcription of the MCP-1 gene (Mezzano *et al.*, 2004). NF-kappaB also stimulated MCP-1 production and infiltration of monocytes and macrophages in STZ-induced diabetic rats (Lee *et al.*, 2004). The mechanism through which this transcription is suggested to take place was shown in cultured mouse mesangial cells. Stimulation of protein kinase C (PKC) by high glucose has been shown to lead to ROS formation, which then activated NF-kappa-B resulting in increased expression of MCP-1 (Ha *et al.*, 2002).

In the current study, MCP-1 protein was not detectable in kidney tissue, however, induction of DM increased the protein content in plasma. A similar effect was shown in a number of studies. In cultured human aortic endothelial cells (HAEC), high glucose was shown to stimulate the activation of NF-kappaB and addition of C-peptide significantly suppressed this activation. In the same study, it was also shown that both high glucose and NF-kappaB induced the secretion of MCP-1. However, C-peptide addition also reduced this secretion (Luppi, *et al.*, 2008) suggesting the same mechanism explained above. In the current study, C-peptide treatment apparently normalized the levels of MCP-1 to those of the control in plasma, possibly through a similar mechanism.

RANTES was shown to have a vital role in the recruitment of T cells, monocytes, and macrophages. It is expressed in a number of renal cells along with other cells such as lymphocytes (Wolf *et al.*, 1993; Satriano *et al.*, 1997). RANTES is involved in mediating chronic inflammation. It was largely found to be associated with the presence of NF-kappa-B suggesting that it is activated in a similar way to MCP-1 as NF-kappa-B was found to bind to promoter sites of RANTES (Zoja *et al.*, 1998; Schmid *et al.*, 2006).

Levels of RANTES were found to correlate with TNF-α, TGF-β, and NF-kappa-B in tubular and mesangial cells (Ruster & Wolf, 2008).

In the current study, 29 weeks of DM was found to have an effect, although not significant, on levels of RANTES protein in diabetic kidney tissue. C-peptide treatment successfully suppressed the secretion of it, possibly in a way similar to that of MCP-1. In the present study, circulating levels of RANTES did not show response to DM, C-peptide treatment also did not significantly affect the levels of RANTES in circulation. Serum levels of RANTES were shown to be elevated in patients with T2DM (Herder *et al.*, 2005) and in the group with progression of the metabolic syndrome into T2DM in the Finnish Diabetes Prevention Study (Herder *et al.*, 2006). A high concentration of C-peptide (in T2DM) was shown to deposit in thoracic arterial intima of diabetic subjects and to exhibit a chemotactic property to induce CD4 cell migration in T2DM patients in a way similar to RANTES without showing additive effect (Walcher, *et al.*, 2004), hence in future it would be interesting to investigate the effect of C-peptide on RANTES in T1DM models in greater detail.

The recruitment of macrophages and T cells has been shown to be associated with the progression of DN (Bohle *et al.*, 1991; Galkina & Ley, 2006a). The mechanism behind this recruitment is not fully understood (Galkina & Ley, 2006a). Adhesion molecules ICAM-1 and VCAM-1 have been shown to be involved in this. In STZ-induced diabetic ICAM-1 deficient mice, macrophage infiltration was shown to diminish and the expression of Col-IV and TGF-β in glomeruli were reduced as well as mesangial matrix expansion, urinary albumin excretion, and glomerular hypertrophy (Okada *et al.*, 2003a). CD4+ T cell accumulation also was shown to be reduced in the glomeruli in ICAM-1 deficient mice (Chow *et al.*, 2005). However, it has been shown that the levels of C-peptide were not affected in ICAM-1 deficient mice in both fasting and fed state compared to wild type mice (Babic *et al*., 2004).

In diabetic mouse kidney, VCAM-1 was found to be expressed predominantly in the vascular endothelium and other infiltrating cells such as monocytes and lymphocytes (Ina *et al.*, 1999). The circulating levels of VCAM-1 were shown to have an association with albuminuria in T1DM patients (Clausen *et al.*, 2000). The levels of circulating VCAM-1 were suggested to possibly be a useful biomarker to detect diabetic renal disease (Lim &

Tesch, 2012). However, the relationship between circulating VCAM-1 and the pathogenesis of DN is yet to be clarified.

In the current study, 29 weeks of DM resulted in a significant increase in ICAM-1 protein in kidney tissue and in plasma. C-peptide treatment successfully normalized the level of ICAM-1 in kidney. Although there was a visible effect of C-peptide treatment on ICAM-1 levels in plasma, this effect did not reach statistical significance. The mechanism by which C-peptide is thought to reduce ICAM-1 is that C-peptide mediates the release of NO, which in turn inhibits the interaction between leukocytes and endothelial cells in rats leading to a decrease in the expression of ICAM-1 (Bhatt *et al.*, 2014). In the current study, C-peptide possibly induces its effect in a similar mechanism.

In cultured HAEC cells, C-peptide was shown to downregulate high glucose induced VCAM-1 (Luppi *et al.*, 2008). This is in agreement with the findings in the current study. DM in this chapter was shown to upregulate the protein levels of VCAM-1, and C-peptide treatment was shown to reduce it to level of the control in plasma. In kidney however, DM had no detectable effect on VCAM-1 protein, neither did C-peptide treatment.

Vascular endothelial growth factor (VEGF) and its receptor have been reported to increase in diabetic kidneys of rat and to have a role in the progression of diabetic nephropathy and it is known to induce macrophage migration into kidney (Cooper *et al.*, 1999; Sato *et al.*, 2008). It was also found that VEGF gene expression and protein content are increased in response to high levels of glucose in cultured mouse podocytes (Hoshi *et al.*, 2002) and cultured rat mesangial cells (Cha *et al.*, 2000). The mechanism by which high glucose induces the expression of VEGF is proposed to be mediated by PKC and ERK pathways (Hoshi *et al.*, 2002). The current study shows that the induction of DM increased the expression of VEGF in diabetic kidney tissue. C-peptide treatment was successful in decreasing this expression. It has been shown that diabetes induces molecular changes such as upregulation of cytokines and growth factors (like TGF-β) and activation of renin-angiotensin system (RAS) (Derubertis & Craven, 1994; Cha *et al.*, 2000). As a result of these changes, the production of VEGF is increased in kidney (Cha *et al.*, 2000). If the same has happened in this study, C-peptide might have induced its effect on VEGF through the suppression of TGF-β (as shown in Figure 5.10 and Figure 5.11). However, the exact underlying mechanism by which C-peptide induces this effect on VEGF is not well understood and needs further investigation.

5.3.2 Effect of C-peptide treatment on proinflammatory cytokines during diabetes

TNF-α is an important cytokine that is involved in the onset of diabetic nephropathy. It is produced by immune cells including macrophages, monocytes, and T cells (Dong *et al.*, 2007) as well as renal cells (Jevnikar *et al.*, 1991). Many studies have shown that both circulating and renal levels of TNF-α correlate with the progression of DN. TNF-α may induce renal injury, necrosis, and apoptosis by causing cytoxicity (Laster *et al.*, 1988; Boyle *et al.*, 2003). It also induces the activation of protein kinase B/phosphatidylinositol-3 kinase and the activation of NADPH oxidase leading to ROS generation thus increasing the glomerular permeability (McCarthy *et al.*, 1998). TNF-α induces its effect during diabetes via TNF-α receptor type II (TNF-aRII) leading to the activation of NF-kappa-B by ubiquitination and degradation of inhibitor of kappa-B proteins (Hayden & Ghosh, 2014; Holbrook *et al*, 2019). It has been shown that use of TNF-α inhibitor resulted in decreasing the intensity of downstream effects of TNF-α such as NF-kappa-B in mouse renal cortex (Omote *et al.*, 2014; Venegas-Pont *et al.*, 2010). The underlying mechanism behind the upregulated expression and secretion of TNF-α during DM is still largely unknown. However, C-peptide has been reported to reduce the apoptotic effects of TNF-α on TNF-α-treated OK cells (Al-Rasheed *et al.*, 2006). In the current study, DM increased the production of TNF-α in kidney tissue, but not in plasma. Treatment with C-peptide apparently reduced the levels of TNF-α. The exact mechanism behind this effect of C-peptide is yet to be investigated in greater detail.

Levels of IL-1β were reported to be increased in early diabetic kidney and were shown to be associated with the upregulation of adhesion molecules, inflammatory cytokines, and growth factors (Brady, 1994). IL-1β induces the expression of Col-IV in mesangial cells as well as TGF-β during diabetes (Melcion *et al.*, 1982; Nakamura *et al.*, 1993). In the current study, the cellular origin of IL-1β was not identified and it could be originating from recruited immune cells or resident renal cells. However, the induction of DM upregulated the levels of IL-1β in kidney tissue, but not in plasma, and C-peptide treatment significantly reduced this regulation. The mechanism through which high glucose induces the secretion of IL-1β in renal resident cells is not fully understood, however, it has been proposed to be mediated by PKCα-dependent activation of p38MAPK, ERK, and NF-kappa-B in human monocytes (Dasu *et al.*, 2007). The underlying mechanism of C-peptide suppressing the secretion of IL-1β is not understood and requires further investigation. This seems a particularly important avenue for future

research in view of a report that blockade of the action of IL-1β using a neutralising antibody blunts diabetic nephropathy in an obese mouse model of T2DM (Lei *et al*, 2019)

Data has shown that local renal cells including podocytes, mesangial cells, endothelial cells, and tubular epithelial cells can produce IL-6 under several conditions including hyperglycaemia (Su *et al.*, 2017). Levels of IL-6 were found to be higher in diabetic patients with DN than those who have not developed DN (Mahadevan *et al.*, 1995). The levels of IL-6 were also found to be associated with mesangium expansion and with the interstitium and tubular cell infiltration (Suzuki *et al.*, 1995; Coleman & Ruef, 1992; Lim & Tesch, 2012). In the current study, the induction of DM failed to produce changes in the levels of IL-6 in kidney tissue and plasma. Hyperglycaemia has been shown to activate both the expression of angiotensin receptor and the effect of angiotensin II (ANGII) (Thaiss *et al.*, 1996; Ihm *et al.*, 2002). One study showed that the expression and the secretion of IL-6 in human mesangial cells in response to high glucose and ANGII was higher than those with high glucose alone and lower than those with ANGII alone, suggesting that ANGII may be antagonistic to high glucose and that the expression of IL-6 in this milieu is rather complicated (Ihm *et al.*, 2002). If the same is happening in this chapter, this could be the explanation behind the failure of DM induction to affect the secretion of IL-6.

5.3.3 Effect of C-peptide treatment on renal fibrosis

In the kidney, one of the main consequences of DM is renal fibrosis which is characterized by expansion of extracellular matrix components and the basement membrane (Zeisberg & Kalluri, 2004; Ziyadeh, 1996). TGF-β is well known as a key component triggering renal fibrosis in diabetic kidney. TGF-β initiates multiple pathways including Smad signalling which is a major pathway in renal fibrosis (Meng *et al.*, 2015). This may lead to overproduction of Col-IV which contributes to extracellular matrix accumulation in DM (Dimas *et al.*, 2017). Thus, the suppression of TGF-β may be a key element in the treatment of renal fibrosis in the case of diabetic nephropathy. C-peptide has an evident role in the reduction of glomerular hyperfiltration and albuminuria in both diabetic animals and T1DM patients as well as reduction of ECM accumulation and mesangial expansion (Brunskill, 2017; Wahren, 2017). C-peptide has been shown to have an antifibrotic effect in a number of studies. Upon stimulation with TGF-β, C-peptide suppressed the expression of TGF-βRI and TGF-βRII as well as the phosphorylation of Smad3 in cultured human proximal tubular cell (Hills, *et al.*, 2009; Hills, *et al.*, 2010).

Administration of C-peptide has been shown to prevent high glucose-induced elevation of TGF-β in STZ mice and rats. *In vitro* studies showed that, in mouse podocytes, C-peptide inhibits the TGF-β-induced elevation of the Col-IV. This shows that C-peptide may be involved in the reduction of the mesangial expansion as well as the renal fibrosis (Samnegård *et al.*, 2005b). More recent evidence shows that C-peptide attenuated pathological changes in the glomeruli of diabetic rats. They also found that C-peptide downregulated the expression of Col-IV and TGF-β mRNA and protein content in both diabetic rats and high glucose stimulated mesangial cells (Li, *et al.*, 2018).

It is evident that C-peptide has an inhibitory effect on the accumulation of ECM, however the underlying mechanism by which C-peptide induces this effect is still poorly understood. A recent study has shown that C-peptide supresses the production of Col-IV by blunting Smad3 binding to the promoters of Col-IV alongside with decreasing the content of TGF-β both in cultured mesangial cells and diabetic rats, suggesting this as the mechanism by which C-peptide acts (Li *et al.*, 2018). In the current study, it has been observed that C-peptide decreases the expression of Col-IV as well as the expression and the protein content of TGF-β in diabetic rat kidney, possibly through the same mechanism.

In summary, elevated levels of Col-IV and TGF-β may possibly be an indication of renal fibrosis in the DM model studied here. Thus, controlling their levels may lead to a better control of the disease. C-peptide treatment successfully achieved this. Hence, C-peptide might attenuate the progression of renal complications associated with diabetes.

5.3.4 Limitations in this study

A limitation of this study was that the control (non-diabetic) experimental group only contained two rats. However, this study was primarily designed to investigate the effect of C-peptide on the parameters studied here in the STZ diabetic model. The control group was included only to allow confirmation of previously reported effects of the STZ model on the parameters that were studied in this chapter. Another limitation of the study was that no effect of DM on IL-6 was observed. This could have arisen because the sensitivity of the IL-6 ELISA that was used was insufficient to detect an effect.

In Chapter 4 it was observed that Pi apparently enhanced the biological effects of C-peptide on ERK signalling *in vitro*. A further limitation of this study is that this Pi-dependence was not investigated directly in the rat model. In future work it would be of interest to determine whether dietary phosphorus restriction or dietary phosphorus supplementation had the effects on the actions of C-peptide *in vivo* that would be predicted from what was observed in Chapter 5.

5.4 Conclusion

This rat study using the STZ model of T1D, which was sufficiently prolonged (29 weeks) to generate significant tubulo-interstitial inflammation and fibrosis, showed a number of significant therapeutic effects of C-peptide on these pathological changes. The potential clinical significance of these findings and avenues for future research are the subject of the next chapter.

6 Chapter 6 General discussion

6.1 Overview

The renal complications in diabetes are very common and can have a major impact on human health. The deficiency of C-peptide during diabetes may contribute to the progression of diabetic nephropathy (Brunskill, 2017). My thesis hypothesised that physiologically-relevant concentrations of C-peptide are important for maintaining normal renal function especially in the tubular epithelium.

C-peptide signalling in the renal epithelium has been an active area of research in the past twenty years. Numerous reports from human and animal studies have shown that C-peptide is an effective therapeutic tool for improving the disturbances of the renal function and structure, including microalbuminuria, glomerular hyperfiltration, mesangial expansion, and increased levels of endothelial nitric oxide synthase during exposure to various injurious stimuli. *In vitro* studies in proximal tubular epithelial cells have shown that physiological concentrations of C-peptide activated ERKs, PI3K, PKC, increased intracellular Ca^{2+}, and stimulated transcription factors NF-kappaB and PPAR-Ɣ (Hills, *et al.*, 2010).

C-peptide activates different signalling pathways in different cell lines. In renal tubular and endothelial cells, C-peptide induced rapid increase in the intracellular levels of $[Ca^{2+}]_I$ (Ohtomo *et al.*, 1996; Shafqat *et al.*, 2002; Wallerath *et al.*, 2003). In lymphocytes, myoblasts, and fibroblasts along with proximal renal tubular cells, C-peptide was shown to activate PI3K (Grunberger *et al.*, 2001; Al-Rasheed *et al.*, 2004; Walcher *et al.*, 2004). The phosphorylation of PKC was also shown to be activated by C-peptide in renal tubular cells (Al-Rasheed *et al.*, 2004). As a downstream effect of PKC phosphorylation, stimulation with C-peptide resulted in phosphorylation of MAPK members including ERK1/2, p38, and JNK (Grunberger *et al.*, 2001; Kitamura *et al.*, 2001; Al-Rasheed *et al.*, 2004; Zhong *et al.*, 2005).

6.2 C-peptide and TERT/1 cells

In the present study, for the first time, RPTEC/ TERT/1 cells were identified as a C-peptide responsive PTEC line. C-peptide activates the key signalling pathway ERK1/2 in TERT/1 cells (Section 3.2.1) This signalling cascade plays a vital role in regulating a number of intracellular physiological processes such as cell growth and survival (Wahren, John & Larsson, 2015). Similar results were seen in another, but less differentiated, renal epithelial cell line HEK-293A (Section 3.2.2) although maximal ERK1/2 response required a higher C-peptide concentration. Janabi in 2017 also showed similar results in a different strain of HEK cells (HEK-293), although interestingly he saw no response to C-peptide in the HEK-293A cells that were used here (Janabi, 2017). The reason for this difference between laboratories is unknown.

The reactivity of TERT/1 cells with C-peptide will provide a new tool for studying C-peptide interactions with cell membranes. Investigating the C-peptide receptor and its downstream signals in TERT/1 cells may be useful as TERT/1 cells are a highly differentiated cell culture model of human proximal tubule (Wieser *et al.*, 2008) and the health of the proximal tubular epithelium is considered an important factor in the progression of DN (Tang & Lai, 2012).

As the receptor of C-peptide has not been conclusively identified, the exact mechanism of action of C-peptide is still uncertain. However, C-peptide's effects were shown to be PTX sensitive, suggesting that C-peptide interacts with a $G\alpha_{i/o}$-coupled receptor (Ido *et al.*, 1997). More recent findings, which agree with these findings, found that C-peptide-mediated phosphorylation of both ERK1/2 and rpS6 were PTX-sensitive in HEK-293 cells (Janabi, 2017). Moreover, C-peptide binding to cell membrane was shown in different cell lines to be PTX sensitive too (Flatt *et al.*, 1986; Rigler *et al.*, 1999). Therefore, it is most likely that C-peptide binds to a $G\alpha_i$-coupled receptor.

6.3 GPR146 and C-peptide

Yosten and colleagues in 2013 have proposed GPCR/GPR146 as C-peptide's receptor (see **Chapter 3**).

In this study, further examination of this hypothesis was made by examining the effect of C-peptide on GPR146 mRNA expression. At least one GPCR (the luteinizing hormone receptor) has been reported to show down-regulation of its mRNA in response to ERK signalling triggered by the receptor's ligand (Menon *et al.*, 2011). However the present experiments failed to reveal any such effect of C-peptide on the GPR146 mRNA expression in both TERT/1 and HEK-293A cells. This does not prove that GPR146 is not the C-peptide receptor, but the result seems consistent with recent findings where overexpression of GPR146 failed to enhance C-peptide-induced phosphorylation of ERK1/2 and rpS6 in HEK-293 cells (Janabi, 2017). In that study, Janabi (2017) generated both EGFP-tagged (EGFP-GPR146) and untagged cDNA clones of GPR146 and stably-transfected these in HEK-293 and HEK-293A cells to study whether this would alter C-peptide's signalling, and in an unsuccessful attempt to detect $G\alpha_i$-linked responses in pools of cDNA clones from an OK cDNA library. However, attempts to follow the same approach to overexpress EGFP-GPR146 in HEK-293A and TERT/1 cells failed in this study. In the TERT/1 cells this presumably reflects the difficulty of transfecting this highly differentiated cell line. The failure here with HEK293A cells is more difficult to explain, but may be consistent with the differences observed between the C-peptide ERK1/2 responses of the HEK293A stocks in the two laboratories i.e. that the HEK293A cells used here are functionally different from those used by Janabi in 2017.

6.4 ERK1/2 signalling and Pi

ERK signalling has been shown to play an important role in triggering renal fibrosis, as it has been shown, when induced by TGF-β, to promote damage in the basement membrane leading eventually to glomerular sclerosis in cultured podocytes (Liu *et al.*, 2005). On the other hand, it was shown to possess beneficial effects. For instance, the inhibition of STZ-induced glomerular cell apoptosis by mitofusion protein 2 was reported to be carried out through ERK1/2 signaling pathway (Tang *et al.*, 2012). Therefore, having a detailed understanding of the stimuli and the mechanism by which ERK is activated by C-peptide is important in DN.

In this study, both Pi and C-peptide were shown to activate ERK1/2 in TERT/1 cells. The activation of ERK1/2 was increased by 2.5mM Pi, a plasma Pi concentration that occurs in hyperphosphataemic type1 diabetic kidney patients and in rodents (Haut *et al.*, 1980). This response to Pi possibly occurs because sensing of extracellular Pi (and possibly also Vi, Phi and HPhi) by SLC20 transporter proteins (PiT1 and PiT2 in the plasma membrane) forming a heterodimer which acts like a receptor for extracellular Pi, allowing the extracellular Pi to bind then signal to ERK1/2 without the need to transport Pi into the cell (Bon *et al.*, 2018).

C-peptide, in this project, decreased the mRNA expression and the activity of Na^+-linked Pi transport by 30% in TERT/1 cells. Interestingly, the concentration at which C-peptide was shown to exert its effect on ^{33}Pi transport and on PiT2 and XPR1 expression occurred at about 3nM, a C-peptide concentration that occurs in circulation after a meal. It has previously been shown that feeding with a high oral load of glucose to stimulate pancreatic beta cell secretion results in an unexplained decrease in the Pi transport in kidney (Rasmussen & Jespersen, 1985; Berthelay *et al.*, 1984). This decrease in renal Pi reabsorption, however, cannot be because of insulin, as insulin has been shown to stimulate renal Pi transporters (Abraham *et al.*, 1990). The effect of C-peptide on TERT/1 Pi transport in Chapter 4 might be the explanation. If this happens *in vivo*, it is important to investigate further the possible involvement of C-peptide as a novel hormone in controlling Pi excretion after a meal.

6.5 The effects of C-peptide on inflammatory and fibrotic cytokines *in vivo*

The *in vivo* study presented in Chapter 5 revealed important observations. The effect of C-peptide on diabetic rat kidney tissue and plasma was investigated. In the present study, STZ-induced diabetes in rats resulted in upregulation of TGF-β and Col-IV; though, C-peptide administration prevented diabetes-induced overexpression of TGF-β and Col-IV mRNA, and TGF-β protein in kidney tissue. The induction of DM resulted in overall decrease in rats' body weight compared to healthy control. It also resulted in an increase in rats' kidney weight, glomerular filtration rate (GFR), and plasma fructosamine concentration (see Appendix 5).

In DN, TGF-β is key to the development of the proximal tubular atrophy, matrix production and tubulointerstitial scarring that accompanies loss of renal excretory

function (Ziyadeh, 1993). Excess TGF-β stimulated Col-IV synthesis is a major contributor to ECM accumulation in DN. STZ-induced diabetes in rats resulted in upregulation of, ICAM-1, VEGF-A, TNF-α, and IL-1β in kidney and MCP-1, ICAM-1 and VCAM-1 in plasma (see Sections, 5.2.1 and 5.2.2). Administration of C-peptide prevented the diabetes-induced overexpression of aforementioned inflammatory markers. These markers, in DN, have crucial roles in the chemoattraction and the adhesion of inflammatory cells which can further lead to release of immune cell products including TNF-*α*, IL-1β, IL-6, and reactive oxygen species (ROS) (Galkina & Ley, 2006c). Furthermore, immune cell accumulation in diabetic kidney is associated with glomerular sclerosis, glomerular immune complex deposition, chemokine production, and fibrosis (Chow *et al.*, 2004). TNF-α and IL-1β were also shown to be induced by diabetes in the present study. Their release, however, is not limited to immune cells, they have been shown to be released by resident cell (Jevnikar *et al.*, 1991). Administration of C-peptide was shown to successfully supress their production in kidney tissue of diabetic rats (see Section 5.2.3).

6.6 Future research in this field

6.6.1 Biological significance of C-peptide effects on adhesion molecules in plasma *in vivo*

In the studies performed in Chapter 5, an interesting feature of the plasma data from the diabetic animals was the significant concentration of endothelial inflammatory adhesion molecules (ICAM-1 and VCAM-1), and for VCAM-1 this was significantly decreased in response to C-peptide treatment in plasma (Figure 5.4). It has been known for at least 20 years that these molecules are elevated in the plasma of T1DM patients (Clausen *et al.*, 2000). As the rat plasma used in the present study was obtained by centrifugation at only 1200 x g (Section 2.17.2) it is likely that any endothelium-derived microparticles (EMPs) in the original blood sample would have been retained in the plasma that was used in these assays, because a much higher g force of 18,000 x g is required to sediment microparticles (Abbasian *et al.*, 2015). ICAM-1 is known to be expressed on circulating EMPs in humans (Simak *et al.*, 2006). It is likely therefore that a significant fraction of the ICAM-1 and VCAM-1 detected here in plasma was in microparticles. This raises the question of whether the suppressive effect of C-peptide on VCAM-1 arose from inhibition of EMP output. No such decrease of EMPs by C-peptide has been reported previously. Indeed in a recent *in vitro* study from this laboratory using nanoparticle tracking analysis

to quantify EMPs released from the human vascular endothelial cell line EA.hy926, no effect of C-peptide on EMP output was observed, even in response to C-peptide concentrations as high as 10nM, and a concentration of 5nM was found to increase EMP output when it was quantified by flow cytometry (Al-Isawi, 2019). In view of the possible pathological role of EMPs in cardiovascular disease, in future work it would therefore be interesting to determine whether C-peptide treatment exerts any effect on EMP numbers in T1DM *in vivo.*

6.6.2 Links between Pi and the anti-inflammatory and anti-fibrotic effects of C-peptide *in vivo*

In view of the interaction observed between Pi and C-peptide signalling in Chapter 4, and the beneficial functional effects of C-peptide *in vivo* in Chapter 5 in a rodent STZ model, it would be interesting in future work to examine the impact of Pi on the effects of C-peptide on inflammation and fibrosis in a T1DM model *in vivo.* Dietary restriction of the Pi concentration in extracellular fluid might be used to determine whether lowering plasma Pi concentration in rodents to the level normally observed in humans has any impact on the effects of C-peptide that were observed in Chapter 5. This would also be of interest because of reports that Pi itself promotes renal fibrosis (Tan *et al.*, 2016) and that the plasma membrane Pi transporter PiT1 (SLC20A1) promotes inflammation in response to lipopolysaccharide (Koumakis *et al.*, 2019).

6.7 Conclusion

In summary, the findings presented in this thesis highlight the important role of C-peptide as an active tool in renal biology and the *in vivo* work strongly suggests that C-peptide is renoprotective in T1DM in rats. Replacement of C-peptide in deficient people may therefore potentially restore normal renal function impaired by various injurious agents.

6.8 Limitations in this project

Overall I have found working with C-peptide difficult and in some cases unpredictable. Others in this field have found this too and these difficulties have hampered progress in C-peptide biology. The absence of a robustly identified receptor for C-peptide is a general limitation in the C-peptide field. Stimulation of TERT/1 and HEK293A cells *in vitro* and prolonged stimulation of diabetic rat kidney *in vivo* with C-peptide, in this study, did not show any effect of C-peptide on the expression of the proposed C-peptide receptor

GPR146. A complication in research on the C-peptide receptor is that several studies have shown that insulin and C-peptide signalling interact, suggesting that it might be necessary to stimulate with insulin along with C-peptide to observe the full interaction between GPR146 and insulin receptor (see Section 3.3). Such experiments would obviously be a priority in future work.

For further examination of the claim that GPR146 is C-peptide's receptor, a transient expression of EGFP-GPR146 was attempted in the two cell lines that had been shown here to respond to C-peptide *in vitro* (i.e. TERT/1 and HEK293A). In spite of repeated attempts, only very low transfection efficiency was observed. However, some of the experiments with the GPR146-EGFP construct were accompanied by declining cell viability. It would therefore be of interest to repeat this work after generating a completely new sample of the GPR146-EGFP construct, to eliminate the possibility that a toxic contaminant in the construct had adversely affected the earlier work.

A limitation of the *in vitro* experiments described in Chapters 3 and 4 is that they were only conducted in immortalised cell lines. In future work it would be of interest to confirm whether the effects of C-peptide and Pi that were reported there also occur in primary cultures of human proximal tubular epithelial cells. Furthermore, in some experiments in Chapter 4, it was noted that the Pi concentration detected in the cell monolayer (Fig 4.6b and Fig 4.7b) showed wide variation between replicate experiments. Although this could be because of calcium phosphate precipitation into the cell monolayer from the culture medium, the exact reason behind this was not investigated directly. This possibility could be investigated in future experiments by measuring deposition of radio-active $^{45}Ca^{2+}$ in the cell monolayer.

The possible physiological significance of inhibition of renal Pi transporters by C-peptide in Chapter 4 by down-regulating the level of mRNA expression of SLC20A2 and SLC53A1 Pi transporters was investigated in TERT/1 cells. However, similar investigations were not conducted on mRNA extracted from rat kidney (Chapter 5). In future such measurements on kidneys exposed to C-peptide *in vivo* would be of interest to determine whether Pi transporters are a physiologically important target for regulation by C-peptide.

Appendix

Appendix 1: Reducing Lysis buffer

Stock Solutions	For 10ml	Final concentration
1M pH 7.4 beta glycerophosphate	100ul	10mM
0.5M pH 8 EDTA	20ul	1mM
40mM EGTA	250ul	1mM
1M pH 7.5 Tris-HCl	500ul	50mM
100mM Na Orthovanadate	100ul	1mM
1M Benzamidine	10ul	1mM
100mM PMSF	20ul	0.2mM
5mg/ml Pepstatin A	10ul	
5mg/ml Leupeptin	10ul	
Beta-Mercaptoethanol	10ul	0.1%
10% Triton X-100	1ml	1%
500mM Na Fluoride	1ml	50mM
Nano-pure water	6.97ml	

Appendix 2: Sample Buffer

Component	Volume (ml)
Water	4.00
0.5m TRIS HCl pH6.8	1.00
Glycerol	0.80
10% (w/v) SDS	1.60
2-β-mercaptoethanol	0.40
0.05% (w/v) bromophenol blue	0.20

Appendix 3: Resolving and Stacking Gel for Western Blot (×1 gel)

Stock solutions	12% Resolving gel	10% Resolving gel	12% Stacking gel
Water (Nano-pure)	3.35 ml	3.1 ml	3.03 ml
Acrylamide1 (30 w/v)	4 ml	2.5 ml	0.65 ml
1.5M Tris HCl (pH:8.8)	2.5 ml	1.875	---
0.5M Tris HCl(pH:6.8)	---	---	1.25 ml
SDS(10% w/v)	100 µl	75 µl	50 µl
APS2	50 µl	37.5 µl	25 µl
TEMED3	5 µl	10 µl	5 µl

Appendix 4: Buffers

Western Transfer buffer (1litre)

3.03g Tris-base

14.4g Glycine

200ml Methanol

SDS-PAGE Running buffer (1litre)

3.03g Tris-base

14.4g glycine

50ml 20% w/v SDS

Tris-buffered saline 10 X (TBS) (1 litre)

6.055g Trizma Base

8.766g NaCl

Adjust to pH 7.6 with HCl

TBS-Tween 1 X (1 litre)

100ml 10X TBS

900ml De-ionised H2O

1ml Tween 20

Appendix 5: Characteristics of the animals used in the diabetic rat study

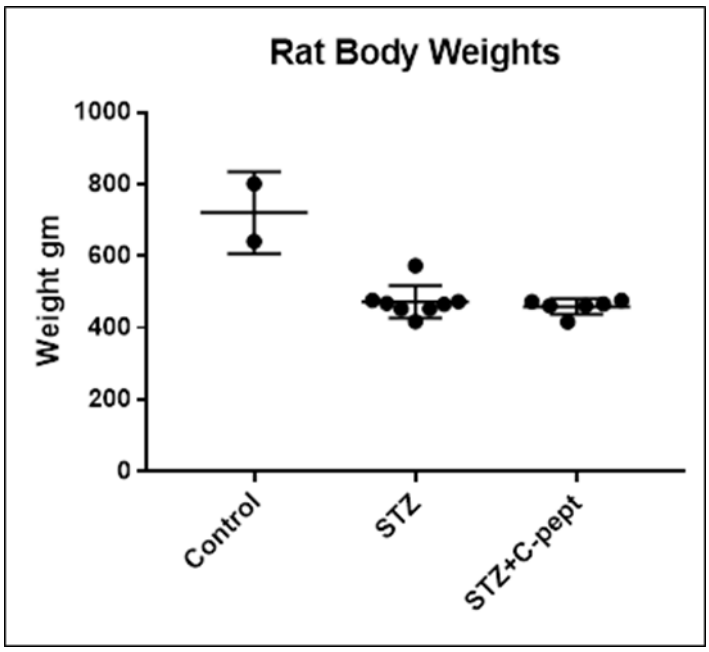

Appendix 5.1 Rat body weight; data are presented from 8 rats from the STZ group, 6 STZ+C-pep group rats, and 2 rats from the healthy (control) group. (Conducted by Mr Jeremy Brown).

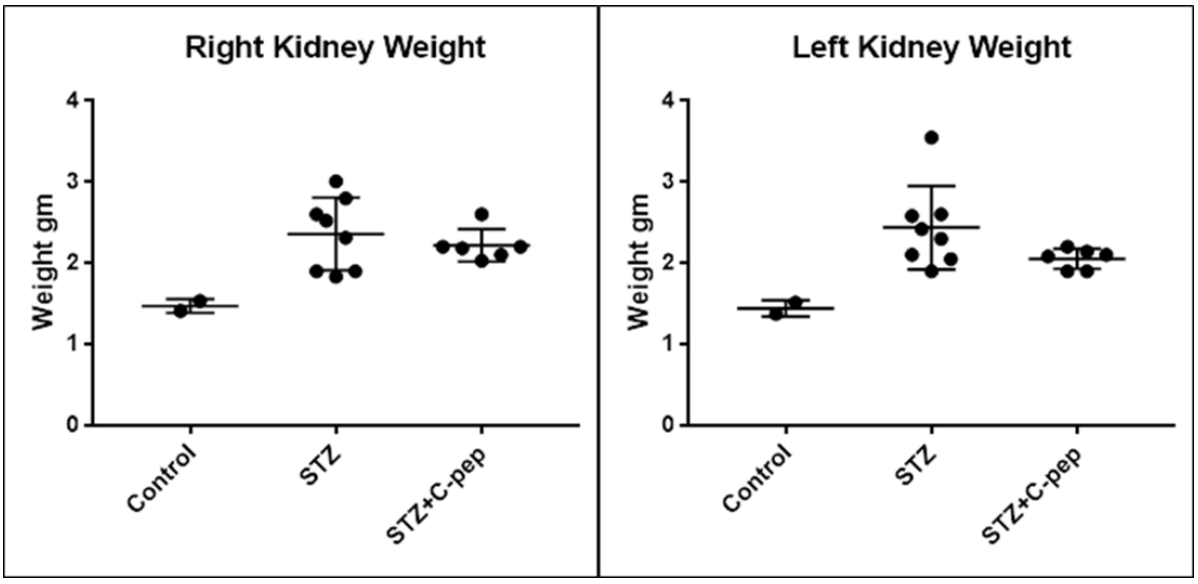

Appendix 5.2 Rat right and left kidney weight; data are presented from 8 rats from the STZ group, 6 STZ+C-pep group rats, and 2 rats from the healthy (control) group. (Conducted by Mr Jeremy Brown).

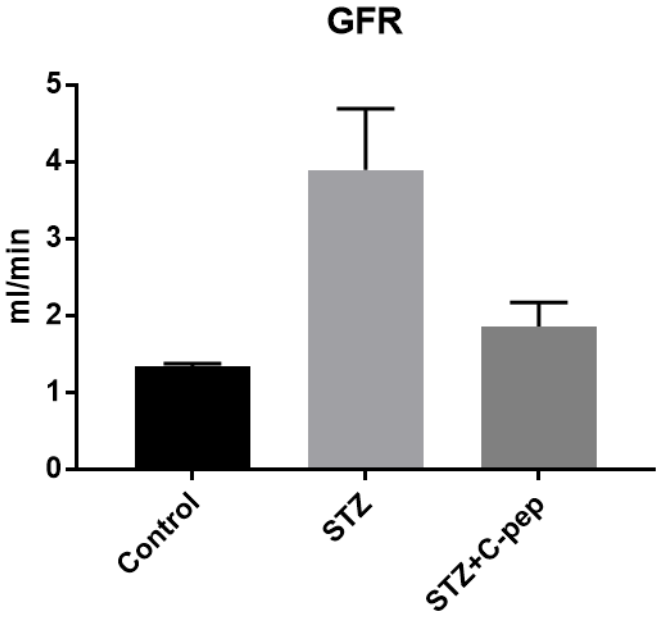

Appendix 5.3 Glomerular filtration rate (GFR) estimated from creatinine clearance; data are presented from 8 rats from the STZ group, 6 STZ+C-pep group rats, and 2 rats from the healthy (control) group. (Conducted by Mr Jeremy Brown).

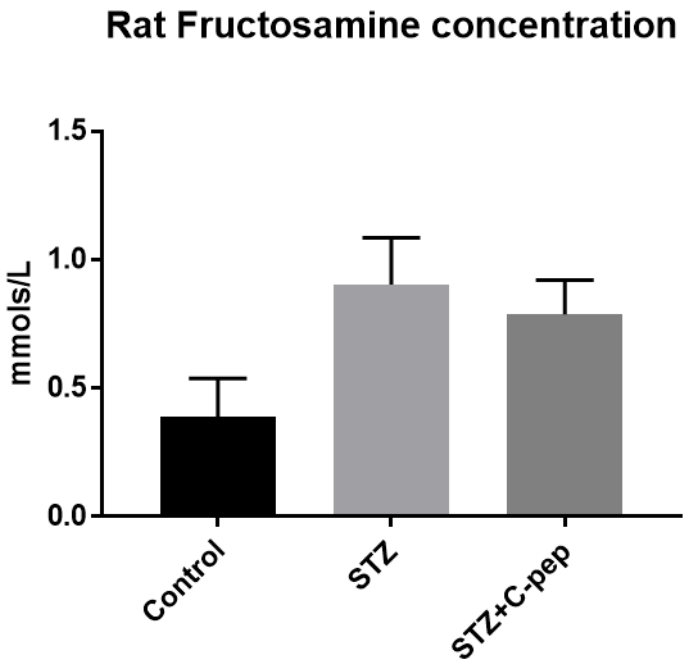

Appendix 5.4 Rat plasma fructosamine concentration; data are presented from 8 rats from the STZ group, 6 STZ+C-pep group rats, and 2 rats from the healthy (control) group. (Conducted by Mr Jeremy Brown).

Bibliography

Abbasian, N., Burton, J.O., Herbert, K.E., Tregunna, B.E., Brown, J.R., Ghaderi-Najafabadi, M., Brunskill, N.J., Goodall, A.H., Bevington, A., 2015. Hyperphosphatemia, Phosphoprotein Phosphatases, and Microparticle Release in Vascular Endothelial Cells. *Journal of the American Society of Nephrology : JASN.* **26,** 2152-2162.

Abell SK, de Courten B, Boyle JA & Teede HJ., 2015. Inflammatory and other biomarkers: role in pathophysiology and prediction of gestational diabetes mellitus. *International Journal of Molecular Sciences* 16 13442–13473.

Abraham, M.I., McAteer, J.A., Kempson, S.A., 1990. Insulin stimulates phosphate transport in opossum kidney epithelial cells. *The American Journal of Physiology.* **258,** F1592-8.

Adam, C., Frame, S., Cohen, P., 2004. Further evidence that the tyrosine phosphorylation of glycogen synthase kinase-3 (GSK3) in mammalian cells is an autophosphorylation event. *Biochemical Journal.* **377,** 249-255.

Adeniyi, F.A., Adeleye, J., Adeniyi, C., 2010. Diabetes, sexual dysfunction and therapeutic exercise: a 20 year review. *Current Diabetes Reviews.* **6,** 201-206.

Ahren, B. 2000. Autonomic regulation of islet hormone secretion--implications for health and disease. *Diabetologia*. 43:393-410.

Al-Isawi, Z.J., 2019. *Role of C-Peptide in the Vasculature.*

Al-Rasheed, N.M., Chana, R.S., Baines, R.J., Willars, G.B., Brunskill, N.J., 2004. Ligand-independent activation of peroxisome proliferator-activated receptor-gamma by insulin and C-peptide in kidney proximal tubular cells: dependent on phosphatidylinositol 3-kinase activity. *The Journal of Biological Chemistry.* **279,** 49747.

Al-Rasheed, N.M., Meakin, F., Royal, E., Lewington, A., Brown, J., Willars, G., Brunskill, N.J., 2004. Potent activation of multiple signalling pathways by C-peptide in opossum kidney proximal tubular cells. *Diabetologia.* **47,** 987-997.

Al-Rasheed, N.M., 2006. *Proinsulin C-peptide : activation of intracellular signalling pathways and modulation of transcription factors in opossum kidney proximal tubular cells.* Ph. D. University of Leicester.

Al-Rasheed, N.M., Willars, G.B., Brunskill, N.J., 2006. C-peptide signals via Galpha i to protect against TNF-alpha-mediated apoptosis of opossum kidney proximal tubular cells. *Journal of the American Society of Nephrology : JASN.* **17,** 986-995.

Anderson, J.W., Kendall, C.W., Jenkins, D.J., 2003. Importance of weight management in type 2 diabetes: review with meta-analysis of clinical studies. *Journal of the American College of Nutrition.* **22,** 331-339.

Ansermet, C., Moor, M.B., Centeno, G., Auberson, M., Hu, D.Z., Baron, R., Nikolaeva, S., Haenzi, B., Katanaeva, N., Gautschi, I., Katanaev, V., Rotman, S., Koesters, R., Schild, L., Pradervand, S., Bonny, O., Firsov, D., 2017. Renal Fanconi Syndrome and Hypophosphatemic Rickets in the Absence of Xenotropic and Polytropic Retroviral Receptor in the Nephron. *Journal of the American Society of Nephrology : JASN.* **28,** 1073-1078.

Ashcroft, F.M. & Rorsman, P., 1989. Electrophysiology of the pancreatic β-cell. *Progress in Biophysics and Molecular Biology.* **54,** 87-143.

Aso, Y., Yoshida, N., Okumura, K., Wakabayashi, S., Matsutomo, R., Takebayashi, K., Inukai, T., 2004. Coagulation and inflammation in overt diabetic nephropathy: association with hyperhomocysteinemia. *Clinica Chimica Acta.* **348,** 139-145.

Atkinson, M.A., Eisenbarth, G.S., Michels, A.W., 2014. Type 1 diabetes. *The Lancet.* **383,** 69-82.

Babic, A.M., Wang, H.W., Lai, M.J., Daniels, T.G., Felbinger, T.W., Burger, P.C., Stricker-Krongrad, A. and Wagner, D.D., 2004. ICAM-1 and β2 integrin deficiency impairs fat oxidation and insulin metabolism during fasting. *Molecular Medicine*, ***10***(7), pp.72-79.

Bansal, V.K., 1990. Serum Inorganic Phosphorus. In 3rd, Walker, H. K., Hall, W. D. and Hurst, J. W., eds, *Clinical Methods: The History, Physical, and Laboratory Examinations.* Boston: Butterworth Publishers, a division of Reed Publishing.

Baud, L. & Ardaillou, R., 1995. Tumor necrosis factor in renal injury. *Mineral and Electrolyte Metabolism.* **21,** 336-341.

Bell, D. & Ovalle, F., 2006. Long-term glycaemic efficacy and weight changes associated with thiazolidinediones when added at an advanced stage of type 2 diabetes. *Diabetes, Obesity and Metabolism.* **8,** 110-115.

Berthelay, S., Saint-Hillier, Y., Nguyen, N.U., Henriet, M.T., Dumoulin, G., Wolf, J.P., Haton, D., 1984. Relations between oral glucose load and urinary elimination of calcium and phosphorus in healthy men with normal body weight. *Nephrologie.* **5,** 205-207.

Bevington, A., Kemp, G., Graham, R., RUSSEL, G., 1992. Phosphate-sensitive enzymes: a possible molecular basis for cellular disorders of phosphate metabolism. *Clinical Chemistry and Enzymology Communications.* **4,** 235-257.

Bevington, A., Kemp, G., Russell, R., 1990. Acquired disorders of phosphate metabolism. *The Metabolic and Molec-Ular Basis of Acquired Disease.London.* **8301,** 1097-1123.

Bhatt, M.P., Lim, Y.C., Kim, Y.M., Ha, K.S., 2013a. C-peptide activates AMPKalpha and prevents ROS-mediated mitochondrial fission and endothelial apoptosis in diabetes. *Diabetes.* **62,** 3851-3862.

Bhatt, M.P., Lim, Y., Ha, K., 2014. C-peptide replacement therapy as an emerging strategy for preventing diabetic vasculopathy. *Cardiovascular Research.* **104,** 234-244.

Bhatt, M.P., Lim, Y.C., Hwang, J., Na, S., Kim, Y.M., Ha, K.S., 2013b. C-peptide prevents hyperglycemia-induced endothelial apoptosis through inhibition of reactive oxygen species-mediated transglutaminase 2 activation. *Diabetes.* **62,** 243-253.

Biga, L., Dawson, S., Harwell, A., Hopkins, R., Kaufmann, J., LeMaster, M., Matern, P., Morrison-Graham, K., Quick, D. and Runyeon, J., 2020. 25.1 *Internal And External Anatomy Of The Kidney*. [online] Open.oregonstate.education. Available at: <https://open.oregonstate.education/aandp/chapter/25-1-internal-and-external-anatomy-of-the-kidney/> [Accessed 10 December 2019].

Binder AM, Larocca J, Lesseur C, Marsit CJ & Michels KB., 2015. Epigenome-wide and transcriptome-wide analyses reveal gestational diabetes is associated with alterations in the human leukocyte antigen complex. *Clinical Epigenetics* 7 79.

Blobe, G.C., Schiemann, W.P., Lodish, H.F., 2000. Role of transforming growth factor β in human disease. *New England Journal of Medicine.* **342,** 1350-1358.

Bo, S., Gentile, L., Castiglione, A., Prandi, V., Canil, S., Ghigo, E., Ciccone, G., 2012. C-peptide and the risk for incident complications and mortality in type 2 diabetic patients: a retrospective cohort study after a 14-year follow-up. *European Journal of Endocrinology.* **167,** 173-180.

Bohle, A., Wehrmann, M., Bogenschütz, O., Batz, C., Müller, G., 1991. The pathogenesis of chronic renal failure in diabetic nephropathy: investigation of 488 cases of diabetic glomerulosclerosis. *Pathology-Research and Practice.* **187,** 251-259.

Bon, N., Couasnay, G., Bourgine, A., Sourice, S., Beck-Cormier, S., Guicheux, J., Beck, L., 2018. Phosphate (Pi)-regulated heterodimerization of the high-affinity sodium-dependent Pi transporters PiT1/Slc20a1 and PiT2/Slc20a2 underlies extracellular Pi sensing independently of Pi uptake. *The Journal of Biological Chemistry.* **293,** 2102-2114.

Boyle, J.J., Weissberg, P.L., Bennett, M.R., 2003. Tumor necrosis factor-α promotes macrophage-induced vascular smooth muscle cell apoptosis by direct and autocrine mechanisms. *Arteriosclerosis, Thrombosis, and Vascular Biology.* **23,** 1553-1558.

Brady, H.R., 1994. *Leukocyte Adhesion Molecules and Kidney Diseases.*

Braga Gomes, K., Fontana Rodrigues, K., Fernandes, A.P., 2014. The role of transforming growth factor-beta in diabetic nephropathy. *International Journal of Medical Genetics.* **2014,** .

Brauner-Osborne H, Wellendorph P, Jensen AA (2007). Structure, pharmacology and therapeutic prospects of family C G-protein coupled receptors. *Curr Drug Targets* 8**:** 169-184.

Brems, D.N., Brown, P.L., Heckenlaible, L.A., Frank, B.H., 1990. Equilibrium denaturation of insulin and proinsulin. *Biochemistry.* **29,** 9289-9293.

Birkner, K., Wasser, B., Loos, J., Plotnikov, A., Seger, R., Zipp, F., Witsch, E. and Bittner, S., 2017. The role of ERK signaling in experimental autoimmune encephalomyelitis. *International journal of molecular sciences*, *18*(9), p.1990.

Brownlee, M., 2001. Biochemistry and molecular cell biology of diabetic complications. *Nature.* **414,** 813.

Brunskill, N., 2017. C-peptide and diabetic kidney disease. *Journal of Internal Medicine.* **281,** 41-51.

Buchanan, T.A. and Xiang, A.H., 2005. Gestational diabetes mellitus. *The Journal of clinical investigation*, ***115***(3), pp.485-491.

Burns D (1988). "Subunit structure and enzymic activity of pertussis toxin". *Microbiol Sci*. 5(9): 285–7.

Burnstock, G., 2014. Purinergic signalling: from discovery to current developments. *Experimental Physiology*. **99,** 16-34.

Buzalaf, M.A., Taga, E.M., Granjeiro, J.M., Ferreira, C.V., Lourença, V.A., Ortega, M.M., Poletto, D.W., Aoyama, H., 1998. Kinetic characterization of bovine lung low-molecular-weight protein tyrosine phosphatase. *Experimental Lung Research.* **24,** 269-272.

Camalier, C.E., Yi, M., Yu, L., Hood, B.L., Conrads, K.A., Lee, Y.J., Lin, Y., Garneys, L.M., Bouloux, G.F., Young, M.R., 2013. An integrated understanding of the physiological response to elevated extracellular phosphate. *Journal of Cellular Physiology.* **228,** 1536-1550.

Campbell, R.K., 2009. Fate of the beta-cell in the pathophysiology of type 2 diabetes. *Journal of the American Pharmacists Association : JAPhA.* **49 Suppl 1,** S10-5.

Cargnello, M. & Roux, P.P., 2011. Activation and function of the MAPKs and their substrates, the MAPK-activated protein kinases. *Microbiology and Molecular Biology Reviews : MMBR.* **75,** 50-83.

Caverzasio, J., Brown, C.D., Biber, J., Bonjour, J.P., Murer, H., 1985. Adaptation of phosphate transport in phosphate-deprived LLC-PK1 cells. *The American Journal of Physiology.* **248,** F122-7.

Ceriello, A., 2005. Postprandial hyperglycemia and diabetes complications: is it time to treat? *Diabetes.* **54,** 1-7.

Cha, D.R., Kim, N.H., Yoon, J.W., Jo, S.K., Cho, W.Y., Kim, H.K., Won, N.H., 2000. Role of vascular endothelial growth factor in diabetic nephropathy. *Kidney International.* **58,** S104-S112.

Chatterjee, S., Khunti, K., Davies, M.J., 2017. Type 2 diabetes. *The Lancet.* **389,** 2239-2251.

Chaudhury, A., Duvoor, C., Dendi, R., Sena, V., Kraleti, S., Chada, A., Ravilla, R., Marco, A., Shekhawat, N.S., Montales, M.T., 2017. Clinical review of antidiabetic drugs: implications for type 2 diabetes mellitus management. *Frontiers in Endocrinology.* **8,** 6.

Chen, L., Yang, X., Tang, J., 2002. Acidic residues on the N-terminus of proinsulin C-peptide are important for the folding of insulin precursor. *The Journal of Biochemistry.* **131,** 855-859.

Chima, R.S., Maltese, G., Lamontagne, T., Piraino, G., Denenberg, A., O'Connor, M., Zingarelli, B., 2011. C-peptide ameliorates kidney injury following hemorrhagic shock. *Shock (Augusta, Ga.).* **35,** 524-529.

Chmielewski, C., 2003. Renal anatomy and overview of nephron function. *Nephrology Nursing Journal.* **30,** 185.

Chow, F.Y., Nikolic-Paterson, D.J., Ozols, E., Atkins, R.C., Tesch, G.H., 2005a. Intercellular adhesion molecule-1 deficiency is protective against nephropathy in type 2 diabetic db/db mice. *Journal of the American Society of Nephrology : JASN.* **16,** 1711-1722.

Chow, F.Y., Nikolic-Paterson, D.J., Atkins, R.C., Tesch, G.H., 2004. Macrophages in streptozotocin-induced diabetic nephropathy: potential role in renal fibrosis. *Nephrology Dialysis Transplantation.* **19,** 2987-2996.

Chow, F.Y., Nikolic-Paterson, D.J., Ozols, E., Atkins, R.C., Tesch, G.H., 2005b. Intercellular adhesion molecule-1 deficiency is protective against nephropathy in type 2 diabetic db/db mice. *Journal of the American Society of Nephrology : JASN.* **16,** 1711-1722.

Cifarelli, V., Luppi, P., Hubert, M.T., He, J., Piganelli, J., Trucco, M., 2008. Human proinsulin C-peptide reduces high glucose-induced proliferation and NF-κB activation in vascular smooth muscle cells. *Atherosclerosis.* **201,** 248-257.

Cifarelli, V., Trucco, M., Luppi, P., 2011. Anti-inflammatory effects of C-peptide prevent endothelial dysfunction in type 1 diabetes. *Immunology, Endocrine & Metabolic Agents in Medicinal Chemistry (Formerly Current Medicinal Chemistry-Immunology, Endocrine and Metabolic Agents).* **11,** 59-70.

Cines, D.B., Pollak, E.S., Buck, C.A., Loscalzo, J., Zimmerman, G.A., McEver, R.P., Pober, J.S., Wick, T.M., Konkle, B.A., Schwartz, B.S., 1998. Endothelial cells in physiology and in the pathophysiology of vascular disorders. *Blood, the Journal of the American Society of Hematology.* **91,** 3527-3561.

Clausen, M.V., Hilbers, F. and Poulsen, H., 2017. The structure and function of the Na, K-ATPase isoforms in health and disease. *Frontiers in physiology*, *8*, p.371.

Clausen, P., Jacobsen, P., Rossing, K., Jensen, J., Parving, H., Feldt-Rasmussen, B., 2000. Plasma concentrations of VCAM-1 and ICAM-1 are elevated in patients with Type 1 diabetes mellitus with microalbuminuria and overt nephropathy. *Diabetic Medicine.* **17,** 644-649.

Coleman, D.L. & Ruef, C., 1992. Interleukin-6: an autocrine regulator of mesangial cell growth. *Kidney International.* **41,** 604-606.

Connolly, D.T., Heuvelman, D.M., Nelson, R., Olander, J.V., Eppley, B.L., Delfino, J.J., Siegel, N.R., Leimgruber, R.M., Feder, J., 1989. Tumor vascular permeability factor stimulates endothelial cell growth and angiogenesis. *The Journal of Clinical Investigation.* **84,** 1470-1478.

Connolly, D.T., Olander, J.V., Heuvelman, D., Nelson, R., Monsell, R., Siegel, N., Haymore, B.L., Leimgruber, R., Feder, J., 1989. Human vascular permeability factor. Isolation from U937 cells. *The Journal of Biological Chemistry.* **264,** 20017-20024.

Cooper, M.E., Vranes, D., Youssef, S., Stacker, S.A., Cox, A.J., Rizkalla, B., Casley, D.J., Bach, L.A., Kelly, D.J., Gilbert, R.E., 1999. Increased renal expression of vascular endothelial growth factor (VEGF) and its receptor VEGFR-2 in experimental diabetes. *Diabetes.* **48,** 2229-2239.

Craven, P.A., Davidson, C.M., DeRubertis, F.R., 1990. Increase in diacylglycerol mass in isolated glomeruli by glucose from de novo synthesis of glycerolipids. *Diabetes.* **39,** 667-674.

Crean, D., Bellwon, P., Aschauer, L., Limonciel, A., Moenks, K., Hewitt, P., Schmidt, T., Herrgen, K., Dekant, W., Lukas, A., 2015. Development of an in vitro renal epithelial disease state model for xenobiotic toxicity testing. *Toxicology in Vitro.* **30,** 128-137.

Creative-diagnostics.com. 2021. Erk Signaling Pathway - Creative Diagnostics. [online] Available at: <https://www.creative-diagnostics.com/Erk-Signaling-Pathway.htm> [Accessed 21 March 2021].

Cukierman, T., Gerstein, H., Williamson, J., 2005. Cognitive decline and dementia in diabetes—systematic overview of prospective observational studies. *Diabetologia.* **48,** 2460-2469.

Dasu, M.R., Devaraj, S., Jialal, I., 2007. High glucose induces IL-1β expression in human monocytes: mechanistic insights. *American Journal of Physiology-Endocrinology and Metabolism.* **293,** E337-E346.

Damm, P., Kühl, C., Buschard, K., Jakobsen, B.K., Svejgaard, A., Sodoyez-Goffaux, F., Shattock, M., Bottazzo, G.F. and Mølsted-Pedersen, L., 1994. Prevalence and predictive value of islet cell antibodies and insulin autoantibodies in women with gestational diabetes. *Diabetic medicine*, *11*(6), pp.558-563.

de Boer, I.H., Rue, T.C., Hall, Y.N., Heagerty, P.J., Weiss, N.S., Himmelfarb, J., 2011. Temporal trends in the prevalence of diabetic kidney disease in the United States. *Jama.* **305,** 2532-2539.

De La Tour, D. Dufayet, Raccah, D., Jannot, M.F., Coste, T., Rougerie, C., Vague, P., 1998. Erythrocyte Na/K ATPase activity and diabetes: relationship with C-peptide level. *Diabetologia.* **41,** 1080-1084.

De Meyts, P., 2016. The insulin receptor and its signal transduction network. In *Endotext [Internet]*. MDText. com, Inc.

Dekker Nitert, M., Barrett, H.L., Kubala, M.H., Scholz Romero, K., Denny, K.J., Woodruff, T.M., McIntyre, H.D. and Callaway, L.K., 2014. Increased placental expression of fibroblast growth factor 21 in gestational diabetes mellitus. *The Journal of Clinical Endocrinology & Metabolism*, *99*(4), pp.E591-E598.

Derubertis, F.R. & Craven, P.A., 1994. Activation of protein kinase C in glomerular cells in diabetes. Mechanisms and potential links to the pathogenesis of diabetic glomerulopathy. *Diabetes.* **43,** 1-8.

Diabetes Control and Complications Trial Research Group, 1993. The effect of intensive treatment of diabetes on the development and progression of long-term complications in insulin-dependent diabetes mellitus. *New England Journal of Medicine.* **329,** 977-986.

Dick, C.F., Dos-Santos, A.L., Meyer-Fernandes, J.R., 2011. Inorganic phosphate as an important regulator of phosphatases. *Enzyme Research.* **2011,** 103980.

Dimas, G.G., Didangelos, T.P., Grekas, D.M., 2017. Matrix Gelatinases in Atherosclerosis and Diabetic Nephropathy: Progress and Challenges. *Current Vascular Pharmacology.* **15,** 557-565.

Djemli-Shipkolye, A., Gallice, P., Coste, T., Jannot, M.F., Tsimaratos, M., Raccah, D., Vague, P., 2000. The effects ex vivo and in vitro of insulin and C-peptide on Na/K adenosine triphosphatase activity in red blood cell membranes of type 1 diabetic patients. *Metabolism: Clinical and Experimental.* **49,** 868-872.

Dong, X., Swaminathan, S., Bachman, L., Croatt, A., Nath, K., Griffin, M., 2007. Resident dendritic cells are the predominant TNF-secreting cell in early renal ischemia–reperfusion injury. *Kidney International.* **71,** 619-628.

Dube, N., Cheng, A., Tremblay, M.L., 2004. The role of protein tyrosine phosphatase 1B in Ras signaling. *Proceedings of the National Academy of Sciences of the United States of America.* **101,** 1834-1839.

Eddy, A.A., Giachelli, C.M., Liu, E., 1995. Renal expression of genes that promote interstitial inflammation and fibrosis in rats with protein-overload proteinuria. *Kidney International.* **47,** 1546-1557.

Edmund Lamb, 2011. Kidney disease. In Nessar Ahmed, ed, Clinical Biochemistry. 1st ed. United States: Oxford University Press. 59-98.

Eisenbarth, G.S., 2007. Update in type 1 diabetes. *The Journal of Clinical Endocrinology & Metabolism.* **92,** 2403-2407.

Ekberg, K., Brismar, T., Johansson, B.L., Lindstrom, P., Juntti-Berggren, L., Norrby, A., Berne, C., Arnqvist, H.J., Bolinder, J., Wahren, J., 2007. C-Peptide replacement therapy and sensory nerve function in type 1 diabetic neuropathy. *Diabetes Care.* **30,** 71-76.

Eknoyan, G. & Quetelet, A., 2008. The average man and indices of obesity. (1796–1874) Nephrol. *Dial.Transplant.* **23,** 47-51.

Engelman, J.A., Luo, J., Cantley, L.C., 2006. The evolution of phosphatidylinositol 3-kinases as regulators of growth and metabolism. *Nature Reviews Genetics.* **7,** 606.

Easom, R.A. 2000. Beta-granule transport and exocytosis. *Semin Cell Dev Biol*. 11:253-66.

Flatt PR, Swanston-Flatt SK, Hampton SM, Bailey CJ, Marks V (1986). Specific binding of the C-peptide of proinsulin to cultured B-cells from a transplantable rat islet cell tumor. *Bioscience reports* 6**:** 193-199.

Fine, L.G., 1995. William Bowman's description of the microscopic anatomy of the kidney. *Nephrology, Dialysis, Transplantation : Official Publication of the European Dialysis and Transplant Association - European Renal Association.* **10,** 2147-2149.

Fioretto, P., Barzon, I., Mauer, M., 2014. Is diabetic nephropathy reversible? *Diabetes Research and Clinical Practice.* **104,** 323-328.

Fioretto, P., Steffes, M.W., Sutherland, D.E., Goetz, F.C., Mauer, M., 1998. Reversal of lesions of diabetic nephropathy after pancreas transplantation. *New England Journal of Medicine.* **339,** 69-75.

Fiorina, P., Folli, F., Maffi, P., Placidi, C., Venturini, M., Finzi, G., Bertuzzi, F., Davalli, A., D'Angelo, A., Socci, C., 2003. Islet transplantation improves vascular diabetic complications in patients with diabetes who underwent kidney transplantation: a comparison between kidney-pancreas and kidney-alone transplantation1. *Transplantation.* **75,** 1296-1301.

Forbes, J.M. & Cooper, M.E., 2013. Mechanisms of diabetic complications. *Physiological Reviews.* **93,** 137-188.

Forbes, J.M., Cooper, M.E., Oldfield, M.D., Thomas, M.C., 2003. Role of advanced glycation end products in diabetic nephropathy. *Journal of the American Society of Nephrology : JASN.* **14,** S254-8.

Forst, T., De La Tour, D.D., Kunt, T., Pfutzner, A., Goitom, K., Pohlmann, T., Schneider, S., Johansson, B.L., Wahren, J., Lobig, M., Engelbach, M., Beyer, J., Vague, P., 2000. Effects of proinsulin C-peptide on nitric oxide, microvascular blood flow and

erythrocyte Na+,K+-ATPase activity in diabetes mellitus type I. *Clinical Science (London, England : 1979).* **98,** 283-290.

Forst, T., Hach, T., Kunt, T., Weber, M.M., Pfutzner, A., 2009. Molecular effects of C-Peptide in microvascular blood flow regulation. *The Review of Diabetic Studies : RDS.* **6,** 159-167.

Forster, I., Hernando, N., Biber, J., Murer, H., 2006. Proximal tubular handling of phosphate: A molecular perspective. *Kidney International.* **70,** 1548-1559.

Fowler, M.J., 2008. Microvascular and macrovascular complications of diabetes. *Clinical Diabetes.* **26,** 77-82.

Frank RN (2004). Diabetic retinopathy. *The New England journal of medicine* 350**:** 48-58.

Fredriksson R, Lagerstrom MC, Lundin LG, Schioth HB (2003). The G-protein-coupled receptors in the human genome form five main families. Phylogenetic analysis, paralogon groups, and fingerprints. *Molecular pharmacology* **63:** 1256-1272.

Fricker, L.D., Evans, C.J., Esch, F.S., Herbert, E., 1986. Cloning and sequence analysis of cDNA for bovine carboxypeptidase E. *Nature.* **323,** 461.

Gaither, K., Quraishi, A.N. and Illsley, N.P., 1999. Diabetes alters the expression and activity of the human placental GLUT1 glucose transporter. *The Journal of Clinical Endocrinology & Metabolism*, ***84***(2), pp.695-701.

Galkina, E. & Ley, K., 2006a. Leukocyte recruitment and vascular injury in diabetic nephropathy. *Journal of the American Society of Nephrology : JASN.* **17,** 368-377.

Galkina, E. & Ley, K., 2006b. Leukocyte recruitment and vascular injury in diabetic nephropathy. *Journal of the American Society of Nephrology : JASN.* **17,** 368-377.

Galkina, E. & Ley, K., 2006c. Leukocyte recruitment and vascular injury in diabetic nephropathy. *Journal of the American Society of Nephrology : JASN.* **17,** 368-377.

Galuska, D., Pirkmajer, S., Barrès, R., Ekberg, K., Wahren, J., Chibalin, A.V., 2011. C-peptide increases Na, K-ATPase expression via PKC-and MAP kinase-dependent activation of transcription factor ZEB in human renal tubular cells. *PLoS One.* **6,** e28294.

Gavin, J.R., Alberti, K.G.M.M., Davidson, M.B., DeFronzo, R.A., 1997. Report of the expert committee on the diagnosis and classification of diabetes mellitus. *Diabetes Care.* **20,** 1183.

Gerbi, A., Barbey, O., Raccah, D., Coste, T., Jamme, I., Nouvelot, A., Ouafik, L., LÚvy, S., Vague, P., Maixent, J., 1997. Alteration of Na, K-ATPase isoenzymes in diabetic cardiomyopathy: effect of dietary supplementation with fish oil (n-3 fatty acids) in rats. *Diabetologia.* **40,** 496-505.

Gilbertson, D.T., Liu, J., Xue, J.L., Louis, T.A., Solid, C.A., Ebben, J.P., Collins, A.J., 2005. Projecting the number of patients with end-stage renal disease in the United

States to the year 2015. *Journal of the American Society of Nephrology : JASN.* **16,** 3736-3741.

Glaucoma Research Foundation. 2020. *Types Of Glaucoma*. [online] Available at: <https://www.glaucoma.org/glaucoma/types-of-glaucoma.php> [Accessed 1 July 2020].

Gloriam, D.E., Schiöth, H.B., Fredriksson, R., 2005. Nine new human Rhodopsin family G-protein coupled receptors: identification, sequence characterisation and evolutionary relationship. *Biochimica Et Biophysica Acta (BBA)-General Subjects.* **1722,** 235-246.

Goldsmith, Z.G. and Dhanasekaran, D.N., 2007. G protein regulation of MAPK networks. *Oncogene*, **26**(22), pp.3122-3142.

Grunberger, G., Qiang, X., Li, Z., Mathews, S., Sbrissa, D., Shisheva, A., Sima, A., 2001. Molecular basis for the insulinomimetic effects of C-peptide. *Diabetologia.* **44,** 1247-1257.

Ha, H., Yu, M.R., Choi, Y.J., Kitamura, M., Lee, H.B., 2002. Role of high glucose-induced nuclear factor-kappaB activation in monocyte chemoattractant protein-1 expression by mesangial cells. *Journal of the American Society of Nephrology : JASN.* **13,** 894-902.

Haffner, S.M., Lehto, S., Rönnemaa, T., Pyörälä, K., Laakso, M., 1998. Mortality from coronary heart disease in subjects with type 2 diabetes and in nondiabetic subjects with and without prior myocardial infarction. *New England Journal of Medicine.* **339,** 229-234.

Haidet, J., Cifarelli, V., Trucco, M., Luppi, P., 2009. Anti-inflammatory properties of C-Peptide. *The Review of Diabetic Studies : RDS.* **6,** 168-179.

Han, D.C., Isono, M., Hoffman, B.B., Ziyadeh, F.N., 1999. High glucose stimulates proliferation and collagen type I synthesis in renal cortical fibroblasts: mediation by autocrine activation of TGF-beta. *Journal of the American Society of Nephrology : JASN.* **10,** 1891-1899.

Hanlon, C.D. and Andrew, D.J., 2015. Outside-in signaling–a brief review of GPCR signaling with a focus on the Drosophila GPCR family. *Journal of cell science*, *128*(19), pp.3533-3542.

Harris, D.C., 2001. Tubulointerstitial renal disease. *Current Opinion in Nephrology and Hypertension.* **10,** 303-313.

Haut, L.L., Alfrey, A.C., Guggenheim, S., Buddington, B., Schrier, N., 1980. Renal toxicity of phosphate in rats. *Kidney International.* **17,** 722-731.

Hayden, M.S. and Ghosh, S., 2014. Regulation of NF-κB by TNF family cytokines, *Seminars in immunology*, 2014, Elsevier pp253-266.

Heilker R, Wolff M, Tautermann CS, Bieler M (2009). G-protein-coupled receptor-focused drug discovery using a target class platform approach. *Drug Discov Today* 14**:** 231-240.

Heino, J., Ignotz, R.A., Hemler, M.E., Crouse, C., Massague, J., 1989. Regulation of cell adhesion receptors by transforming growth factor-beta. Concomitant regulation of integrins that share a common beta 1 subunit. *The Journal of Biological Chemistry.* **264,** 380-388.

Henriksson, M., Nordling, E., Melles, E., Shafqat, J., Ståhlberg, M., Ekberg, K., Persson, B., Bergman, T., Wahren, J., Johansson, J., 2005. Separate functional features of proinsulin C-peptide. *Cellular and Molecular Life Sciences CMLS.* **62,** 1772-1778.

Herder, C., Haastert, B., Muller-Scholze, S., Koenig, W., Thorand, B., Holle, R., Wichmann, H.E., Scherbaum, W.A., Martin, S., Kolb, H., 2005. Association of systemic chemokine concentrations with impaired glucose tolerance and type 2 diabetes: results from the Cooperative Health Research in the Region of Augsburg Survey S4 (KORA S4). *Diabetes.* **54 Suppl 2,** S11-7.

Herder, C., Peltonen, M., Koenig, W., Kraft, I., Muller-Scholze, S., Martin, S., Lakka, T., Ilanne-Parikka, P., Eriksson, J.G., Hamalainen, H., Keinanen-Kiukaanniemi, S., Valle, T.T., Uusitupa, M., Lindstrom, J., Kolb, H., Tuomilehto, J., 2006. Systemic immune mediators and lifestyle changes in the prevention of type 2 diabetes: results from the Finnish Diabetes Prevention Study. *Diabetes.* **55,** 2340-2346.

Hill, C., Flyvbjerg, A., Grønbaek, H., Petrik, J., Hill, D., Thomas, C., Sheppard, M., Logan, A., 2000. The renal expression of transforming growth factor-β isoforms and their receptors in acute and chronic experimental diabetes in rats. *Endocrinology.* **141,** 1196-1208.

Hills, C.E., Brunskill, N.J., Squires, P.E., 2010a. C-peptide as a therapeutic tool in diabetic nephropathy. *American Journal of Nephrology.* **31,** 389-397.

Hills, C.E. & Brunskill, N.J., 2009. Cellular and physiological effects of C-peptide. *Clinical Science (London, England : 1979).* **116,** 565-574.

Hills, C.E., Al-Rasheed, N., Al-Rasheed, N., Willars, G.B., Brunskill, N.J., 2009. C-peptide reverses TGF-β1-induced changes in renal proximal tubular cells: implications for treatment of diabetic nephropathy. *American Journal of Physiology-Renal Physiology.* **296,** F614-F621.

Hills, C.E., Brunskill, N.J., Squires, P.E., 2010b. C-peptide as a therapeutic tool in diabetic nephropathy. *American Journal of Nephrology.* **31,** 389-397.

Hladky, S. & Rink, T., 1986. *Body fluid and kidney physiology.* Edward Arnold.

Hodgkins, K.S. & Schnaper, H.W., 2012. Tubulointerstitial injury and the progression of chronic kidney disease. *Pediatric Nephrology.* **27,** 901-909.

Hoshi, S., Nomoto, K., Kuromitsu, J., Tomari, S., Nagata, M., 2002. High glucose induced VEGF expression via PKC and ERK in glomerular podocytes. *Biochemical and Biophysical Research Communications.* **290,** 177-184.

Howell, S.L. 1984. The mechanism of insulin secretion. *Diabetologia*. 26:319-27.

Hu, G.M., Mai, T.L. and Chen, C.M., 2017. Visualizing the GPCR network: classification and evolution. *Scientific reports*, *7*(1), pp.1-15.

Huang, D., Richter, K., Breidenbach, A., Vallon, V., 2002. Human C-peptide acutely lowers glomerular hyperfiltration and proteinuria in diabetic rats: a dose-response study. *Naunyn-Schmiedeberg's Archives of Pharmacology.* **365,** 67-73.

Huang, W., Gallois, Y., Bouby, N., Bruneval, P., Heudes, D., Belair, M.F., Krege, J.H., Meneton, P., Marre, M., Smithies, O., Alhenc-Gelas, F., 2001. Genetically increased angiotensin I-converting enzyme level and renal complications in the diabetic mouse. *Proceedings of the National Academy of Sciences of the United States of America.* **98,** 13330-13334.

Huang, W.H. & Askari, A., 1984. Regulation of (Na K)-ATPase by inorganic phosphate: pH dependence and physiological implications. *Biochemical and Biophysical Research Communications.* **123,** 438-443.

Hutton, J.C. 1994. Insulin secretory granule biogenesis and the proinsulin-processing endopeptidases. *Diabetologia*. 37 Suppl 2:S48-56.

Huyer, G., Liu, S., Kelly, J., Moffat, J., Payette, P., Kennedy, B., Tsaprailis, G., Gresser, M.J., Ramachandran, C., 1997. Mechanism of inhibition of protein-tyrosine phosphatases by vanadate and pervanadate. *The Journal of Biological Chemistry.* **272,** 843-851.

Ido, Y., Vindigni, A., Chang, K., Stramm, L., Chance, R., Heath, W.F., DiMarchi, R.D., Di Cera, E., Williamson, J.R., 1997. Prevention of vascular and neural dysfunction in diabetic rats by C-peptide. *Science (New York, N.Y.).* **277,** 563-566.

Ihm, C.G., Park, J.K., Kim, H.J., Lee, T.W., Cha, D.R., 2002. Effects of high glucose on interleukin-6 production in human mesangial cells. *Journal of Korean Medical Science.* **17,** 208-212.

Illsley NP., 2000. Glucose transporters in the human placenta. *Placenta* 21 14–22.

Ina, K., Kitamura, H., Okeda, T., Nagai, K., Liu, Z.Y., Matsuda, M., Fujikura, Y., 1999. Vascular cell adhesion molecule-l expression in the renal interstitium of diabetic KKAy mice. *Diabetes Research and Clinical Practice.* **44,** 1-8.

INTERNATIONAL_DIABETES_FEDERATION. 2017. IDF Diabetes Atlas [Online]. Brussels, Belgium. Available: http://www.diabetesatlas.org [Accessed 8 October 2019].

Islam, M.S. & Wilson, R.D., 2012. Experimentally induced rodent models of type 2 diabetes. *Animal models in diabetes research.* Springer. 161-174.

Iwano, M., Plieth, D., Danoff, T.M., Xue, C., Okada, H., Neilson, E.G., 2002. Evidence that fibroblasts derive from epithelium during tissue fibrosis. *The Journal of Clinical Investigation.* **110,** 341-350.

Jacquillet, G. & Unwin, R.J., 2019. Physiological regulation of phosphate by vitamin D, parathyroid hormone (PTH) and phosphate (Pi). *Pflügers Archiv-European Journal of Physiology.* **471,** 83-98.

Jägerbrink, T., Lindahl, E., Shafqat, J., Jörnvall, H., 2009. Proinsulin C-peptide interaction with protein tyrosine phosphatase 1B demonstrated with a labeling reaction. *Biochemical and Biophysical Research Communications.* **387,** 31-35.

Janabi, A.M.H., 2017. *Proinsulin C-Peptide-Mediated Signalling and the Search for its Receptor.*

Jansson, N., Greenwood, S.L., Johansson, B.R., Powell, T.L. and Jansson, T., 2003. Leptin stimulates the activity of the system A amino acid transporter in human placental villous fragments. *The Journal of Clinical Endocrinology & Metabolism*, *88*(3), pp.1205-1211.

Jansson, T., Ekstrand, Y., Björn, C., Wennergren, M. and Powell, T.L., 2002. Alterations in the activity of placental amino acid transporters in pregnancies complicated by diabetes. *Diabetes*, *51*(7), pp.2214-2219.

Javierre, B.M., Hernando, H., Ballestar, E., 2011. Environmental triggers and epigenetic deregulation in autoimmune disease. *Discovery Medicine.* **12,** 535-545.

Jevnikar, A.M., Brennan, D.C., Singer, G.G., Heng, J.E., Maslinski, W., Wuthrich, R.P., Glimcher, L.H., Kelley, V.E.R., 1991. Stimulated kidney tubular epithelial cells express membrane associated and secreted TNFα. *Kidney International.* **40,** 203-211.

Jewell, J. L., Oh, E. and Thurmond, D. C. (2010) Exocytosis mechanisms underlying insulin release and glucose uptake: conserved roles for Munc18c and syntaxin 4. *American Journal of Physiology-Regulatory, Integrative and Comparative Physiology, 298*(3), pp. R517-R531.

Jinde, K., Nikolic-Paterson, D.J., Huang, X.R., Sakai, H., Kurokawa, K., Atkins, R.C., Lan, H.Y., 2001. Tubular phenotypic change in progressive tubulointerstitial fibrosis in human glomerulonephritis. *American Journal of Kidney Diseases.* **38,** 761-769.

Johansson, B.L., Borg, K., Fernqvist-Forbes, E., Kernell, A., Odergren, T., Wahren, J., 2000. Beneficial effects of C-peptide on incipient nephropathy and neuropathy in patients with Type 1 diabetes mellitus. *Diabetic Medicine.* **17,** 181-189.

Johansson, B.L., Kernell, A., Sjöberg, S., Wahren, J., 1993. Influence of combined C-peptide and insulin administration on renal function and metabolic control in diabetes type 1. *The Journal of Clinical Endocrinology & Metabolism.* **77,** 976-981.

Johansson, B.L., Linde, B., Wahren, J., 1992. Effects of C-peptide on blood flow, capillary diffusion capacity and glucose utilization in the exercising forearm of type 1 (insulin-dependent) diabetic patients. *Diabetologia.* **35,** 1151-1158.

Johansson, B., Sjöberg, S., Wahren, J., 1992. The influence of human C-peptide on renal function and glucose utilization in type 1 (insulin-dependent) diabetic patients. *Diabetologia.* **35,** 121-128.

Julien, M., Khoshniat, S., Lacreusette, A., Gatius, M., Bozec, A., Wagner, E.F., Wittrant, Y., Masson, M., Weiss, P., Beck, L., 2009. Phosphate-dependent regulation of MGP in osteoblasts: Role of ERK1/2 and Fra-1. *Journal of Bone and Mineral Research.* **24,** 1856-1868.

Kelley, L.A., Mezulis, S., Yates, C.M., Wass, M.N., Sternberg, M.J., 2015. The Phyre2 web portal for protein modeling, prediction and analysis. *Nature Protocols.* **10,** 845.

Khajah, M.A., Mathew, P.M. and Luqmani, Y.A., 2018. Na+/K+ ATPase activity promotes invasion of endocrine resistant breast cancer cells. *PloS one*, ***13***(3), p.e0193779.

Khandelwal, R.L. & Kamani, S.A., 1980. Studies on inactivation and reactivation of homogeneous rabbit liver phosphoprotein phosphatases by inorganic pyrophosphate and divalent cations. *Biochimica Et Biophysica Acta (BBA)-Enzymology.* **613,** 95-105.

King, A. & Bowe, J., 2016. Animal models for diabetes: understanding the pathogenesis and finding new treatments. *Biochemical Pharmacology.* **99,** 1-10.

Kirwan JP, Hauguel-De Mouzon S, Lepercq J, Challier JC, Huston- Presley L, Friedman JE, Kalhan SC & Catalano PM., 2002. TNF-alpha is a predictor of insulin resistance in human pregnancy. *Diabetes* 51 2207–2213.

Kitabchi, A.E., Umpierrez, G.E., Miles, J.M., Fisher, J.N., 2009. Hyperglycemic crises in adult patients with diabetes. *Diabetes Care.* **32,** 1335-1343.

Kitamura, T., Kimura, K., Makondo, K., Furuya, D., Suzuki, M., Yoshida, T., Saito, M., 2003. Proinsulin C-peptide increases nitric oxide production by enhancing mitogen-activated protein-kinase-dependent transcription of endothelial nitric oxide synthase in aortic endothelial cells of Wistar rats. *Diabetologia.* **46,** 1698-1705.

Kitamura, T., Kimura, K., Jung, B.D., Makondo, K., Okamoto, S., Canas, X., Sakane, N., Yoshida, T., Saito, M., 2001. Proinsulin C-peptide rapidly stimulates mitogen-activated protein kinases in Swiss 3T3 fibroblasts: requirement of protein kinase C, phosphoinositide 3-kinase and pertussis toxin-sensitive G-protein. *The Biochemical Journal.* **355,** 123-129.

Kitamura, T., Kimura, K., Jung, B.D., Makondo, K., Sakane, N., Yoshida, T., Saito, M., 2002. Proinsulin C-peptide activates cAMP response element-binding proteins through the p38 mitogen-activated protein kinase pathway in mouse lung capillary endothelial cells. *The Biochemical Journal.* **366,** 737-744.

Koumakis, E., Millet-Botti, J., El Benna, J., Leroy, C., Boitez, V., Codogno, P., Friedlander, G., Forand, A., 2019. Novel function of PiT1/SLC20A1 in LPS-related inflammation and wound healing. *Scientific Reports.* **9,** 1808.

Kristiansen K (2004). Molecular mechanisms of ligand binding, signaling, and regulation within the superfamily of G-protein-coupled receptors: molecular modeling and mutagenesis approaches to receptor structure and function. *Pharmacol Ther* 103**:** 21-80.

Kulkarni, R. N. (2004) The islet β-cell. *The international journal of biochemistry & cell biology, 36*(3), pp. 365-371.

Laing, S.P., Swerdlow, A., Slater, S., Burden, A., Morris, A., Waugh, N.R., Gatling, W., Bingley, P., Patterson, C., 2003. Mortality from heart disease in a cohort of 23,000 patients with insulin-treated diabetes. *Diabetologia.* **46,** 760-765.

Lam, S., van der Geest, Reinier N, Verhagen, N.A., Daha, M.R., van Kooten, C., 2004. Secretion of collagen type IV by human renal fibroblasts is increased by high glucose via a TGF-β-independent pathway. *Nephrology Dialysis Transplantation.* **19,** 1694-1701.

Lam, S., Verhagen, N.A., Strutz, F., Van Der Pijl, Johan W, Daha, M.R., Van Kooten, C., 2003. Glucose-induced fibronectin and collagen type III expression in renal fibroblasts can occur independent of TGF-β1. *Kidney International.* **63,** 878-888.

Lamb, E., 2011. Assessment of kidney function in adults. *Medicine.* **39,** 306-311.

Landreh, M., Östberg, L.J., Jörnvall, H., 2014a. A subdivided molecular architecture with separate features and stepwise emergence among proinsulin C-peptides. *Biochemical and Biophysical Research Communications.* **450,** 1433-1438.

Landreh, M., Johansson, J., Wahren, J. and Jörnvall, H., 2014b. The structure, molecular interactions and bioactivities of proinsulin C-peptide correlate with a tripartite molecule. *Biomolecular concepts*, *5*(2), pp.109-118.

Laster, S.M., Wood, J.G., Gooding, L.R., 1988. Tumor necrosis factor can induce both apoptic and necrotic forms of cell lysis. *Journal of Immunology (Baltimore, Md.: 1950).* **141,** 2629-2634.

Law KP & Zhang H., 2017. The pathogenesis and pathophysiology of gestational diabetes mellitus: deductions from a three-part longitudinal metabolomics study in China. *Clinica Chimica Acta: International Journal of Clinical Chemistry* **468** 60–70.

Leahy, J.L., 2005. Pathogenesis of type 2 diabetes mellitus. *Archives of Medical Research.* **36,** 197-209.

Lee, F.T., Cao, Z., Long, D.M., Panagiotopoulos, S., Jerums, G., Cooper, M.E., Forbes, J.M., 2004. Interactions between angiotensin II and NF-kappaB-dependent pathways in modulating macrophage infiltration in experimental diabetic nephropathy. *Journal of the American Society of Nephrology : JASN.* **15,** 2139-2151.

Lei Y, Devarapu SK, Motrapu M, Cohen CD, Lindenmeyer MT, Moll S, Kumar SV and Anders H-J (2019) Interleukin-1β Inhibition for Chronic Kidney Disease in Obese Mice With Type 2 Diabetes. Front. *Immunol.* 10:1223. doi: 10.3389/fimmu.2019.01223

Lenzen, S., 2008. The mechanisms of alloxan-and streptozotocin-induced diabetes. *Diabetologia.* **51,** 216-226.

Lenzen, S., 2014. A fresh view of glycolysis and glucokinase regulation: history and current status. *Journal of Biological Chemistry*, *289*(18), pp.12189-12194.

Leslie, R.D., 2010. Predicting adult-onset autoimmune diabetes: clarity from complexity. *Diabetes.* **59,** 330-331.

Li, Y., Zhong, Y., Gong, W., Gao, X., Qi, H., Liu, K., Qi, J., 2018. C-peptide prevents SMAD3 binding to alpha promoters to inhibit collagen type IV synthesis. *Journal of Molecular Endocrinology.* **61,** 47-56.

Li, Z.G. & Sima, A.A.F., 2004. C-peptide and central nervous system complications in diabetes. *Experimental Diabesity Research.* **5,** 79-90.

Li, Z., Zhang, W., Sima, A.A., 2003. C-peptide enhances insulin-mediated cell growth and protection against high glucose–induced apoptosis in SH-SY5Y cells. *Diabetes/Metabolism Research and Reviews.* **19,** 375-385.

Lim, A.K.H. & Tesch, G.H., 2012. Inflammation in diabetic nephropathy. *Mediators of Inflammation.* **2012,** .

Lim, Y., Bhatt, M.P., Kwon, M., Park, D., Na, S., Kim, Y., Ha, K., 2015. Proinsulin C-peptide prevents impaired wound healing by activating angiogenesis in diabetes. *Journal of Investigative Dermatology.* **135,** 269-278.

Lindahl, E., Nyman, U., Melles, E., Sigmundsson, K., Ståhlberg, M., Wahren, J., Öbrink, B., Shafqat, J., Joseph, B., Jörnvall, H., 2007. Cellular internalization of proinsulin C-peptide. *Cellular and Molecular Life Sciences.* **64,** 479.

Lloyd, C.M., Minto, A.W., Dorf, M.E., Proudfoot, A., Wells, T.N., Salant, D.J., Gutierrez-Ramos, J.C., 1997. RANTES and monocyte chemoattractant protein-1 (MCP-1) play an important role in the inflammatory phase of crescentic nephritis, but only MCP-1 is involved in crescent formation and interstitial fibrosis. *The Journal of Experimental Medicine.* **185,** 1371-1380.

Loeffler, I. & Wolf, G., 2013. Transforming growth factor-β and the progression of renal disease. *Nephrology Dialysis Transplantation.* **29,** i37-i45.

Lote, C., 2001. Applied physiology: the renal tubule. *Current Paediatrics.* **11,** 207-211.

Lu, B., Ennis, D., Lai, R., Bogdanovic, E., Nikolov, R., Salamon, L., Fantus, C., Le-Tien, H., Fantus, I.G., 2001. Enhanced sensitivity of insulin-resistant adipocytes to vanadate is associated with oxidative stress and decreased reduction of vanadate (5) to vanadyl (4). *Journal of Biological Chemistry.* **276,** 35589-35598.

Luppi, P., Cifarelli, V., Tse, H., Piganelli, J., Trucco, M., 2008. Human C-peptide antagonises high glucose-induced endothelial dysfunction through the nuclear factor-κB pathway. *Diabetologia.* **51,** 1534.

Luppi, P., Cifarelli, V., Wahren, J., 2011. C-peptide and long-term complications of diabetes. *Pediatric Diabetes.* **12,** 276-292.

Luzi, L., Zerbini, G., Caumo, A., 2007. C-peptide: a redundant relative of insulin? *Diabetologia.* **50,** 500-502.

Madsbad, S., 1983. Prevalence of residual B cell function and its metabolic consequences in type 1 (insulin-dependent) diabetes. *Diabetologia.* **24,** 141-147.

Maezawa, Y., Yokote, K., Sonezaki, K., Fujimoto, M., Kobayashi, K., Kawamura, H., Tokuyama, T., Takemoto, M., Ueda, S., Kuwaki, T., 2006a. Influence of C-peptide on early glomerular changes in diabetic mice. *Diabetes/Metabolism Research and Reviews.* **22,** 313-322.

Maezawa, Y., Yokote, K., Sonezaki, K., Fujimoto, M., Kobayashi, K., Kawamura, H., Tokuyama, T., Takemoto, M., Ueda, S., Kuwaki, T., 2006b. Influence of C-peptide on early glomerular changes in diabetic mice. *Diabetes/Metabolism Research and Reviews.* **22,** 313-322.

Magalhaes AC, Dunn H, Ferguson SS (2012). Regulation of GPCR activity, trafficking and localization by GPCR-interacting proteins. *British journal of pharmacology* 165**:** 1717-1736.

Mahadevan, P., Larkins, R., Fraser, J., Fosang, A., Dunlop, M., 1995. Increased hyaluronan production in the glomeruli from diabetic rats: a link between glucose-induced prostaglandin production and reduced sulphated proteoglycan. *Diabetologia.* **38,** 298-305.

Marx, N., Walcher, D., Raichle, C., Aleksic, M., Bach, H., Grüb, M., Hombach, V., Libby, P., Zieske, A., Homma, S. and Strong, J., 2004. C-peptide colocalizes with macrophages in early arteriosclerotic lesions of diabetic subjects and induces monocyte chemotaxis in vitro. *Arteriosclerosis, thrombosis, and vascular biology*, **24**(3), pp.540-545.

McCarthy, M.I., 2010. Genomics, type 2 diabetes, and obesity. *New England Journal of Medicine.* **363,** 2339-2350.

McCarthy, E.T., Sharma, R., Sharma, M., Li, J.Z., Ge, X.L., Dileepan, K.N., Savin, V.J., 1998. TNF-alpha increases albumin permeability of isolated rat glomeruli through the generation of superoxide. *Journal of the American Society of Nephrology : JASN.* **9,** 433-438.

Melcion, C., Lachman, L., Killen, P.D., Morel-Maroger, L., Striker, G.E., 1982. Mesangial cells, effect of monocyte products on proliferation and matrix synthesis. *Transplantation Proceedings.* **14,** 559-564.

Meneghini, L.F., 2009. Early insulin treatment in type 2 diabetes: what are the pros? *Diabetes Care.* **32 Suppl 2,** S266-9.

Meng, X., Tang, P.M., Li, J., Lan, H.Y., 2015. TGF-β/Smad signaling in renal fibrosis. *Frontiers in Physiology.* **6,** 82.

Menon, B., Franzo-Romain, M., Damanpour, S., Menon, K., 2011. Luteinizing hormone receptor mRNA down-regulation is mediated through ERK-dependent induction of RNA binding protein. *Molecular Endocrinology.* **25,** 282-290.

Mezzano, S., Aros, C., Droguett, A., Burgos, M.E., Ardiles, L., Flores, C., Schneider, H., Ruiz-Ortega, M., Egido, J., 2004. NF-κB activation and overexpression of regulated

genes in human diabetic nephropathy. *Nephrology Dialysis Transplantation.* **19,** 2505-2512.

Michigami, T., 2013. Extracellular phosphate as a signaling molecule. *Phosphate and Vitamin D in Chronic Kidney Disease.* Karger Publishers. 14-24.

Millar RP, Newton CL (2010). The year in G protein-coupled receptor research. *Molecular endocrinology* 24**:** 261-274.

Miller, C.G., Pozzi, A., Zent, R., Schwarzbauer, J.E., 2014. Effects of high glucose on integrin activity and fibronectin matrix assembly by mesangial cells. *Molecular Biology of the Cell.* **25,** 2342-2350.

Mochizuki N, Ohba Y, Kiyokawa E, Kurata T, Murakami T, Ozaki T et al. (1999). Activation of the ERK/MAPK pathway by an isoform of rap1GAP associated with Gai. *Nature 400*: 891–894.

Moinuddin, Z. & Dhanda, R., 2015. Anatomy of the kidney and ureter. *Anaesthesia & Intensive Care Medicine.* **16,** 247-252.

Morran, M.P., Omenn, G.S., Pietropaolo, M., 2008. Immunology and genetics of type 1 diabetes. *Mount Sinai Journal of Medicine: A Journal of Translational and Personalized Medicine: A Journal of Translational and Personalized Medicine.* **75,** 314-327.

Mostafa, N. M. E.-S. B. (2012) Hormonal and nutrient signalling to protein kinase B and mammalian target of rapamycin in pancreatic beta-cells. Unpublished, University of Leicester.

Muller, L. & Lindberg, I., 1999. The cell biology of the prohormone convertases PCI and PC2. *Progress in nucleic acid research and molecular biology.* Elsevier. 69-108.

Muoio, D.M. & Newgard, C.B., 2008. Molecular and metabolic mechanisms of insulin resistance and β-cell failure in type 2 diabetes. *Nature Reviews Molecular Cell Biology.* **9,** 193.

Nakamura, T., Fukui, M., Ebihara, I., Osada, S., Nagaoka, I., Tomino, Y., Koide, H., 1993. mRNA expression of growth factors in glomeruli from diabetic rats. *Diabetes.* **42,** 450-456.

Navarro, J.F., Milena, F.J., Mora, C., Leon, C., Garcia, J., 2006. Renal pro-inflammatory cytokine gene expression in diabetic nephropathy: effect of angiotensin-converting enzyme inhibition and pentoxifylline administration. *American Journal of Nephrology.* **26,** 562-570.

Nguyen-Ngo, C., Jayabalan, N., Salomon, C. and Lappas, M., 2019. Molecular pathways disrupted by gestational diabetes mellitus. *Journal of molecular endocrinology*, *63*(3), pp.R51-R72.

Noble, J.A. & Erlich, H.A., 2012. Genetics of type 1 diabetes. *Cold Spring Harbor Perspectives in Medicine.* **2,** a007732.

Nordquist, L., Brown, R., Fasching, A., Persson, P., Palm, F., 2009. Proinsulin C-peptide reduces diabetes-induced glomerular hyperfiltration via efferent arteriole dilation and inhibition of tubular sodium reabsorption. *American Journal of Physiology-Renal Physiology.* **297,** F1265-F1272.

Nordquist, L., Lai, E.Y., Sjoquist, M., Patzak, A., Persson, A.E.G., 2008. Proinsulin C-peptide constricts glomerular afferent arterioles in diabetic mice. A potential renoprotective mechanism. *American Journal of Physiology-Regulatory, Integrative and Comparative Physiology.* **294,** R836-R841.

Nordquist, L., Palm, F., Andresen, B.T., 2008. Renal and vascular benefits of C-peptide: Molecular mechanisms of C-peptide action. *Biologics : Targets & Therapy.* **2,** 441-452.

Nouwen, A., Nefs, G., Caramlau, I., Connock, M., Winkley, K., Lloyd, C.E., Peyrot, M., Pouwer, F., European Depression in Diabetes Research Consortium, 2011. Prevalence of depression in individuals with impaired glucose metabolism or undiagnosed diabetes: a systematic review and meta-analysis of the European Depression in Diabetes (EDID) Research Consortium. *Diabetes Care.* **34,** 752-762.

Nowicki, M., Fliser, D., Fode, P., Ritz, E., 1996. Changes in plasma phosphate levels influence insulin sensitivity under euglycemic conditions. *The Journal of Clinical Endocrinology & Metabolism.* **81,** 156-159.

Obrosova, I.G., 2009. Diabetic painful and insensate neuropathy: pathogenesis and potential treatments. *Neurotherapeutics.* **6,** 638-647.

Ohtomo, Y., Aperia, A., Sahlgren, B., Johansson, B., Wahren, J., 1996. C-peptide stimulates rat renal tubular Na , K -ATPase activity in synergism with neuropeptide Y. *Diabetologia.* **39,** 199-205.

Okada, S., Shikata, K., Matsuda, M., Ogawa, D., Usui, H., Kido, Y., Nagase, R., Wada, J., Shikata, Y., Makino, H., 2003a. Intercellular adhesion molecule-1-deficient mice are resistant against renal injury after induction of diabetes. *Diabetes.* **52,** 2586-2593.

Okada, S., Shikata, K., Matsuda, M., Ogawa, D., Usui, H., Kido, Y., Nagase, R., Wada, J., Shikata, Y., Makino, H., 2003b. Intercellular adhesion molecule-1-deficient mice are resistant against renal injury after induction of diabetes. *Diabetes.* **52,** 2586-2593.

Omote, K., Gohda, T., Murakoshi, M., Sasaki, Y., Kazuno, S., Fujimura, T., Ishizaka, M., Sonoda, Y., Tomino, Y., 2014. Role of the TNF pathway in the progression of diabetic nephropathy in KK-Ay mice. *American Journal of Physiology-Renal Physiology.* **306,** F1335-F1347.

Osmond, D.T.D., King, R.G., Brennecke, S.P. and Gude, N.M., 2001. Placental glucose transport and utilisation is altered at term in insulin-treated, gestational-diabetic patients. *Diabetologia*, ***44***(9), pp.1133-1139.

Ozcan, U., Cao, Q., Yilmaz, E., Lee, A.H., Iwakoshi, N.N., Ozdelen, E., Tuncman, G., Gorgun, C., Glimcher, L.H., Hotamisligil, G.S., 2004. Endoplasmic reticulum stress links obesity, insulin action, and type 2 diabetes. *Science (New York, N.Y.).* **306,** 457-461.

Pace AM, Faure M, Bourne HR. (1995). Gi2-mediated activation of the MAP kinase cascade. *Mol Biol Cell 6*: 1685–1695.

Panee, J., 2012. Monocyte Chemoattractant Protein 1 (MCP-1) in obesity and diabetes. *Cytokine.* **60,** 1-12.

Pearson, J., 2000. Normal endothelial cell function. *Lupus.* **9,** 183-188.

Perez-Morales, R.E., Del Pino, M.D., Valdivielso, J.M., Ortiz, A., Mora-Fernandez, C., Navarro-Gonzalez, J.F., 2019. Inflammation in Diabetic Kidney Disease. *Nephron.* **143,** 12-16.

Pendergrass, M., Fazioni, E. and DeFronzo, R.A., 1995. Non-insulin-dependent diabetes mellitus and gestational diabetes mellitus: same disease, another name?. *Diabetes reviews*, *3*(4), pp.566-583.

Pfeilschifter, J., Pignat, W., Vosbeck, K., Märki, F., 1989. Interleukin 1 and tumor necrosis factor synergistically stimulate prostaglandin synthesis and phospholipase A2 release from rat renal mesangial cells. *Biochemical and Biophysical Research Communications.* **159,** 385-394.

Phillips, D., Aponte, A.M., French, S.A., Chess, D.J., Balaban, R.S., 2009. Succinyl-CoA synthetase is a phosphate target for the activation of mitochondrial metabolism. *Biochemistry.* **48,** 7140-7149.

Pivovarov, A.S., Calahorro, F. and Walker, R.J., 2019. Na+/K+-pump and neurotransmitter membrane receptors. *Invertebrate Neuroscience*, *19*(1), p.1.

Plows, J.F., Stanley, J.L., Baker, P.N., Reynolds, C.M. and Vickers, M.H., 2018. The pathophysiology of gestational diabetes mellitus. *International journal of molecular sciences*, *19*(11), p.3342.

Pramanik, A., Ekberg, K., Zhong, Z., Shafqat, J., Henriksson, M., Jansson, O., Tibell, A., Tally, M., Wahren, J., Jörnvall, H., 2001. C-peptide binding to human cell membranes: importance of Glu27. *Biochemical and Biophysical Research Communications.* **284,** 94-98.

Prentki, M. & Nolan, C.J., 2006. Islet beta cell failure in type 2 diabetes. *The Journal of Clinical Investigation.* **116,** 1802-1812.

Pries, A. & Kuebler, W., 2006. Normal endothelium. *The Vascular Endothelium I.* Springer. 1-40.

Pugsley, M. & Tabrizchi, R., 2000. The vascular system: An overview of structure and function. *Journal of Pharmacological and Toxicological Methods.* **44,** 333-340.

Quigley, H.A., Addicks, E.M., Green, W.R. and Maumenee, A.E., 1981. Optic nerve damage in human glaucoma: II. The site of injury and susceptibility to damage. *Archives of ophthalmology*, *99*(4), pp.635-649.

Radeke, H.H., Meier, B., Topley, N., Flöge, J., Habermehl, G.G., Resch, K., 1990. Interleukin 1-α and tumor necrosis factor-α induce oxygen radical production in mesangial cells. *Kidney International.* **37,** 767-775.

RASMUSSEN, A. & JESPERSEN, L., 1985. Reduced tubular reabsorption of phosphate during post-operative glucose infusions in humans. *European Journal of Clinical Investigation.* **15,** 157-160.

Rath, D.P., Bailey, M., Zhang, H., Jiang, Z., Abduljalil, A.M., Weisbrode, S., Hamlin, R.L., Robitaille, P., 1995. 31P-nuclear magnetic resonance studies of chronic myocardial ischemia in the Yucatan micropig. *The Journal of Clinical Investigation.* **95,** 151-157.

Razzaque, M., Koji, T., Horita, Y., Nishihara, M., Harada, T., Nakane, P., Taguchi, T., 1995. Synthesis of type III collagen and type IV collagen by tubular epithelial cells in diabetic nephropathy. *Pathology-Research and Practice.* **191,** 1099-1104.

Rebsomen, L., Pitel, S., Boubred, F., Buffat, C., Feuerstein, J., Raccah, D., Vague, P., Tsimaratos, M., 2006. C-peptide replacement improves weight gain and renal function in diabetic rats. *Diabetes & Metabolism.* **32,** 223-228.

Reeves, W.B. & Andreoli, T.E., 2000. Transforming growth factor beta contributes to progressive diabetic nephropathy. *Proceedings of the National Academy of Sciences of the United States of America.* **97,** 7667-7669.

Reidy, K., Kang, H.M., Hostetter, T., Susztak, K., 2014. Molecular mechanisms of diabetic kidney disease. *The Journal of Clinical Investigation.* **124,** 2333-2340.

Rigler, R., Pramanik, A., Jonasson, P., Kratz, G., Jansson, O.T., Nygren, P., Stahl, S., Ekberg, K., Johansson, B., Uhlen, S., Uhlen, M., Jornvall, H., Wahren, J., 1999. Specific binding of proinsulin C-peptide to human cell membranes. *Proceedings of the National Academy of Sciences of the United States of America.* **96,** 13318-13323.

Ross, J., 1995. mRNA stability in mammalian cells. *Microbiological Reviews.* **59,** 423-450.

Ruan, H. and Lodish, H. F. (2003) Insulin resistance in adipose tissue: direct and indirect effects of tumor necrosis factor-α. *Cytokine & Growth Factor Reviews, 14*(5), pp. 447-455.

Rudberg, S., Rasmussen, L.M., Bangstad, H.J., Osterby, R., 2000. Influence of insertion/deletion polymorphism in the ACE-I gene on the progression of diabetic glomerulopathy in type 1 diabetic patients with microalbuminuria. *Diabetes Care.* **23,** 544-548.

Ruef, C., Budde, K., Lacy, J., Northemann, W., Baumann, M., Sterzel, R.B., Coleman, D.L., 1990. Interleukin 6 is an autocrine growth factor for mesangial cells. *Kidney International.* **38,** 249-257.

Rorsman, P. and Renström, E. (2003) Insulin granule dynamics in pancreatic beta cells. *Diabetologia, 46*(8), pp. 1029-1045.

Ruster, C. & Wolf, G., 2008. The role of chemokines and chemokine receptors in diabetic nephropathy. *Front Biosci.* **13,** 944-955.

Saltiel, A. R. and Kahn, C. R. (2001) Insulin signalling and the regulation of glucose and lipid metabolism. *Nature, 414*(6865), pp. 799-806.

Samnegård, B., Jacobson, S.H., Jaremko, G., Johansson, B., Ekberg, K., Isaksson, B., Eriksson, L., Wahren, J., Sjöquist, M., 2005a. C-peptide prevents glomerular hypertrophy and mesangial matrix expansion in diabetic rats. *Nephrology Dialysis Transplantation.* **20,** 532-538.

Samnegård, B., Jacobson, S.H., Jaremko, G., Johansson, B., Ekberg, K., Isaksson, B., Eriksson, L., Wahren, J., Sjöquist, M., 2005b. C-peptide prevents glomerular hypertrophy and mesangial matrix expansion in diabetic rats. *Nephrology Dialysis Transplantation.* **20,** 532-538.

Samnegård, B., Jacobson, S.H., Jaremko, G., Johansson, B., Sjöquist, M., 2001. Effects of C-peptide on glomerular and renal size and renal function in diabetic rats. *Kidney International.* **60,** 1258-1265.

Samnegård, B., Jacobson, S.H., Johansson, B., Ekberg, K., Isaksson, B., Wahren, J., Sjöquist, M., 2004. C-peptide and captopril are equally effective in lowering glomerular hyperfiltration in diabetic rats. *Nephrology Dialysis Transplantation.* **19,** 1385-1391.

Sato, W., Kosugi, T., Zhang, L., Roncal, C.A., Heinig, M., Campbell-Thompson, M., Yuzawa, Y., Atkinson, M.A., Grant, M.B., Croker, B.P., 2008. The pivotal role of VEGF on glomerular macrophage infiltration in advanced diabetic nephropathy. *Laboratory Investigation.* **88,** 949.

Satriano, J.A., Banas, B., Luckow, B., Nelson, P., Schlondorff, D.O., 1997. Regulation of RANTES and ICAM-1 expression in murine mesangial cells. *Journal of the American Society of Nephrology : JASN.* **8,** 596-603.

Scalia, R., Coyle, K.M., Levine, B.J., Booth, G., Lefer, A.M., 2000. C-peptide inhibits leukocyte–endothelium interaction in the microcirculation during acute endothelial dysfunction. *The FASEB Journal.* **14,** 2357-2364.

Schmid, H., Boucherot, A., Yasuda, Y., Henger, A., Brunner, B., Eichinger, F., Nitsche, A., Kiss, E., Bleich, M., Grone, H.J., Nelson, P.J., Schlondorff, D., Cohen, C.D., Kretzler, M., European Renal cDNA Bank (ERCB) Consortium, 2006. Modular activation of nuclear factor-kappaB transcriptional programs in human diabetic nephropathy. *Diabetes.* **55,** 2993-3003.

Segura, M.T., Demmelmair, H., Krauss-Etschmann, S., Nathan, P., Dehmel, S., Padilla, M.C., Rueda, R., Koletzko, B. and Campoy, C., 2017. Maternal BMI and gestational diabetes alter placental lipid transporters and fatty acid composition. *Placenta, 57,* pp.144-151.

Serhan, C.N., Ward, P.A. and Gilroy, D.W., 2010a. *Fundamentals of inflammation.* Cambridge University Press.

Serhan, C.N., Ward, P.A. and Gilroy, D.W., 2010b. *Fundamentals of inflammation.* Cambridge University Press.

Seron, D., Cameron, J., Haskard, D., 1991. Expression of VCAM-1 in the normal and diseased kidney. *Nephrology Dialysis Transplantation.* **6,** 917-922.

Sestoft, L., 1979. *Is the Relationship between the Plasma Concentration of Inorganic Phosphate and the Rate of Oxygen Consumption of Significance in Regulating Energy Metabolism in Mammals?.*

Shafqat, J., Juntti-Berggren, L., Zhong, Z., Ekberg, K., Köhler, M., Berggren, P., Johansson, J., Wahren, J., Jörnvall, H., 2002. Proinsulin C-peptide and its analogues induce intracellular Ca2 increases in human renal tubular cells. *Cellular and Molecular Life Sciences CMLS.* **59,** 1185-1189.

Sharma, K., Jin, Y., Guo, J., Ziyadeh, F., 1996. Neutralization of TGF-by anti-TGF-antibody attenuates kidney hypertrophy and enhanced ECM expression in streptozotocin-induced diabetic mice. *Diabetes.* **45,** 522-530.

Sharma, K. & Ziyadeh, F.N., 1997. Biochemical events and cytokine interactions linking glucose metabolism to the development of diabetic nephropathy. *Seminars in Nephrology.* **17,** 80-92.

Sharma, K. & Ziyadeh, F.N., 1995. Hyperglycemia and diabetic kidney disease. The case for transforming growth factor-beta as a key mediator. *Diabetes.* **44,** 1139-1146.

Sheetz, M.J. & King, G.L., 2002. Molecular understanding of hyperglycemia's adverse effects for diabetic complications. *Jama.* **288,** 2579-2588.

Sima, A.A., Zhang, W., Kreipke, C.W., Rafols, J.A., Hoffman, W.H., 2009. Inflammation in Diabetic Encephalopathy is Prevented by C-Peptide. *The Review of Diabetic Studies : RDS.* **6,** 37-42.

Sima, A.A.F., 2003. C-peptide and diabetic neuropathy. *Expert Opinion on Investigational Drugs.* **12,** 1471-1488.

Sima, A.A.F. & Sugimoto, K., 1999. Experimental diabetic neuropathy: an update. *Diabetologia.* **42,** 773-788.

Sima, A., Zhang, W., Sugimoto, K., Henry, D., Li, Z., Wahren, J., Grunberger, G., 2001. C-peptide prevents and improves chronic type I diabetic polyneuropathy in the BB/Wor rat. *Diabetologia.* **44,** 889-897.

Simak, J., Gelderman, M., Yu, H., Wright, V., Baird, A., 2006. Circulating endothelial microparticles in acute ischemic stroke: a link to severity, lesion volume and outcome. *Journal of Thrombosis and Haemostasis.* **4,** 1296-1302.

Simmons, N., 1990. A cultured human renal epithelioid cell line responsive to vasoactive intestinal peptide. *Experimental Physiology: Translation and Integration.* **75,** 309-319.

Sjöquist, M., Huang, W., Johansson, B., 1998. Effects of C-peptide on renal function at the early stage of experimental diabetes. *Kidney International.* **54,** 758-764.

Song, B.J., Aiello, L.P. and Pasquale, L.R., 2016. Presence and risk factors for glaucoma in patients with diabetes. *Current diabetes reports*, *16*(12), p.124.

Sowa ME, He W, Wensel TG, Lichtarge O (2000). A regulator of G protein signaling interaction surface linked to effector specificity. *Proceedings of the National Academy of Sciences of the United States of America* 97**:** 1483-1488.

Steck, A.K., Dong, F., Waugh, K., Frohnert, B.I., Yu, L., Norris, J.M., Rewers, M.J., 2016. Predictors of slow progression to diabetes in children with multiple islet autoantibodies. *Journal of Autoimmunity.* **72,** 113-117.

Steiner, D.F., S.Y. Park, J. Stoy, L.H. Philipson, and G.I. Bell. 2009. A brief perspective on insulin production. *Diabetes Obes Metab*. 11 Suppl 4:189-96.

Stevens RC, Cherezov V, Katritch V, Abagyan R, Kuhn P, Rosen H, *et al.* (2013). The GPCR Network: a large-scale collaboration to determine human GPCR structure and function. *Nat Rev Drug Discov* 12**:** 25-34.

Strutz, F., Zeisberg, M., Hemmerlein, B., Sattler, B., Hummel, K., Becker, V., Müller, G.A., 2000. Basic fibroblast growth factor expression is increased in human renal fibrogenesis and may mediate autocrine fibroblast proliferation. *Kidney International.* **57,** 1521-1538.

Su, H., Lei, C., Zhang, C., 2017. Interleukin-6 signaling pathway and its role in kidney disease: an update. *Frontiers in Immunology.* **8,** 405.

Suzuki, D., Miyazaki, M., Naka, R., Koji, T., Yagame, M., Jinde, K., Endoh, M., Nomoto, Y., Sakai, H., 1995. In situ hybridization of interleukin 6 in diabetic nephropathy. *Diabetes.* **44,** 1233-1238.

Sweeney G, Klip A. Regulation of the Na+/K+-ATPase by insulin: why and how?. *Mol Cell Biochem*. 1998;182(1-2):121-133.

Swinnen, S.G., Hoekstra, J.B., DeVries, J.H., 2009. Insulin therapy for type 2 diabetes. *Diabetes Care.* **32 Suppl 2,** S253-9.

Szajerka, G. & Kwiatkowska, J., 1984. The effect of cortisol on rabbit red cell acid phosphatase isoenzymes. *Molecular and Cellular Biochemistry.* **59,** 183-186.

Takahashi, T. & Harris, R.C., 2014. Role of endothelial nitric oxide synthase in diabetic nephropathy: lessons from diabetic eNOS knockout mice. *Journal of Diabetes Research.* **2014,** 590541.

Tan, X., Xu, X., Zeisberg, E.M., Zeisberg, M., 2016. High inorganic phosphate causes DNMT1 phosphorylation and subsequent fibrotic fibroblast activation. *Biochemical and Biophysical Research Communications.* **472,** 459-464.

Tang, S.C. & Lai, K.N., 2012. The pathogenic role of the renal proximal tubular cell in diabetic nephropathy. *Nephrology Dialysis Transplantation.* **27,** 3049-3056.

Taniguchi, C. M., Emanuelli, B. and Kahn, C. R. (2006) Critical nodes in signalling pathways: insights into insulin action. *Nat Rev Mol Cell Biol, 7*(2), pp. 85-96.

Tarr, J.M., Kaul, K., Wolanska, K., Kohner, E.M. and Chibber, R., 2013. Retinopathy in diabetes. *Diabetes.* Springer. 88-106.

Thaiss, F., Wolf, G., Assad, N., Zahner, G., Stahl, R., 1996. Angiotensinase A gene expression and enzyme activity in isolated glomeruli of diabetic rats. *Diabetologia.* **39,** 275-280.

Thermo-Fisher (2016) Growth and Maintenance of the 293A Cell Line USER GUIDE Publication Number MAN0000303. Thermo Fisher Scientific Catalogue Number R705-07.

Thorve, V.S., Kshirsagar, A.D., Vyawahare, N.S., Joshi, V.S., Ingale, K.G., Mohite, R.J., 2011. Diabetes-induced erectile dysfunction: epidemiology, pathophysiology and management. *Journal of Diabetes and its Complications.* **25,** 129-136.

Tortora, G.J. & Bryan, D., 2014. Principles of anatomy and physiology.

Tsimaratos, M., Roger, F., Chabardes, D., Mordasini, D., Hasler, U., Doucet, A., Martin, P., Feraille, E., 2003. C-peptide stimulates Na , K -ATPase activity via PKC alpha in rat medullary thick ascending limb. *Diabetologia.* **46,** 124-131.

Tuso, P., 2014. Prediabetes and lifestyle modification: time to prevent a preventable disease. *The Permanente Journal.* **18,** 88-93.

Ueda, A., Ishigatsubo, Y., Okubo, T., Yoshimura, T., 1997. Transcriptional regulation of the human monocyte chemoattractant protein-1 gene. Cooperation of two NF-kappaB sites and NF-kappaB/Rel subunit specificity. *The Journal of Biological Chemistry.* **272,** 31092-31099.

Umpierre, D., Ribeiro, P.A., Kramer, C.K., Leitão, C.B., Zucatti, A.T., Azevedo, M.J., Gross, J.L., Ribeiro, J.P., Schaan, B.D., 2011. Physical activity advice only or structured exercise training and association with HbA1c levels in type 2 diabetes: a systematic review and meta-analysis. *Jama.* **305,** 1790-1799.

Umpierrez, G. & Korytkowski, M., 2016. Diabetic emergencies—ketoacidosis, hyperglycaemic hyperosmolar state and hypoglycaemia. *Nature Reviews Endocrinology.* **12,** 222.

Unger, J. & Parkin, C.G., 2010. Type 2 diabetes: an expanded view of pathophysiology and therapy. *Postgraduate Medicine.* **122,** 145-157.

Varadarajan, D.K., Karthikeyan, A.S., Matilda, P.D., Raghothama, K.G., 2002. Phosphite, an analog of phosphate, suppresses the coordinated expression of genes under phosphate starvation. *Plant Physiology.* **129,** 1232-1240.

Vasic, D. & Walcher, D., 2012. Proinflammatory effects of C-Peptide in different tissues. *International Journal of Inflammation.* **2012,** .

Venegas-Pont, M., Manigrasso, M.B., Grifoni, S.C., LaMarca, B.B., Maric, C., Racusen, L.C., Glover, P.H., Jones, A.V., Drummond, H.A., Ryan, M.J., 2010. Tumor necrosis factor-α antagonist etanercept decreases blood pressure and protects the kidney in a mouse model of systemic lupus erythematosus. *Hypertension.* **56,** 643-649.

Verma, S. & Anderson, T.J., 2002. Fundamentals of endothelial function for the clinical cardiologist. *Circulation.* **105,** 546-549.

Vesey, D.A., Cheung, C., Cuttle, L., Endre, Z., Gobe, G., Johnson, D.W., 2002. Interleukin-1β stimulates human renal fibroblast proliferation and matrix protein production by means of a transforming growth factor-β-dependent mechanism. *Journal of Laboratory and Clinical Medicine.* **140,** 342-350.

Vish, M.G., Mangeshkar, P., Piraino, G., Denenberg, A., Hake, P.W., O'Connor, M., Zingarelli, B., 2007. Proinsulin c-peptide exerts beneficial effects in endotoxic shock in mice. *Critical Care Medicine.* **35,** 1348-1355.

Vleming, L.J., Baelde, J.J., Westendorp, R.G., Daha, M.R., van Es, L.A., Bruijn, J.A., 1995. Progression of chronic renal disease in humans is associated with the deposition of basement membrane components and decorin in the interstitial extracellular matrix. *Clinical Nephrology.* **44,** 211-219.

Wada, J. & Makino, H., 2012. Inflammation and the pathogenesis of diabetic nephropathy. *Clinical Science.* **124,** 139-152.

Wahren, J., 2017. C-peptide and the pathophysiology of microvascular complications of diabetes. *Journal of Internal Medicine.* **281,** 3-6.

Wahren, J., Ekberg, K., Johansson, J., Henriksson, M., Pramanik, A., Johansson, B.L., Rigler, R., Jornvall, H., 2000. Role of C-peptide in human physiology. *American Journal of Physiology.Endocrinology and Metabolism.* **278,** E759-68.

Wahren, J., Foyt, H., Daniels, M., Arezzo, J.C., 2016a. Long-Acting C-Peptide and Neuropathy in Type 1 Diabetes: A 12-Month Clinical Trial. *Diabetes Care.* **39,** 596-602.

Wahren, J. & Larsson, C., 2015. C-peptide: New findings and therapeutic possibilities. *Diabetes Research and Clinical Practice.* **107,** 309-319.

Wahren, J., Shafqat, J., Johansson, J., Chibalin, A., Ekberg, K., Jornvall, H., 2004. Molecular and cellular effects of C-peptide--new perspectives on an old peptide. *Experimental Diabesity Research.* **5,** 15-23.

Wahren, J., Foyt, H., Daniels, M., Arezzo, J.C., 2016b. Long-Acting C-Peptide and Neuropathy in Type 1 Diabetes: A 12-Month Clinical Trial. *Diabetes Care.* **39,** 596-602.

Wahren, J., Kallas, A., Sima, A.A., 2012. The clinical potential of C-peptide replacement in type 1 diabetes. *Diabetes.* **61,** 761-772.

Wahren, J. & Larsson, C., 2015. C-peptide: New findings and therapeutic possibilities. *Diabetes Research and Clinical Practice.* **107,** 309-319.

Wakisaka, M., Spiro, M.J., Spiro, R.G., 1994. Synthesis of type VI collagen by cultured glomerular cells and comparison of its regulation by glucose and other factors with that of type IV collagen. *Diabetes.* **43,** 95-103.

Walcher, D.C., Poletek, P., Rosenkranz, S., Bach, H., Betz, S., Durst, R., Grüb, M., Hombach, V., Strong, J., 2006. C-Peptide induces vascular smooth muscle cell proliferation: involvement of SRC-kinase, phosphatidylinositol 3-kinase, and extracellular signal-regulated kinase 1/2. *Circulation Research.* **99,** 1181-1187.

Walcher, D., Aleksic, M., Jerg, V., Hombach, V., Zieske, A., Homma, S., Strong, J., Marx, N., 2004. C-peptide induces chemotaxis of human CD4-positive cells: involvement of pertussis toxin-sensitive G-proteins and phosphoinositide 3-kinase. *Diabetes.* **53,** 1664-1670.

Walcher, D., Babiak, C., Poletek, P., Rosenkranz, S., Bach, H., Betz, S., Durst, R., Grüb, M., Hombach, V., Strong, J. and Marx, N., 2006. C-Peptide induces vascular smooth muscle cell proliferation: involvement of SRC-kinase, phosphatidylinositol 3-kinase, and extracellular signal-regulated kinase 1/2. *Circulation research*, *99*(11), pp.1181-1187.

Wallerath, T., Kunt, T., Forst, T., Closs, E.I., Lehmann, R., Flohr, T., Gabriel, M., Schäfer, D., Göpfert, A., Pfützner, A., 2003. Stimulation of endothelial nitric oxide synthase by proinsulin C-peptide. *Nitric Oxide.* **9,** 95-102.

Wang, S., Wei, W., Zheng, Y., Hou, J., Dou, Y., Zhang, S., Luo, X., Cai, X., 2012. The role of insulin C-peptide in the coevolution analyses of the insulin signaling pathway: a hint for its functions. *PloS One.* **7,** e52847.

Wang, Z., Xie, Z., Lu, Q., Chang, C., Zhou, Z., 2017. Beyond genetics: what causes type 1 diabetes. *Clinical Reviews in Allergy & Immunology.* **52,** 273-286.

Weiss, M.A., Frank, B.H., Khait, I., Pekar, A., Heiney, R., Shoelson, S.E., Neuringer, L.J., 1990. NMR and photo-CIDNP studies of human proinsulin and prohormone processing intermediates with application to endopeptidase recognition. *Biochemistry.* **29,** 8389-8401.

Wendt, T.M., Tanji, N., Guo, J., Kislinger, T.R., Qu, W., Lu, Y., Bucciarelli, L.G., Rong, L.L., Moser, B., Markowitz, G.S., 2003. RAGE drives the development of glomerulosclerosis and implicates podocyte activation in the pathogenesis of diabetic nephropathy. *The American Journal of Pathology.* **162,** 1123-1137.

Werner, A., Dehmelt, L., Nalbant, P., 1998. Na+-dependent phosphate cotransporters: the NaPi protein families. *The Journal of Experimental Biology.* **201,** 3135-3142.

Wieser, M., Stadler, G., Jennings, P., Streubel, B., Pfaller, W., Ambros, P., Riedl, C., Katinger, H., Grillari, J., Grillari-Voglauer, R., 2008. hTERT alone immortalizes epithelial cells of renal proximal tubules without changing their functional characteristics. *American Journal of Physiology-Renal Physiology.* **295,** F1365-F1375.

Wild, S., Roglic, G., Green, A., Sicree, R., King, H., 2004. Global prevalence of diabetes: estimates for the year 2000 and projections for 2030. *Diabetes Care.* **27,** 1047-1053.

Wolf, G., Aberle, S., Thaiss, F., Nelson, P.J., Krensky, A.M., Neilson, E.G., Stahl, R.A., 1993. TNFα induces expression of the chemoattractant cytokine RANTES in cultured mouse mesangial cells. *Kidney International.* **44,** 795-804.

Wolf M, Sauk J, Shah A, Vossen Smirnakis K, Jimenez-Kimble R, Ecker JL & Thadhani R., 2004. Inflammation and glucose intolerance: a prospective study of gestational diabetes mellitus. *Diabetes Care* **27** 21–27.

Wortzel, I. and Seger, R., 2011. The ERK cascade: distinct functions within various subcellular organelles. *Genes & cancer*, ***2***(3), pp.195-209.

Yang, L., Zheng, L., Chng, W.J. and Ding, J.L., 2019. Comprehensive analysis of ERK1/2 substrates for potential combination immunotherapies. *Trends in pharmacological sciences*, 40(11), pp.897-910.

Yosten, G.L., Kolar, G.R., Redlinger, L.J., Samson, W.K., 2013. Evidence for an interaction between proinsulin C-peptide and GPR146. *The Journal of Endocrinology.* **218,** B1-8.

Yosten, G.L., Maric-Bilkan, C., Luppi, P., Wahren, J., 2014a. Physiological effects and therapeutic potential of proinsulin C-peptide. *American Journal of Physiology.Endocrinology and Metabolism.* **307,** E955-68.

Yosten, G.L., Maric-Bilkan, C., Luppi, P., Wahren, J., 2014b. Physiological effects and therapeutic potential of proinsulin C-peptide. *American Journal of Physiology.Endocrinology and Metabolism.* **307,** E955-68.

Yosten, G.L., Redlinger, L.J., Samson, W.K., 2012. Evidence for an interaction of neuronostatin with the orphan G protein-coupled receptor, GPR107. *American Journal of Physiology.Regulatory, Integrative and Comparative Physiology.* **303,** R941-9.

Young, L.H., Ikeda, Y., Scalia, R., Lefer, A.M., 2000. C-peptide exerts cardioprotective effects in myocardial ischemia-reperfusion. *American Journal of Physiology-Heart and Circulatory Physiology.* **279,** H1453-H1459.

Yu, H., Rimbert, A., Palmer, A.E., Toyohara, T., Xia, Y., Xia, F., Ferreira, L.M., Chen, Z., Chen, T., Loaiza, N., 2019. GPR146 Deficiency Protects against Hypercholesterolemia and Atherosclerosis. *Cell.* **179,** 1276-1288. e14.

Zeisberg, M. & Kalluri, R., 2004. The role of epithelial-to-mesenchymal transition in renal fibrosis. *Journal of Molecular Medicine.* **82,** 175-181.

Zerif, E., Maalem, A., Gaudreau, S., Guindi, C., Ramzan, M., Véroneau, S., Gris, D., Stankova, J., Rola-Pleszczynski, M., Mourad, W., 2017. Constitutively active Stat5b signaling confers tolerogenic functions to dendritic cells of NOD mice and halts diabetes progression. *Journal of Autoimmunity.* **76,** 63-74.

Zeng, Y (2019) MSc thesis, University of Leicester.

Zhang, W. and Liu, H.T., 2002. MAPK signal pathways in the regulation of cell proliferation in mammalian cells. *Cell research*, ***12***(1), pp.9-18.

Zhang, Z. & VanEtten, R., 1991. Pre-steady-state and steady-state kinetic analysis of the low molecular weight phosphotyrosyl protein phosphatase from bovine heart. *Journal of Biological Chemistry.* **266,** 1516-1525.

Zhong, Z., Kotova, O., Davidescu, A., Ehren, I., Ekberg, K., Jörnvall, H., Wahren, J., Chibalin, A., 2004. C-peptide stimulates Na , K -ATPase via activation of ERK1/2 MAP kinases in human renal tubular cells. *Cellular and Molecular Life Sciences CMLS.* **61,** 2782-2790.

Zhou, A., Webb, G., Zhu, X., Steiner, D.F., 1999. Proteolytic processing in the secretory pathway. *The Journal of Biological Chemistry.* **274,** 20745-20748.

Ziyadeh, F.N., 1998. Evidence for the involvement of transforming growth factor-β in the pathogenesis of diabetic kidney disease: Are Koch's postulates fulfilled. *Curr Pract Med.* **1,** 87-89.

Ziyadeh, F.N., 1996. Significance of tubulointerstitial changes in diabetic renal disease. *Kidney International.Supplement.* **54,** S10-3.

Ziyadeh, F.N., Sharma, K., Ericksen, M., Wolf, G., 1994. Stimulation of collagen gene expression and protein synthesis in murine mesangial cells by high glucose is mediated by autocrine activation of transforming growth factor-beta. *The Journal of Clinical Investigation.* **93,** 536-542.

Ziyadeh, F.N., 1993. The extracellular matrix in diabetic nephropathy. *American Journal of Kidney Diseases.* **22,** 736-744.

Zoja, C., Donadelli, R., Colleoni, S., Figliuzzi, M., Bonazzola, S., Morigi, M., Remuzzi, G., 1998. Protein overload stimulates RANTES production by proximal tubular cells depending on NF-kB activation. *Kidney International.* **53,** 1608-1615.